

**Investigation on moisture buffering of hygroscopic materials  
by full-scale experiments and HAM simulations**

Xiangjin Yang

A Thesis

In the Department

of

Building, Civil and Environmental Engineering

Presented in Partial Fulfillment of the Requirements

For the Degree of Doctor of Philosophy at

Concordia University

Montreal, Quebec, Canada

April 2010

© Xiangjin Yang, 2010



Library and Archives  
Canada

Published Heritage  
Branch

395 Wellington Street  
Ottawa ON K1A 0N4  
Canada

Bibliothèque et  
Archives Canada

Direction du  
Patrimoine de l'édition

395, rue Wellington  
Ottawa ON K1A 0N4  
Canada

*Your file* *Votre référence*  
ISBN: 978-0-494-67328-7  
*Our file* *Notre référence*  
ISBN: 978-0-494-67328-7

**NOTICE:**

The author has granted a non-exclusive license allowing Library and Archives Canada to reproduce, publish, archive, preserve, conserve, communicate to the public by telecommunication or on the Internet, loan, distribute and sell theses worldwide, for commercial or non-commercial purposes, in microform, paper, electronic and/or any other formats.

The author retains copyright ownership and moral rights in this thesis. Neither the thesis nor substantial extracts from it may be printed or otherwise reproduced without the author's permission.

**AVIS:**

L'auteur a accordé une licence non exclusive permettant à la Bibliothèque et Archives Canada de reproduire, publier, archiver, sauvegarder, conserver, transmettre au public par télécommunication ou par l'Internet, prêter, distribuer et vendre des thèses partout dans le monde, à des fins commerciales ou autres, sur support microforme, papier, électronique et/ou autres formats.

L'auteur conserve la propriété du droit d'auteur et des droits moraux qui protègent cette thèse. Ni la thèse ni des extraits substantiels de celle-ci ne doivent être imprimés ou autrement reproduits sans son autorisation.

---

In compliance with the Canadian Privacy Act some supporting forms may have been removed from this thesis.

While these forms may be included in the document page count, their removal does not represent any loss of content from the thesis.

Conformément à la loi canadienne sur la protection de la vie privée, quelques formulaires secondaires ont été enlevés de cette thèse.

Bien que ces formulaires aient inclus dans la pagination, il n'y aura aucun contenu manquant.

■ ■ ■  
**Canada**

## **Abstract**

### **Investigation on moisture buffering of hygroscopic materials by full-scale experiments and HAM simulations**

Xiangjin Yang, Ph. D.  
Concordia University, 2010

The moisture buffering effect of interior hygroscopic materials can reduce the variation of indoor RH, thus to achieve a desired indoor environment and to obtain a better building envelope performance while saving energy consumed in operating HVAC equipment. Even though a large number of studies have been conducted to investigate the moisture buffering effect, additional studies are still required for several major questions including: 1) How to evaluate the impact of different parameters on moisture buffering potential under different conditions? 2) Is the local moisture buffering of surface materials influenced by non-uniform indoor conditions? 3) Can hygroscopic materials be categorized and ranked in order to achieve a better moisture buffering application?

Aiming to answer these questions, this research is developed and carried out to define an index to quantitatively evaluate the impact of different parameters on moisture buffering potential of interior surface materials and furniture, to investigate moisture buffering of surface materials under non-uniform indoor conditions and to classify hygroscopic materials.

These objectives are achieved through both experiments and simulations including 1) analysis of the moisture balance established in a full-scale experimental testing (28 cases) and whole building Heat, Air and Moisture (HAM) simulations (54 cases BSim simulations); 2) investigation of local moisture buffering of interior surface

materials through both measurements obtained in the experiment and HAM simulations (WUFI) applied on test walls; and 3) analyses of moisture buffering capacity at material level using WUFI simulations.

A new index, maximum accumulated moisture buffering value (MAMBV), is developed to quantify the impact of different parameters on the moisture buffering effect. The great advantage of this index is that it can provide a direct comparison of moisture buffering potential in different test scenarios. The parameters investigated include daily moisture load rate and schemes, ventilation rates, supply air conditions, volume rates, and different interior surface materials and furniture. The distribution of local moisture buffering of surface materials are analyzed for the first time and the locations where surface materials provide higher moisture buffering is identified. The moisture response, including moisture buffering capacity, moisture history effect, and time factor involved are fully investigated. Based on these analyses, hygroscopic materials are categorized into three groups, which are determined by materials' moisture capacity and vapor transfer resistance factor.

This thesis presents a comprehensive evaluation of the impact of different parameters on the moisture buffering effect under realistic indoor conditions, advances the current understanding of moisture buffering capacity of materials, and brings forward a new contribution toward moisture buffering design and application.

## Acknowledgements

I would like to acknowledge firstly the support of my thesis supervisors, Drs. Paul Fazio and Hua Ge for their guidance and supervision. Not only did they provide financial support and academic advice for me, but also helped me to build my own motivation, enthusiasm, creativity, and patience.

I would like to express my sincere gratitude to Dr. Jiwu Rao, who helped me to build test facility and set up instruments and equipments, and more importantly to give me a lot of advices on data analyses.

I would like to thank Mr. Luc Demers who provided great help on experimental facility and techniques for instruments and measurements. Many thanks are also due to our department staffs, Jacques Payer, Joe Hrib, Olga Soares for their unfailing services.

I would like also to express my gratitude to many students, who have assisted me on the hard experimental work. They are Jianfeng (Jeff) Qin, Wenzheng (Cary) Zhu, Junxiang (Kevin) Guan, Nazmi Boran, Saba Owji, Liebin Chen, Zhichao Zhang, Bruno Lee, Jiejun Zhao, and a visiting student from France, Amandine Piot.

I would like to give my thanks to my friends, Qian Mao, Caroline Hachem, Ying (Wendy) Ye, Qinru Li, Yang Wu, Xiangyang Tan, and Yang Li for their support. Many thanks are due to Sergio Vera. We built and shared the same test facility delivering different research focuses.

Finally, and most importantly, I wish to express my warmest appreciation and love for my family. Without their support and encouragement, nothing would come up today. I would like to dedicate my thesis to my father (Wuchang Yang), my mother (Fengying Hao), my sister (Xiangzhu Yang), my brother in law (Fengfei Huang) and their little boy (Boyang Huang). Thank you all for your care, love, understanding, trust and belief, which make me who I am.

# Table of Content

<i>List of Figures</i> .....	<i>xi</i>
<i>List of Tables</i> .....	<i>xvii</i>
<i>Abbreviations</i> .....	<i>xviii</i>
<i>Nomenclature</i> .....	<i>xx</i>
<b>Chapter 1 Introduction</b> .....	<b>1</b>
1.1 Background.....	1
1.2 Introduction of moisture buffering effect.....	3
1.3 Objectives and approaches.....	5
1.4 Thesis outline.....	8
<b>Chapter 2 Literature review</b> .....	<b>9</b>
2.1 Moisture balance and its components.....	9
2.1.1 Moisture production in indoor environment.....	10
2.1.2 Ventilation, air tightness and air infiltration.....	12
2.2 Material level and small-scale experiment study.....	13
2.2.1 Experiment setup and parameters studied.....	14
2.2.2 Moisture buffering value (MBV).....	17
2.3 Large -scale experimental study.....	21
2.3.1 Ventilation rate.....	22
2.3.2 Moisture generation protocols.....	24
2.3.3 Indoor environment.....	24
2.3.4 Performance of building envelope and interior surface materials.....	25
2.3.5 Evaluation of moisture buffering effect... ..	25
2.3.6 Other factors and sensitive analyses.....	26
2.4 Fundamental theory on moisture transfer .....	27
2.4.1 Moisture in materials.....	27
2.4.2 Moisture transfer in materials.....	28
2.4.3 Moisture transfer to and from surface.....	31
2.4.4 Balance of moisture buffering and storage.....	31
2.5 Latest HAM models with consideration of moisture buffering effect.....	31
2.5.1 Analytical solution.....	32
2.5.2 Simplified models.....	32
2.5.3 Commercial and research models.....	35
2.6 Material properties and terms related to moisture buffering effect.....	38

2.6.1	<i>Material properties or parameters</i> .....	38
2.6.2	<i>Terms evaluating moisture buffering capacity</i> .....	41
2.7	<i>Limitation in previous researches</i> .....	43
	<b>Chapter 3 Experiment setup and test procedure</b> .....	<b>45</b>
3.1	<i>Test hut and environmental chamber</i> .....	45
3.2	<i>Test cases</i> .....	48
3.3	<i>Test conditions</i> .....	50
3.3.1	<i>Outdoor conditions</i> .....	50
3.3.2	<i>Indoor conditions and its initial conditions</i> .....	51
3.3.3	<i>Ventilation rate and conditions of supply air</i> .....	52
3.4	<i>Equipments</i> .....	54
3.4.1	<i>Moisture generation equipments</i> .....	54
3.4.2	<i>Ventilation system</i> .....	56
3.4.3	<i>AHU (Air Handling Unit)</i> .....	59
3.5	<i>Monitoring and measurements</i> .....	61
3.5.1	<i>Outdoor environmental conditions</i> .....	64
3.5.2	<i>Indoor conditions</i> .....	64
3.5.3	<i>Hygrothermal conditions of building envelopes, including surface materials</i> .....	64
3.5.4	<i>Monitoring and control of the AHU and ventilation system</i> .....	68
3.5.5	<i>Monitoring of moisture generation rate</i> .....	68
3.5.6	<i>Air leakage measurement</i> .....	68
3.6	<i>Furniture and its location in test rooms</i> .....	69
	<b>Chapter 4 Moisture balance analyses</b> .....	<b>72</b>
4.1	<i>Moisture balance and its components in experimental study</i> .....	72
4.1.1	<i>Moisture balance</i> .....	72
4.1.2	<i>Moisture removed by ventilation and air leakage</i> .....	73
4.1.3	<i>Correction: baseline correction</i> .....	76
4.1.4	<i>Maximum amount of moisture buffered by surface materials</i> .....	77
4.2	<i>Observation and data analyses of the full-scale experiment</i> .....	77
4.2.1	<i>RH method vs. condensed water method</i> .....	77
4.2.2	<i>Impact of ventilation rates</i> .....	80
4.2.3	<i>Impact of moisture generation protocol</i> .....	82
4.2.4	<i>Wood paneling vs. uncoated gypsum board</i> .....	86
4.2.5	<i>Impact of furniture</i> .....	88
4.3	<i>Whole building simulation (BSim)</i> .....	90



4.3.1	<i>Introduction of BSim and assumptions of model</i>	90
4.3.2	<i>Simulation setup, validation and case studied</i>	91
4.3.3	<i>Moisture balance in BSim simulations and MAMBV</i>	94
4.4	<i>Impacts of various parameters on moisture buffering effect</i>	96
4.4.1	<i>Impact of ventilation rates</i>	96
4.4.2	<i>Impact of supply air humidity</i>	98
4.4.3	<i>Impact of outdoor conditions</i>	100
4.4.4	<i>Impact of material properties</i>	101
4.4.5	<i>Impact of volume rates</i>	103
4.5	<i>Summary</i>	105
<b>Chapter 5 Moisture response of materials and application of MBV at room level</b>		<b>108</b>
5.1	<i>Material properties</i>	108
5.2	<i>Moisture response of hygroscopic materials</i>	110
5.2.1	<i>Introduction of WUFI pro 4</i>	110
5.2.2	<i>Cases studied</i>	111
5.3	<i>Results and discussion</i>	114
5.3.1	<i>Comparison between uncoated gypsum board vs. wood paneling</i>	114
5.3.2	<i>Other materials</i>	121
5.3.3	<i>Summary</i>	131
5.4	<i>Using effective capacitance method (EC) to predict indoor RH and MAMBV</i>	135
5.4.1	<i>Methodology of effective capacitance (EC) model</i>	135
5.4.2	<i>Application in cases studied in this thesis research</i>	138
5.4.3	<i>Calculations and discussion</i>	141
<b>Chapter 6 Local moisture buffering of interior surface materials</b>		<b>149</b>
6.1	<i>Local moisture content of surface materials measured from experiment</i>	149
6.1.1	<i>Temperature and RH along test walls</i>	149
6.1.2	<i>Moisture content and temperature distribution of surface materials</i>	152
6.2	<i>Local moisture buffering of surface materials and impact of ventilation rates</i>	160
6.2.1	<i>WUFI simulation set up and case scenarios</i>	160
6.2.2	<i>WUFI simulation validation</i>	165
6.2.3	<i>Simulation results analyses and discussion</i>	171
6.3	<i>Impact of furniture blocking on local moisture buffering of surface materials</i>	176
<b>Chapter 7 Conclusions and contributions</b>		<b>179</b>
7.1	<i>Summary of findings</i>	179
7.2	<i>Contributions</i>	185
7.3	<i>Recommendations for future research</i>	186

*7.4 Related publications*.....188  
***Reference***.....190  
***Appendix***.....199  
*Appendix A: Material properties of materials used in experiment and simulation.*  
*Appendix B: Moisture content sensor calibration.*  
*Appendix C: Non-uniform indoor environment.*  
*Appendix D: Building envelope performance in moisture buffering experimental investigation.*

## List of Figures

<i>Figure 2.1. Moisture balance in building</i> .....	10
<i>Figure 2.2. Schedule of the moisture generation for living room and main bedroom (from Satio, 2005 b)</i> .....	12
<i>Figure 2.3. Material level experiment carried in a small chamber (from Roels, 2008)</i> .....	14
<i>Figure 2.4. Material level experiment carried out in TMT (from Osanyintola, 2005)</i> .....	15
<i>Figure 2.5. Moisture taken in a small scale experiment (from Rode et al, 2005)</i> .....	17
<i>Figure 2.6. Moisture Buffering Value (from Wu, 2007)</i> .....	18
<i>Figure 2.7. Moisture Buffering Value depending on RH load (from Osanyintola, 2005)</i> .....	19
<i>Figure 2.8. MBC depending on Reynolds number (from Osanyintola and Simonson 2005)</i> .....	21
<i>Figure 2.9. Indoor RH comparison between cases using aluminum sheet or plaster painted as surface materials (from Kunzel et al., 2004)</i> .....	26
<i>Figure 2.10. Moisture storage regions (from Hagentoft, 2001)</i> .....	27
<i>Figure 2.11. Hypothetical total isothermal moisture transport function (Adapted from Straube and Burnett, 2005)</i> .....	29
<i>Figure 2.12. Moisture transport mechanisms (Ojanen, 1989)</i> .....	29
<i>Figure 2.13. Representation of the humidity buffering layer</i> .....	34
<i>Figure 2.14. Sorption curve for different building materials. (from Rode and Grau, 2008)</i> .....	38
<i>Figure 3.1. Test room inside of environmental chamber</i> .....	46
<i>Figure 3.2. Configuration of test hut</i> .....	47
<i>Figure 3.3. Repeatability of results after the second cycle (case 1)</i> .....	50
<i>Figure 3.4. Conditions of chamber (outdoor) environment, indoor, and AHU</i> .....	51
<i>Figure 3.5. Example of ventilation air conditions (RH, T, and ACH), in case 1</i> .....	53
<i>Figure 3.6. Photo of moisture generation components</i> .....	55
<i>Figure 3.7. Moisture loading in two successive days (measured by load cell)</i> .....	56
<i>Figure 3.8. Pressure distribution diagram of the ventilation system</i> .....	57

<i>Figure 3.9. Location and dimensions of inlet and outlets</i> .....	58
<i>Figure. 3.10. Components of AHU (Air Handling Unit)</i> .....	60
<i>Figure 3.11. Photo of RH sensor installation and sensor location diagram</i> .....	65
<i>Figure 3.12. Location of anemometers on pole and plan view(dimensions are in meter)</i> .....	66
<i>Figure 3.13. Three types of moisture content installation</i> .....	66
<i>Figure 3.14. Locations of sensors through building envelope</i> .....	67
<i>Figure 3.15 Location of furniture for fully furnished room</i> .....	70
<i>Figure 4.1. Air mass balance and moisture involved in ventilation and air leakage</i> .....	74
<i>Figure 4.2. Water collector and condensed water method</i> .....	76
<i>Figure 4.3 Indoor HR in case 1 and case 2</i> .....	79
<i>Figure 4.4. Calculation of <math>M_v + M_l + M_d</math> and moisture generated in case 1</i> .....	79
<i>Figure 4.5 MAMBV and <math>M_b^*</math>(accumulated moisture buffering value) in case 1</i> .....	80
<i>Figure 4.6. Indoor HR at different ventilation rates for cases using uncoated gypsum board</i> .....	81
<i>Figure 4.7. <math>M_b^*</math> at different ventilation rates for cases using uncoated gypsum board</i> ...	81
<i>Figure 4.8 Example of maximum moisture content measured on uncoated gypsum board at different ventilation rates</i> .....	82
<i>Figure 4.9. Indoor HR under two moisture generation rates (case 1 and 9 are hygroscopic cases, case 2 and case 10 are non-hygroscopic cases) in cases using uncoated gypsum board</i> .....	83
<i>Figure 4.10 Example of maximum moisture content measured on uncoated gypsum board, at two different moisture generation rates</i> .....	84
<i>Figure 4.11 Indoor RH comparison between case 1, 11 and case 2, 12</i> .....	85
<i>Figure 4.12 MAMBV under different moisture load schemes</i> .....	86
<i>Figure 4.13 Accumulated moisture buffering value in cases using wood paneling vs. uncoated gypsum board</i> .....	87
<i>Figure 4.14 Humidity ratio of test room in case 13 (without furniture), case 23 (added books and bookshelf), case 25 (added curtains, desk and chair), and case 27 (fully furnished)</i> .....	89

Figure 4.15. Interface and room model in BSim simulation.....	92
Figure 4.16. Indoor humidity ratio comparison between simulation results and experimental data.....	93
Figure 4.17. Accumulated moisture buffering value ( $M_b^*$ ) profile in a daily moisture generation cycle at different ventilation rate, gypsum board. (ventilation air humidity is 4.7g/kg HR).....	97
Figure 4.18. Maximum accumulated moisture value at different ventilation rates, gypsum board and wood paneling, (supply air humidity is 4.7g/kg HR).....	97
Figure 4.19. MAMBV under different ventilation air humidity.....	99
Figure 4.20. Maximum accumulated moisture value of cases using OSB, ACC and TBP as interior surface materials, under two different moisture generation protocols.....	102
Figure 4.21. (a)Maximum accumulated moisture value vs. the volume rate, (b) Optimum volume rate.....	104
Figure 5.1. Classification of hygroscopic materials based on their moisture capacity and vapor transfer resistance factor.....	110
Figure 5.2. Equilibrium point for wood paneling and gypsum board.....	115
Figure 5.3. Moisture buffering of gypsum board over a 10/14 moisture load cycles....	116
Figure 5.4. Moisture content of wood paneling in the first 40 cycles under a 10/14 moisture load cycles.....	116
Figure 5.5. Moisture residual for the cases using wood paneling, in the second stage WUFI simulations.....	118
Figure 5.6. Total amount of moisture absorbed (40th cycle): (a) wood paneling, and (b) gypsum board, under 2 hours and 10 hours moisture load schemes.....	119
Figure 5.7. Moisture residual under two different moisture initial conditions.....	120
Figure 5.8. Moisture content of wood paneling under two different moisture initial conditions.....	125
Figure 5.9. Relationship between the time required to reach new equilibrium condition vs. vapor resistance factor and moisture capacity.....	127
Figure 5.10. Correlation between penetration depth and the time required to reach new equilibrium state.....	127
Figure 5.11. Penetration depths of the ten hygroscopic materials under daily moisture	

<i>cycles</i> .....	125
<i>Figure 5.12. Moisture absorption under 10/14 hours and 2/12 hours moisture load schemes (obtained from the 40th moisture load cycle)</i> .....	126
<i>Figure 5.13. Stable moisture buffering profile of different materials in the first 10 hours of daily moisture load</i> .....	128
<i>Figure 5.14. Moisture residual in the first moisture load cycle, under three different moisture load schemes</i> .....	129
<i>Figure 5.15. Non-linear factor introduced into the effective capacitance calculation</i> ..	140
<i>Figure 5.16. Predicted accumulated moisture buffering value using effective capacitance (EC) method, compared to those calculated from experimental investigation (uncoated gypsum board and wood paneling)</i> .....	143
<i>Figure 5.17. Predicted accumulated moisture buffering value using effective capacitance (EC) method, compared to those calculated from BSim simulations (wood fiberboard)</i> .....	144
<i>Figure 5.18. Predicted indoor HR using effective capacitance (EC) method, compared to the average indoor HR measured in experiment (wood paneling and uncoated gypsum board)</i> .....	145
<i>Figure 5.19. Predicted indoor HR using effective capacitance (EC) method vs. BSim simulations (wood fiberboard)</i> .....	146
<i>Figure 5.20. Range of indoor HR, using effective capacitance (EC) method and BSim simulation, under 10 hours moisture generation regime</i> .....	148
<i>Figure 5.21. Range of indoor HR, using effective capacitance (EC) method and BSim simulation, under 2 hours moisture generation regime</i> .....	148
<i>Figure 6.1. Temperatures measured by RH&amp;T sensors close to the test wall in case 1</i> .....	150
<i>Figure 6.2. Humidity ratio close to the test wall measured in case 1</i> .....	151
<i>Figure 6.3. Location of moisture content sensors on interior surface materials, (a) uncoated gypsum board, (b) wood paneling (dimensions are in meter)</i> .....	153
<i>Figure 6.4. Example of interior surface temperature vs. local indoor air temperature</i> .....	155

Figure 6.5. Interior surface temperature distribution on gypsum board in case 1, (a) moisture generation period, (b) no-moisture generation period.....	155
Figure 6.6. The moisture content (%) distribution on gypsum board in case 1: (a) at the end of the moisture generation period, (b) at the end of no moisture generation period, (c) maximum moisture variation in one daily moisture cycle.....	156
Figure 6.7. Temperature distribution on wood paneling in case 13: (a) moisture generation period, (b) no moisture generation period.....	158
Figure 6.8. Moisture content distribution on wood paneling in case 13: (a) at the end of moisture generation period, (b) at the end of no-moisture generation period, (c) maximum moisture content variation in one daily moisture cycle.....	159
Figure 6.9. The locations of the areas analyzed in WUFI simulations.....	160
Figure 6.10. The model of WUFI simulations on local area of interior surface materials.....	161
Figure 6.11. Air velocity profile close to test walls, at different planes (east and west).....	164
Figure 6.12. Moisture content comparison between WUFI simulations and experimental measurements: (a) uncoated gypsum board, (b) wood paneling.....	167
Figure 6.13. Moisture content distribution in case 1(10/14 hours load) at different times in one day period.....	168
Figure 6.14. Average moisture content in gypsum board in area a, b, c at 0.5 ACH....	169
Figure 6.15. Surface moisture content (at 0.5 mm) on gypsum board simulated (WUFI simulation) vs. moisture content measured, at 0.5 ACH. (locations of sensors and the corresponding area are shown in Figure 6.2).....	169
Figure 6.16. Average moisture content in wood paneling in areas a, b, c at 0.5 ACH.....	170
Figure 6.17. Surface moisture content on wood paneling measured and simulated (WUFI simulation) at area a, b, c at 0.5 ACH.....	170
Figure 6.18. Moisture content in gypsum board at area c at different ventilation rates, 0.5, 0.75 and 1 ACH: (a) average vs. surface moisture content, (b) simulation results vs. measurement data.....	173

*Figure 6.19. Moisture content in wood paneling at area c at different ventilation rates, 0.5 and 0.75 ACH: (a) average vs. surface moisture content, (b) simulation results vs. measurement data.....174*

*Figure 6.20. Examples of moisture content behind the curtains in case 25 vs. those in case 23.....177*

*Figure 6.21. Examples of other moisture content measured in case 23 and case 25.....177*

*Figure 6.22. Examples of temperate on the surface blocked by curtain in case 25 compared to those in case 23.....178*



## List of Tables

<i>Table 2.1. Literature on moisture production in residential houses</i> .....	11
<i>Table 2.2 Parameters studied in the material-level experiments</i> .....	17
<i>Table 2.3. MBV standard test (adapted from Roels, 2008)</i> .....	19
<i>Table 2.4. MBV corresponding to different surface mass transfer coefficient</i> .....	20
<i>Table 2.5. Summary of large-scale experiments</i> .....	23
<i>Table 3.1. Components of wall assembly</i> .....	46
<i>Table 3.2. Test cases (Part I)</i> .....	48
<i>Table 3.3. Test cases (Part II)</i> .....	49
<i>Table 3.4. Test conditions</i> .....	50
<i>Table 3.5. The variation of supply air conditions</i> .....	53
<i>Table 3.6. The comparison of the moisture generation rates measured by load cell and manually</i> .....	55
<i>Table 3.7. Operation pressure of AHU at different ventilation rates</i> .....	57
<i>Table 3.8. Equipments and instruments used in AHU system</i> .....	60
<i>Table 3.9. Sensors or instruments used in measurements</i> .....	61
<i>Table 3.10. The air leakage rates under different ventilation rates</i> .....	68
<i>Table 3.11. Description of furniture, added in three steps</i> .....	70
<i>Table 4.1. Maximum accumulated moisture value under different moisture generation rates</i> .....	83
<i>Table 4.2. MAMBV in cases with furniture added</i> .....	88
<i>Table 4.3. Comparison of MAMBV obtained from simulation results and experimental data</i> .....	93
<i>Table 4.4. Case scenarios studied in BSim simulations</i> .....	95
<i>Table 4.5. Maximum accumulated moisture buffering value under different outdoor conditions</i> .....	100
<i>Table 5.1. Moisture capacity and vapor resistance factor between 33% and 75% RH</i> .....	109
<i>Table 5.2. Cases studied in WUFI simulations</i> .....	113
<i>Table 5.3. Comparison of three groups' materials under first stage WUFI</i>	

<i>simulations</i> .....	122
<i>Table 5.4. Moisture absorption and moisture under three different moisture load regime</i> .....	126
<i>Table 5.5. Days to reach quasi-steady moisture response under three different moisture load schemes</i> .....	129
<i>Table 5.6. Moisture residual and days to reach stable moisture buffering cycle under two different initial conditions</i> .....	131
<i>Table 5.7. MBV1h and MBV8h of materials used in effective capacitance method</i> .....	139
<i>Table 5.8. MBV1h and MBV8h of materials used in effective capacitance method</i> .....	139
<i>Table 5.9. MAMAV obtained from effective capacitance model vs. MAMAV calculated based on experiments and BSim simulations</i> .....	144
<i>Table 6.1 Mass transfer coefficient and air velocity at different locations, at different ventilation rates (gypsum board)</i> .....	164

## Abbreviations

<b>ACH</b>	<i>Air Change Rate</i>	<b>JIS</b>	<i>Japanese Industry Standard</i>
<b>AHU</b>	<i>Air Handling Unit</i>	<b>MAMBV</b>	<i>Maximum Accumulated Moisture Buffering Value</i>
<b>ASHARE</b>	<i>The American Society of Heating, Refrigerating and Air-Conditioning Engineers</i>	<b>MC</b>	<i>Moisture Content</i>
<b>BESTEST</b>	<i>Building Energy Simulation Test</i>	<b>MBV</b>	<i>Moisture Buffering Value</i>
<b>CFD</b>	<i>Computational Fluid Dynamics</i>	<b>MBC</b>	<i>Moisture Buffering Capacity</i>
<b>DAS</b>	<i>Data Acquisition System</i>	<b>NORDTEST</b>	<i>Nordic Country Test</i>
<b>DTU</b>	<i>Technical University of Denmark</i>	<b>NRCC</b>	<i>National Research Council Canada</i>
<b>EMPD</b>	<i>Effective Moisture Penetration Depth</i>	<b>ORNL</b>	<i>Oak Ridge National Laboratory</i>
<b>ECBCS</b>	<i>Energy Conservation in Buildings and Community Systems</i>	<b>PAQ</b>	<i>Perceived Air Quality</i>
<b>HAM</b>	<i>Heat, Air and Moisture</i>	<b>PID</b>	<i>Proportional, Integral, and Differential</i>
<b>HVAC</b>	<i>Heating, Ventilation and Air Conditioning</i>	<b>PMV</b>	<i>Predicted Mean Vote</i>
<b>HIR</b>	<i>Hygric Inertia per cubic meter of Room</i>	<b>RH</b>	<i>Relative Humidity</i>
<b>HR</b>	<i>Humidity Ratio</i>	<b>TMT</b>	<i>Transient Moisture and Temperature Facility</i>
<b>IAQ</b>	<i>Indoor Air Quality</i>	<b>U of S</b>	<i>University of Saskatchewan</i>
<b>IDIS</b>	<i>International Standard Organization /Draft International Standard</i>	<b>VTT</b>	<i>Technical Research Centre of Finland</i>
<b>IEA</b>	<i>International Energy Agency</i>	<b>WBHAM</b>	<i>Whole Building Heat, Air and Moisture</i>
<b>ISO</b>	<i>International Standard Organization</i>	<b>LBNL</b>	<i>Lawrence Berkley National Lab</i>

## Nomenclature

$\beta$	Surface coefficient of water vapor transfer, $m/s$
$\delta$	Vapor permeability, $kg/Pa \cdot m \cdot s$
$\xi$	Moisture capacity, $kg/m^3$ per %RH, or $kg/kg$
$\theta_b$	Temperature of buffering layer, $^{\circ}C$
$\mu$	Vapor transfer resistance factor
$\mu_o$	Viscosity of dry air at $T_o$ , $1.71E-5$ $kg/m \cdot s$
$\phi$	Relative humidity
$A$	Area, $m^2$
$b$	Effusivity, $kg/m^2 \cdot Pa \cdot s^{0.5}$
$c_a$	Heat capacity of air, $J/m^3 K$
$c_p$	Effective specific heat capacity, $J/kg \cdot K$
$C(t)$	Condensed water over time, $g$
$D_w$	Diffusivity, $m^2/s$
$D_\phi$	Liquid diffusivity, $m^2/s$
$d_p$	Penetration depth, $m$
$e$	Moisture correction term, $g$
$G$	Moisture generation, $g$
$h_c$	Heat transfer coefficient, $W/m^2 K$
$h_m$	Mass transfer coefficient, (humidity ratio based), $kg/m^2 Pa \cdot s$
$H$	Enthalpy of humid air, $J/m^3$
$h_v$	Latent heat of phase change, $J/kg$
$l$	Length of flow path, $m$

$M_a$	Accumulated change of the water vapor mass in the room air, $g$
$M_b^*$	Accumulated moisture buffering value, $g$
$M_{vl}$	Total water mass removed from the test room by ventilation and air leakage, $g$
$M_d$	Moisture loss due to vapor diffusion, $g$
$m$	Weight of material samples, $g$
$n$	Ventilation rate, $l/hr$
$N_{br}$	The number of bedrooms
$P_v$	Vapor pressures, $Pa$
$P_{vi}$	Vapor pressures of indoor, $Pa$
$P_{vo}$	Vapor pressure of outdoor (environmental chamber) air, $Pa$
$P_{suc}$	Suction pressure, $Pa$
$p_b$	Vapor pressure in the buffering layer, $Pa$
$p_{sat}$	Saturation vapor pressure, $Pa$
$q_v$	Vapor diffusion flux, $kg/m^2$
$q_w$	Liquid flow, $kg/m^2$
$Q_v$	Mass air flow rate at the outlet, $kg/hr$
$Q_l$	Infiltrating air leakage rate, $kg/hr$
$Q_v$	Air flow rate through the outlet, $kg/hr$
$Q_l$	Air flow of air leakage, $kg/hr$
$R_{vi}$	The total vapor resistance of the wall components, $Pa\ m^2/g$
$R_i$	The interior surface heat resistance, $m^2K/W$
$R_v$	The gas constant of water vapour, $462\ J/kg\cdot K$
$t_p$	load cycle period, $s$
$t_{rev}$	The time point at which the most recent moisture generation starts, $s$
$\Delta t_m$	The time period for the current (at time $t$ ) moisture load, $s$

$S$	Constant temperature, $110.4\text{ K}$
$T_o$	Constant temperature, $273\text{ K}$
$T_f$	Film temperature, $K$
$T_s$	The average temperature on the surface of gypsum board or wood paneling, $^{\circ}\text{C}$
$T_{in}$	The indoor air temperature close to the test walls, $^{\circ}\text{C}$
$v_a$	Vapor content of air, $\text{kg}/\text{m}^3$
$v_{suf}$	Vapor content of the surface material, $\text{kg}/\text{m}^3$
$V$	Volume of the room, $\text{m}^3$
$V_m$	Volume of materials, $\text{m}^3$
$V_{\infty}$	External air velocity out of the boundary layer, $\text{m}/\text{s}$
$w$	Humidity ratio, $\text{g}/\text{kg}$
$w_o$	Humidity ratios of outlet air, $\text{g}/\text{kg}$
$w_i$	Humidity ratios of inlet air, $\text{g}/\text{kg}$
$w_l$	Humidity ratios of outdoor (environmental chamber) air, $\text{g}/\text{kg}$
$w_a$	Average humidity ratio of room air, $\text{g}/\text{kg}$
$w_h$	Humidity ratio of the air exiting the AHU system, $\text{g}/\text{kg}$
$w_{cap}$	Capillary saturation moisture content, $\text{kg}/\text{kg}$
$w_{sat}$	The maximum saturation water content, $\text{kg}/\text{kg}$
$Z_b$	Diffusion resistance between surface and center of moisture buffering layer, $\text{s}/\text{m}$

# CHAPTER 1

## INTRODUCTION

### 1.1 Background

Building envelopes are designed to create an indoor environment that is expected to provide both healthy and comfortable living place for human beings.

Typically, people spend about 90% of their time indoor. Therefore maintaining desired indoor environment is important for human health and productivity (Bornehag, et al., 2001). Research on the indoor environment focuses on thermal comfort, indoor air quality (IAQ), and its effect on human health. Indoor temperature, indoor humidity, surface temperature, air velocity, and concentration of contaminants are recognized as basic indoor environmental parameters.

Building envelopes are exposed to heat, air, and moisture (HAM) loads from both indoor and outdoor environments. The performance of building envelopes under the HAM loads influences the service life of building and the health of occupants. Building failures due to moisture problems are frequently observed. For example, rain penetration and poor moisture management were the major causes for the systematic building envelope failures which occurred in the lower mainland of British Columbia. The repair cost was estimated over one billion dollars (Barrett, 1998). Based on a survey conducted by the

Seattle Department of Design, Construction and Land Use, Karagiozis (2004) indicated that moisture damages affected approximately 20% of the multifamily structures built in the Seattle area over the past 15 years. Research on building envelope performance has been focused on the HAM response of building envelopes to the loads from outdoor environment such as solar radiation, wind driven rain, and temperature variations.

Indoor environment and building envelope performance are interrelated. Past studies tend to partly ignore this interaction by focusing on one aspect at one time only in order to simplify the modeling of complex physical phenomena. For instance, when CFD (Computational Fluid Dynamics) is used to study the indoor flow pattern and the distribution of indoor conditions, a fixed boundary condition (e.g. interior surface temperature and humidity) is normally assumed. While in the HAM response study of building envelopes, a constant indoor condition is typically assumed. However, in reality, both indoor conditions and hygrothermal characteristics of interior surface are variable and interrelated.

Integrating both indoor environment and building envelope performance research into a whole building hygrothermal performance study has become a new trend recently. An international collaboration project, Annex 41, organized by the International Energy Agency (IEA) was carried out during 2004 to 2008. This project studied the heat, air and moisture response of whole building (WBHAM), including indoor environment, building envelope and outdoor environment.

Moisture buffering effect is one of the research topics that focus on the interaction between indoor environment and the building envelope.



## **1.2 Introduction of moisture buffering effect**

Moisture buffering effect is defined as the ability of hygroscopic materials to reduce the amplitude of indoor relative humidity variations when they are applied in indoor environment (Padfield, 1998, Rode et al., 2004, and Mitamura et al., 2004).

Implementation of moisture buffering in buildings may lead to significant improvements of the indoor environment in term of thermal comfort, indoor air quality (IAQ), and human health. It may improve the hygrothermal performance of building envelope and prolongs its durability. More important, the application of moisture buffering in indoor environment can help to achieve the desired indoor humidity through passive energy means.

Thermal comfort is defined as “condition of mind that expresses satisfaction with the thermal environment” (ASHRAE Standard 55). The application of hygroscopic materials shows a significant improvement of the thermal comfort. Simonson et al.’s studies (2002, and 2004) indicated that there is a 10% drop in the number of people, who are dissatisfied with the inadequate respiratory cooling due to high indoor RH in bedrooms in field tests at the end of the occupancy (7am), when hygroscopic materials are used in Belgium climate.

Moderation effect from moisture buffering materials can significantly reduce the extreme variation of indoor humidity, and consequently has a great potential to improve the air quality (Kurnitski et al., 2007). Numerical study from Simonson et al. (2002, and 2004) noted that there is a 25% drop in dissatisfaction PAQ (perceived air quality) during the morning peak RH hours when hygroscopic materials are applied.

In addition, moisture buffering effect can reduce health risks, such as asthma, allergic symptoms, and airway infections caused mainly by mold growth, by preventing extreme indoor RH (Bornehag et al., 2001, 2004, 2005).

Moisture problems of building envelope are due to high moisture accumulation in building envelope components. Condensation on cold interior surfaces and interstitial condensation within building envelope may lead to deterioration of finishing materials and serious damage of structure. The moisture accumulation within the building envelope is caused not only by outdoor environment sources (i.e. rain, snow, water from underground), but also affected by indoor environment conditions. The main solution of moisture problems in the building envelope is to control moisture loads from both outdoor and indoor environments. Numerous studies have indicated that the reduction of high indoor humidity due to moisture buffering can decrease the risk of condensation on interior surfaces and in building structures (Downing and Bayer, 1993, Toftum and Fanger, 1999, Toftum et al., 1998a, 1998b, Berglund, 1998, Ojanen and Kumaran, 1996, Lucus et al., 2002).

The desired indoor environment can be achieved by HVAC (Heating, Ventilation, and Air conditioning) systems. However, HVAC systems use up to 50% of the total energy consumed for buildings (Sherman and Matson 1997). Moisture buffering due to the use of hygroscopic materials can help maintaining the desired indoor humidity with reduced ventilation rate and operation hours of dehumidification, thus, achieving a significant energy saving. Osanyintola and Simonson (2006) estimated that up to 5% heating load and 30% cooling load may be reduced when moisture buffering effect is taken into account, in the condition that the ventilation system is well controlled.

### **1.3 Objectives and approaches**

A large number of studies have been conducted to investigate the moisture buffering effect using both experimental and modelling techniques (reviewed in chapter 2). Additional studies are still required, however, to resolve issues related to various aspects of moisture buffering effect. For instance, methods to evaluate moisture buffering potential are not consistent in large-scale laboratory experiments or field tests. The different moisture responses of materials under different moisture load are noticed, but no thorough investigations have been carried out. The local variation of moisture buffering of interior surface materials, caused by the non-uniform distribution of indoor conditions, is a dominant phenomenon in reality, but very few studies especially experimental measurements have been performed to study the local effect. There is no classification of hygroscopic materials for their practical application. More important, no guidelines exist on how to choose hygroscopic materials for taking advantage of the moisture buffering effect under different realistic moisture loads for different usage of the building or room. There is also the lack of specific guidelines on conducting large-scale experiments or field tests on moisture buffering potential.

This research aims to bridge the knowledge gaps identified above and extend the knowledge base in understanding the impacts of different parameters on moisture buffering potential and moisture buffering behaviour of surface hygroscopic materials.

The specific objectives of this research include:

1. to quantitatively evaluate the impact of different parameters on moisture buffering potential of interior surface materials and furniture under realistic room conditions.
2. to analyze the influence of material properties on the moisture buffering capacity under different moisture load schemes and to classify materials based on their responses to moisture load.
3. to investigate the influence of non-uniform indoor environment on the local moisture buffering of surface materials.
4. to make recommendations for practical application of materials used for moisture buffering effect, and recommendations for large-scale experimental investigation on moisture buffering effect.

These objectives are achieved through a full-scale experimental study and simulations.

The methodology used in this study is summarized as follows:

- Moisture balance and moisture buffering potential at room level

Moisture balance calculation is established in both a full-scale single room experimental testing and a WBHAM (whole building heat, air, and moisture) simulation using BSim. There are totally 28 cases carried out in the experimental study and 54 cases conducted in BSim simulation. A new index, maximum accumulated moisture buffering value (MAMBV), is developed to evaluate the impact of parameters on moisture buffering potential of surface materials and furniture. The parameters include ventilation rate, supply air conditions, moisture generation rate and regime, outdoor conditions, volume rate, material properties

(moisture capacity and vapor permeability). In this approach, the test room is considered as a single zone with uniform conditions.

- Moisture response of materials studied at material level

Moisture response of materials under different moisture load schemes is analyzed using WUFI simulation. The moisture responses include the time required to reach new equilibrium conditions under one step moisture load (materials were exposed to a higher level of ambient RH for a long period), the time period required to reach a stable moisture buffering cycle, and moisture residuals in each load cycle under daily moisture loads. Materials are categorized into three groups based on their different moisture response patterns. This moisture response study provides insights for explaining the impact of different parameters observed from large-scale experimental and simulation study.

A simplified analytical method, the effective capacitance method, is used to predict indoor humidity and MAMBV.

- Impact of non-uniform indoor environment on moisture buffering of surface materials

The impact of non-uniform indoor conditions on local moisture buffering of interior surface materials is investigated by analyzing the maximum moisture content measured on the interior surface of the test wall, and the moisture content profile in the whole volume of surface materials obtained by WUFI Pro 4

simulations. The impact of ventilation rate on the moisture buffering of three areas of test wall is also investigated.

#### **1.4 Thesis outline**

In Chapter 2, fundamental theories on moisture transport, experimental investigation and models developed for studying moisture buffering effect are reviewed. Chapter 3 describes the experimental design, setup and test procedure, including the test hut configurations, test cases, test conditions, equipments, and measurement systems. In Chapter 4, moisture balance equations based on experimental data and BSim simulation results are developed and presented. A new index, MAMBV, is introduced and used to evaluate the impact of different parameters on moisture buffering potential of materials in this chapter. Moisture responses of materials are investigated using WUFI simulation in Chapter 5. The simplified method, effective capacitance model, used to predict MAMBV and indoor RH using moisture buffering value (MBV) is developed. Chapter 6 focuses on the impact of non-uniform indoor environment on local moisture buffering of surface materials. The last chapter summarizes the contributions of this thesis research and points out future research directions.

## CHAPTER 2

### LITERATURE REVIEW

The components of the moisture balance in buildings are introduced in the first section of this chapter. The existing research on moisture buffering effect, including experimental studies and modeling, is reviewed. Experimental investigation carried out at both material level and room level are introduced and discussed. Fundamental of moisture transports is first reviewed, followed by the presentation of simplified models and simulation tools. Material properties and terms used to describe moisture buffering effect are listed and discussed. Limitations of the existing studies are summarized at the end of this chapter.

#### 2.1 Moisture balance and its components

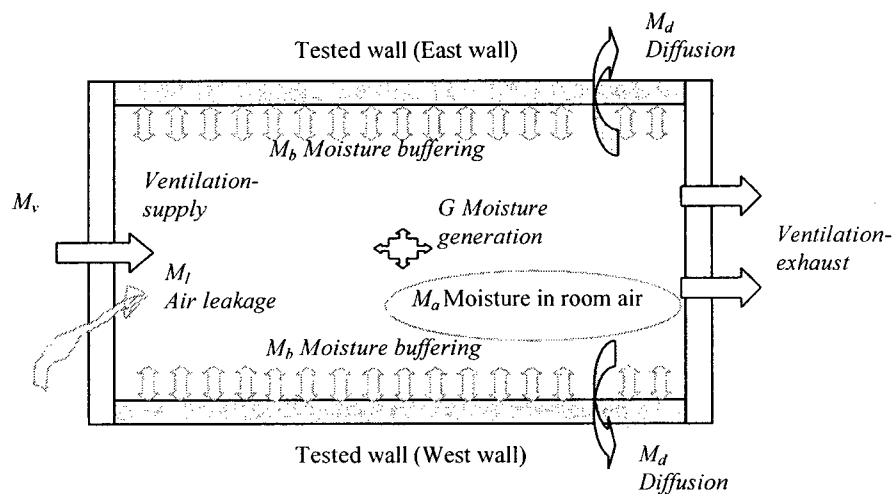
As shown in Figure 2.1, the gains and losses of moisture mass within an enclosed air space are governed by the law of conservation. This moisture balance involves moisture generated  $G$ , moisture removed by ventilation and air leakage  $M_v$  and  $M_l$ , moisture absorbed or released by surface hygroscopic materials  $M_b$  (moisture buffering), and moisture held by indoor air  $M_a$ . The moisture balance can be described as,

$$M_a(t) = -M_b(t) - M_v(t) - M_l(t) + G(t) \quad (2.1)$$

where all the terms are accumulated mass changes from the start of the moisture loading

cycle (g).

The moisture components on the right hand side of Eq. 2.1 determine the amount of indoor humidity on the left hand side, which has to meet the requirement of thermal comfort, indoor air quality, health, etc., as introduced in the previous chapter. The two important factors, moisture source  $G$  and ventilation in residential houses  $M_v$ , which hold most of moisture in the balance, are discussed in the following sections.



**Figure 2.1. Moisture balance in building.**

### 2.1.1 Moisture production in indoor environment

Moisture source in the indoor space can be generated by transpiration from the human body, evaporation from plants, personal hygiene activities, cleaning of dwellings, washing up, laundering, and subsequent drying, cooking, etc. (Straube, 2002, Aoki-Kramer and Karagiozis, 2004).

Many field tests and literature provide the typical moisture production rates for residential houses, as shown in Table 2.1. The literature review indicates that the average



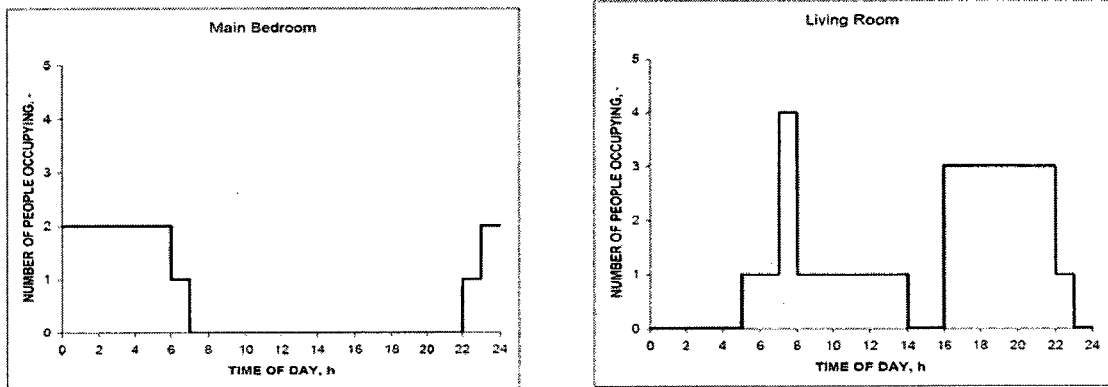
moisture production rate is between 300-600g/hr, depending on outdoor climate, ventilation condition, occupancy, as well as physical conditions and life style of the occupants.

**Table 2.1. Literature on moisture production in residential houses.**

Sources	Moisture Production
Christian, 1994	Europe, a family without children has the average production rate of 341 g/hr; and rate of 504-600 g/hr for a family with one to three children.
Tenwolde and Walker, 2001	Average value of 300g/hr for a family without kids, and 490g/hr to 600g/hr for a family with children from 1 to 3.
Aoki-Kramer and Karagiozis, 2004	Typical household of four people generates 4-14 kg/day based on the field measurements.
ASHRAE Handbook, 2004	A family of four produces an average of 320g/hr of moisture.

Moisture production is not evenly distributed throughout the day. Harriman et al. (2001) and Christian (1994) summarized the peak hourly load by the types of domestic activities. Satio (2005 b) displayed the daily schedule of moisture production measured in Japan, as shown in Figure 2.2.

The profile of the moisture generation rate is normally simplified in the experiment work. The amount, rate and profile (loading scheme) of moisture generation are all important factors that influence the moisture buffering effect (Roles and Janssen, 2006, Janssen and Roles, 2007). These topics are discussed in sections 2.2.2 and 2.3.2.



**Figure 2.2. Schedule of the moisture generation for living room and main bedroom (from Satio, 2005 b).**

### 2.1.2 Ventilation, airtightness and air infiltration

The ventilation requirement for residential buildings is traditionally met by air infiltration (natural ventilation). The reported average air leakage rates of the old houses vary between 0.2 ACH and 2 ACH (air changes per hour) (ASHRAE, 2005). However, with the consideration for the energy conservation, ASHRAE (ASHRAE Standard 119, 1988) and the National Building Code of Canada (NRCC, 2005) encourage tighter envelopes and recommend to meet the ventilation requirement using mechanical ventilation. Since 1980-90s, the tract-built Canadian house<sup>1</sup> showed a 30% increase of airtightness. 82% of the new houses had natural air exchange rates less than 0.3 ACH in March (Hamlin, 1991). Ventilation and air leakage have strong influence on the moisture buffering effect, which will be discussed in Section 2.3.

The minimum ventilation rate for residential building has to meet the requirement of the indoor air quality, thermal comfort, and health. Canadian Standard (CAN/CSA-F326-

<sup>1</sup> Houses built simulating identical occupancies

M91, 1991) categorized the minimum ventilation rate according to rooms' function. For example a master bedroom requires a minimum of 10 L/s ventilation rate, while a single bedroom necessitates a minimum of 5 L/s ventilation rate. However, a minimum requirement of a whole residential house is not provided. The recent ASHRAE Standard 62.1-2007 requires the ventilation rate to be calculated using the equation:

$$Q_{fan} = 0.05 \times A_{floor} + 3.5 \times (N_{br} + 1) \quad (2.2)$$

where  $Q_{fan}$  is the fan flow in L/s;  $A_{floor}$  is the area of floor in  $m^2$ ; and  $N_{br}$  is the number of bedrooms.

Therefore, the minimum air change rate for a family of 4 is between 0.31 to 0.81 ACH, given that the volume of the house is between 200-500  $m^3$ .

It can be concluded that, although various ventilation rates are suggested by different standards, 0.3 ACH is the minimum ventilation rate recommended.

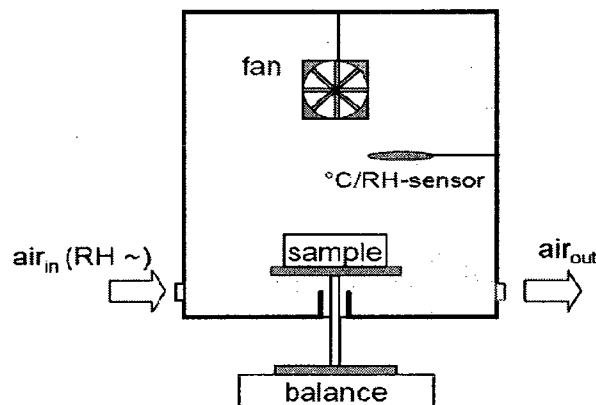
## **2.2 Material level and small-scale experiment study**

Since the 1980's, many experimental investigations have been carried out at two levels: the material or small-scale experiment level and large-scale or field test level.

### **2.2.1 Experiment setup and parameters studied**

Several small scale tests studying moisture buffering capacity were conducted in Europe, Japan and Canada. One of the purposes was to define the moisture buffering value (MBV) as a composite material property to represent the capacity of moisture buffering.

Most of the tests were performed in small environmental chambers, where the samples of hygroscopic materials were generally exposed to two different levels of RH. The amount of moisture involved in moisture buffering was obtained by monitoring the weight change of the samples, as shown in Figure 2.3. Such tests were carried out by NORDTEST (Rode et al., 2005), JIS (JIS A 1470-1, 2002), IDIS (ISO/DIS 24353, 2008), Wu (2007) or Wu et al, (2008) and DTU (Rode et al., 2005). (NORDTEST, JIS, IDIS, DTU stand for Nordic Country Test Standard, Japanese Industry Standard, International Standard Organization /Draft International Standard, and Technical University of Denmark, respectively.)

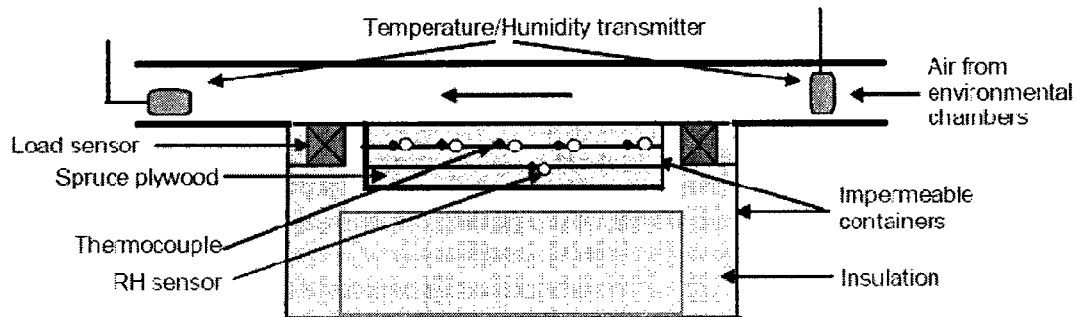


**Figure 2.3. Material level experiment carried in a small chamber (from Roels, 2008).**

A different experimental design was implemented by Osanyintola (2005) and Talukar et al. (2007 a, b) to study the transient behavior of gypsum boards and plywood, using a transient moisture and temperature facility (TMT) (see Figure 2.4). The main concept of this experiment consists of exposing a material sample to a stream of conditioned air, which was switched between two RH levels. Afterwards, the author(s) monitored the RH

& T of different layers of the sample, the RH & T of the upstream and downstream air, and the weight change of the material sample.

The parameters studied in all investigations mentioned above are: moisture loading protocol, material thickness, and mass transfer coefficient, as listed in Table 2.2.



**Figure 2.4. Material level experiment carried out in TMT (from Osanyintola, 2005).**

Table 2.2 Parameters studied in the material-level experiments.

Sources	Materials Tested	RH Levels high/low (%)	Time Intervals high/low (h)	Surface Transfer Coefficient Velocity or Re number	Sample Thickness
Padfield, 1998	wood/ plaster/cellular concrete /wool insulation/clay tile/ brick	0/100*	10/10	Not reported	30mm
Rode et al., 2005 a	Spruce board/ brick/gypsum/ concrete/laminated wood/ cellular concrete/birch panel	75/33	8/16	$2.0 \times 10^{-8}$ kg·m <sup>2</sup> /s/Pa	As applied in practice
Rofés, 2008	Gypsum board, painted or not	80/54	12/12	0.8, 3.39, 3.9, 5.0 x10 <sup>-8</sup> kg·m <sup>2</sup> /s/Pa	As applied in practice
Ramos et al., 2004	Cement plaster/gypsum plaster or board, painted or not	85/65	12/12	Not reported	As applied in practice
Ojanen and Salonvaara, 2004	Wood pine/ gypsum board, painted or not/wood fiberboard/ gypsum board with insulation	50/23 75/50	8/16	Not reported	As applied in practice
Wu, 2007 and Wu et al., 2008	Gypsum board/ Plywood/ OSB/ Fiberboard/ Stucco	75/33	8/16	1.3m/s	As applied in practice
Osanyintola, 2005, Talukar et al., 2007 a, b	Uncoated gypsum board/ coated gypsum board/plywood	71/30	8/8 24/24	Re = 2000 Re = 5000	Three layers of the materials as applied in practice
Osanyintola, O. F., 2005	plywood	75/33	8/16	Re = 2000 Re = 5000	Three layers of the materials as applied in practice

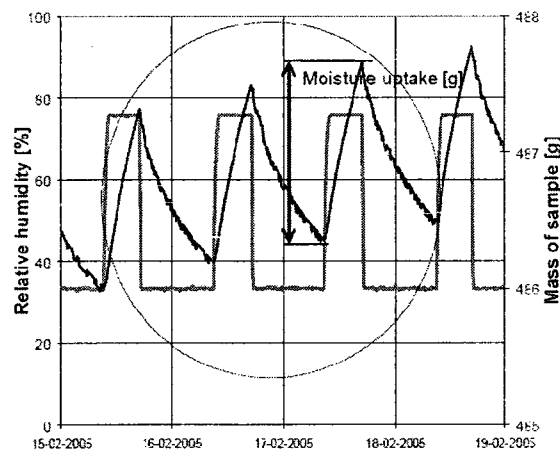
\* Specially designed moisture flux generation provided the linear change of RH between two levels.

### 2.2.2 Moisture Buffering Value (MBV)

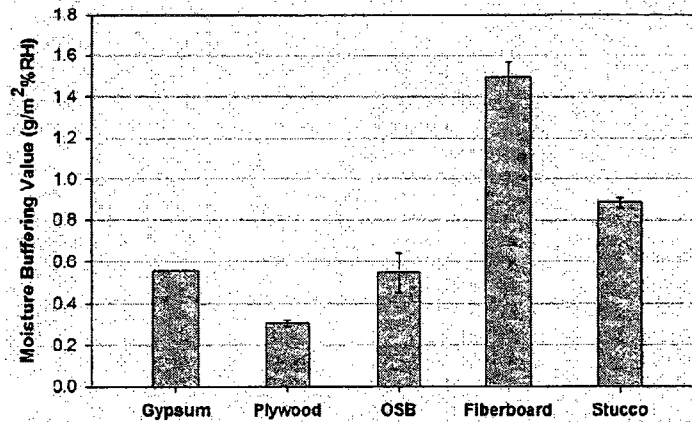
One of the most important contributions of the tests mentioned in the previous section is the introduction of the moisture buffering value (MBV) concept. MBV is defined as:

$$MBV = \frac{m_{\max} - m_{\min}}{A \cdot (RH_{\text{high}} - RH_{\text{low}})} \quad (2.3)$$

where  $A$  is the area of materials exposed to ambient environment,  $RH_{\text{high}}$  and  $RH_{\text{low}}$  are two RH levels of the environment the materials are exposed to, and  $m_{\max}$  and  $m_{\min}$  are the maximum and minimum weight measured during one cycle of test as shown in Figure 2.5.



**Figure 2.5. Moisture uptake profile in a small scale experiment (from Rode et al., 2005).**



**Figure 2.6. Moisture Buffering Value (from Wu, 2007).**

MBV represents the ability of the material to absorb moisture when the ambient RH varies between two different RH levels. Figure 2.6 displays an example of the MBV for different materials (Wu, 2007).

It is reported that three factors, namely, loading protocol, mass transfer coefficient, and sample thickness, significantly affect the MBV.

- *Loading protocol*

Different loading protocols were adopted by various standard tests (listed in Table 2.3). Depending on the level of RH and the time interval, MBV shows different values in the simulation (Osanyintola, 2005 and Roels, 2008), as observed in Figure 2.7. However, currently there is no experimental data that clearly support the influence of moisture loading protocol on different materials.



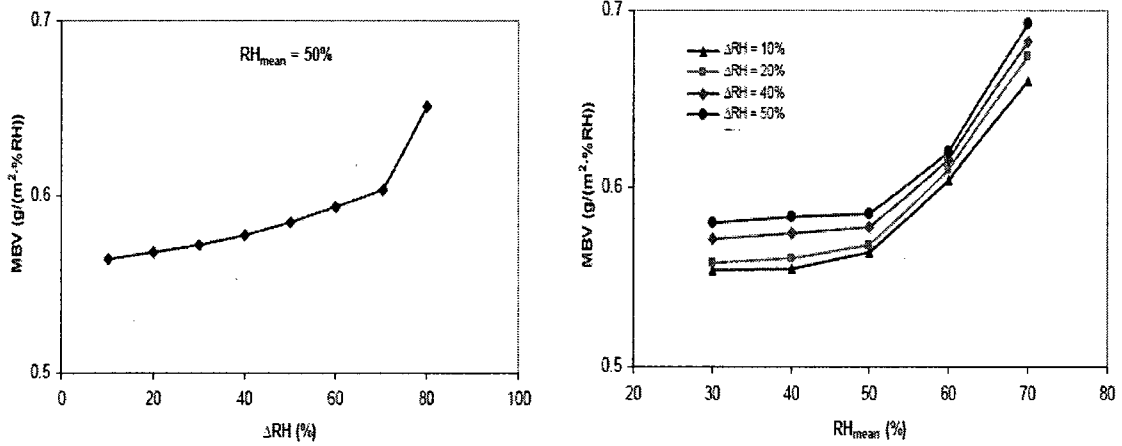


Figure 2.7. Moisture Buffering Value depending on RH load (from Osanyintola, 2005).

Table 2.3. MBV standard test (adapted from Roels, 2008).

Sources	RH Levels high/low (%)	Time Intervals high/low (h)	Surface Transfer Coefficient (kg·m <sup>2</sup> ·s/Pa)	Sample Thickness
JIS A 1470-1, 2002	53/33, 75/53, 93/75	24/24	2.1x10 <sup>-8</sup>	As applied in practice
IDIS 24353, 2008	53/33, 75/53, 93/75	12/12	2.7 x10 <sup>-7</sup>	As applied in practice
NORDTEST protocol, 2005	75/33	8/16	2.0x10 <sup>-8</sup>	>1% daily penetration depth

▪ *Surface mass transfer coefficient*

Surface mass transfer coefficient is defined as:

$$q_v = \beta \cdot (v_a - v_{surf}) \quad (2.4)$$

where  $\beta$  is the mass transfer coefficient (m/s);  $v_a$  (kg/m<sup>3</sup>) is the vapor content of air; and  $v_{surf}$  (kg/m<sup>3</sup>) is the vapor content of the surface material.

A commonly used analogous relation between moisture transfer coefficient and heat transfer coefficient is,

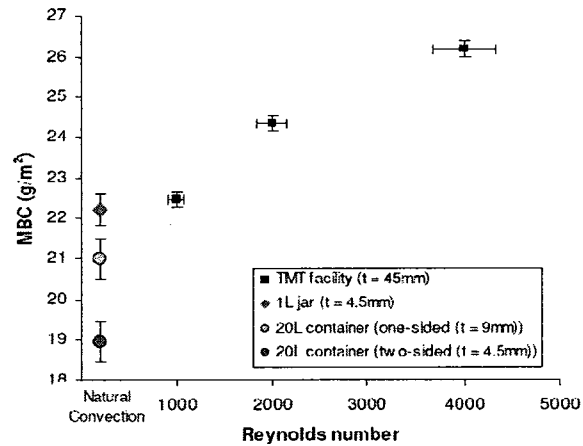
$$\beta = \frac{h_c}{\rho c_p} \quad (2.5)$$

where  $h_c$  is heat transfer coefficient (W/m<sup>2</sup>K);  $\rho$  is the density of material (kg/m<sup>3</sup>); and  $c_p$  is the heat capacity of the material (J/kg·K). However the relationship presented by Eq. (2.5) is more applicable to turbulent flow.

Osanyintola and Simonson (2005 a, b) found that the change of Reynold number (Re), which is correlated to the surface mass transfer coefficient, results in a large change of moisture buffering capacity (MBC) (Figure 2.8). MBC is defined as the amount of moisture involved in moisture buffering on unit surface area. Moreover, Roles and Janssen (2005) reported in numerical study that the variation of mass transfer coefficient has a great impact on MBV (as shown in Table 2.4).

**Table 2.4. MBV corresponding to different surface mass transfer coefficient.**

Moisture Transfer Coefficient (kg·m <sup>2</sup> s/Pa)	MBV (g/m <sup>2</sup> ·%RH)	
	Plywood	Gypsum Board
1.0x10 <sup>-8</sup>	0.7	0.95
3.0x10 <sup>-8</sup>	0.77	1.06
10.0x10 <sup>-8</sup>	0.81	1.11



**Figure 2.8. MBC depending on Reynolds number (from Osanyintola and Simonson 2005).**

▪ *Samples thickness*

The sample thickness influences the moisture buffering effect as well. It is reported in a numerical study that if the thickness of the sample is lower than the penetration depth the MBV changes dramatically (Roles and Janssen, 2005). The definition of penetration depth can be found in section 5.3.2.

**2.3 Large-scale experimental study**

Several large-scale lab experiments and field tests were carried out recently in Japan, Denmark (DTU) and Finland (VTT - Technical Research Centre of Finland). The impacts of different surface materials and furniture on indoor humidity were investigated under designed daily moisture generation (see Table 2.5).

Due to the large number of factors influencing the results of moisture buffering effect in field tests, such as complicated moisture schedule and poorly controlled ventilation, the

review in the following sections focuses on the large-scale experiments performed in the laboratories. These tests were carried out in three test huts respectively, 4.62 m<sup>3</sup> chamber in Japan, 50 m<sup>3</sup> test room at VTT, and 38 m<sup>3</sup> chamber at DTU. The first test hut was placed inside a conditioned room, and the latter two were set up in the outdoor environment.

### **2.3.1 Ventilation rate**

Ventilation rate is one of the main factors influencing the moisture buffering effect. The increasing of ventilation rate results in the reduction of moisture buffering effect on indoor humidity (Simonson et al., 2004). Experimental data shows that, when the ventilation rate exceeds 1 ACH, the moisture buffering effect is less than a half of the case without ventilation. No significant effect is found above 5.0 ACH (Mitamura et al., 2004).

**Table 2.5. Summary of large-scale experiments.**

Sources	Materials Tested	Moisture Generation Protocol	Ventilation Rate (ACH)	Notes
Japan (Mitamura et al., 2004)	Hygroscopic material (porous soil)	20 g/hr for 6 hours followed by 6 hours without moisture (bedroom)	1.5, 10	room volume of 4.62 m <sup>3</sup> locations of the hydrothermal materials are tested
Japan, (Saito, 2005 a)	Furnished room (carpet, plywood, gypsum, etc.)	Based on survey in Japan, had peak hours of cooking, bath and base moisture generation profile	Real operation	Field test, multi-rooms
VTT (Simonson and Salonvaara, 2000 a, b)	Gypsum board coated with single primer, wooden floor board	87 g/hr for 8 hours at night (bedroom)	0, 0.25, 0.55, 1	Field test, room dimension: 3.15 m x 2.15 m x 2.3 m (h)
VTT (Ojanen and Salonvaara, 2004)	Uncoated wood paneling	6-8am, 0.4, 4-10pm, 0.2, rest of 0.02 (kg/hrm <sup>3</sup> ), (living room)	0.5	Volume 50 m <sup>3</sup> , air tightness 1 ACH at 50 Pa, placed outside
VTT (Holm and Lengsfeld, 2007)	Gypsum board, coated and uncoated	6-8am, 0.4, 4-10pm, 0.2, rest of 0.02 (kg/hrm <sup>3</sup> )	0.66 and 0.63	Different locations of surface materials are tested Air tightness, 0.02 ACH for test room at 4 Pa, Volume 50 m <sup>3</sup> , placed outside
DTU (Rode et al., 2001)	Plywood	16 g/hr for 12 hours followed by 12 hours condensation period	No ventilation	13.8 m <sup>2</sup> x 2.75 m(h), air tightness 0.2ACH at 50 Pa, placed outside
DTU (Hedeegard et al., 2005 a, b)	cellular concrete and plaster board (coated and uncoated)	25 g/hr for 12 hours followed by 12 hours condensation period	No ventilation	13.8 m <sup>2</sup> x 2.75 m (h), air tightness 0.2ACH at 50 Pa, placed outside
DTU (Svennberg et al., 2004)	Furnished room, desk, table, bookcase, book, chair, carpet, curtain	25 g/hr for 12 hours followed by 12 hours condensation period	No ventilation	13.8 m <sup>2</sup> x 2.75 m (h), air tightness 0.2ACH at 50 Pa, placed outside
BESTEST (Rode et al., 2004, a)	Gypsum board, coated and uncoated	0.18 kg/hr 9am-5pm (bedroom)	0.5	Field test, room dimension: 6 m x 8 m x 2.7 m (h)

### **2.3.2 Moisture generation protocols**

Indoor moisture generation serves as a moisture source for moisture buffering effect. Indoor humidity, which is the combined results of moisture generation, ventilation and moisture buffering effect, acts as the moisture load for moisture buffering on the interior surface materials in large-scale experiments. The effect of indoor humidity in large-scale experiment on moisture buffering is similar to the effect of the moisture load in the material level experiments (shown in section 2.2.2).

The moisture modes differ from one study to another, as shown in Table 2.5. These protocols were designed based on moisture generation in different room type (bedroom, living room) observed in real residential houses. The impact of different moisture generation rates has not been tested. Further studies need to be performed for better understanding of this effect.

### **2.3.3 Indoor environment**

The indoor conditions (RH & T) were measured by either one or more sensors, placed at the center of the test rooms, and were typically considered as one node in existing experimental studies. However, in reality, temperature stratification and uneven moisture distribution are the prevalent conditions within these rooms. These conditions affect the moisture transfer between the indoor air-film and the surface materials, and consequently affect the moisture buffering of surface materials (Hedegaard et al., 2005b). For that reason, non-uniform indoor environment should be considered in the experimental work.

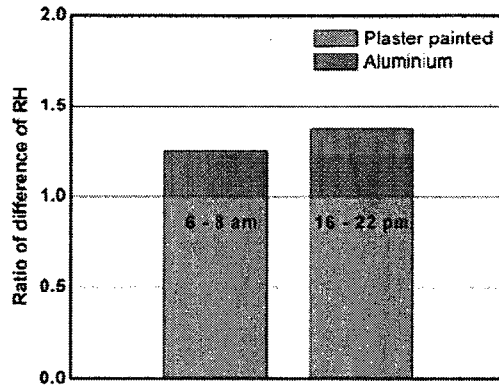
### **2.3.4 Performance of building envelope and interior surface materials**

The HAM response of building envelope is mostly neglected in previous experimental study on moisture buffering effect. The building envelope is constructed either with metal panel (DTU) or sealed with aluminum sheets (Japan), to avoid air leakage, which do not simulate the real structure of houses. Even when a real house structure is presented (VTT), there is no recording of HAM response of the building envelope. More importantly, there is no measurement (specially of moisture content) taken on the surface materials, where the moisture buffering happens. Only the indoor RH can be analyzed as the measurement results from these tests. Therefore, information concerning the whole building HAM response that can be obtained from such tests is very limited.

### **2.3.5 Evaluation of moisture buffering effect**

The evaluation of moisture buffering effect in the large-scale experiment was typically performed by comparing the decreasing of the peak indoor RH level and the reduction of RH variation (e.g. the comparison presented by Kunzel et al. (2004)) (Figure 2.9). However, at the material level test, MBV is used to evaluate moisture buffering capacity. There is no direct link between these two evaluation methods. Thus, it is required to evaluate the moisture buffering capacity in large experiments the same way as in small-scale experiments in terms of the amount of moisture that is involved in the moisture buffering effect.

This approach calls for the accurate measurements of all the components involved in the moisture balance (Eq. 2.1) in a large-scale experiment.



**Figure 2.9. Indoor RH comparison between cases using aluminum sheet or plaster painted as surface materials (from Kunzel et al., 2004).**

### 2.3.6 Other factors and sensitivity analyses

The impact of material properties on moisture buffering effect is also important. Sensitivity analyses were carried out by some researchers employing simulation work. However, the conclusions are not consistent. For example, Malonvaara et al. (2004) in a numerical analyses, indicated that surface mass transfer coefficient and moisture capacity of the material play a more important role on moisture buffering effect compared to permeability. By contrast, Annex 41 in the final report (Roels, 2008) concluded that the permeability and moisture capacity exert the same impact on moisture buffering effect. The possible explanation is the impact of the material properties (moisture capacity and permeability) on moisture buffering effect may be influenced by other factors such as moisture load, and therefore, differs from case to case.

Other factors such as initial condition and moisture history of daily cycle in the materials were observed from the previous tests, however no further analyses were provided.



## 2.4 Fundamental theory on moisture transfer

### 2.4.1 Moisture in materials

Most building materials are porous materials, so they have the capacity to store moisture. The moisture storage capacity of materials is described by the relation between the moisture content and the relative humidity, so-called sorption isotherms curve. There are three regions in the absorption procedure distinguished in porous building materials as shown in Figure 2.10:

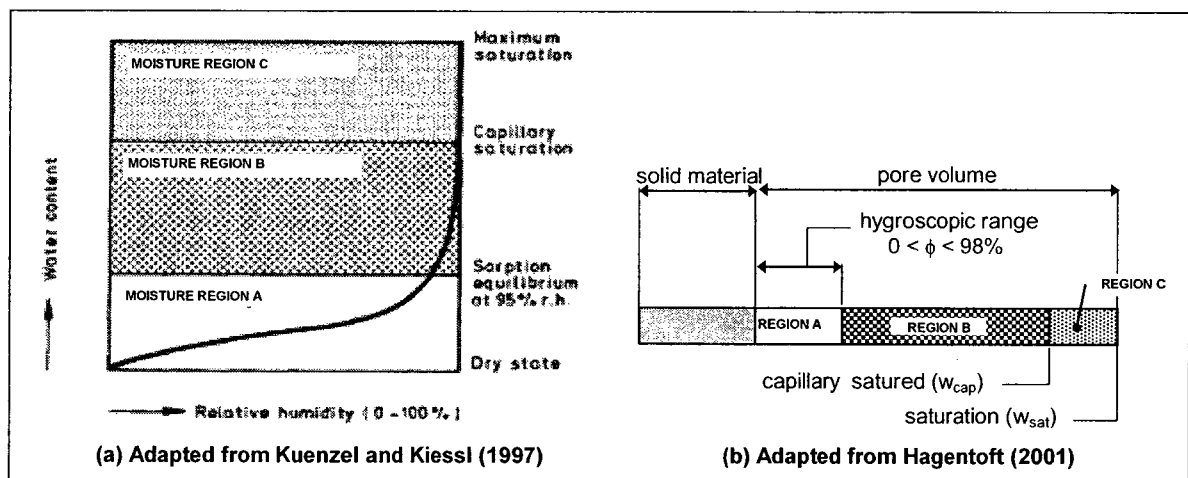


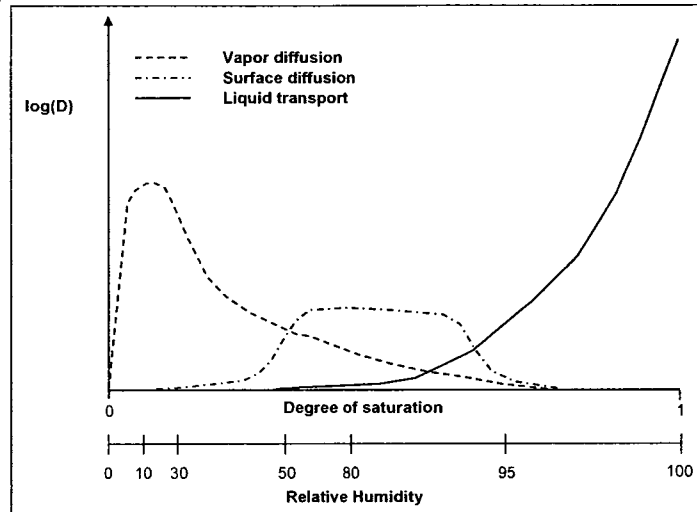
Figure 2.10. Moisture storage regions (from Hagentoft, 2001).

- Region A (hygroscopic region) is the range where the material absorbs vapor water from the surrounding environment to the pore walls in single layer, and then multilayer, until the relative humidity reaches to 98% RH (Hagentoft, 2001) or 95%RH (Kuenzel and Kiessl, 1997).
- Region B is characterized by capillary suction when the material is in contact with liquid water. The moisture content is increased significantly until the capillary saturation moisture content ( $w_{cap}$ ) is reached.

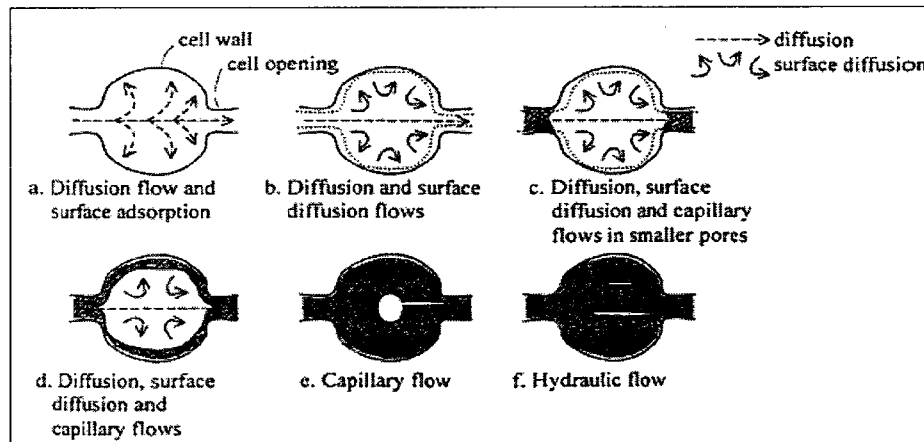
- Region C (supersaturated region) occurs between  $w_{cap}$  and  $w_{sat}$  (the maximum possible water content).  $w_{sat}$  is the water content level when the material is saturated at 100% of relative humidity, which could only take place under special conditions such as in vacuum.

#### **2.4.2 Moisture transfer in materials**

Moisture can migrate in porous materials in both vapor and liquid phases. Straube and Burnett (2005) described the combined vapor and liquid moisture transport as a function of the moisture diffusivities, as shown in Figure 2.11. The moisture transport mechanism is also illustrated in Figure 2.12. At the lowest moisture contents, diffusion controls vapor flow and adsorbed water molecules are tightly bound to the pore walls. As the moisture content increases, small pores are filled with water and vapor diffusion is reduced. Over 30% RH, surface diffusion begins and becomes important between 50% and 90% RH. Liquid transport may begin when water condenses in small pores over 30% RH and dominates the moisture transfer over 90% RH. The different physical phases are introduced in the following sections.



**Figure 2.11. Hypothetical total isothermal moisture transport function (Adapted from Straube and Burnett, 2005).**



**Figure 2.12. Moisture transport mechanisms (Ojanen, 1989).**

- Vapor diffusion

Vapor diffusion takes into account mainly vapor diffusion, effusion or Knudsen diffusion, and thermo-diffusion (Hens, 1996). Most research investigations indicated that the driving force of Fick's diffusion is by partial vapor pressure as,

$$q_v = -\delta(w, T) \cdot \nabla p_v \quad (2.6)$$

where  $q_v$  is the vapor flow (kg/m),  $\delta$  is vapor permeability (kg/Pa·m·s), and  $p_v$  is the vapor pressure (Pa).

- Surface diffusion

Water molecules in regions with thicker layers jump and settle on sites with fewer layers, due to different surface diffusion (Ojanen et al., 1989). The true potential of surface diffusion is the mass gradient density. However, the increase of moisture content or RH causes thicker adsorbed layers. For that reason, it is easy and accurate to use RH or moisture content as driving potentials (Straube and Burnett, 2005; Kuenzel, 1995). Surface diffusion is usually considered as a phase of liquid transfer.

- Liquid transport

According to Karagiozis (2001b), liquid flow is transported mainly by capillary flow in region B and gravitation effect in supersaturated region C. The driving potentials commonly used for liquid flow are relative humidity ( $\phi$ ), moisture content ( $w$ ) or suction pressure ( $P_{suc}$ ) (Hagentoft et al., 2004). Künzel and Kiessl (1997) and Karagiozis (2001b) used relative humidity as driving potential, described as

$$q_w = -D_\phi \cdot \nabla \phi \quad (2.7)$$

where  $D_\phi$  is liquid coefficient (m<sup>2</sup>/s), and  $\phi$  is relative humidity. Surface diffusion effect is included in the liquid coefficient.

### 2.4.3 Moisture transfer to and from surface

The convective moisture transfer between material surface and ambient air can be calculated as,

$$q_v = \beta \cdot (v_a - v_{surf}) \quad (2.8)$$

where  $\beta$  is the mass transfer coefficient (m/s);  $v_a$  (kg/m<sup>3</sup>) is the vapor content of air; and  $v_{surf}$  (kg/m<sup>3</sup>) is the vapor content of the surface materials.

### 2.4.4 Balance of moisture transfer and storage

The moisture transfer in materials and its storage can be described as,

$$\underbrace{\frac{\partial w}{\partial t}}_{\text{moisture storage}} = -\nabla \left\{ \underbrace{-D_\phi \cdot \nabla \phi}_{\text{liquid - transfer}} - \underbrace{\delta_p(w, T) \cdot \nabla p}_{\text{vapor - diffusion}} \right\} \quad (2.9)$$

Applying the Eq. 2.8 as the boundary conditions, the moisture transfer in materials and between the ambient air can be calculated and modeled.

## 2.5 Latest HAM models with consideration of moisture buffering effect

In the following sections, analytical, numerical and research commercially available models are reviewed. The shortcoming and the advantages of all these models are presented as well.

### 2.5.1 Analytical solution

Based on the moisture balance, explained in the section 2.1, the indoor humidity in the cases without moisture buffering can be calculated as (Hagentoft, 2001):

$$w_i(t) = w_o + G / nV\rho \cdot (1 - e^{-nt}) \quad (2.10)$$

where  $w_i$  is the humidity ratio of indoor air (g/kg·dry air),  $w_o$  (g/kg·dry air) is the humidity ratio of outdoor air (or ventilation air),  $G$  is the moisture generation (kg), and  $n$  is the ventilation rate (1/hr).

This equation is built under the assumption that the indoor air is well mixed and the air leakage is included in the ventilation.

Hens (2005) introduced a simplified analytical solution for the calculation with the consideration of moisture buffering effect using Fourier analysis. However, this method has not been widely used due to it need to be solved in a large matrix.

### 2.5.2 Simplified models

- Effective moisture penetration depth (EMPD)

In this method, it is assumed that within the very thin inner (surface) layer, moisture is distributed uniformly and discontinuously from the outer layer (Kerestecioglu et al., 1990, Cunningham, 1992), as shown in Figure 2.13. The moisture transfer between the inner layer and outer layer is neglected. The moisture buffering only happens between the inner layer and the ambient indoor air and can be described as:

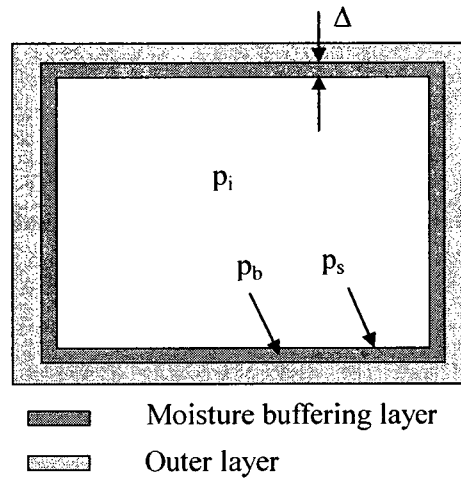
$$\frac{v_i - v_b}{\frac{1}{\beta'} + Z_b} = \rho \xi(\phi_b) \Delta \frac{d}{dt} \left( \frac{p_b}{p_{sat}(\theta_b)} \right) \quad (2.11)$$

where  $v_i$  is the indoor moisture content ( $\text{kg/m}^3$ );  $v_b$  is the moisture content in the buffering layer ( $\text{kg/m}^3$ );  $p_{sat}$  is saturation vapor pressure in the buffering layer (Pa);  $\beta$  is the mass transfer coefficient (m/s);  $Z_b$  is the diffusion resistance between surface and center of moisture buffering layer (s/m);  $\theta_b$  is the temperature of buffering layer (K);  $\Delta$  is the thickness of the buffering layer (m);  $\rho$  is the density ( $\text{kg/m}^3$ ); and  $\xi$  is the moisture capacity (kg/kg), which is the function of the RH ( $\phi_b$ ).

The thickness of the moisture buffering layer,  $\Delta$ , is associated with EMPD, which is defined as (Cunningham, 1992):

$$EMPD = \sqrt{\frac{\delta \cdot p_{sat}(\theta) \cdot T}{\rho \xi \cdot \pi}} \quad (2.12)$$

where  $T$  is the period of the cyclic variation (s);  $\xi$  is the moisture capacity (kg/kg);  $\delta$  is vapor permeability ( $\text{kg/Pa}\cdot\text{m}\cdot\text{s}$ );  $p_{sat}$  is the local saturation vapor pressure (Pa), which is the function of temperature  $\theta$ , and  $\rho$  is the density ( $\text{kg/m}^3$ ).



**Figure 2.13. Representation of the humidity buffering layer.**

The choice of  $\Delta$  is very sensitive and should be backed up by experimental study and careful judgments in the application (Kerestecioglu et al., 1990, Zhao, 2004). The EMPD approach has been adopted in several simulation programs such as Energy Plus 2005, TRNSYS and Clim 2000.

- The distributed method

The commonly used distributed method is evaporation and condensation theory. In this model the combined heat and moisture transfer, taking place in the building envelope, is solved by the finite element method. However, the energy and moisture balance are formulated by lumped models assuming one node indoor conditions. (Kerestecioglu and Gu 1990)

Another distributed model, Biot model, was developed by El Diasty, Fazio, and Budaiwi . (1993). Analogue to the Biot method in heat transfer, the moisture transfer between materials and surrounded air is slow when Bi is closed to 0. On the contrary, when the Bi



is big enough materials can reach moisture transfer equilibrium with surround air very soon. The Biot number is considered as:

$$B_i = \frac{\beta V_m / A_e}{\delta} \quad (2.13)$$

where  $h_m$ , mass transfer coefficient, (kg/m<sup>2</sup>Pa·s) (humidity ratio based);  $V_m$ , material volume (m<sup>3</sup>);  $A_e$  exposed area (m<sup>2</sup>); and  $\delta$ , vapor permeability in materials (kg/m·Pa·s).

- Numerical model

In the numerical model for indoor comfort developed by Teodosiu et al., (2003), wall turbulence model, describing convection-diffusion conservation of vapor mass function, is added into the existing  $k$ - $\varepsilon$  model. Some other models (Barringer and Mcgugan 1989, Thomas and Burch, 1990) also provide simplified method to calculate the moisture absorption and desorption on the surface.

In summary, these simplified or numerical models are hard to be applied in practice because most of them need the users to have a fully understanding of moisture transfer mechanism and strong mathematical skills.

### 2.5.3 Commercial and research models

In Europe and North America, many hygrothermal models have been developed and validated to predict the moisture behavior of building materials and building enclosures, such as WUFI, MOISTURE EXPERT and hygIRC. All these models consider that indoor

condition is the input for interior boundary conditions and moisture transport through the envelope does not affect the indoor conditions.

WBHAM (Whole Building Heat, Air and Moisture) model was developed recently to solve this shortcoming by integrating building envelope HAM response (moisture buffering effect), indoor environment, and ventilation. For example, TRNSYS (Kwiatkowski et al., 2007), EnergyPlus (Crawley et al., 2002), ESP-r (Koronyhalyova et al., 2004) are well known energy analysis tools and now moisture buffering effect is integrated; WUFI-Plus is developed from hygrothermal model WUFI and now has the capacity to simulate the moisture buffering effect (Künzel and Holm, 2003); and HAMFitPlus is newly developed model at NRC (Tariku, 2008). Different models have their own advantages and shortcomings depending on their considerations in the physical model for indoor environment, moisture transfer in building envelope, outdoor environment, and on other factors such as interface, output, and material database.

- *Indoor environment*

Most of the models assume a well-mixed indoor environment and use lumped model to calculate their conditions, which are based on the heat and moisture balance:

$$c_a \cdot \rho_a \cdot V \cdot \frac{dT_i}{dt} = Q_{ventilation} + Q_{window} + Q_{structure} + Q_{adjacentzones} + Q_{source} + Q_{heatingssystem} \quad (2.14)$$

$$V \rho_a \cdot \frac{dw_a}{dt} = G_{ventilation} + G_{structure} + G_{adjacentzones} + G_{source} + G_{airhandingsystem} \quad (2.15)$$

where  $c_a$  is the heat capacity of air (J/m<sup>3</sup>K);  $V$  is the volume of the room (m<sup>3</sup>);  $w_a$  is the humidity ratio of the indoor air (kg/kg); and  $\rho_a$  is the density of the indoor air (kg/ m<sup>3</sup>).

Another approach is to use CFD to integrate the indoor environment air flow model (non-well mixed) into the whole building simulation. Because of the large number of driving forces and assumptions to be made in the simulations, it has to be done very carefully and validated by intensive experimental data (Woloszyn and Rode, 2008 a, b).

- *Moisture transfer in building envelope*

The model for heat transfer through building envelope has been well developed and validated. But the accuracy of the moisture transfer heavily relies on the physical models and the assumptions. Woloszyn and Rode (2008, b) made a brief summary of these simulation tools in term of their considerations on moisture transfer as following.

1) Not all the commercial software has complicated physical model for moisture transfer, for example, EnergyPlus and TRNSYS used EMPD method and capacitance buffering storage to simplify the calculation.

2) For the simulation tools having complicated moisture transfer model, there are differences on the consideration of coupling heat and moisture transfer, liquid transfer, air flow, driving potentials, and hysteresis.

- i) Heat and moisture transfer are not independent from each other (Kunzel, 1995).

So the model considering coupled heat and moisture models is more powerful, such as WUFI-Plus, and HAMFitPlus.

- ii) Moisture transfer through building envelope materials is in both vapor and liquid phase. But some models included only vapor transfer, such as BSim (Rode and Grau 2001).

iii) The air leakage passing through the building envelope is found to be the most important factor of moisture transfer in practice. However, most of the models have no capacity to calculate this phenomenon so far.

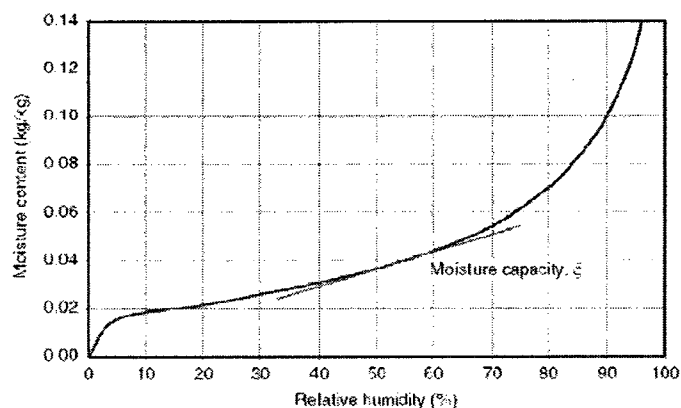
iv) Hysteresis is not significant according to the existing experiment and simulation works (Carmeliet et al., 2004). Only BSim included it.

## 2.6 Material properties and terms related to moisture buffering effect

### 2.6.1 Material properties or parameters

- Sorption isotherms and moisture capacity

Sorption isotherm is the curve, characterizing the equilibrium between relative humidity and moisture content of the materials, as shown in Figure 2.14. Moisture capacity is the slope of the sorption curve, representing the moisture storage ability of the material.



**Figure 2.14. Sorption curve for different building materials (from Rode and Grau, 2008).**

- *Vapor permeability*

Vapor permeability is defined as

$$q_w = \delta \cdot A \cdot t \cdot \frac{(p_1 - p_2)}{l} \quad (2.16)$$

where  $q_w$  is the vapor moisture flow (kg);  $A$  is the cross-section area of the flow path ( $m^2$ );  $t$  is the time during which flow occurs (s);  $l$  is the length of the flow path (m); and  $\delta$  is moisture permeability ( $kg/m \cdot s \cdot Pa$ ).

- *Moisture transfer coefficient*

The moisture transfer coefficient has been introduced in section 2.2.1, and is normally calculated by Lewis formula (see Eq. 2.5), which is appropriate for turbulent flow. However, the air velocity is very low on the interior surface of the building material and the flow mostly near the wall cannot develop into fully turbulent flow. Several tests were carried out to determine the moisture transfer coefficients by Iskara et al. (2007), and the results will be used in the calculation or simulation in this research.

- *Moisture diffusivity*

The diffusivity describes how fast moisture transfers through materials and is defined as:

$$D_w = \frac{\delta \cdot p_s}{\rho \cdot \xi} \quad (2.17)$$

where  $p_s$  is the saturation vapor pressure (Pa), and  $D_w$  is the diffusivity ( $m^2/s$ ).

- *Discussion*

It is expected that high vapor permeability doesn't resemble the high moisture storage capacity. The material with high capacity to store moisture normally has low vapor permeability (Padfield, 1998).

These two material properties cannot be used to evaluate the moisture buffering effect directly, but their influence, together with the impact of moisture transfer coefficient is important for moisture buffering effect. Ojanen and Salonvaara (2004) believed that vapor transfer resistance (reciprocal of vapor permeability) from the surface to the active layer is not significant, and mass transfer coefficient and the moisture capacity of the material play a more decisive role in the performance. However, Annex 41 (Roels, 2008) concluded that materials with high moisture capacity and average vapour permeability may have the similar moisture buffering capacity to the materials with average moisture capacity and high vapour permeability. The sensitivity analyses (Talukar et al. 2007 a, b) found that the change of permeability has the dominant effect on moisture buffering on coated gypsum board; however, moisture capacity has a greater influence on uncoated gypsum board.

In summary, it is agreed by most researchers that the vapor permeability, moisture capacity and surface mass transfer coefficient are important factors influencing the moisture buffering capacity. But the degree of impact by vapor permeability and moisture capacity may be different from material to material, and possibly depends on the ambient environment (moisture load, surface conditions and etc.). This difference will be studied in this research.

## 2.6.2 Terms evaluating moisture buffering capacity

Padfield (1998) and Rode et al., (2004, b) summarized the terms related to moisture buffering capacity, which are MBV (Moisture Buffering Value), diffusion thickness or moisture penetration depth, and available water.

- *MBV (Moisture buffering value)*

The definition of the MBV has been introduced in Section 2.2.1. It is dependent on moisture loading protocol, surface mass transfer coefficient, and the thickness of the samples. When the concept is applied to room, or building, the term named as hygric inertia is defined as:

$$HIR = \left( \sum A_k \cdot MBV + \sum MBV' \right) / V \quad (2.18)$$

where  $A_k$  are the area of surface materials,  $MBV$  is the moisture buffering value of surface materials,  $MBV'$  is the equivalent  $MBV$  of the elements inside the room.

- *Penetration depth*

Short term variation (hourly or daily) of indoor humidity was found to mainly affect the moisture content of the interior surface in a few millimetres. The penetration depth is defined as, (Salonvaara et al., 2003, 2004)

$$d_p = 4.61 \sqrt{\frac{D_w \cdot t_p}{\pi}} \quad (2.19)$$

where  $t_p$  is the load cycle period (s).

It is the depth of the surface material where the amplitude of moisture content is dampened to 1% of that on the surface. It describes the amount of the material involved in the moisture buffering effect.

- *Available water*

Available water is the quantity of water in hygrothermal materials that takes part in the buffering effect under a periodic oscillation of RH.

There are other terms used for evaluating moisture buffering capacity. For example, index of moisture buffering effect (Mitamura et al., 2004) and inertia classes (Ramos and de Freitas, 2004). They provide a rough classification and may have their advantages for practical application.

- *Discussion*

MBV is now the most commonly accepted method to describe the moisture buffering capacity of materials. The shortcoming of this method is its dependence on factors including the moisture loading protocol, the moisture transfer coefficient on the surface, and the thickness of the samples. Penetration depth has its physical meaning, but it is hard to be obtained directly from tests. Available water can be obtained from the experiments. However, its value depends on the test conditions and, thus, cannot be used directly to evaluate moisture buffering potential at room level.



## **2.7 Limitations in previous research work**

Based on the literature review and discussion, it is found that even though a lot of research studying moisture buffering has been carried out, additional research is still required in this field.

Firstly, existing large-scale experiments do not provide sufficient data or data analyses on the local moisture buffering and its distribution along the interior surfaces of the test rooms caused generally by the non-uniform indoor environment. Moreover, the investigation on the impact of moisture generation rate, moisture load schemes, initial conditions, supply air conditions, and hygric properties of surface materials in the large-scale experiment is very limited.

Secondly, in most large-scale experimental studies, the effect of moisture buffering is evaluated by comparing the reduction of the indoor RH variation. However, the amount of moisture involved in the moisture buffering under different moisture loads has not been calculated precisely from large-scale experiments. This approach has been employed at the material level (the MBV method), as motioned in section 2.2.2. The calculation of the amount of moisture involved at the large-scale level could be used to evaluate the moisture buffering potential, to quantify the impact of different parameters, and moreover to identify the impact of moisture history.

Furthermore, there are no general guidelines for large-scale experimental investigation or field test to follow. Several standard test procedures are available on moisture buffering value (MBV) tests, even though there are disagreements on the test conditions. However,

in large-scale experiment or field tests, due to the limitation of extensive test results and analyses, basic guidelines are still not available.

Considering the moisture buffering application in practice, the recommendations on how to choose different materials under different moisture load schemes, which is relevant to the usage of buildings or rooms, are still missing. This information should be concluded from the moisture buffering behaviour of hygroscopic materials under different moisture loads. Thus, the materials used for moisture buffering can be classified and recommendations on the material selection under different moisture load schemes can be made.

## CHAPTER 3

### EXPERIMENT SETUP AND TEST PROCEDURE

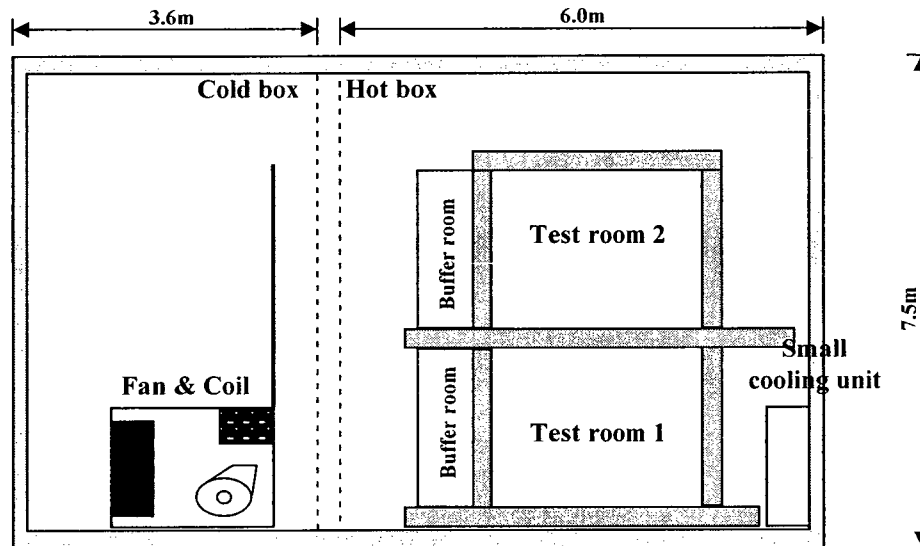
In this chapter, a large scale experiment setup for moisture buffering effect is described. The test conditions, scenario, parameters studied, equipments and the measurement are all presented.

#### **3.1 Test hut and environmental chamber**

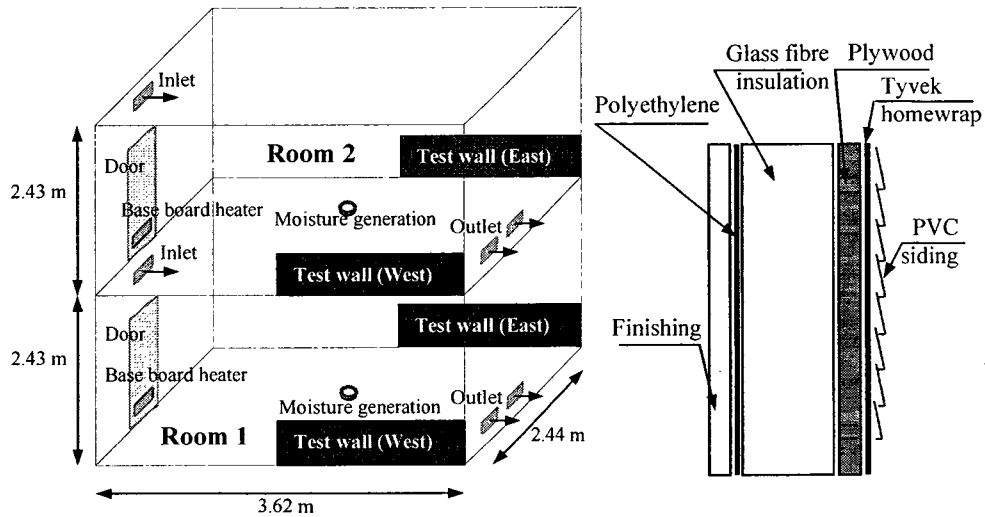
A two-story test-hut was assembled in a large-scale environmental chamber at Concordia University (Figure 3.1). The chamber was designed to test large scale building envelope systems between a cold box and a hot box (Fazio et al., 1997). The two boxes could also be assembled into a single climatic chamber with an internal space of 7 m (H) × 4 m (W) × 6.6 m (L), which was the configuration adopted to test a two-storey hut in this study. The temperature condition in this large chamber was controlled by two cooling systems and two electric heaters from -40 to 40°C with an accuracy of 0.1°C and the variation of humidity was 1% RH. A fan (5.7 m<sup>3</sup>/s or 12,000 CFM) that drives air through the evaporator provided the air circulation for the large chamber. In addition, portable small fans were used to promote mixing for a uniform condition of the chamber.

**Table 3.1 Components of wall assembly.**

Wall Component	Material
Outdoor surface	PVC siding
Air cavity	19 mm
Air/ weather barrier	Tyvek house wrap
Sheathing	Plywood (Canply, 12.5 mm thick)
Stud cavity	Studs (2'x6" by 24"long), Glass fibre batt insulation
Vapor barrier	Polyethylene 6mil or 0.15 mm
Indoor surface material	Uncoated gypsum board (12.5 mm) Or wood paneling (11/16 in or 17.5 mm) Or covered by polyethylene sheet (0.15 mm)



**Figure 3.1. Test room inside of the environmental chamber.**



**Figure 3.2. Configuration of test hut.**

The construction of the test hut represents the typical residential wood-framed construction. The main components of the wall assembly are presented in Table 3.1. On the east and west walls, uncoated gypsum board or wood paneling was the two different interior finishing materials tested in this experimental program. The rest of the interior surfaces were covered with aluminum sheets (0.8 mm) to avoid any moisture absorption or transport. There were tests carried out with east and west wall surfaces covered with polyethylene sheets. These tests were considered as non-hygroscopic surface studies. Each room had the dimension of 3.62 m x 2.44 m x 2.43 m (height). The layout of the test hut is shown in Figure 3.2.

A buffer room was located at the entrance of the test room (door side). The DAS (Data Acquisition System) and the moisture generation setup (pump, water bottle, and load cell) were placed inside of the buffer room.

**Table 3.2 Test cases (Part I).**

Hygroscopic cases		Non-hygroscopic cases		Conditions of supply air	Moisture generation (g/hr)	Ventilation rate (ACH)	
#	Interior finishing	#	Interior finishing				
1	Uncoated	2	Polyethylene	4.7 g/kg HR, 19 °C	103.6	0.50	
3	gypsum board	4	sheets		103.7	0.75	
5		6			101.6	1.02	
7		8			51.7	0.33	
9		10			53.3	0.51	
11		12			200.2 (2)*	0.52	
13	Wood paneling	14			7 g/kg HR, 19 °C	96.6	0.5
15		16				96.8	0.75
17		18				44.6	0.33
19		20				55.5	0.50
21		22				188.3 (2)*	0.51

\*notes the moisture generation regime is 2/22 hours.

**Table 3.3 Test cases (Part II).**

Furniture	Hygroscopic cases		Non-hygroscopic cases		Conditions of supply air	Moisture generation (g/hr)	Ventilation rate (ACH)
	#	Interior finishing	#	Interior finishing			
Bookshelf and books	23	Wood paneling	24	Polyethylene sheets	7 g/kg HR, 19 °C	99.2	0.51
Add: desk, chair and curtain	25		26			98.5	0.51
Fully furnished*	27		28			101.6	0.50

\*Furniture is introduced in Section 3.6.

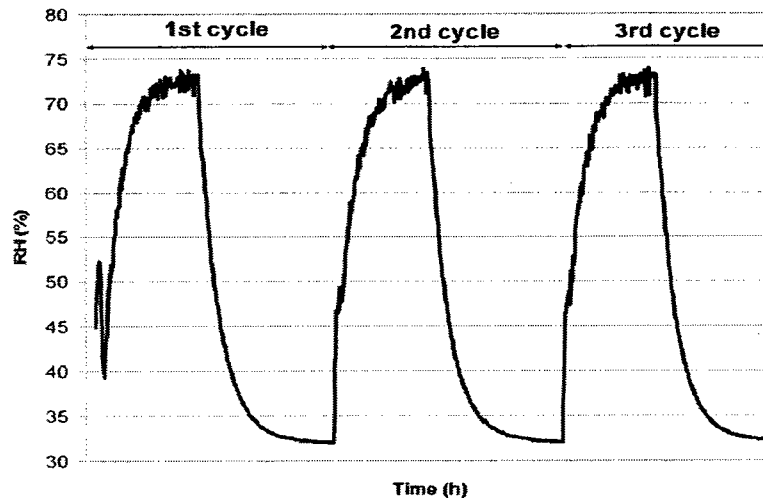
### 3.2 Test cases and procedure

There were totally 28 test cases, 12 cases using uncoated gypsum board and 10 cases using wood paneling as surface materials, and 6 cases with rooms furnished. Each case with tested surface materials (uncoated gypsum board or wood paneling) was paired with

another test with the polyethylene sheet covering surfaces, representing the non-hygroscopic case. The parameters studied were different ventilation rates: 0.33, 0.5, 0.75, 1 ACH, moisture generation rates: 50, 100 g/hr for 10 hours, and 200 g/hr for 2 hours in each 24-hour period, and two different surface materials, uncoated gypsum board and wood paneling (as shown in Table 3.2). The furniture was added in three steps: firstly, bookshelf and books; secondly, desk, chair and curtain; and thirdly, the bed with mattress (shown in Table 3.3).

Each test lasted for more than 3 daily cycles. The beginning of the first cycle is always influenced by unstable initial conditions, which is due to the interruption between tests. But the second and the third cycle are almost identical to each other (as shown in Figure 3.3).

The second day or the third day data were normally selected for analyses depending on whether there was interruption in the test performed.



**Figure 3.3: Repeatability of results after the second cycle (case 1, uncoated gypsum board, 0.5 ACH, 100 g/hr).**

### 3.3 Test conditions

The conditions of outdoor, indoor and AHU (Air Handling Unit), (after dehumidifier section) are shown in Figure 3.4 and Table 3.4.

**Table 3.4 Test conditions.**

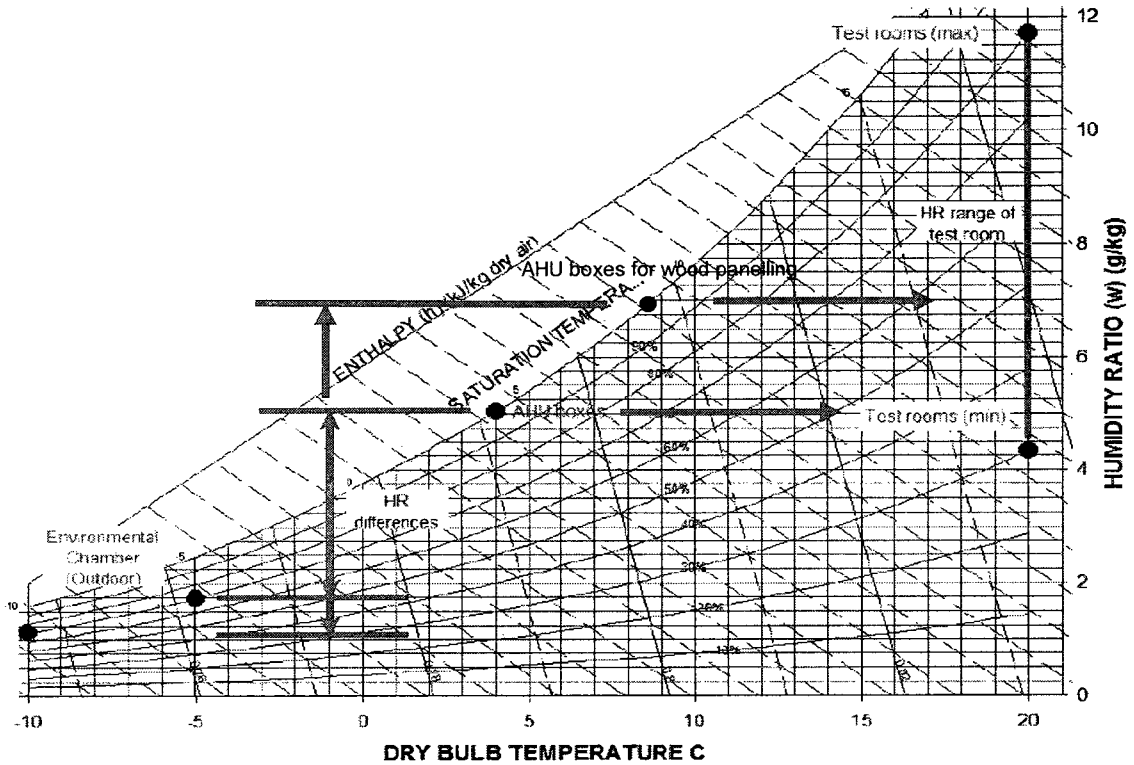
Location	Temperature (°C)	RH (%)	Humidity Ratio (g/kg dry air)
Chamber (Outdoor)	-10	45	0.72
	-5	70	1.73
AHU	4	100	5.03
	8.7	100	6.98
Test rooms	20	30 to 85	4.33 to 12.45

#### 3.3.1 Outdoor conditions

The tests using uncoated gypsum board were carried out under typical winter conditions of Montreal (-10 °C, 45% RH outdoor). The cases using the wood paneling (including cases with furniture) were tested at -5 °C, 70% RH outdoor conditions. Different settings were applied due to the fact that the tests with wood paneling and furniture were carried



out in the hot and humid summer season, during which the cooling unit for the environmental chamber had reached its limits and could not provide the same conditions as those for the gypsum board cases.



**Figure 3.4. Conditions of chamber (outdoor) environment, indoor, and AHU.**

### 3.3.2 Indoor conditions

The indoor temperature was kept constant throughout the test at 20-21.5 °C and the RH was left floating, which is the result of the moisture generation, ventilation and the moisture buffering.

The test rooms were pre-conditioned before each test run to achieve an initial HR (humidity ratio) of 4.68 to 4.99 g/kg·dry air for cases using gypsum board and 6.91 to 7.08 g/kg·dry air for cases using wood paneling.

### **3.3.3 Ventilation rate and conditions of supply air**

The minimum ventilation rate of 0.3ACH was designed to meet the requirements for indoor air quality, thermal comfort, and health in houses (as reviewed in section 2.1.2). The humidity ratio of supply air for cases using uncoated gypsum board was set at around 4.67 to 4.99 g/kg-dryair HR. For the cases using wood paneling and cases with furniture, the humidity ratio of supply air was set to be higher than 6.9 g/kg-dryair, which corresponded to 50% RH at around 19.5 °C. The reason for this different setting was to keep the indoor RH no lower than 50% RH, corresponding to 6% MC on wood paneling, which is the minimum moisture content that can be measured by electric moisture pins on wood paneling.

The stability of ventilation air conditions is an important factor in the test set up, which could influence further data analyses. It can be observed from Figure 3.5 that RH and T of supply air and the ventilation rate of return air are very stable throughout the test run. The supply air conditions for all cases are listed in Table 3.5. It shows that the HR of supply air achieved is in the range of 4.67-4.99 g/kg-dry air for cases using gypsum board (cases 1-12), and 6.91-7.28 g/kg-dry air for cases using wood paneling and furniture (cases 13-29). The HR variation of supply air is less than 0.3 g/kg-dry air, while the deviation of the ventilation rate is less than 0.08 ACH.

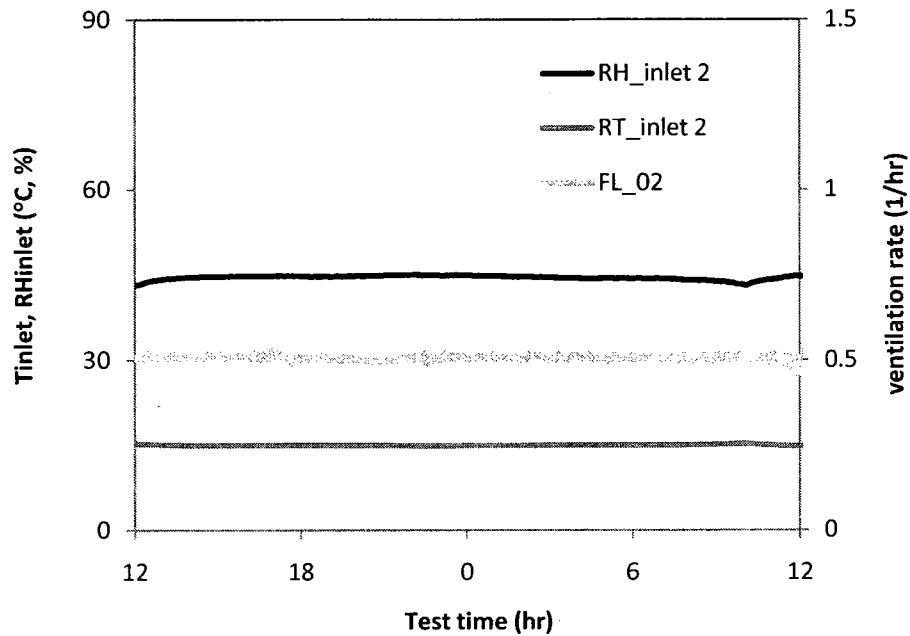


Figure 3.5. Example of ventilation air conditions (RH, T, and ACH) in case 1.

Table 3.5. The variation of supply air conditions.

Case No.	HR (g/kg dry air)	ACH (/hr)	Case No.	HR (g/kg dry air)	ACH (/hr)
1	4.69 ± 0.17	0.50±0.04	13	7.08±0.25	0.50±0.03
2	4.66 ± 0.22	0.50±0.02	14	7.18±0.24	0.50±0.03
3	4.68 ± 0.30	0.76±0.08	15	7.01±0.27	0.75±0.03
4	4.68 ± 0.12	0.76±0.08	16	7.03±0.28	0.75±0.03
5	4.99 ± 0.10	1.02±0.05	17	6.95±0.31	0.33±0.01
6	4.99± 0.21	1.02±0.06	18	6.98±0.15	0.33±0.01
7	4.84± 0.10	0.33±0.01	19	6.91±0.28	0.50±0.05
8	4.85± 0.18	0.33±0.01	20	6.91±0.28	0.51±0.05
9	4.86±0.09	0.52±0.01	21	6.95±0.41	0.51±0.01
10	4.86±0.27	0.52±0.03	22	6.95±0.34	0.51±0.10
11	4.86±0.24	0.52±0.02	23	7.01±0.19	0.50±0.05
12	4.67±0.18	0.52±0.02	24	7.00±0.16	0.50±0.03
			25	7.01±0.16	0.50±0.01
			26	7.01±0.06	0.51±0.10
			27	7.10±0.12	0.51±0.02
			28	7.10±0.12	0.51±0.02

### **3.4 Equipment**

#### **3.4.1 Moisture generation equipment**

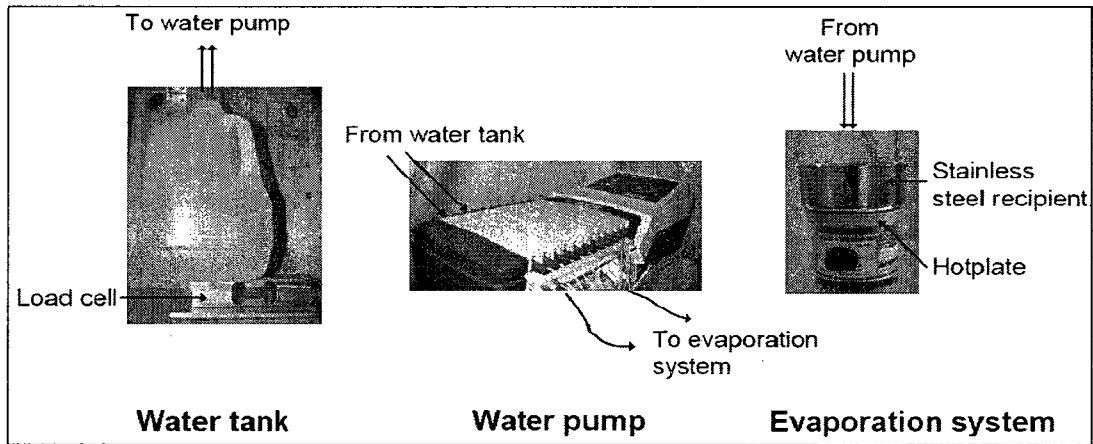
The bedroom scenario was simulated as a 10-hour of moisture generation at two rates of  $4.6 \text{ g/hr m}^3$  (100 g/hr) and  $2.3 \text{ g/hr m}^3$  (50 g/hr) followed by a 14-hour period of no moisture generation. This profile is based on the literature review of moisture sources in houses in Section 2.1.1. In addition, to further analyze the impact of short term moisture generation regime, cases with 200 g/hr for two hours moisture generation followed by a 22-hour period of no moisture generation were tested. The moisture generation rates used for all cases are listed in Table 3.2 and 3.3.

A moisture generation setup was located in the center of the rooms and represented one single source at 0.45 m height (as shown in Figure 3.2), with the exception of cases with furniture (Figure 3.15).

Components of the moisture generation setup are shown in Figure 3.6. Water was pumped (Multichannel cartridge pump: model Watson-Marlow Sci-Q205, Thermo Scientific) from the water tank, which was located in the buffer room, through thin plastic tubes ( $\phi 1/16''$ ) and dripped onto a pot, which was placed on a hot plate (Micro Hotplate: model 120, Thermo Scientific; electrical heater with capacity control), located in the centre of the test room. Water droplets evaporated immediately and vapor dispersed into the indoor air as soon as the drops touched the pot.

The weight of the water tank was monitored continuously by a load cell (SCAIME type AG, range 2.5 kg, accuracy of  $\pm 0.025\%$ ) underneath. The weight of the water tank was

also recorded manually by a scale (Denver Instruments, TR 4102,  $4100 \pm 0.01$  g) before and after moisture generation in the cases using wood paneling to verify the measurements from load cells. It is found that the moisture generation measured by two methods (load cell and manually) has a maximum difference of 2.3% and less than 1% difference in most cases, as shown in Table 3.6. Using this system, the amount of water added into the moisture balance of the test room can be controlled and monitored precisely.

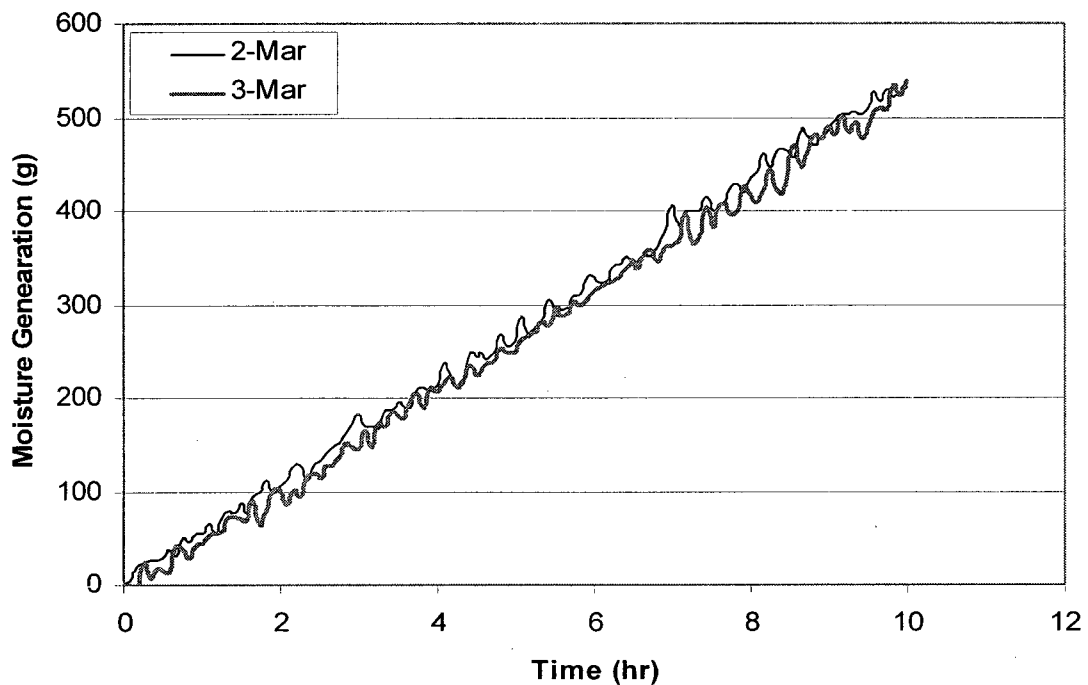


**Figure 3.6. Photo of moisture generation components.**

**Table 3.6. Comparison of the moisture generation rates measured by load cell and manually.**

Case No.	Measured by load cell (g/hr)	measured manually (g/hr)	Difference (%)
13	96.6	94.4	2.3
14	101.0	98.9	2.1
15	96.8	96.0	0.8
16	101.6	99.5	2.0
17	44.4	44.9	-1.2
18	44.6	44.8	-0.4
19	55.5	55.5	0.0
20	54.7	54.4	0.6
21	188.3	188.6	-0.1
22	192.7	190.8	1.0

The reliability of the system was tested. When the water pump was shut down, the water stopped dripping from the pipe immediately and water filled the plastic tubes. Once the water pump was started back, the dripping began right away. Also the repeatability of daily moisture generation in each test run is double checked by computing moisture load profile for each test day. Figure 3.7 shows an example of moisture generation profile in two successive days.



**Figure 3.7. Moisture loading in two successive days (measured by load cell).**

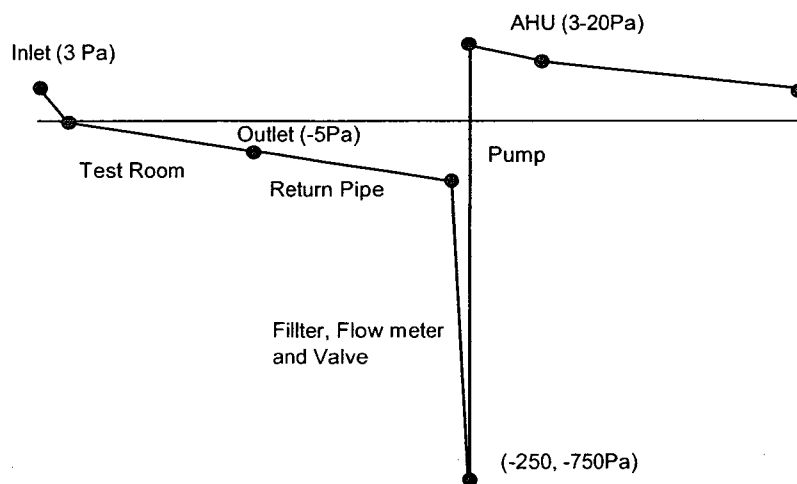
### 3.4.2 Ventilation system

The ventilation system was a closed-loop system, in which the supply air was taken directly from the test room and treated by an air handling unit (AHU) and then the

conditioned air was sent back to the test room. The ventilation rates investigated were  $0.3 \text{ hr}^{-1}$ ,  $0.5 \text{ hr}^{-1}$ ,  $0.75 \text{ hr}^{-1}$ , and  $1 \text{ hr}^{-1}$ .

A circulation air pump (6) (Gast regenerative blower), as shown in Figure 3.10, was installed on the return air pipe to generate a slight negative pressure in the test rooms ( $-5 \text{ Pa}$ ), thus avoiding exfiltration of the humid indoor air. The pressure of the AHU box was positive and highly depending on the ventilation rate. In Table 3.7, the pressures of the AHU box at different ventilation rates are listed.

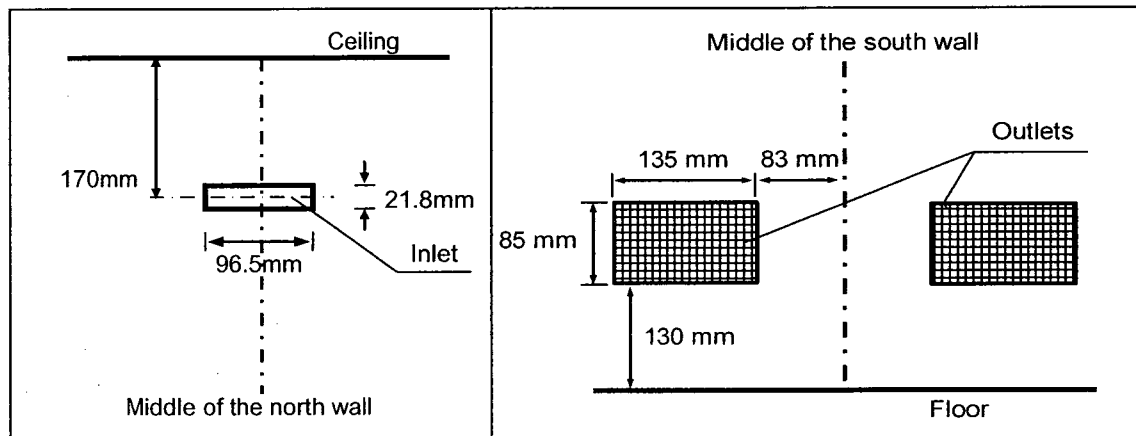
The air pressures (e.g. pressure differentials with respect to the lab air pressure) varied along the ventilation system loop, as shown in Figure 3.8. Precautions were taken to seal all the ventilation components and pipes to avoid air leakage. The segments of the air filter, flow meter (laminar flow element), and flow rate adjusting valve were assembled with PVC plumbing pipes and were well sealed at joints with PVC glue or gasket. The air pump was placed inside the AHU box to nullify the effect of its high pressure drop (gain) and any air leakage from the pump.



**Figure 3.8. Pressure distribution diagram of the ventilation system.**

**Table 3.7. Operation pressure of AHU at different ventilation rates.**

Ventilation Rate (ACH)	Operation Pressure of AHU Box (Pa)	
	Room 1	Room 2
0.3	3.7	N/A
0.5	7.1	7.5
0.75	N/A	11.9
1.0	N/A	22.2



**Figure 3.9. Location and dimensions of inlet and outlets.**

The air pressures (e.g. pressure differentials with respect to the lab air pressure) varied along the ventilation system loop, as shown in Figure 3.8. Precautions were taken to seal all the ventilation components and pipes to avoid air leakage. The segments of the air filter, flow meter (laminar flow element), and flow rate adjusting valve were assembled with PVC plumbing pipes and were well sealed at joints with PVC glue or gasket. The air pump was placed inside the AHU box to nullify the effect of its high pressure drop (gain) and any air leakage from the pump.

The air inlet had a rectangular section with the dimension of 96.5 mm (W) and 21.8 mm (H). The inlet was installed in the middle plane of the north wall at 2.26 m height (distance between the floor and the center of the inlet). Two rectangular outlets were



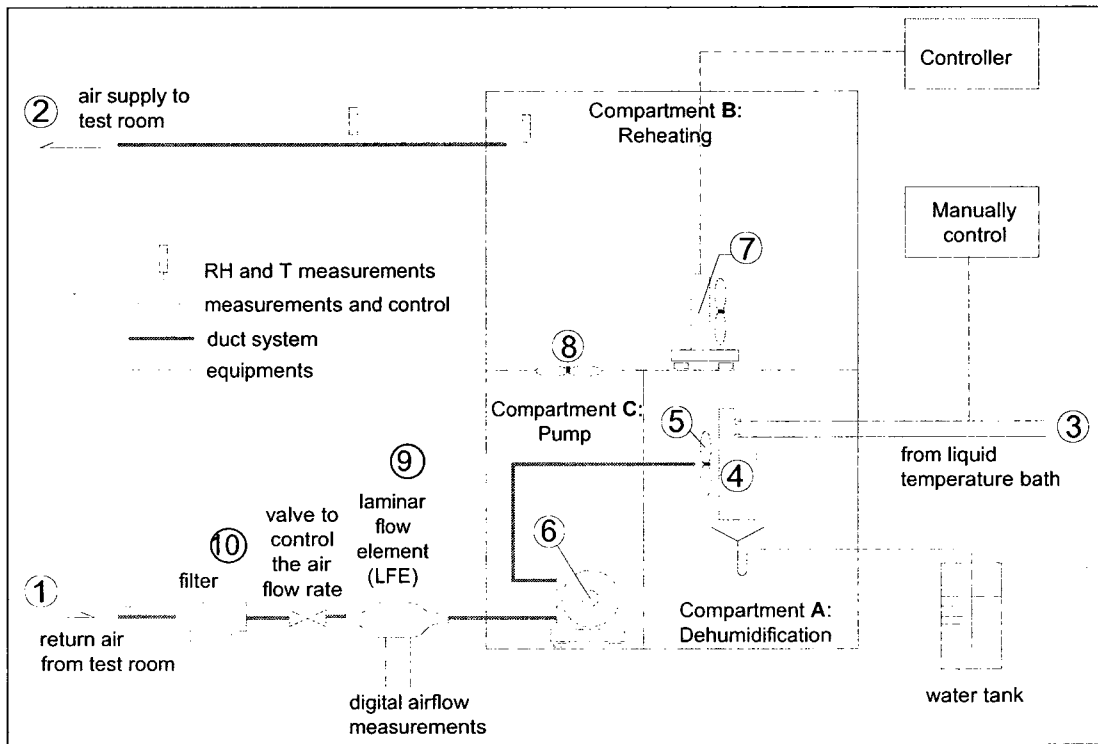
placed on the south wall with the dimension of 135 mm (W) and 8 mm (H). The location of the inlet and outlet are shown in Figure 3.9.

An electrical baseboard heater was placed at the lower portion of the entrance door (as shown in Figure 3.2) and was controlled by a thermostat inside of the test room to maintain a desirable temperature in the test room. The thermostat was an electronic type and regulated the heater power with a time proportion algorithm (with a duty cycle of approximately 30 s). Since the temperature was distributed non-uniformly within the test room, the set point temperature of the thermostat is used as a nominal value.

### **3.4.3 AHU (Air Handling Unit)**

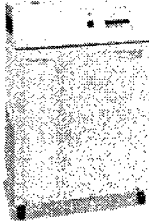
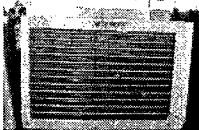
The Air Handling Unit (AHU) was used to control and maintain the conditions of the supply air. A diagram of the AHU is shown in Figure 3.10. A chilled-water temperature bath (NESLAB HX300w from Thermo Scientific) provided cold water for the liquid-air heat exchanger (4) that served as a dehumidifier. The dehumidifier treated the return air to a very low and constant temperature (4 or 8 °C), accompanied by condensation on the coils of the heat exchanger. An air circulation fan (5) within the dehumidifier had a large flow rate to assure the air leaving the dehumidification compartment to be maintained at a constant humidity ratio. This guaranteed a constant humidity level of the supply air. The variation of the humidity ratio during test was only 0.3 g/kg·dry air at maximum. The heater (7) in the compartment B with a PID (proportional, integral and differential) controller reheated the air to the set temperature with the deviation of 0.61 °C during testing. The small axial fan (8) in the middle divider circulated a small fraction of the

cooled air from the dehumidification compartment (compartment A) to the compartment C in order to avoid overheat of the air pump.

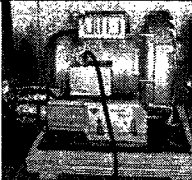

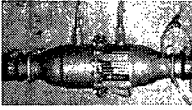
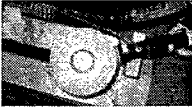


**Figure. 3.10 Components of AHU (Air Handling Unit).**

**Table 3.8. Equipments or instruments used in AHU system.**

Equipments	Descriptions	Photos
③ Liquid temperature bath	NESLAB HX300w, Thermo Scientific	
④ Dehumidifier	Modified from AC unit	

---

⑥ Air pump	GAST Regenerative Blowers R3105	
⑦ Heater	1kW with a time proportional control at 2 second duty cycle	
⑨ Laminar flow element	50 MC2-2, (100cfm) with 2110F smart flow gauge $\pm 1\%$ reading	
⑩ Filter	Inlet filter AJ126C	

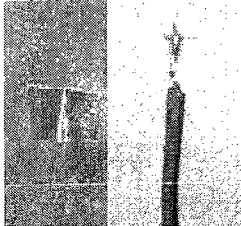
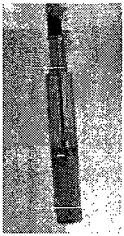
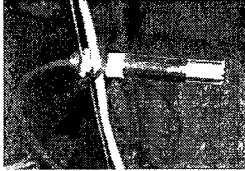
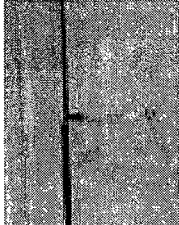
---

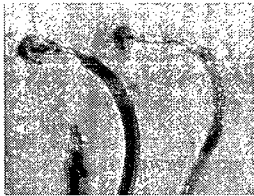
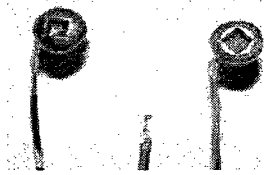
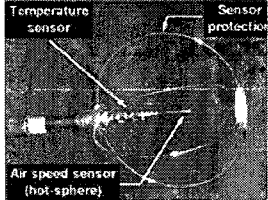
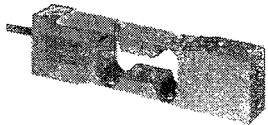

The condensed water was collected and monitored with a load cell (SCAIME type AG, 1 kg, accuracy  $\pm 0.25$  g). Given that a constant thin layer of condensation water film accumulated during pre-conditioning before the second day test, the water flowing down from the coil corresponds to the water actually taken out from the air by the condensation. This is the most significant feature in this design. Using this method, the amount of water condensed from the return air can be recorded easily and accurately. This amount of water represented the moisture difference between return air and supply air and was the moisture removal part by ventilation and air leakage from AHU box. The calculations and applications of this amount of water in the estimation of the moisture buffering effect will be presented in detail in Chapter 4. The equipment and instruments used in AHU system are listed in Table 3.8.

### 3.5 Monitoring and measurements

The monitored parameters include the thermal and moisture responses of the east wall and west wall, the surface temperature of floors and ceilings, the indoor environment conditions (temperature, RH and air speed), condition of the ventilation system, and moisture generating conditions. All the measurements were taken by the DAS (data acquisition system) at 5-min intervals. Additional details are provided by Vera et al. (2006 and 2007). The list of sensors and their description are presented in Table 3.9.

**Table 3.9. Sensors or instruments used in measurements**

Sensors or instruments	Application	Description	Photos
Thermocouples	Outdoor air (12), PVC siding (20), sheathing board (36), interior surface (72), compartments in AHU box (10)	Type T30 AWG, PVC insulated & jacketed, Accuracy: $\pm 0.3^{\circ}\text{C}$ .	
1% RH sensors	Centre of the room (2), inlets and outlets (4), AHU compartment B(2)	HMT333, Vaisala instruments Accuracy: $\pm 0.6\%$ RH(0-40% RH); $\pm 1.0\%$ RH (40-97%); $\pm 0.1^{\circ}\text{C}$ .	
2% RH sensors	Across the test rooms(64)	HMP50, Vaisala instruments Accuracy: $\pm 2\%$ RH (10- 90% RH) $\pm 0.5^{\circ}\text{C}$ .	
3% RH sensors	Stud cavity (36)	HMP50, Vaisala instruments Accuracy: $\pm 3\%$ RH (10- 90% RH) $\pm 0.6^{\circ}\text{C}$ .	

Moisture content by golden pins	Wood paneling (interior surface, 72) Plywood (sheathing, 36)	Transmitter: MTC-60 Delmhorst Instruments co., Accuracy: $\pm 2$ to $\pm 3\%$ MC	
Moisture content by stainless steel screws	Uncoated gypsum board (60)	Transmitter: MTC-60 Delmhorst Instruments co. Accuracy: $\pm 0.1\%$ MC	
Omni-directional anemometers	Close to the test walls (12) Inlet (2)	Probe HT412 Transducer: HT428, Sensor electronics. Accuracy: $\pm 0.02\text{m/s}$ or $\pm 2$ of reading (0-1m/s) $\pm 0.2$ °C.	
Load cells	Water tank (2)	SCAIME type AG2.5 kg, Scale-Tron Inc. Accuracy: 1/4000	
Load cells	Condensation collector (2)	SCAIME type AG1 kg Scale-Tron Inc. Accuracy: 1/4000	

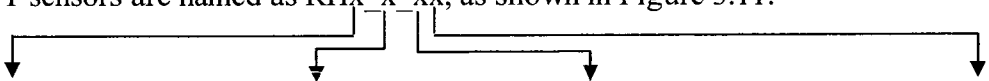
### 3.5.1 Outdoor environmental conditions

Temperature and relative humidity were controlled within the environmental chamber and monitored by two sets of RH & T sensors in the hot box and cold box.

### 3.5.2 Indoor conditions

There were totally 32 sets of RH & T sensors (2% RH accuracy, HMP 50, Vaisala Inc.) across each test room. Of these sensors, 9 sensors were placed along the west wall and 5 sensors were attached on the east wall (as shown in Figure 3.11) at heights of 0.13, 1.13, 1.80 and 2.26 m. An additional RH & T sensor with 1% accuracy in RH (HMT333, Vaisala Inc.) was installed in the center of the room at the height of 1.8m. The air speed was monitored by 12 anemometers (HT412-428, Sensor Electronic & Measurement Equipment, Poland) along the test wall (west wall), as shown in Figure 3.12.

The RH&T sensors are named as RHx<sub>x</sub>xx, as shown in Figure 3.11.

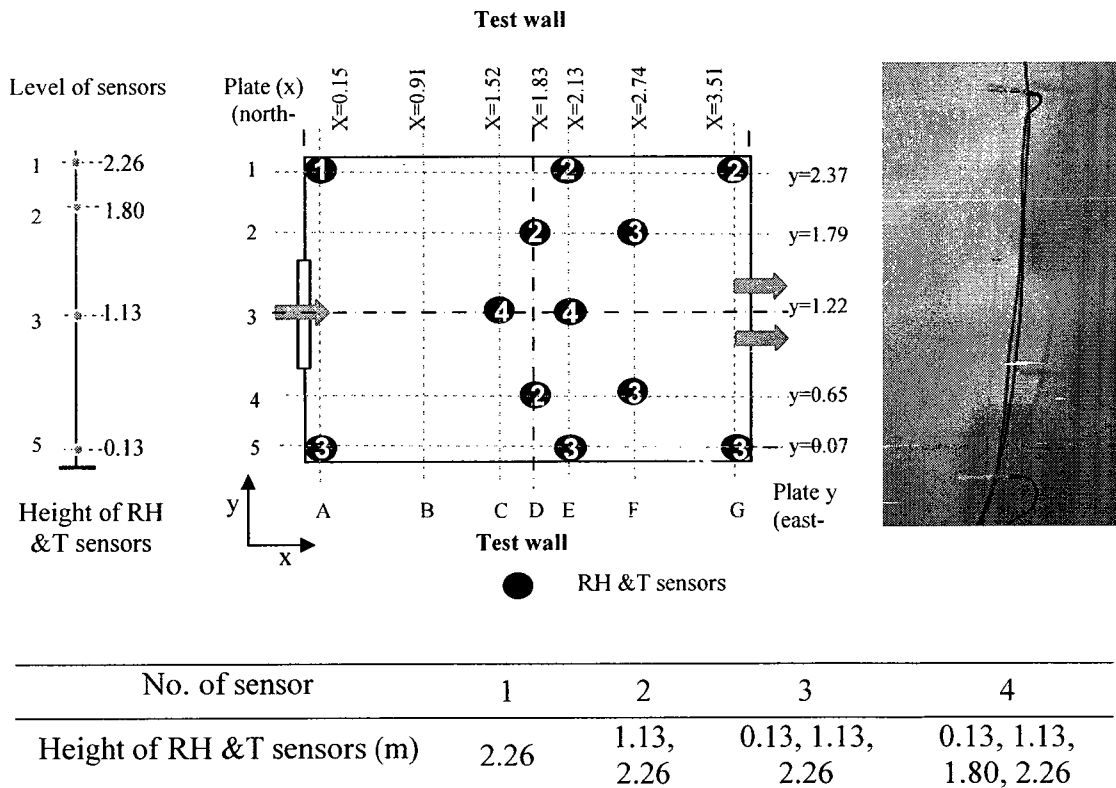


Number of test room; Letter of plane (east-west); Number of plate (south-north); level of RH & T sensors.

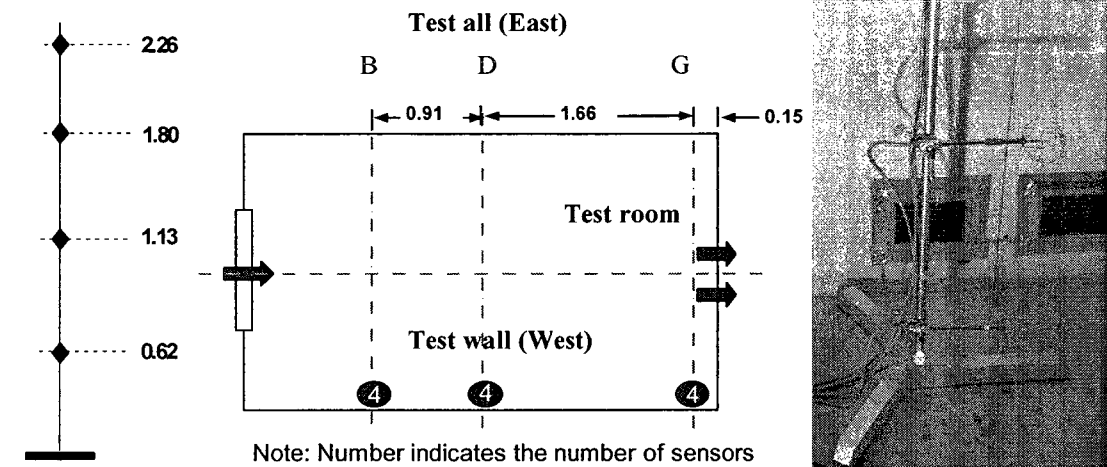
### 3.5.3 Hygrothermal conditions of building envelopes including surface materials

Temperature of outdoor air and exterior surface, temperature and moisture content on the sheathing board (18 sets), RH & T in the insulation cavity (18 sets) were measured by RH & T probes (HMP 50, Vaisala Inc, 3% accuracy) in each test room.

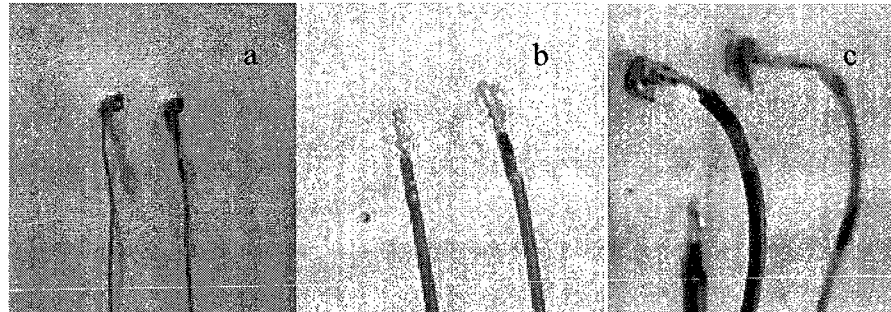
Three different types of moisture content installations were used in this experiment, as shown in Figure 3.13. On gypsum boards, stainless steel screws were inserted to around 5-8 mm deep (a). Screws instead of pins were used because screws can provide much tighter contact between the metal and gypsum. This tight contact is critical for moisture content measurement for gypsum board. Gold-plated copper pins were applied on the wood paneling (c). Both of these two types of probes aimed at measuring the maximum moisture content of an interior layer of the surface materials. Moisture pins attached on the surface materials were used to measure the surface moisture content (b). The location of moisture content sensors and the name of sensors can be found in Figure 6.3.



**Figure 3.11. Photo of RH sensor installation and sensor location diagram (dimensions are in meter).**



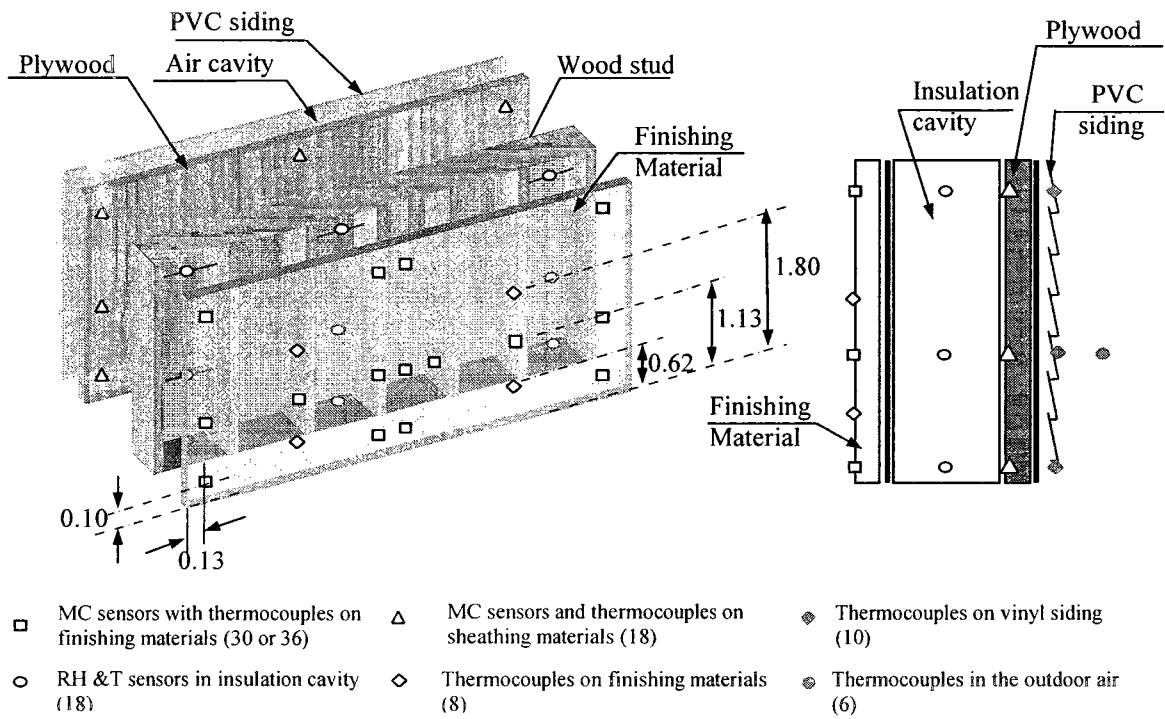
**Figure 3.12. Location of anemometers on pole and plan view (dimensions are in meter).**



**Figure 3.13. Three types of moisture content installation.**

**a: Screws on uncoated gypsum board, b: Surface measurement, c: Moisture pins on wood paneling**





**Figure 3.14. Locations of sensors through building envelope.**

### **3.5.4 Monitoring and control of the AHU and ventilation system**

One load cell (SCAIME type AG, 1.0 kg capacity,  $\pm 1/4000$  accuracy) was used to monitor the weight of the collected condensation water from the dehumidifier section (as shown in Figure 3.10). The conditions of supply and return air were recorded by two RH & T sensors ( $\pm 1\%$  RH and  $\pm 0.2$  °C accuracy, HMT333), inside the ventilation air ducts near the outlet and inlet. The ventilation rate was controlled by a manually adjusted valve before the circulating pump (see Figure 3.10), and measured by a laminar flow element (50MC) with the accuracy of  $\pm 1\%$  of the reading (inch water).

### **3.5.5 Monitoring of moisture generation rate**

The weight of the water tank in the moisture generation system was monitored by a load cell (SCAIME type AG, 2.5 kg,  $1/4000$  accuracy) underneath the tank. In addition, the tank was also weighted manually every day during no-moisture generation period to verify the load cell reading, as presented in Section 3.4.1.

### **3.5.6 Air leakage measurement**

Air leakage is a very important factor influencing the result of the test. Air leakage tests were carried out in two steps. In the first step test, the outlet of the test room was blocked, and the return air pipe was disconnected from the outlet. So the test room and the AHU box were pressurized at different pressures up to 50 Pa. The objective of this test is to identify the air leakage paths and put more efforts on sealing. In the second step test, the inlet was blocked. The test room was depressurized and the AHU box was pressurized during the test. The flow rates were kept very small to generate a negative pressure of test

room less than 10 Pa. The detail procedure can be found in Appendix D in the report submitted to the Annex 41 (Fazio, et al., 2007) in this thesis.

Based on the second step air leakage test, the air leakage rate as a function of pressure in test room was calculated. The operating pressure of the test room and the AHU box was measured during the test corresponding to different ventilation rates. The air leakage rates corresponding to different ventilation rates are presented in Table 3.10.

**Table 3.10. Air leakage rates under different ventilation rates.**

Room 1		Room2		Ventilation Rate (ACH)
Air leakage (kg/hr)	Pressure of test room (Pa)	Air leakage (kg/hr)	Pressure of test room (Pa)	
0.30	-1.7	N/A	N/A	0.3
0.39	-1.9	0.41	-2.1	0.5
N/A	N/A	0.65	-3.5	0.75
N/A	N/A	1.21	-6.1	1

### **3.6 Furniture and its location in test rooms**

Tests studying the moisture buffering effect of furniture were carried out in case 23-28.

The description of the furniture is listed in Table 3.11. The plan view of the fully furnished room is shown in Figure 3.15.

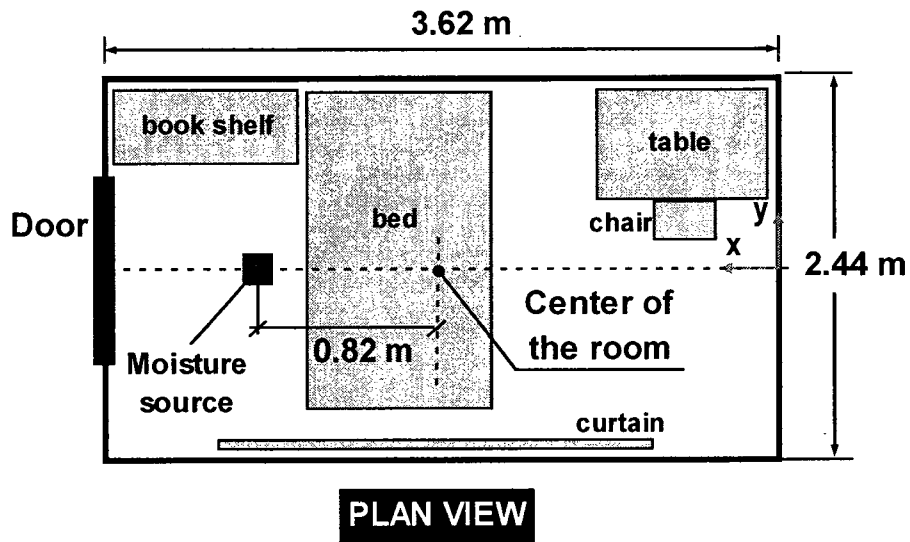
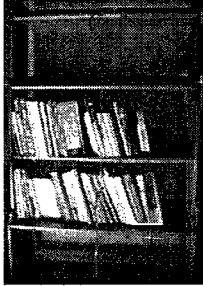
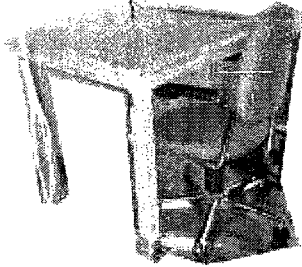
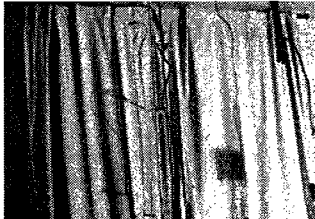
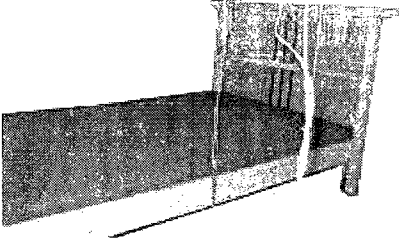


Figure 3.15 Location of furniture for fully furnished room.

Table 3.11. Description of furniture added in three steps.

Test Steps	Furniture	Materials	Dimensions or Area	Picture
1	Book shelf	Solid pine, stain, clear acrylic lacquer	1.0 m (L) 0.32 m (W) 1.98 m (H)	
	Books	Old and new books	1.16 m <sup>2</sup>	
2	Table	Varnished wood	0.56 m <sup>2</sup>	
	Chair	Polyurethane foam Cushion covered with fabric	0.21 m <sup>2</sup>	
	Curtain	Cotton	6.90 m <sup>2</sup>	

3	Bed	Polyurethane foam	2.3 m <sup>2</sup>	
	Mattress	Solid wood		
	Frame			

In summary, totally 28 cases were carried out in this full-scale experiment study. Different moisture generation rates and schemes, ventilation rates, and surface materials were the parameters investigated. The design of the moisture generation equipment and of the AHU allowed precise monitoring of the moisture produced and moisture taken from the return air. HAM response of building envelope, conditions of indoor air, and supply air were monitored.

## CHAPTER 4

### MOISTURE BALANCE ANALYSES

Moisture balance is established in experimental study and whole building HAM simulations. A new index, maximum accumulated moisture buffering value (MAMBV), is developed and used to quantitatively evaluate the impact of parameters on moisture buffering capacity of materials. The parameters investigated include ventilation rate, supply air conditions, moisture generation rate and regime, outdoor conditions, volume rate, material properties (moisture capacity and vapor permeability), and the addition of furniture.

#### 4.1 Moisture Balance and its components in experimental study

##### 4.1.1 Moisture balance

As introduced in Chapter 2, the moisture balance can be expressed as

$$M_a(t) = -M_b(t) - M_{vl}(t) - M_d(t) + G(t) \quad (4.1)$$

By re-arranging Eq. 4.1 the amount of moisture absorbed or released by hygroscopic materials at any time (t), can be calculated as:

$$M_b(t) = -M_a(t) - M_{vl}(t) - M_d(t) + G(t) \quad (4.2)$$

The accumulated moisture change in the room air ( $M_a$ ) is proportional to the change in the humidity ratio ( $w_a$ ):

$$M_a(t) = \rho V [w_a(t) - w_a(0)], \quad (4.3)$$

where  $\rho$  is the room air density ( $\text{kg/m}^3$ ),  $V$  is the volume of the room ( $\text{m}^3$ ), and  $w_a$  is the average humidity ratio of room air ( $\text{g/kg}$  of dry air), obtained from 32 sets of RH & T sensors.

The vapor diffusion can be calculated by

$$M_d(t) = A \times \int_0^t \frac{1}{R_{vi}} [P_{vi}(\tau) - P_{vo}(\tau)] d\tau \quad (4.4)$$

where  $P_{vi}$  and  $P_{vo}$  are vapor pressures of indoor and outdoor air (Pa);  $R_{vi}$  the total vapor resistance ( $\text{Pa}\cdot\text{m}^2/\text{g}$ ) of the wall components, and  $A$  is the area of wall surfaces ( $\text{m}^2$ ).

The moisture generation ( $G$ ) and moisture removal by ventilation and air leakage ( $M_v$ ,  $M_l$ ) are critical parts of this calculation in terms of the amount of moisture involved. The moisture generation  $G$  was recorded by a load cell beneath the water tank (see Section 3.4.1). The calculation on moisture removal by ventilation and air leakage is introduced in the following section.

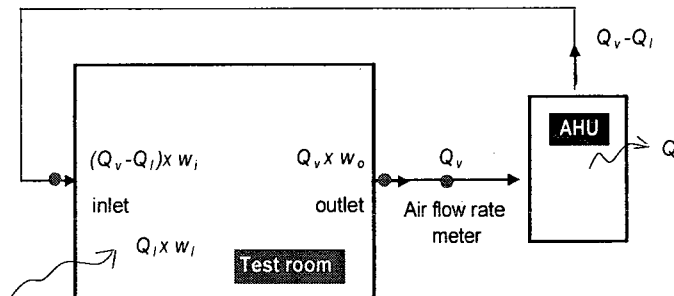
#### **4.1.2 Moisture removed by ventilation and air leakage**

##### ***RH method***

The moisture removed by ventilation and air leakage can be calculated by equation 4.5: (as shown in Figure 4.1):

$$M_{v,i}(t) = \underbrace{\int_0^t [Q_v \cdot w_o(\tau) - (Q_v - Q_l) \cdot w_i(\tau)] d\tau}_{\text{Ventilation}} - \underbrace{Q_l w_l \cdot t}_{\text{Infiltration}} \quad (4.5)$$

where  $Q_v$  is the mass air flow rate at the outlet (kg/hr),  $Q_l$  the infiltrating air leakage rate (kg/hr), and their difference,  $(Q_v - Q_l)$ , is the air flow rate through the inlet. The three terms,  $w_o$ ,  $w_i$  and  $w_l$  (g/kg of dry air) are the humidity ratios of outlet air, inlet air and the "outdoor" (environmental chamber) air, respectively. The values of the humidity ratio are calculated based on the RH values and temperatures obtained through the RH probes installed in the ducts near the inlet and outlet. This calculation based on data from RH probes is referred to as the *RH method*.



**Figure 4.1. Air mass balance and moisture involved in ventilation and air leakage**

(Air flow rates are in kg per hour, AHU is short for Air Handling Unit).

The accuracy of using the RH method to calculate the moisture removed by ventilation and air leakage is highly depending on the accuracy of RH sensors and flow meter (laminar flow element) used in the experiment. Even though they had very high accuracies ( $\pm 1\%$  for RH,  $\pm 0.2$  °C for temperature and  $\pm 1\%$  of reading for air flow rate), the error would still be carried on and accumulate over the calculation time span (24 hours) to the final estimation of the moisture buffering capacity. In addition, since the



amount of moisture absorbed/released (buffering) by interior finishing is only a small portion of the total moisture that is involved in the transport and exchange, the experimental error can be large for estimating the moisture buffering capacity.

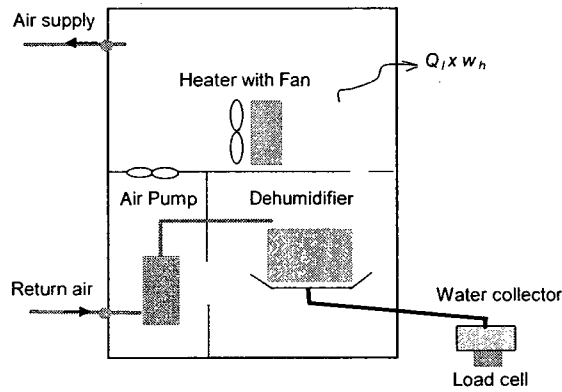
### ***Condensed water method***

To overcome this shortcoming, a close-loop AHU is designed. The amount of moisture removed by ventilation is directly measured by weighing the condensed water collected from the cooling coils by a load cell, as described in Section 3.4.3. This condensed water collected plus the moisture leaking out from the AHU system represents the moisture difference between the supply air and the return air, and is deemed to be the accumulated moisture removed by ventilation (as shown in Figure 4.2). The accumulated moisture removal by ventilation and air leakage can thus be calculated by:

$$M_{vi}(t) = C(t) + Q_l(w_h - w_l) \cdot t \quad (4.6)$$

where  $C(t)$  is the condensed water over time;  $w_h$  is the humidity ratio of the air exiting the AHU system (g/kg of dry air); and  $w_l$  is the humidity ratio of the air in the environmental chamber (g/kg of dry air).

This method of using the amount of condensed water to determine the moisture removed by ventilation air is referred to as the *condensed water method*. The accumulative error due to the error in flow rate measurement is not of concern in this method, since the weight of condensed water is independent from the air flow measurement. Consequently, this method should be more accurate than the RH method in terms of accumulated values during a one-day cycle, which will be discussed in Section 4.2.1.



**Figure 4.2. Water collector and condensed water method.**

Due to the fact that the film of condensed water on the coil surface was fully developed and reached (quasi) steady-state after the first day of testing and water condensed from the second day of the test would all drip down to the collector underneath. Hence, the error caused by the water film forming on the coil surface in the first day can be neglected from the second day of the test.

#### **4.1.3 Correction: baseline correction**

The tests were performed in pairs. In the non-hygroscopic test of each pair (by covering the east and west walls with polyethylene sheets), a moisture correction term,  $e$ , is determined from the measured moisture parameters, as in:

$$e(t) = -M_v(t) - M_d(t) - M_a(t) + G(t) \quad (4.7)$$

There are always measurement errors in experimental studies, even though intensive care was taken. Since the paired tests (a non-hygroscopic test and a moisture buffering test) were carried out under the same test conditions, this correction term is assumed to be the same for both tests.

The actual accumulated moisture buffering value,  $M_b^*$ , of a hygroscopic test can then be calculated as:

$$M_b^*(t) = M_b(t) - e(t) \quad (4.8)$$

where  $M_b$  is the moisture buffering value (g) estimated directly from the measurements in the hygroscopic test using Eq. 4.2, and  $e$  is the moisture correction term obtained from the paired non-hygroscopic test using Eq. 4.7. This correction approach is referred to as the baseline correction.

#### **4.1.4 Maximum amount of moisture buffered by surface materials**

The accumulated moisture buffering value ( $M_b^*$ ) can be plotted as a function of time using Eq. 4.8. The maximum accumulated moisture buffering value (MAMBV) in a daily moisture cycle, is defined as the maximum value taken from the curve shown in Figure 4.5, representing the moisture buffering capacity of hygroscopic materials in a specific scenario tested in this large-scale experimental study. This value is used in the following data analysis section to compare and evaluate the impact of parameters (surface material, ventilation rates, moisture generation rates and schemes, supply air conditions, furniture) on the moisture buffering effect in different cases.

## **4.2 Observation and data analyses of the full-scale experiment**

### **4.2.1 RH method vs. condensed water method**

The average indoor HR (humidity ratio) for case 1 (uncoated gypsum board) and case 2 (polyethylene) tested with 0.5 ACH and 100 g/hr moisture generation rate for 10 hours is

shown in Figure 4.3. The moisture buffering effect is indicated by the reduction of indoor HR.

The moisture input should be equal to the sum of the moisture removed by ventilation and air leakage, and vapor diffusion through the building envelope at the end of each moisture loading cycle, since the indoor condition returned back to the initial condition. However, as shown in Figure 4.4, there are 37.0g and 111.7g difference between the  $M_v + M_l + M_d$  and  $G$  by using two different methods. These differences are due mainly to the errors from air flow rate measurements using RH method, and errors from water collection using the condensed water method.

It is also noticed that the  $M_v + M_l + M_d$  using condensed water method is 74.6g closer to the total moisture generation compared with the value using the RH method at the end of one moisture loading cycle. From this observation, the condensed water method can be considered more accurate.

Another phenomenon observed at the beginning of the test as shown in Figure 4.4 is that the  $M_v + M_l + M_d$  value obtained from the condensed water method is smaller than that obtained from the RH method. This difference is mostly due to a delay that occurs in the condensed water collection process. This delay is always within 20 minutes. However, for the reason that the same delay occurs in the non-hygroscopic case, the error due to this delay can be corrected by the baseline method. So the error carried by this delay can be ignored.

$M_b^*$  thus can be calculated based on the condensed water method, as shown in Figure 4.5. The maximum value of this curve is the MAMBV for this case. The calculations in this

thesis are performed using the condensed water method.

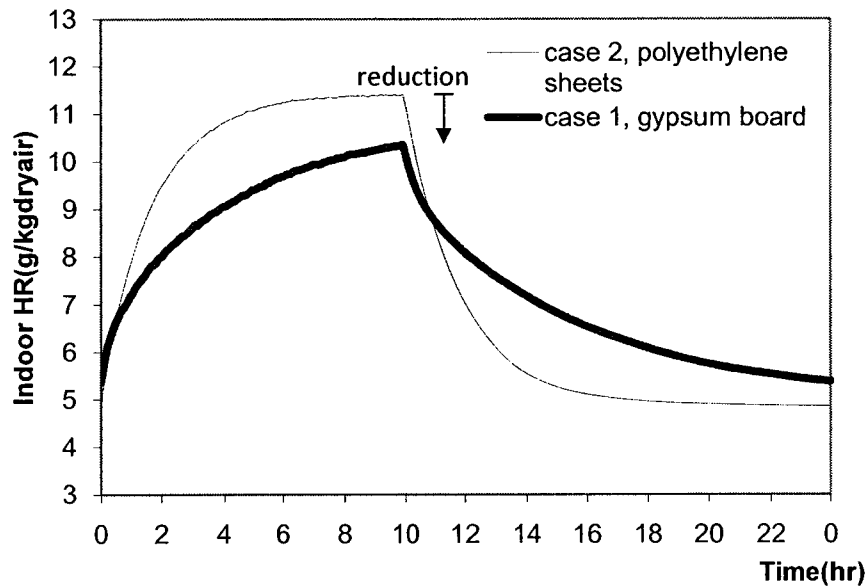


Figure 4.3 Indoor HR in case 1 and case 2.

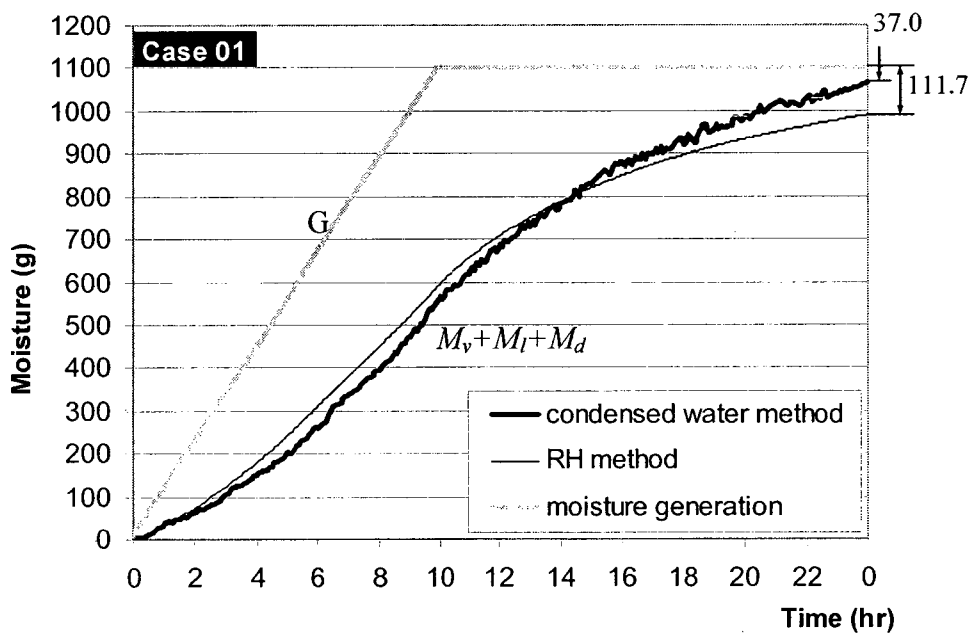
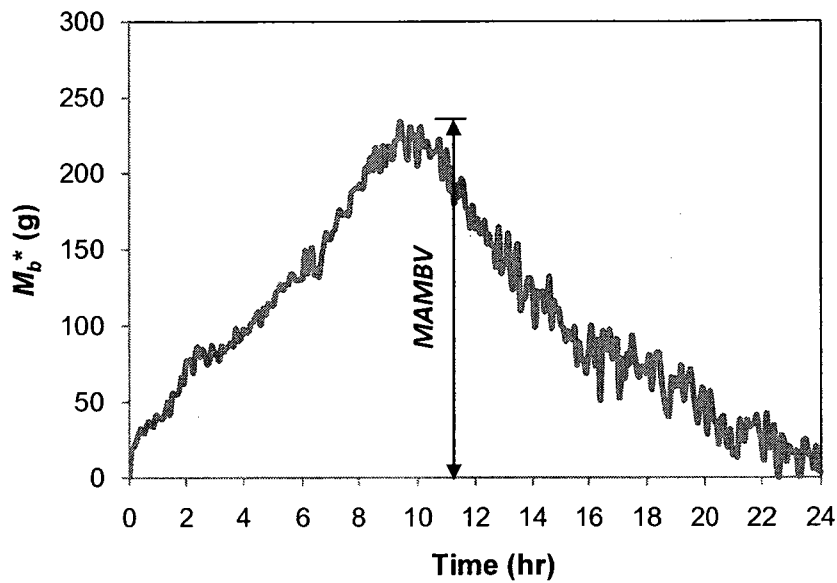


Figure 4.4. Calculation of  $M_v + M_l + M_d$  and moisture generated in case 1.



**Figure 4.5. MAMBV and  $M_b^*$ (accumulated moisture buffering value) in case 1.**

#### **4.2.2 Impact of ventilation rates**

The typical comparison of the moisture buffering effect 0.5, 0.75 and 1 ACH is shown in Figure 4.6. The moisture buffering effect is reduced with the increase of ventilation rate by comparing the reduction range of the indoor HR.

From Figure 4.7, it can be noted that MAMBV are 226 g ( $13.8 \text{ g/m}^2$ ), 155 g ( $8.8 \text{ g/m}^2$ ), and 114g ( $6.4 \text{ g/m}^2$ ) at 0.5, 0.75 and 1 ACH, respectively. With the increase of the same 0.25 ACH, the MAMBV decreases by  $5\text{g/m}^2$  from 0.5 to 0.75 ACH, while  $2.4/\text{m}^2$  from 0.75 to 1.0 ACH. The reduction of the moisture buffering is not proportional to the increase of the ventilation rate and the reduction rate increases as the ventilation rates decreases. The maximum moisture content measured on the surface materials is higher at a lower ventilation rate, following the same trend as indoor humidity, as shown in Figure 4.8. The impact of larger range of ventilation rates is discussed in the Section 4.4.1.

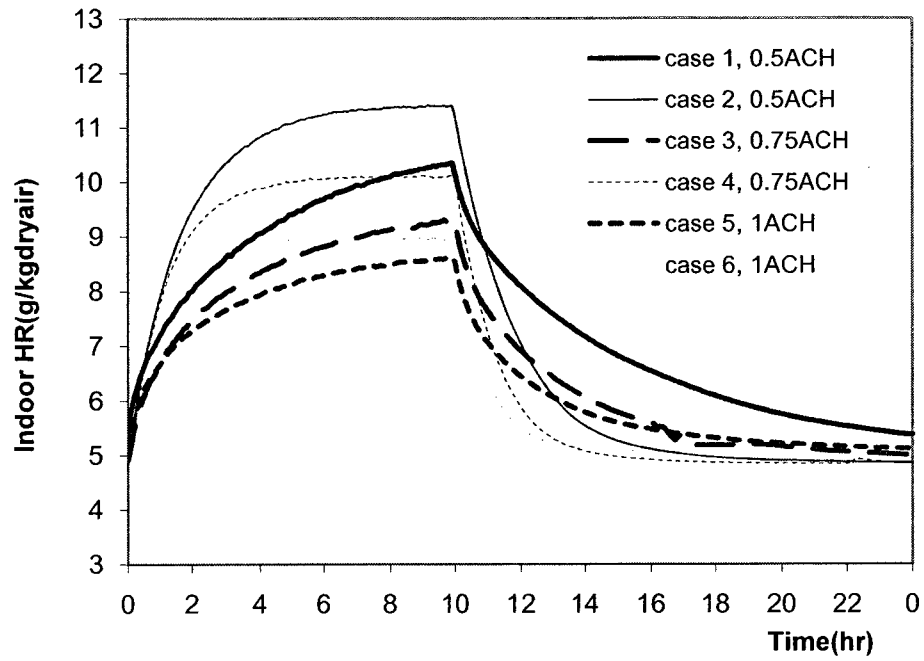


Figure 4.6. Indoor HR at different ventilation rates for cases using uncoated gypsum board.

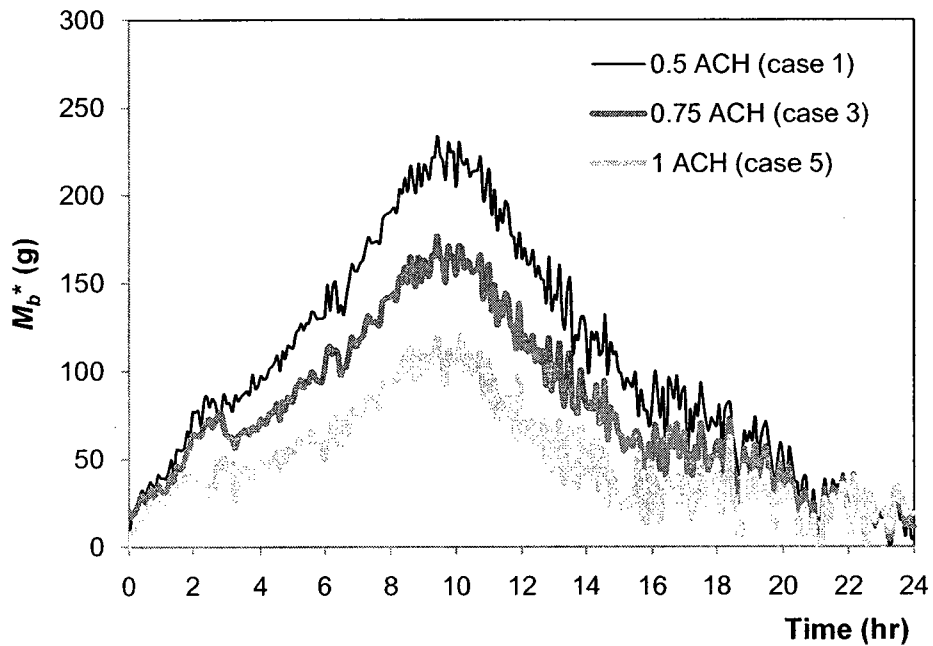
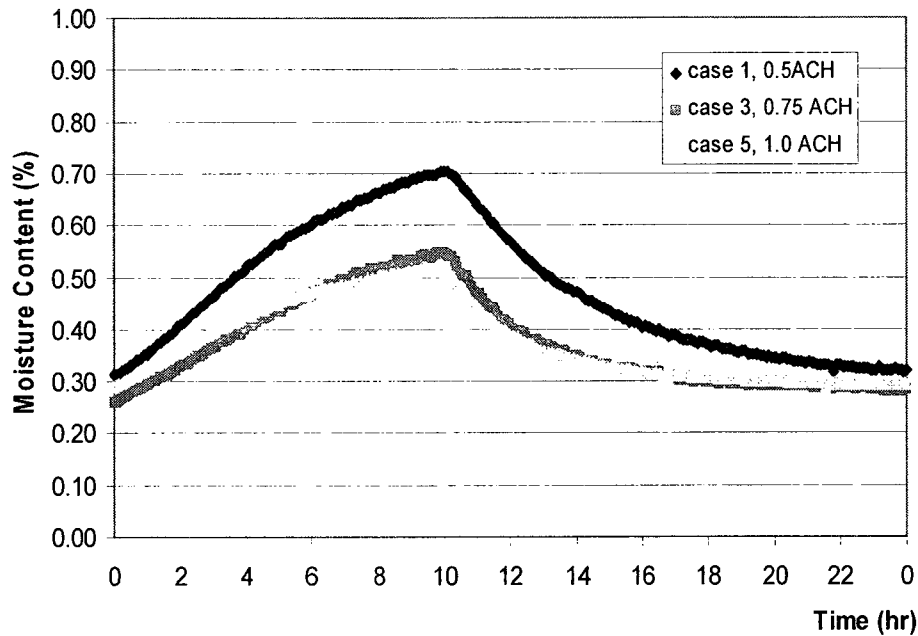


Figure 4.7.  $M_b^*$  at three ventilation rates for cases using uncoated gypsum board.



**Figure 4.8. Example of maximum moisture content measured on uncoated gypsum board at different ventilation rates.**

#### **4.2.3 Impact of moisture generation rate and schemes**

Moisture generated in the indoor environment, providing the moisture sources for the moisture buffering, influences moisture buffering effect significantly. The more moisture generated, the more significant moisture buffering effect.

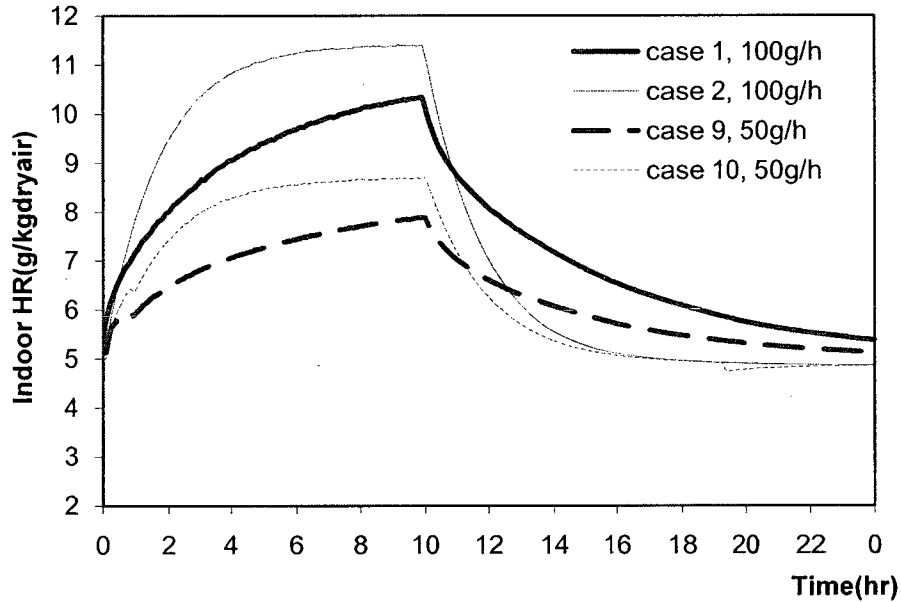
As shown in Figure 4.9, it is difficult to quantitatively compare the moisture buffering potential between hygroscopic cases and non-hygroscopic cases by comparison indoor RH variation. However, it is very easy to make the direct comparison by using MAMBV, as presented in Table 4.1. For example, the moisture buffering capacity (MAMBV) in case 9 is reduced to almost half of the MAMBV in case 1 when the moisture generation rates in case 9 is cut down to half of that in case 1. The impact of moisture generation rate



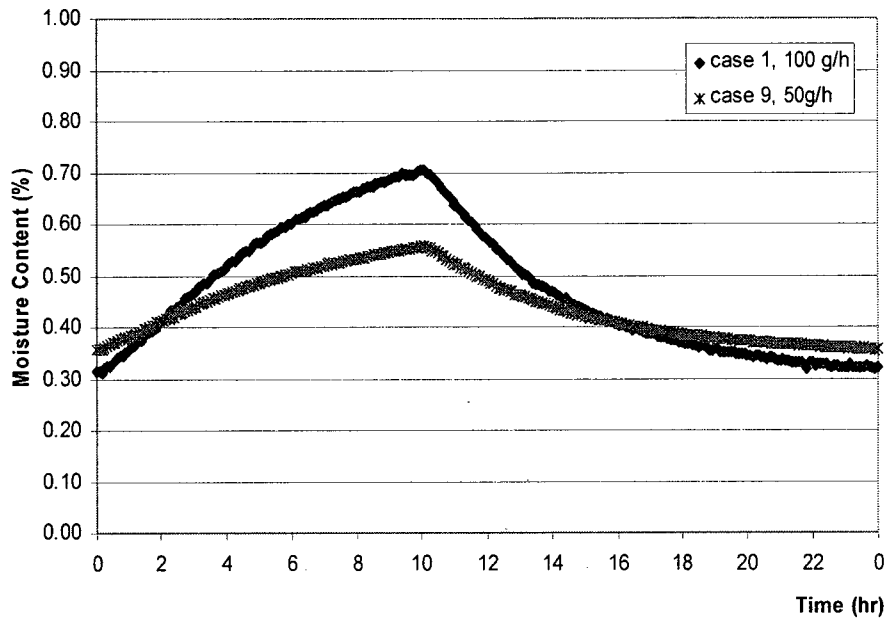
on the MAMBV in case 13 is similar to that in case 19. The impact of moisture generation rate can also be observed from the variation of maximum moisture content, as shown in Figure 4.10. Higher moisture buffering can be detected in case 1 as shown by the larger variation of MC when it is compared to case 9.

**Table 4.1. Maximum accumulated moisture buffering value under different moisture generation rates.**

Case No.	Case 1	Case 9	Case 13	Case 19
Moisture generation rate (g/hr)	103.6	53.3	96.6	55.5
MAMBV (g)	226	113	236	141



**Figure 4.9. Indoor HR under two different moisture generation rates (case 1 and 9 are hygroscopic cases, case 2 and case 10 are non-hygroscopic cases) in the cases using uncoated gypsum board.**

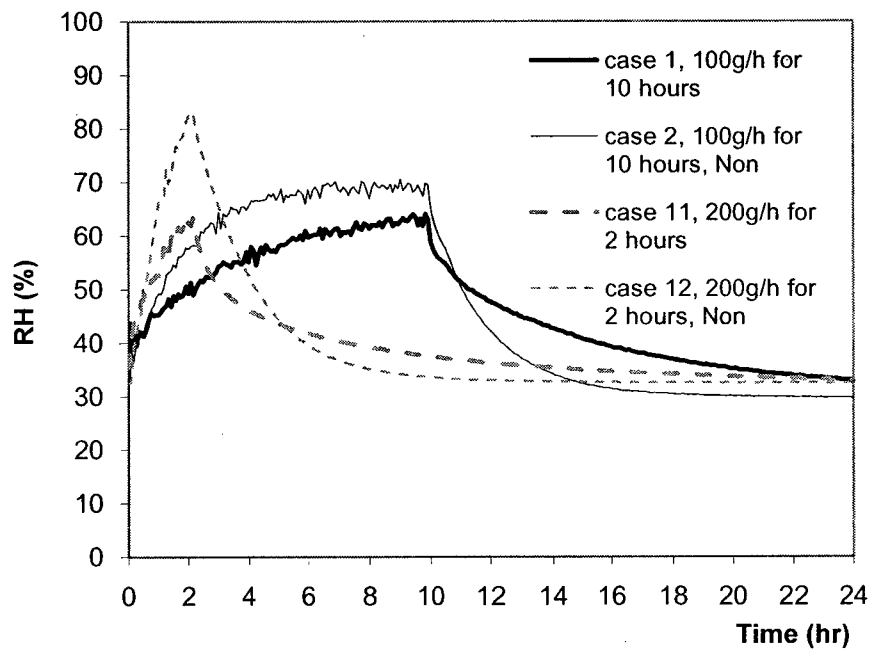


**Figure 4.10. Example of maximum moisture content measured on uncoated gypsum board, at two different moisture generation rates.**

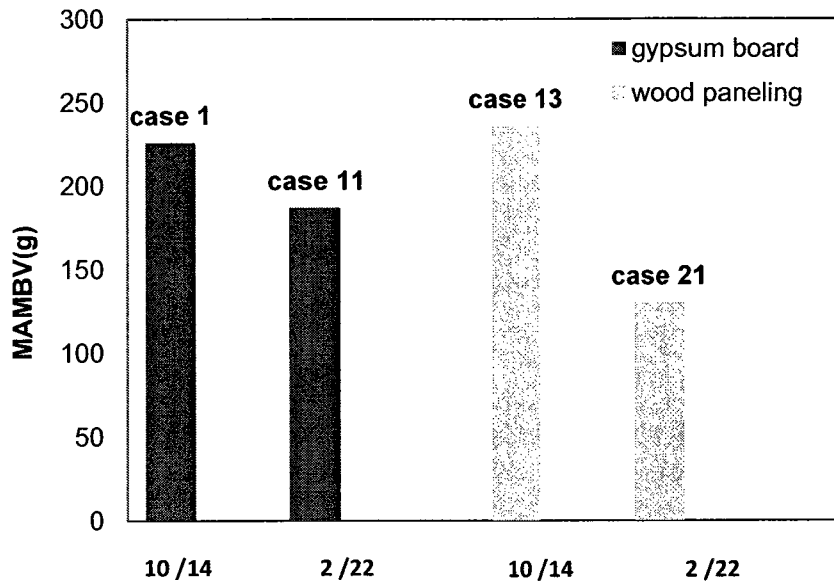
Besides moisture generation rate, the moisture generation regime also has a significant impact on the moisture buffering effect. Two different moisture generation schemes are studied, including 100 g/hr for 10 hours moisture generation in 24 hours (case 1 and case 13) and 200 g/hr for 2 hours in 24 hours (case 11 and case 21) when uncoated gypsum board and wood paneling are applied as interior hygroscopic materials.

Figure 4.11 shows the comparison in indoor RH between case 11 and 1 and the non-hygroscopic cases 12 and 2. It is found that the reduction of indoor RH by moisture buffering is more significant under shorter moisture load schemes (case 11). However, in term of the moisture buffering capacities of surface materials, as shown in Figure 4.12, the total amount of moisture buffered by surface materials is smaller under shorter moisture load schemes (case 11). This reduction of moisture buffering capacity of surface

materials is because of the reduced amount of moisture available for buffering. For example, the MAMBV is reduced from 226 g to 186 g when the moisture generation period is reduced from 10 hours (case 1) to 2 hours (case 11) for the cases using uncoated gypsum board. The same reduction trend can be observed in the cases using wood paneling, as seen in Figure 4.12.



**Figure 4.11. Indoor RH comparison between case 1, 11 and case 2, 12.**



**Figure 4.12. MAMBV under different moisture generation schemes.**

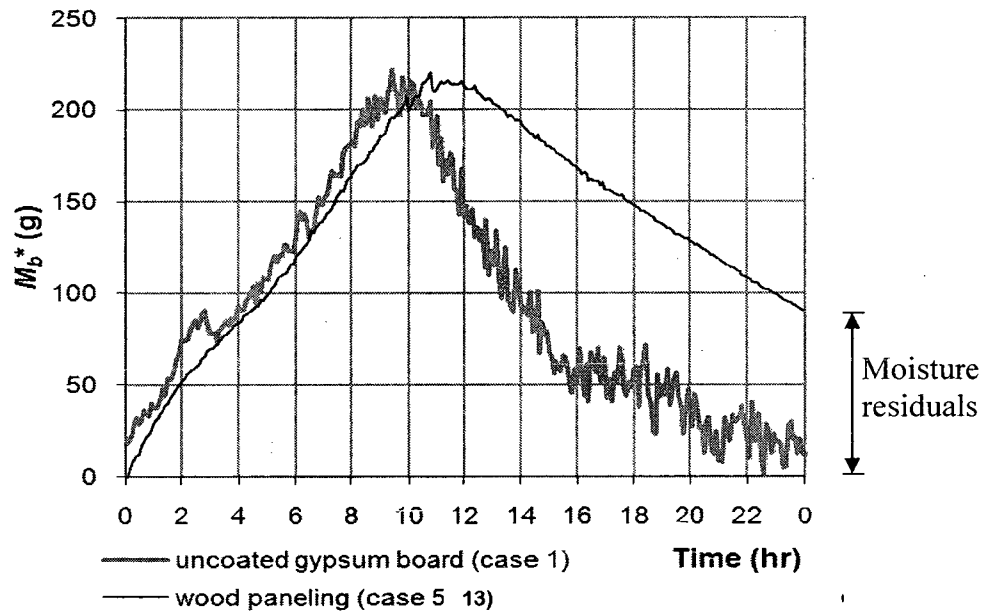
#### **4.2.4 Wood paneling vs. uncoated gypsum board**

As shown in Figure 4.13, gypsum board and wood paneling have almost the same MAMBV (226 g for case 1 using uncoated gypsum board vs. 236 g for case 13 using wood paneling), at 0.5 ACH, 100g/hr moisture generation rate. This similarity is because the moisture buffering effect is determined not only by the sorption capacity of the material but also the vapor permeability of the material. Gypsum board has higher permeability and wood paneling has higher sorption capacity), and the impact of these properties will be further discussed in Chapter 5. The impact of the different supply air conditions in the cases using uncoated gypsum board and in the cases using wood paneling (introduced in Section 3.1.3), is not discussed in this section but will be presented in Section 4.4.2.

Another phenomenon worth of considering is that at the end of one daily moisture cycle, there is 89.0 g (37% of the moisture buffered) moisture remaining in wood paneling in

case 13, as shown in Figure 4.13. However, the moisture remaining in uncoated gypsum board at the end of daily moisture load cycle in case 1 is only 12g (5% the of moisture buffered). This difference in moisture remaining is attributed to the differences in their moisture properties, and will be analyzed in Chapter 5.

This large moisture residual at the end of first several daily moisture load cycles in cases using wood paneling (42 g, 27% of moisture buffered) can also be observed in case 21 under shorter moisture load schemes (2 /22 hours).



**Figure 4.13. Accumulated moisture buffering value in cases using wood paneling vs. uncoated gypsum board.**

MAMBV in the cases using wood paneling shows a much higher reduction (106 g) compared to that in cases using uncoated gypsum board (40 g), when the moisture generation period is shorten from 10 hours to 2 hours, as observed from Figure 4.12. This much higher reduction is due to the fact that wood paneling is less permeable than gypsum board although it has good moisture absorption capacity. It takes much longer

time for wood paneling to react to the humidity change of ambient air. As a result, wood paneling shows a smaller moisture buffering capacity when a shorter moisture generation regime (2/22 hours) is applied.

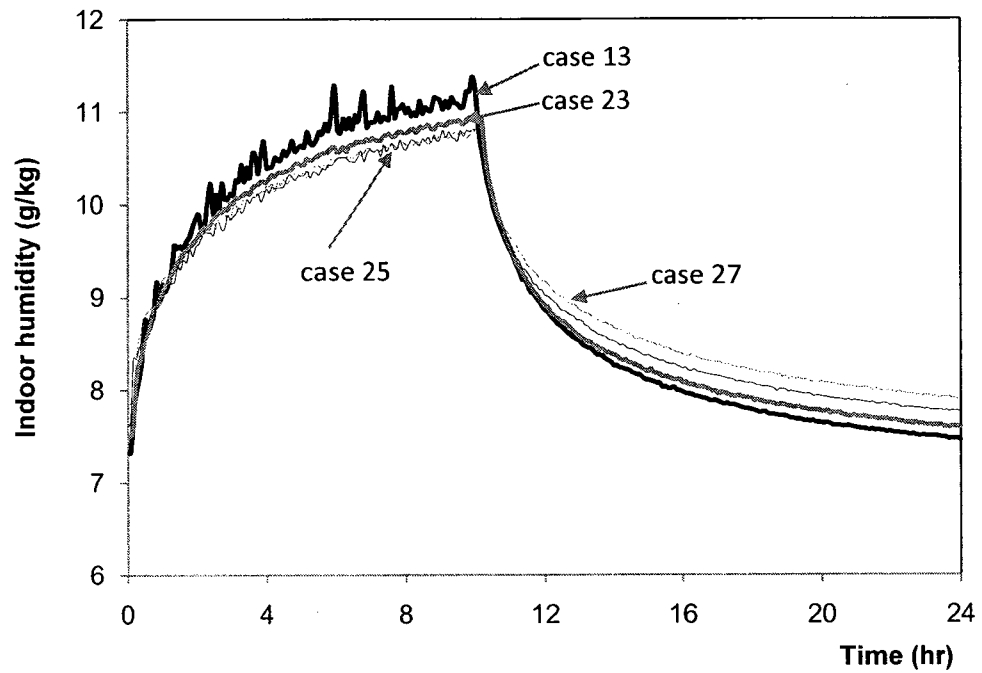
#### 4.2.5 Impact of furniture

With more furniture added in the test room, the indoor humidity variation is decreased, as shown in Figure 4.14, and the moisture buffering potential of the room is increased, as indicated by MAMBV in Table 4.2, because of the combined effect of surface materials and furniture. The moisture buffering potential of surface materials, however, is not increased, which can be observed from moisture content measurements taken on the interior surface materials, as discussed in Section 6.3.

It is also shown that a bookshelf with books and a bed with mattress provide a relatively higher moisture buffering capacity as compared to table, chair and curtains. The increase of MAMBVs is higher in case 23 and case 27 (53 g) compared to the increase in case 25 (23 g).

**Table 4.2. MAMBV in cases with furniture added.**

Case No.	Case 13	Case 23	Case 25	Case 27
Furniture added	No	Bookshelf with books	Table, chair and curtains	Bed with mattress
MAMBV (g)	236	289	312	365



**Figure 4.14. Humidity ratio of test room in case 13 (without furniture), case 23 (added books and bookshelf), case 25 (added curtains, desk and chair), and case 27 (fully furnished).**

### 4.3 Whole building simulation (BSim)

#### 4.3.1 Introduction of BSim and assumption of the model

For the reason that the experimental investigation is usually expensive and time consuming, practically only a limited number of test scenarios can be studied. Validated computer simulation model can be a useful tool to complement the experimental investigation to cover more cases. In this thesis BSim is adopted to evaluate room moisture balances for a large number of test scenarios.

BSim is a multi-zone model developed at the Danish Building Research Institute in Denmark (Rode and Grau 2001). The moisture and heat balance are built in each zone under the assumption of a well-mixed indoor environment. The moisture mass balance of BSim (Rode and Crau, 2001, b) is

$$\begin{aligned}
 \underbrace{V \cdot \rho \cdot (w^n - w^{n-1})}_{\text{indoor air moisture}} = & \underbrace{\Delta t \cdot \left( \sum_{\text{construction}} A_{\text{surf}} \cdot \beta \cdot \left( p_{\text{surf}} - \frac{P}{w^{n-1} + 0.622} \right) \right)}_{\text{moisture buffering}} \\
 + \underbrace{\Delta t \cdot \sum n \cdot V \cdot \rho \cdot (w_{\text{vent}} - w^{n-1})}_{\text{air source}} + & \underbrace{\Delta t \cdot G}_{\text{moisture source}} \\
 \underbrace{\hspace{10em}}_{\text{ventilation and airleakage removal}} & 
 \end{aligned} \tag{4.9}$$

For the building envelope response simulation part, a simplified 1D HAM model is used in BSim. The moisture transfer mechanism of this HAM model includes only the vapor transfer and is not coupled with heat transfer. The driving potential is the partial vapor pressure. The heat and moisture transfer within the building envelope is calculated by using the implicit method in each divided control volume.

A great advantage of this model compared to other similar simulation tools is that it is powerful in setting up the ventilation system control and air leakage, which allows users to set their specified ventilation control methodology and supply air conditions. The



physical model of this tool integrates all the necessary moisture transfer elements, which is proved accurate enough for zone simulations (Rode and Grau 2008), even though it is a simplified model, compared to some research models used for research purpose. In addition, sufficient outputs including the original setting of simulation conditions allow users to easily track and correct mistakes.

#### **4.3.2 Simulation setup, validation and cases studied**

The BSim model is applied and validated first by simulating test cases in the experimental investigation. The conditions of the environmental chamber are input as outdoor conditions for the simulation. No solar radiation, rain, or wind effect is considered. The moisture source and air infiltration are set according to the moisture generation rate and air leakage measured or estimated from experiments. The test room is built in the model as constructed in the experiment with the following modifications:

- The test room and its ventilation systems are modeled as a building with two rooms, of which only one simulates the test room, as shown in Figure 4.15. In the test room, walls a and b are walls covered with interior surface materials being tested. The interior surface of walls c and d and the rest of interior surfaces of test room are covered by aluminum sheets.
- Since the available control algorithms for the ventilation system in BSim are not suitable to provide the same ventilation air conditions as tested in the experiment, a second room called conditioned ventilation room is added, as shown in Figure 4.15. Instead of being taken from outdoor, the ventilation air is taken from this conditioned ventilation room, which has steady state indoor conditions close to the

conditions of ventilation air. Using this method, the conditions of the ventilation air can be set to the same conditions as those measured from the experiment.

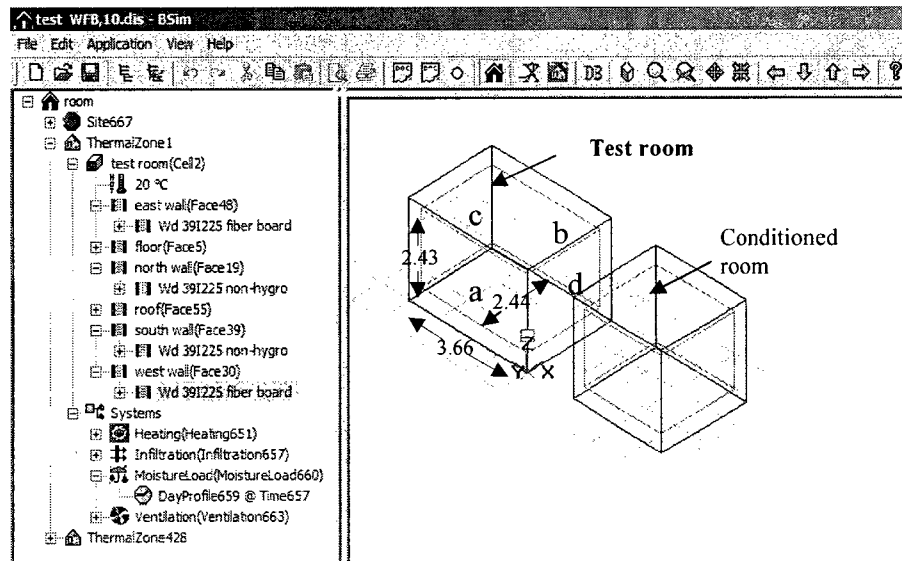
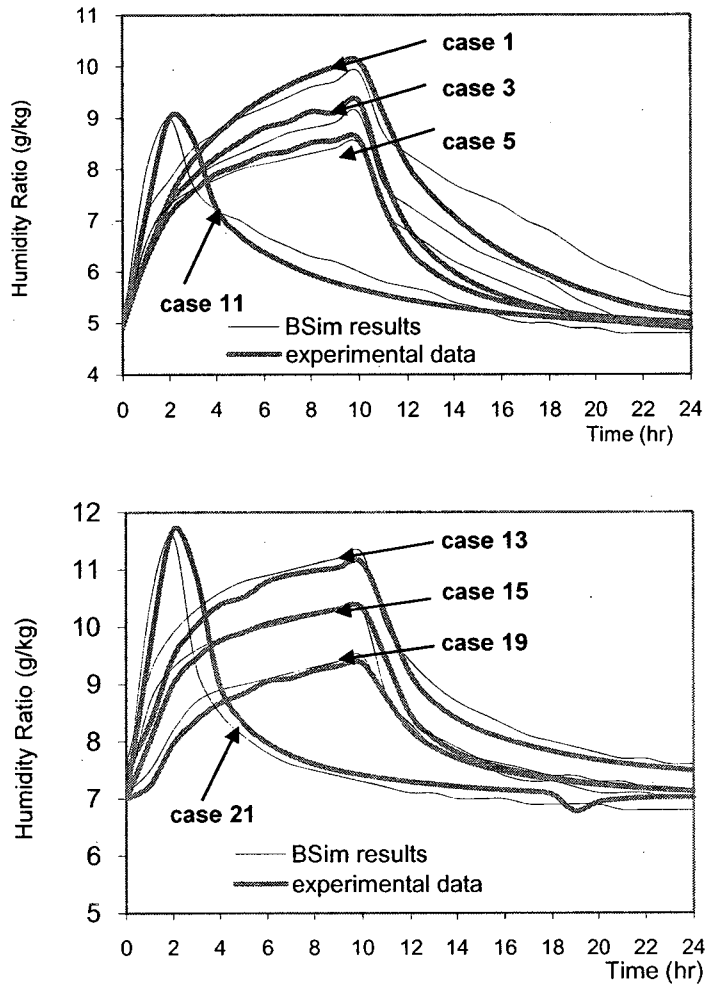


Figure 4.15. Interface and room model in BSim simulation.

### *Model validation*

The BSim model is validated by comparing the simulation results to the experimental measurements. As shown in Figure 4.16, the BSim simulation results agree well with the experimental data with an average of 0.2 g/kg (around 2%) difference in humidity ratio (HR) for all cases.



**Figure 4.16. Indoor humidity ratio comparison between simulation results and experimental data.**

The MAMBVs calculated from BSim simulations are compared to those obtained from experimental results, as shown in Table 4.3. The difference in MAMBV is less than 10% for all the cases.

**Table 4.3. Comparison of MAMBV obtained from simulation results and experimental data.**

Case No.	MAMBV in experiments	MAMBV in simulations	Difference (%)
1	226	217	4.1
3	155	167	7.7
5	114	121	6.1
9	113	125	10.6
11	186	191	2.7
13	236	245	3.8
15	154	170	10.3
19	141	146	3.5
21	110	121	10.0

To study the effect of ventilation conditions, outdoor conditions, moisture generation protocol, material properties and room configuration, extended cases are performed in BSim simulation, as shown in the Table 4.4.

### 4.3.3 Moisture balance in BSim simulation and *MAMBV*

The moisture absorption for cases by BSim simulations can be calculated from

$$M_b^*(t) = -M_a(t) - (M_v(t) + M_l(t)) - M_d(t) + G(t) \quad (4.10)$$

in which,  $M_v$  is calculated based on the conditions of inlet air and indoor air,

$$M_v(t) = Q_v w_v \cdot t - (Q_v + Q_l) w_i \cdot t \quad (4.11)$$

where,  $w_v$  is the humidity ratio of inlet air;  $w_i$  is the average humidity ratio of indoor air, which can be assumed as humidity ratio of outlet air; and  $Q_v$  is the mass flow of supply air.

*MAMBV* is defined as the maximum value of  $M_b^*$  in the simulation cases.

**Table 4.4. Case scenarios studied in BSim simulations.**

Case No.	Surface materials	Supply air conditions <sup>1</sup>	Moisture generation (g/hr)	Ventilation rate (ACH)	Outdoor condition
B1-22	Same scenarios tested in experimental study as listed in Table 3.1				
B23	GB	7 g/kg HR	100 g/hr for 10 hours	0.5	Winter
B24	GB			0.75	
B25	GB			1	
B26	GB		50 g/hr for 10 hours	0.5	Winter
B27	GB		200 g/hr for 2 hours	0.5	
B28	WP	4.7 g/kg HR	100 g/hr for 10 hours	0.5	
B29	WP			0.75	Winter
B30	WP			1	
B31	WP		50 g/hr for 10 hours	0.5	
B32	WP		200 g/hr for 2 hours	0.5	Winter
B33	GB	4.7 g/kg HR	100 g/hr for 10 hours	1.5	
B34	GB			2	
B35	GB			3	Winter
B36	GB			5	
B37	WP			1.5	
B38	WP			2	Winter
B39	WP			3	
B40	WP			5	
B41	GB	4.7 g/kg HR	100 g/hr for 10 hours	0.5	Summer 20 °C, 70% winter
B42	WP	7 g/kg HR		0.5	
B43	OSB	4.7 g/kg HR	100 g/hr for 10 hours	0.5	Winter
B44	ACC				
B45	TBP				
B46	OSB	4.7 g/kg HR	200 g/hr for 2 hours		Winter
B47	ACC				
B48	TBP				
B49 <sup>2</sup>	GB	4.7 g/kg HR	100 g/hr for 10 hours	0.5	Winter
B50 <sup>2</sup>	WP	7 g/kg HR			
B51 <sup>3</sup>	GB	4.7 g/kg HR			Winter
B52 <sup>3</sup>	WP	7 g/kg HR			
B53 <sup>3</sup>	GB	4.7 g/kg HR			Winter
B54 <sup>4</sup>	WP	7 g/kg HR			

Notes: <sup>1</sup> The temperature of all the supply air was set to 19 °C. <sup>2</sup> Two other wall surfaces were covered with finishing materials. <sup>3</sup> Ceiling added as hygroscopic surface. <sup>4</sup> Floor added as hygroscopic surface.

## **4.4 Impact of various parameters on moisture buffering effect**

The impact of different parameters on moisture buffering effect will be discussed in this section based on results from simulations. Parameters include ventilation rate and supply air condition, moisture generation protocol, outdoor environment, type of hygroscopic materials, and room configuration.

### **4.4.1 Impact of ventilation rates**

In total, 14 cases are investigated to evaluate the impact of ventilation rates including case B1 (GB, 0.5 ACH), case B3 (GB, 0.75 ACH), case B5 (GB, 1 ACH), case B33 (GB, 1.5 ACH), case B34 (GB, 2 ACH), case B35 (GB, 3 ACH), case B36 (GB, 5 ACH), case B28(WP, 0.5 ACH), case B29 (WP, 0.75 ACH), case B30 (WP, 1 ACH), case B37(WP, 1.5 ACH), case B38(WP, 2 ACH), case B39(WP, 3 ACH), case B40(WP, 5 ACH). The air supply conditions are the same for all cases at 19 °C, 37% RH.

The increase of ventilation rate results in the reduction of indoor RH variation, which in turn reduces the moisture buffering effect. The profile of the amount of moisture buffered by surface hygroscopic materials ( $M_b^*$ ) in one day moisture load (100g for 10 hours in 24 hours period) for uncoated gypsum board under different ventilation rates is presented in Figure 4.17. This figure shows that when the ventilation rate increase from 0.5 to 5 ACH, the maximum accumulated moisture buffering value (*MAMBV*) of gypsum board reduces from 226g to 15g. The moisture buffering effect is hardly to be noticed when the ventilation rate is over 3 ACH. The moisture buffering potential in the cases using wood paneling as interior surface materials shows the same tendency, as seen in Figure 4.18.

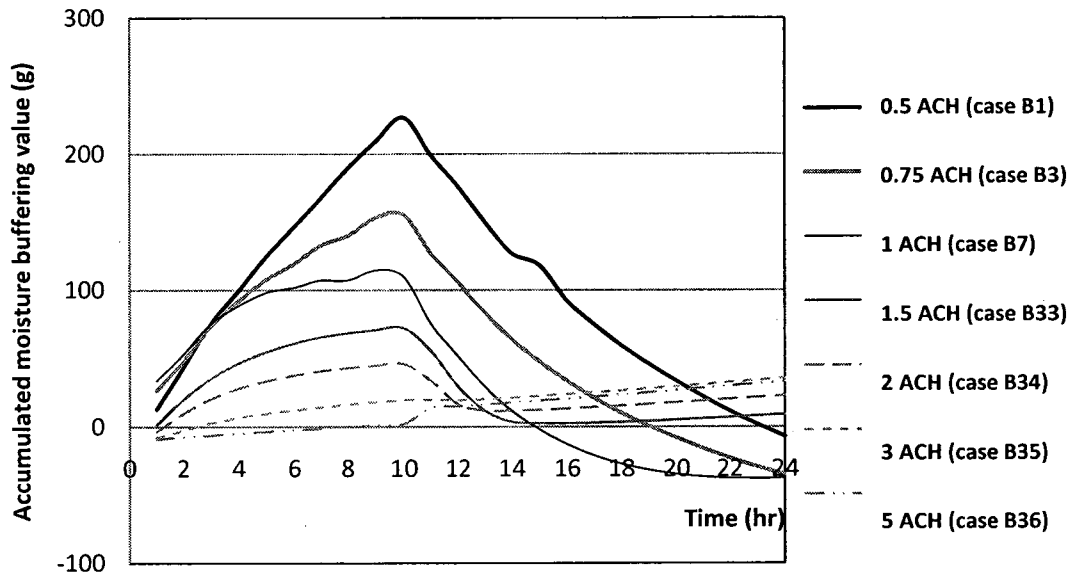


Figure 4.17. Accumulated moisture buffering value ( $M_b^*$ ) profile in a 10/14 daily cycle at different ventilation rates, for cases using uncoated gypsum board (supply air humidity is 4.7g/kg HR).

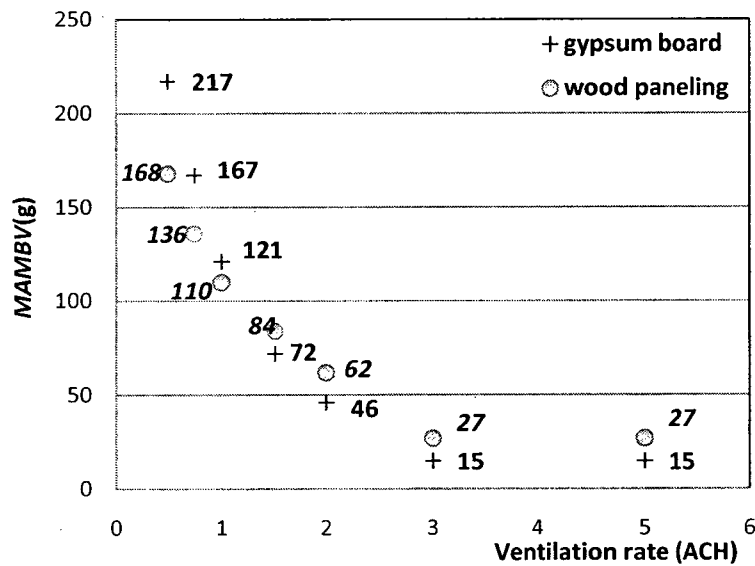


Figure 4.18. Maximum accumulated moisture buffering value at different ventilation rates for uncoated gypsum board and wood paneling (supply air humidity is 4.7g/kg).

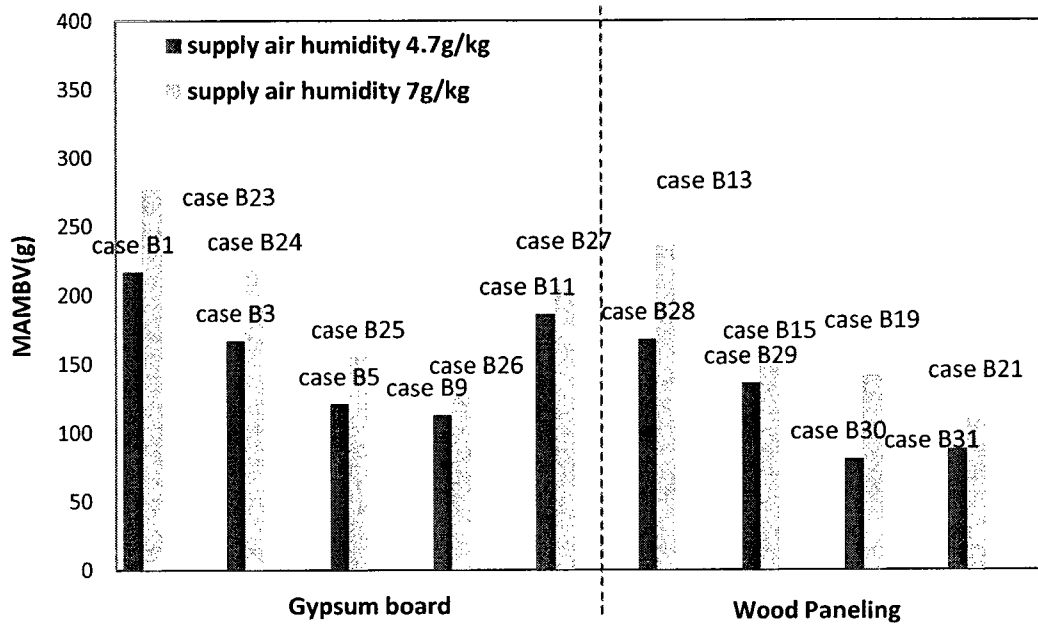
The impact of ventilation rate is more significant when the ventilation rate is low, especially under 1ACH, as shown in Figure 4.18. For example, when the ventilation rate increases from 0.5 ACH to 1 ACH, and from 1 to 1.5 ACH, the reductions of MAMBV are 112 g (50% reduction) and 42 g (19% reduction), respectively, for cases using uncoated gypsum board. Equivalent reductions for cases using wood paneling are 58 g (35% reduction) and 26 g (15% reduction), respectively.

#### **4.4.2 Impact of supply air humidity**

To investigate the impact of ventilation air humidity on moisture buffering effect, additional simulations are carried out to include case B23-27 with supply air conditions of 19 °C, 50% (7 g/kg HR) using uncoated gypsum board and case (B28-31) with supply air conditions of 19 °C, 37% (4.7 g/kg HR) using wood paneling. These cases are compared to cases using uncoated gypsum board (cases B1, B3, B5, B7, and B11) with supply air conditions of 19 °C, 37% RH, and cases using wood paneling (cases B13, B15, B19, and B21), with supply air condition of 19 °C, 50% RH.

It can be concluded that, with the increase of humidity level of ventilation air, the moisture buffering effect is more significant, which can be observed in Figure. 4.19. MAMBV has higher values in the cases with ventilation air humidity of 7g/kg HR. For example, MAMBV is 277 g for case B23 with ventilation air humidity at 7g/kg and 215 g for case B1 with ventilation air humidity at 4.7 g/kg HR. In both cases, uncoated gypsum board is used with 100g/hr for 10 hours moisture generation rate in 24 hours at 0.5 ACH.





**Figure 4.19. MAMBV under different ventilation air humidity.**

It can also be noticed that the impact of supply air humidity is more significant for uncoated gypsum board cases, especially at lower ventilation rate. The differences of MAMBV at two level of supply air humidity are 60 g at 0.5 ACH (case B1 and 23), 52 g at 0.75 ACH (case B3 and B24), and 34g at 1 ACH (case B5 and 25) for cases using uncoated gypsum board, as shown in Figure 4.19. In reality, the humidity of the supply air is not at a fixed level; rather it is fully determined or partly affected by the conditions of the outdoor air depending on the ventilation strategy. The typical strategy of ventilation should be to take in the minimum amount of outdoor air during winter and summer, and to take in full outdoor air during spring and fall season. So the moisture buffering effect can vary seasonally depending on the outdoor air conditions and the ventilation strategy.

#### 4.4.3 Impact of outdoor conditions

Due to the limited capacity of the environmental chamber when operated in summer season, the tests for wood paneling were carried out under outdoor conditions (chamber condition) at -5 °C, 70% RH, which are different from the outdoor conditions applied for tests using uncoated gypsum board (-10 °C, 45% RH). Moreover, in reality, buildings are exposed to different outdoor conditions. Therefore, the impact of outdoor conditions on moisture buffering process needs to be analyzed.

The typical summer conditions of Montreal, 20 °C, 70% (Candanedo et al., 2006), are applied in case B41 and case B42 to compare case B1 and B13 (simulated under winter outdoor conditions)

Table 4.5 shows that the MAMBV under summer conditions (case 41 and case 42) is almost the same as in tested cases B1 and B13. That is because only a very thin inner layer of hygroscopic materials participates in the moisture buffering and the moisture condition of this thin layer of hygroscopic material is independent from the outdoor environment (Hedeegard et al., 2005 a, b).

It should be noted that only the impact of the steady state outdoor environment is considered in this study.

**Table 4.5. Maximum accumulated moisture value under different outdoor conditions.**

Outdoor condition	winter	summer	winter	summer
Case No.	Case B1	Case B41	Case B13	Case 42
MAMBV (g)	217	226	245	247

#### **4.4.4 Impact of material properties**

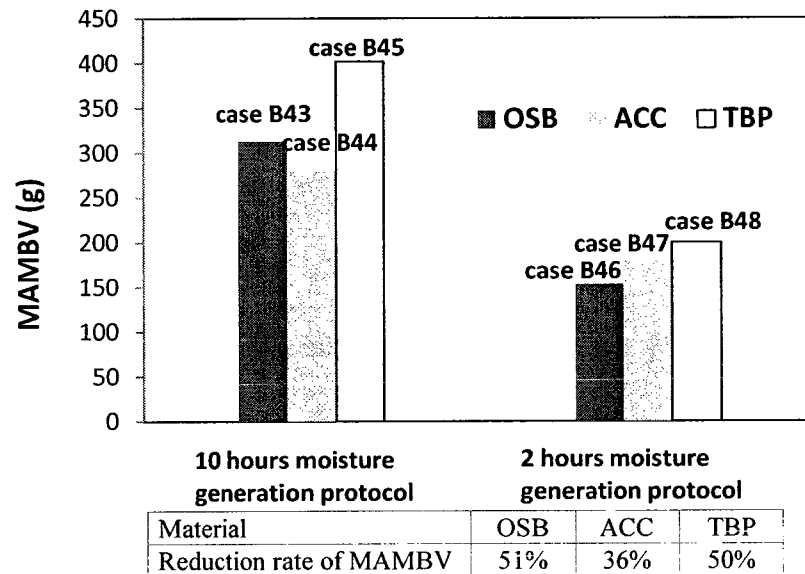
Three other hygroscopic materials, aerated cellular concrete (ACC), oriented strand board (OSB), and telephone book paper (TBP), are studied in this section. ACC has high vapor permeability but low moisture absorption capacity, similar to uncoated gypsum board. OSB has high moisture absorption capacity but low vapor permeability, which is similar to wood paneling. TBP is good at both moisture absorption capacity and vapor permeability. These three materials represent three types of hygroscopic materials, which are categorized in Chapter 5. The materials properties of these three materials can be found in Appendix A.

These three materials are applied on two wall surfaces, where wood paneling or uncoated gypsum board applied in the experimental investigation. In order to study moisture buffering effect under different moisture generation protocols, cases B43, B44, B45 are conducted under long term moisture generation (100g/hr for 10 hour in 24 hours period, while cases B46, B47, B48 are performed under short term moisture generation (200g for 2 hours in 24 hours).

It is noticed in Figure 4.20 that, case using OSB (case B43) and case using ACC (case B44) have almost the same moisture buffering potential (10% difference in MAMBV) under a 10- hour moisture generation regime. The case using TBP (case B45) results in a much higher moisture buffering potential (407 g in MAMBV) under a 10-hour moisture generation regime.

Under a shorter moisture generation regime (2 hours moisture generation in 24 hours), the moisture buffering capacity of the case using OSB (case B46) shows a greater

reduction of moisture buffering effect compared to the case using ACC (case B47). This larger reduction of MAMBV is the same as observed in cases using wood paneling. This greater reduction can be explained by the fact that materials having lower vapor permeability take longer time to absorb or release moisture. This phenomenon is further discussed in Chapter 5. The case using TBP (case B48) also shows a reduction of moisture buffering effect under shorter moisture generation regime, however, the MAMBV is still higher than the cases using the other two materials.



**Figure 4.20. Maximum accumulated moisture buffering value of cases using OSB, ACC and TBP as interior surface materials, under two different moisture generation protocols.**

Another phenomenon observed in the cases using OSB and TBP is the moisture remaining in the first several daily moisture load cycles. There are 92 g (29% of MAMBV) and 101 g (24% of MAMBV) of moisture remaining detected in case B43 (using OSB) and in case B45 (using TBP) in the first cycle, respectively. Smaller amount of moisture remaining is also observed in cases B46 and B48 under 2 hours moisture load

schemes. No significant moisture remaining is found in the cases using ACC (case 44 and 47).

#### **4.4.5 Impact of volume rate**

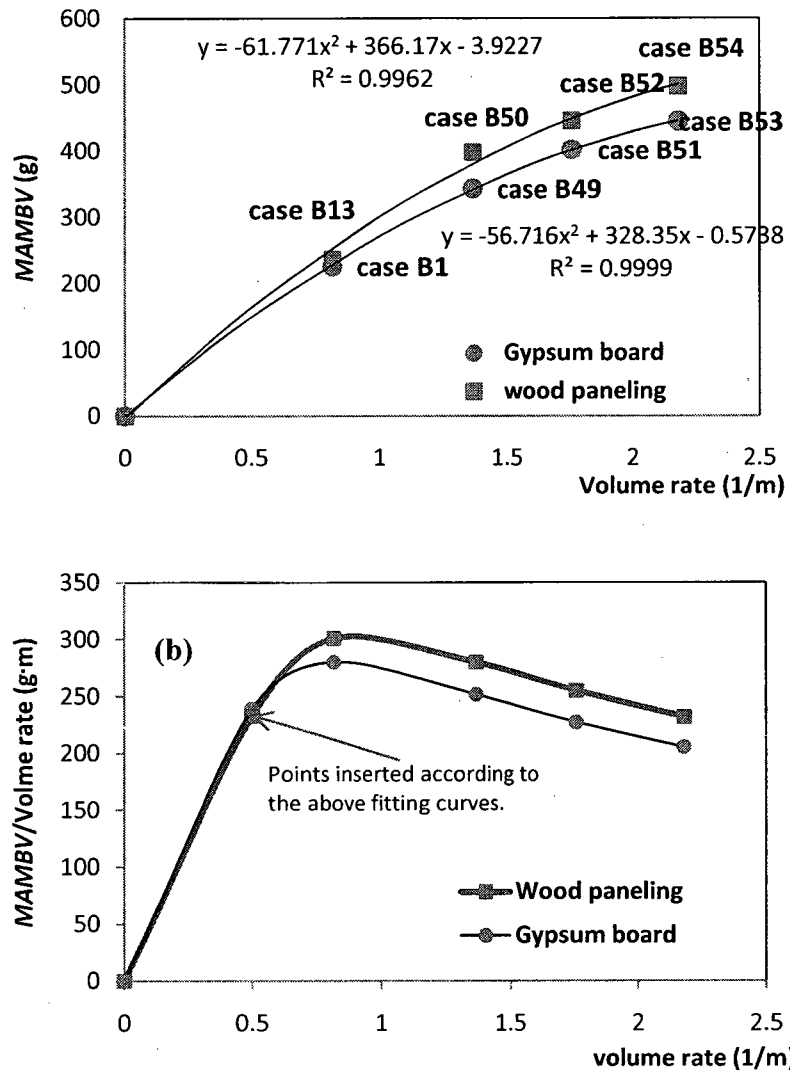
The hygroscopic materials surface area divided by the total volume of the room is defined as the volume rate (Mitamura, et. al., 2004, Cunningham,1992). It is an important room configuration factor influencing the moisture buffering effect.

In this study, two more interior surface areas (north and south walls) are added as hygroscopic material surfaces in cases B49 (using uncoated gypsum board) and B50 (using wood paneling). In addition, hygroscopic materials are applied on the ceiling surface and floor surface, step by step, in cases B51 and B52 (using uncoated gypsum board) and cases B53 and B54 (using wood paneling). So the volume rate is increased from 0.81 to 1.36, 1.76, and finally 2.18. The ventilation rate in these cases is 0.5 ACH and the humidity of supply air is at 4.7 g/kg-dry air.

The maximum accumulated moisture buffering values (*MAMBV*) in these cases are shown in Figure 4.21 (a). These values indicate that the larger area (higher volume rate) of hygroscopic surface materials is exposed to the indoor environment, the higher moisture absorption is observed (higher *MAMBV*).

However, the increase of the moisture buffering effect is not proportional to the increase of the volume rate. The proportion, *MAMBV*/volume rate, is calculated and presented in Figure 4.21 (b), based on the fitting correlation obtained from Figure 4.21 (a). There is an optimum volume rate, at which *MAMBV*/volume rate reaches the peak value. When the volume rate is smaller than this optimum value, *MAMBV*/volume rate can be considered

to be proportional to the increase of volume rate. By contrast,  $MAMBV$ /volume rate decreases with the increase of volume rate when the volume rate is larger than the optimum value. This optimum volume rate could vary with other factors, for example, ventilation rate, supply air conditions, and moisture generation protocols.



**Figure 4.21. (a) Maximum accumulated moisture buffering value as a function of volume rate; (b) Optimum volume rate.**

## 4.5 Summary

A full-scale experimental investigation on moisture buffering effect was conducted in an environmental chamber in this study. More test scenarios were studied in simulation application using BSim.

Moisture absorption value profile ( $M_b^*$ ) is computed based on moisture balance calculation established using experimental data and simulation results. The maximum accumulated moisture buffering value (*MAMBV*) is defined as a quantitative index used to evaluate moisture buffering effect and the impact of parameters on moisture buffering effect. The great advantage of this index is that, it provides a direct comparison of moisture buffering potential in different test scenarios, especially among the cases where the reductions of indoor RH (or HR) variation are hard to compare. In addition, *MAMBV* gives an absolute amount of moisture absorbed in materials, which is very important on the further investigation on the moisture response of interior surface materials.

Parameters discussed include ventilation rate, supply air conditions, moisture generation protocol, type of hygroscopic materials, and volume rates.

It is concluded that with the increase of ventilation rate, indoor humidity variation decreases, and therefore moisture buffering effect is also reduced. No significant moisture buffering effect can be found when the ventilation rate is over 3 ACH. The reduction of moisture buffering effect is much more sensitive to the increase of ventilation rate when the ventilation rate is lower than 1 ACH.

Supply air condition partly determines the level of indoor humidity. The higher humidity level of supply air increases the indoor humidity level. As a result, the moisture buffering effect of surface materials is enhanced. It is observed also that the impact of the humidity level of supply air is more significant at low ventilation rates.

Moisture generation protocol, including moisture generation rate and the regime of moisture generation, affects the moisture buffering of surface materials. The higher moisture generation rate, the more moisture source is available for moisture buffering, and thus the more significant moisture buffering effect appears.

Moisture buffering capacity is influenced by the material properties including moisture capacity and vapor permeability. Moisture buffering capacities of uncoated gypsum board (GB), aerated cellular concrete (ACC), wood paneling (WP) and oriented strand board (OSB) under long term moisture generation regime are within the same range. However, for GB and ACC, materials with higher vapor permeability have higher moisture buffering capacity under short term moisture generation regime (2 hours moisture generation), compared to WP and OSB. Materials, like TBP, which have both high vapor permeability and high moisture capacity, have better moisture buffering capacity under both short term and long term moisture generation protocol. The determination of properties of materials on moisture buffering capacity under different moisture load is fully investigated in Chapter 5.

Another important phenomenon observed in cases using WP, OSB and TBP is the moisture remaining at the first several daily moisture load cycles. No significant moisture remaining is detected in the cases using WP and ACC. The phenomenon is also further analyzed in Chapter 5.



When more areas of hygroscopic materials are involved in the moisture balance of the indoor environment, more moisture can be buffered. However, the increase in the moisture buffering effect is not proportional to the increase of the volume rate for hygroscopic materials. This impact is more significant when the volume rate is under the optimum value.

## CHAPTER 5

# MOISTURE RESPONSE OF MATERIALS AND APPLICATION OF MOISTURE BUFFERING VAULE (MBV) AT ROOM LEVEL

The moisture response of materials under different moisture load schemes is analyzed, using WUFI Pro simulations. The moisture response includes moisture absorption speed, the time required to reach a new equilibrium condition or a stable moisture buffering cycle, the amount of moisture absorbed, and moisture residuals. Materials are categorized into three groups based on their different moisture response patterns. The method to predict MAMBV and indoor RH using MBV, the effective capacitance method, is introduced as well.

### 5.1 Material properties

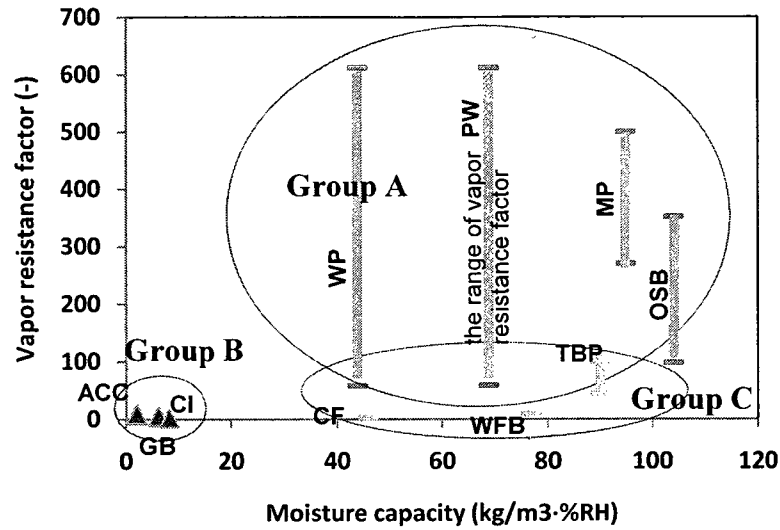
The calculated MAMBVs of uncoated gypsum boards and wood paneling in the large-scale experiment investigation and MAMBV of OSB, ACC and TBP obtained from BSim simulations indicate that the moisture buffering potential of surface materials is highly dependent on the material properties (moisture capacity and vapor permeability) and moisture load schemes, as discussed in Section 4.2.4 and 4.4.4. In addition, the moisture residuals as the result of moisture load history are observed in the cases using OSB, WP, and TBP, while no moisture residual occurs in the cases using GB and ACC.

To confirm this explanation and to further investigate these dependencies, 10 materials including uncoated gypsum board and wood paneling are categorized into three groups by their material properties and the moisture response of these materials under different load schemes are further investigated using WUFI simulation in this chapter.

Materials in group A have higher moisture capacity ( $\xi$  is over  $20\text{kg/m}^3$  per %RH) but low permeability (with vapor transfer resistance factor  $\mu > 100$ ). Group A materials include normally wood based materials, such as wood paneling (WP), plywood (PW), oriented strand board (OSB), and magazine paper (MP). Materials in group B have higher permeability (vapor transfer resistance factor  $\mu$  is in the order of 10) but low moisture capacity ( $\xi < 10 \text{ kg/m}^3$  per % RH) and consist of uncoated gypsum board (GB), aerated cellular concrete (ACC) and cellulose insulation (CI). Materials in group C include telephone book paper (TBP), cotton fiber (CF) and wood fiber board (WFB). These materials have both high moisture capacity and high vapor permeability. The moisture capacities (calculated from the values at 33% and 75% RH in the isotherm curves) for 10 materials and their vapor resistance factors between 33% to 75% RH are shown in Table 5.1 and Figure. 5.1. Additional properties for all the materials used in the simulations are presented in Appendix A.

**Table 5.1 Moisture capacity and vapor resistance factor between 33% and 75% RH**

Group	A				B			C		
Materials	WP	OSB	MP	PW	GB	CI	ACC	WFB	TBP	CF
Moisture capacity ( $\text{kg/m}^3 \cdot \%RH$ )	44	104	95	69	6	8	2	77	90	46
$\mu$ value (-)	58- 612	98- 352	270- 500	59- 612	4- 6	2	8- 10	9- 10	45- 100	1- 3



**Figure 5.1. Classification of hygroscopic materials based on their moisture capacity and vapor transfer resistance factor.**

## 5.2 Moisture response of hygroscopic materials

### 5.2.1 Introduction of WUFI pro 4

WUFI-Pro 4 is a 1D simulation program for predicting hygrothermal transport in multilayered walls. It is developed by Oak Ridge National Laboratory (ORNL) of the United States and the Fraunhofer Institute of Building Physics in Germany. It couples heat and moisture transfer by including the latent heat term (due to condensation or evaporation in the heat balance) and  $P_{sat}$ , which depends on temperature in the moisture balance. The balance is given by (Kunzel, 1995) as:

$$\frac{\partial H}{\partial T} \cdot \frac{\partial T}{\partial t} = \underbrace{\nabla(k \cdot \nabla T)}_{\text{conduction}} + \underbrace{h_v \nabla(\delta_p \nabla(\phi \cdot P_{sat}))}_{\text{latent heat of condensation or evaporation}} \quad (5.1)$$

$$\frac{\partial w}{\partial \phi} \cdot \frac{\partial \phi}{\partial t} = \nabla \cdot \left( \underbrace{D_{\phi} \nabla \phi}_{\text{liquid transfer}} + \underbrace{\delta \nabla (\phi \cdot p_{sat})}_{\text{vapor diffusion}} \right) + \underbrace{S_w}_{\text{water source}} \quad (5.2)$$

where  $H$  is the total enthalpy ( $\text{J/m}^3$ );  $k$  is thermal conductivity of the moist building materials ( $\text{w/m}\cdot\text{K}$ );  $h_v$  latent heat of phase change ( $\text{J/kg}$ );  $\delta$  is water vapor permeability of building materials ( $\text{kg/m}\cdot\text{s}\cdot\text{Pa}$ );  $\phi$  is relative humidity;  $w$  is water content of the building material layer ( $\text{kg/m}^3$ );  $D_{\phi}$  is liquid conduction coefficient ( $\text{kg/m}\cdot\text{s}$ ); and  $p_{sat}$  is water vapor saturation pressure ( $\text{Pa}$ ).

Liquid transport due to gravity and vapor transfer caused by air flow movement is not included in this moisture transfer model. The partial vapor pressure and relative humidity are considered as driving potential for vapor and liquid transfer respectively. Finite volume technique is used to discretize energy and moisture differential equations into numerical equations on volumes.

WUFI Pro 4 is validated in Section 6.2.2, under the test conditions, which shows a good agreement with the measured moisture content on the interior surface materials.

## 5.2. 2 Cases studied

The surface materials in the simulations were set with one surface sealed by aluminum sheets to avoid moisture transfer across the sealed surface and with the other surface exposed to the moisture load. Two relative humidity levels, 75% and 33%, were set as the ambient conditions for the unsealed surface, which are the same as the RH levels specified in the moisture buffering value (MBV) measurements by Nordtest Standard (Rode, 2005 and Roels, 2008).

Three stages of WUFI simulations were conducted as shown in Table 5.2.

In the first stage, the materials were exposed to 75% RH ambient air for 900 hours (i.e. a single step-change in the moisture load) starting from an initial moisture condition of 33% RH (equilibrium condition). The settling time required to reach a new equilibrium and the amount of moisture absorbed were used for analysis.

In the second stage, materials were exposed to daily cycles in the ambient air humidity that switches between 33% and 75% RH. Three types of moisture load schemes were applied, which are 10 hours 75% RH/14 hours 33% RH, 2 hours 75% RH/ 20 hours 33% RH, and 1 hour 75% RH/23 hours 33% RH. The time period for materials to reach a stable moisture buffering profiles (quasi-equilibrium) and the amount of moisture buffered under different moisture load schemes were analyzed. The initial moisture condition in materials was set at equilibrium conditions of 33% RH at 23 °C.

The impact of different initial conditions on the moisture buffering capacity was studied in the third stage simulation. Materials were exposed to 10 hours 75% RH/14 hours 33% RH load with the initial condition of 50% RH at 23 °C.

**Table 5.2 Cases studied in WUFI simulations.**

<b>Material</b>		<b>Stage 1 Case ID</b>	<b>Stage 2 Case ID</b>	<b>Stage 3 Case ID</b>
<b>Wood paneling (WP)</b>		WP-1	WP-2-10/2/1	WP-3-10
<b>Oriented strand board (OSB)</b>		OSB-1	OSB-2-10/2/1	OSB-3-10
<b>Magazine paper (MP)</b>		MP-1	MP-2-10/2/1	MP-3-10
<b>Plywood (PW)</b>		PW-1	PW-2-10/2/1	PW-3-10
<b>Uncoated gypsum board (GB)</b>		GB-1	GB-2-10/2/1	GB-3-10
<b>Cellulose insulation (CI)</b>		CI-1	CI-2-10/2/1	CI-3-10
<b>Aerated cellular concrete (ACC)</b>		ACC-1	ACC-2-10/2/1	ACC-3-10
<b>Wood fiber board (WFB)</b>		WFB-1	WFB-2-10/2/1	WFB-3-10
<b>Tel. book paper (TBP)</b>		TBP-1	TBP-2-10/2/1	TBP-3-10
<b>Cotton fiber (CF)</b>		CF-1	CF-2-10/2/1	CF-3-10
<b>Simulation setting</b>	<b>Indoor temperature</b>	23 °C.	23 °C.	23 °C.
	<b>Initial RH</b>	33%	33%	50%
	<b>Moisture load scheme</b>	N/Z	10/14, 2/22, 1/23	10/14
	<b>Low RH</b>	75%	33%	33%
	<b>High RH</b>	75%	75%	75%

notes: xxx-x-x

material, stage of simulation, time period for high RH applied on materials in a daily cycle.

## **5.3 Results and discussion**

### **5.3.1 Comparison between uncoated gypsum board and wood paneling**

In the first stage simulations, it can be observed that the moisture absorption of wood paneling is much higher than that of uncoated gypsum board when materials reach new equilibrium at 75% RH, as shown in Figure 5.2. The moisture absorption of wood paneling is around 309 g/m<sup>2</sup> and 38 g/m<sup>2</sup> uncoated gypsum board. The high moisture absorption of wood paneling shows that wood paneling has much high moisture absorption potential compared to uncoated gypsum board.

The time period required for wood paneling to reach new equilibrium is significantly longer than that of gypsum board. As shown in Figure 5.2, it takes 342 hours for wood paneling and 10 hours for uncoated gypsum board to reach a new equilibrium state. A new equilibrium state is reached once the daily weight change of materials is less than 1% of the total weight change.

This phenomenon can be explained that vapor permeability determines the moisture distribution speed in the materials. By contrast, moisture capacity determines the maximum amount of moisture that can be absorbed by the material when sufficient time is given for it to reach a new equilibrium state.



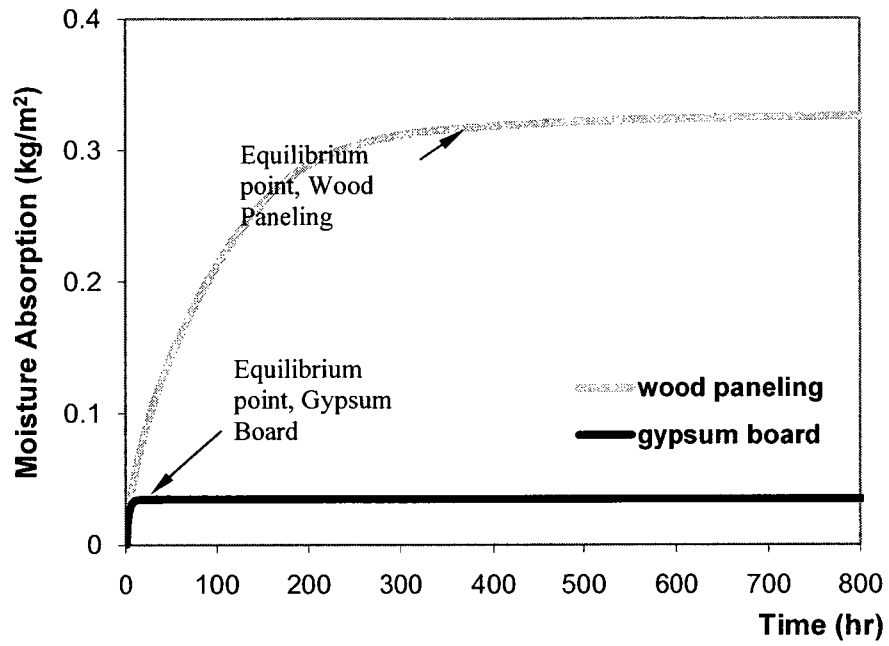
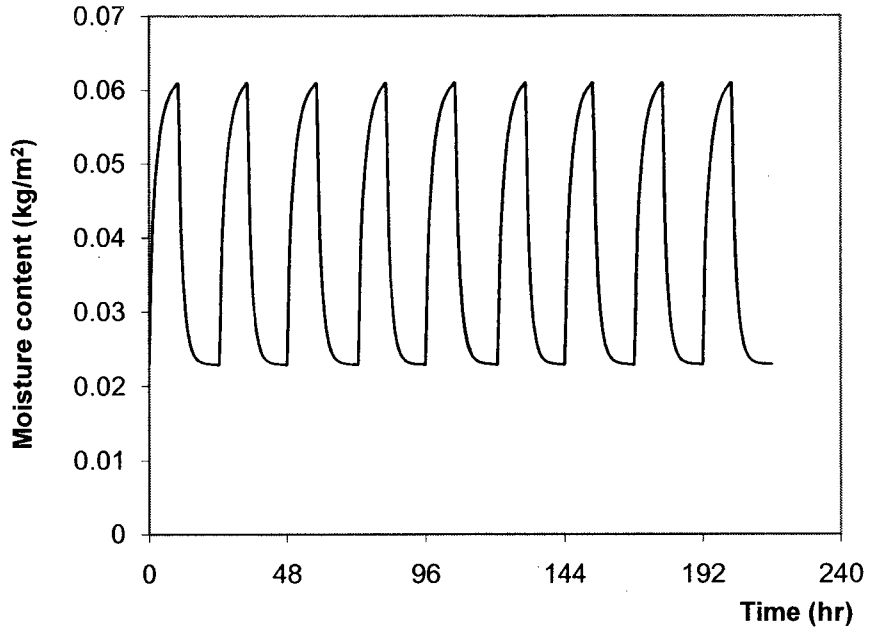
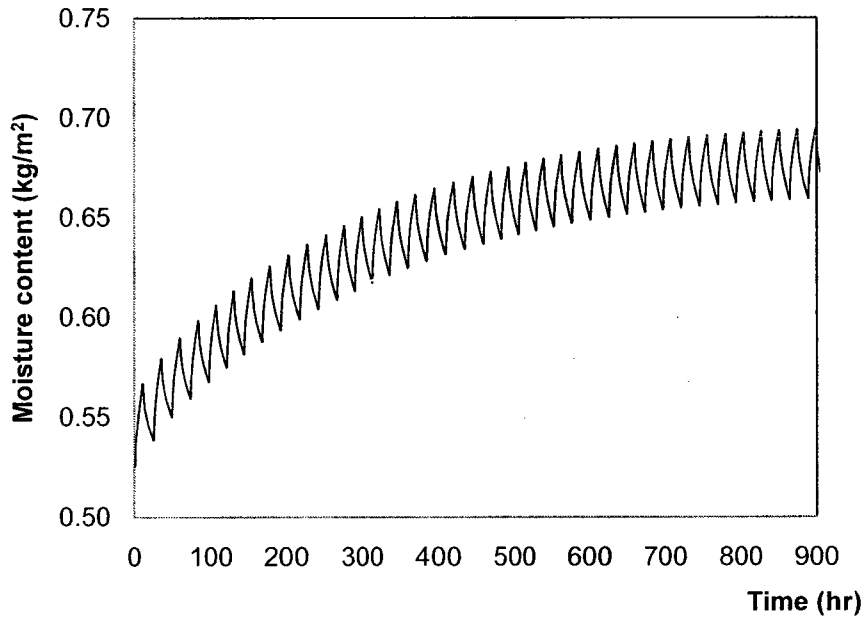


Figure 5.2. Equilibrium point for wood paneling and gypsum board.



**Figure 5.3. Moisture buffering of gypsum board over a 10/14 moisture load cycles.**

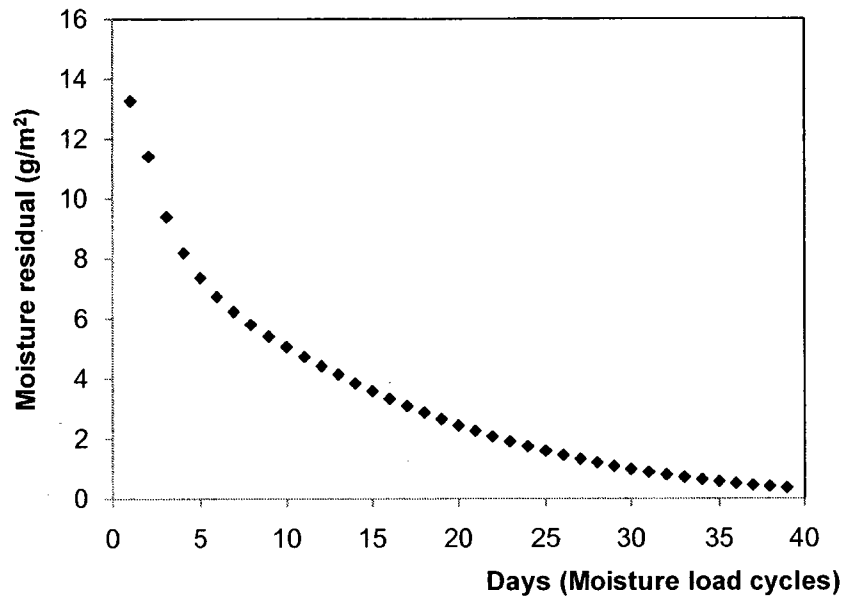


**Figure 5.4. Moisture content of wood paneling in the first 40 cycles under a 10/14 moisture load cycles.**

In the second stage simulations, wood paneling and uncoated gypsum board are exposed to three different moisture load profiles.

The moisture content profiles of uncoated gypsum board and wood paneling under 10/14 hours moisture load cycles are compared in Figure. 5.3 and 5.4. A stable moisture buffering cycle is considered to be reached at the point when the moisture residual of one daily cycle is less than 1% of the total daily moisture absorption. In the case of the uncoated gypsum board, this state is reached after one daily cycle; whereas, in the case of wood paneling this state is reached only after some 40 daily cycles. There is always some amount of moisture residual in the wood paneling for the first tens of moisture load cycles. The maximum moisture remaining in the first cycle for wood paneling is 13.3 g/m<sup>2</sup> or 39% of the total weight change. This moisture residual diminishes as more moisture load cycles are applied, as shown in Figure. 5.5. This explains the moisture remained in the wood paneling at the end of each daily moisture load cycle observed in the large-scale experiment in term of accumulated moisture buffering value ( $M_b^*$ ), as shown in Figure 4.13.

The stable moisture absorption curves of wood paneling and uncoated gypsum board are compared, as shown in Figure.5.6. Under the 10/14 moisture load, uncoated gypsum board and wood paneling have the same range of moisture absorption (36 g/m<sup>2</sup> and 38 g/m<sup>2</sup> for wood paneling and uncoated gypsum board respectively). However, under 2 hour load cycles, uncoated gypsum board has a higher moisture absorption value of 24 g/m<sup>2</sup> which is 37% lower than that for the 10/14 cycles, as compared to 18 g/m<sup>2</sup> (50% reduction) for wood paneling.



**Figure 5.5. Moisture residual for the cases using wood paneling, in the second stage WUFI simulations.**

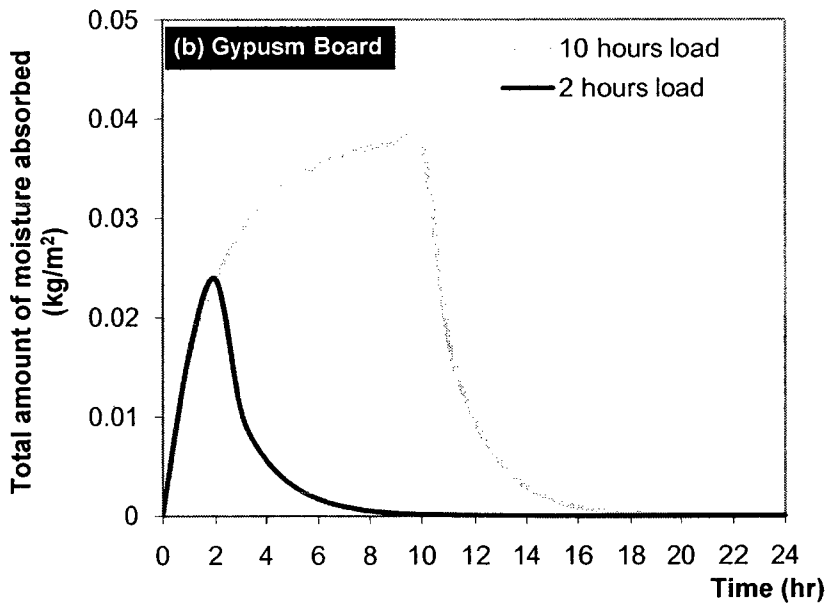
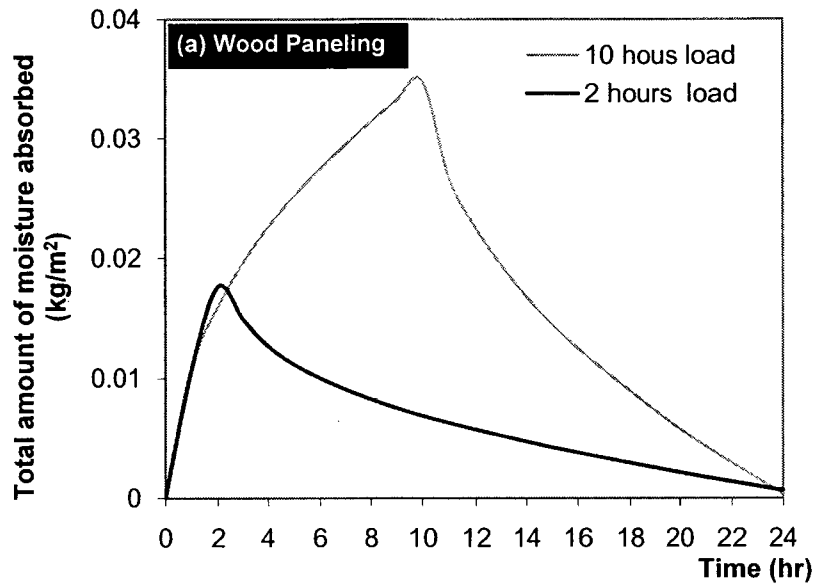
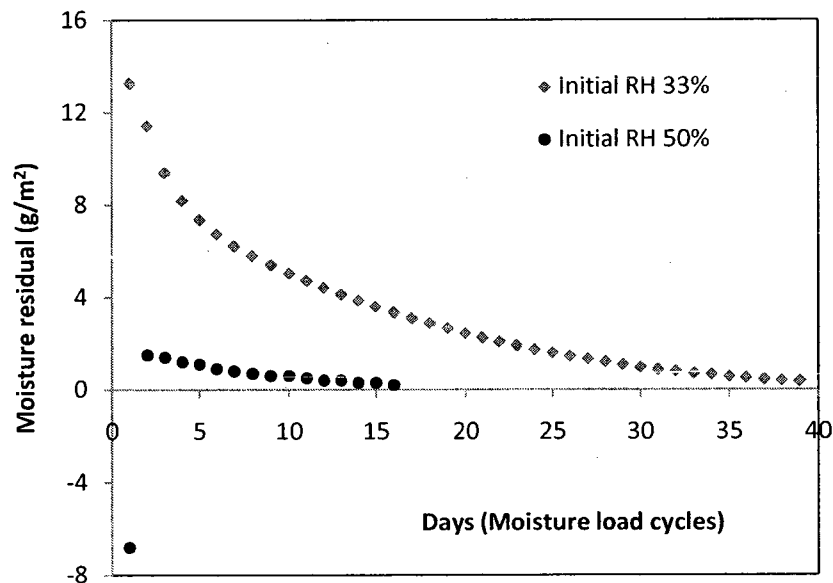
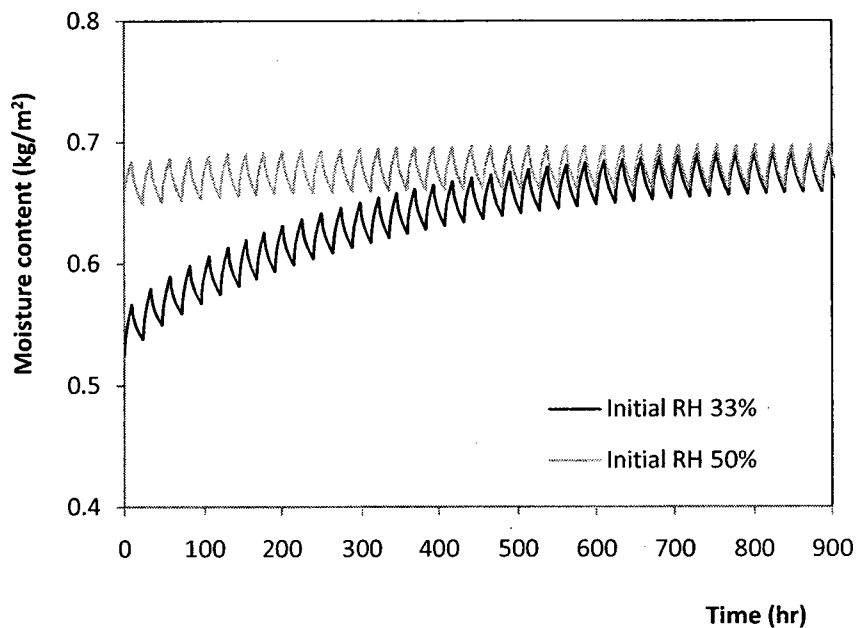


Figure 5.6. Total amount of moisture absorbed (40<sup>th</sup> cycle) (a) wood paneling, and (b) gypsum board, under 2 hours and 10 hours moisture load schemes.

The impact of initial moisture conditions of wood paneling and uncoated gypsum board were investigated in the third stage simulation. It is proved that the change of initial conditions only has impact on the first moisture absorption cycle of uncoated gypsum board. However, the change of initial conditions has great effect on moisture buffering of wood paneling. The effect presents in two aspects: the time required to reach the stable moisture buffering cycle and the moisture residual in each moisture load cycle. As shown in Figure 5.7, under 54% RH initial conditions, the moisture residuals in wood paneling of each moisture load cycle are much smaller compared to those under 33% RH initial conditions. Also, it takes 15 days for wood paneling to reach stable moisture buffering cycle, which is much shorter than that is required under 33% RH initial conditions (40 days), as also shown in Figure 5.8.



**Figure 5.7. Moisture residual under two different initial moisture conditions.**



**Figure 5.8. Moisture content of wood paneling under two different initial moisture conditions.**

### 5.3.2 Other materials

In the first stage of the WUFI simulations, the moisture absorption at the new equilibrium and the times required to reach new equilibrium conditions under the one step-change in the ambient RH from 33% to 75% RH are analyzed and presented in Table 5.3. The total moisture absorptions of materials in group A are much higher (around 300 g/m<sup>2</sup>) than those of materials in group B (14 - 42 g/m<sup>2</sup>), and are determined by their moisture isotherm curves. The total moisture absorptions of materials in group C are also high in the range of 190-365 g/m<sup>2</sup>.

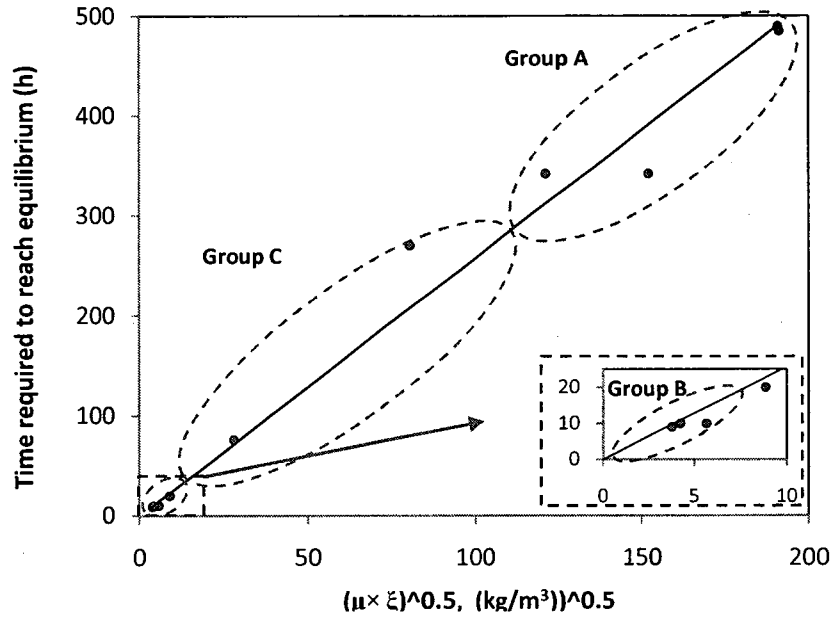
Materials in group A take more than 300 hours, while materials in group B take less than 10 hours to reach the new equilibrium state. Materials in group C require 85-220 hours to reach new equilibrium state. It is also found that, as shown in Figure.5.9, the time

required for materials to reach the new equilibrium state under the one step-change moisture load is proportional to the square root of the product of vapor resistance factor and moisture capacity (points in the figure stand for the materials studied in this simulation).

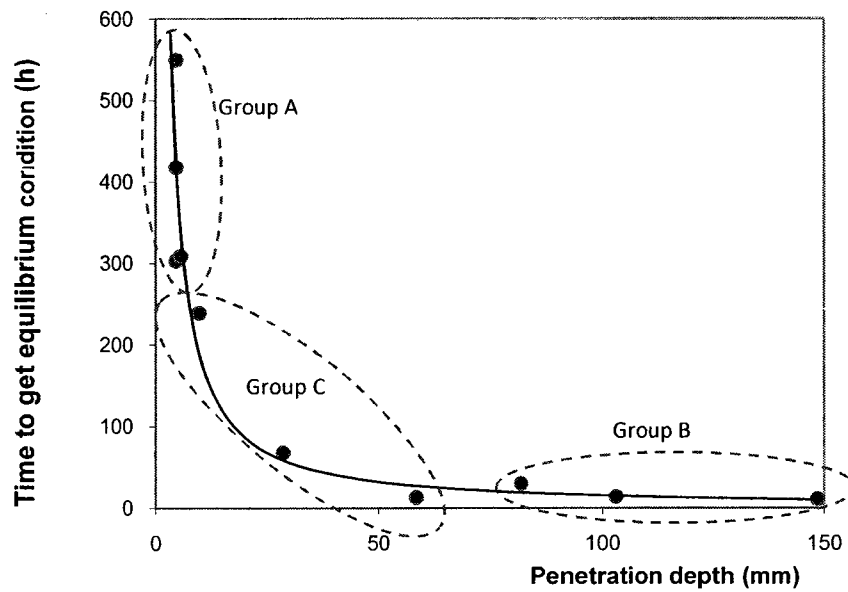
**Table 5.3. Comparison of three groups of materials under first stage WUFI simulations.**

<b>Group</b>	<b>Materials</b>	<b>Time to reach equilibrium (h)</b>	<b>Moisture absorption (g/m<sup>2</sup>)</b>
A	WP	342	313
	OSB	490	360
	MP	485	228
	PW	342	355
B	GB	10	38
	CI	9	45
	ACC	10	41
C	WFB	85	334
	TBP	220	365
	CF	20	190





**Figure 5.9. Relationship between the time required to reach new equilibrium condition and the vapor resistance factor and moisture capacity.**



**Figure 5.10. Correlation between penetration depth and the time required to reach new equilibrium state.**

This linear relationship can also be described by the relationship between effective moisture penetration depth (EMPD) and the time required to reach the new equilibrium state. EMPD is defined as the distance between the material surface to the point where the amplitude of vapor pressure variation is 1% of that on the surface and was estimated by Rode et al. (2005) as:

$$\text{EMPD} \approx 4.61 \sqrt{\frac{D_w \tau}{\pi}} \quad (5.3)$$

where  $D_w$  ( $\text{m}^2/\text{s}$ ) is the water vapor diffusivity and can be calculated as

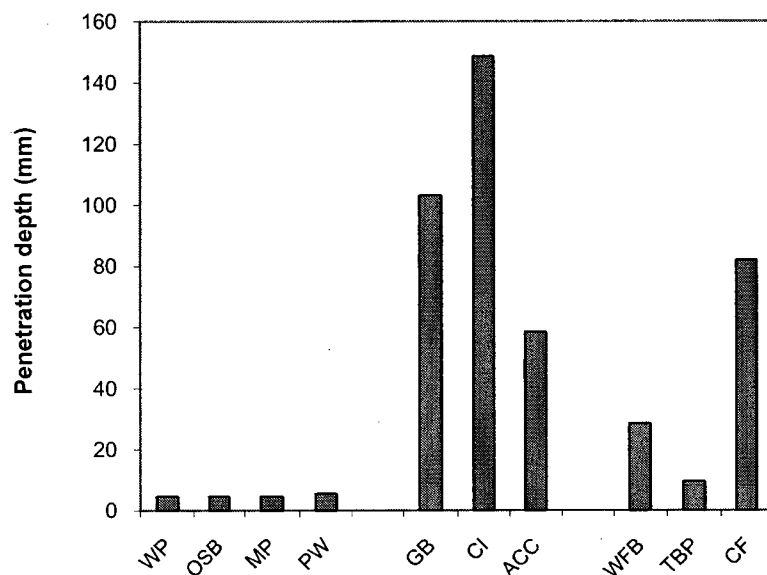
$$D_w = \frac{\delta \cdot P_{sat}}{\xi \cdot \mu} \quad (5.4)$$

where  $\delta$  is vapor permeability of air ( $\text{kg}/\text{m} \cdot \text{s} \cdot \text{Pa}$ );  $P_{sat}$  is the saturation vapor pressure (Pa); and  $\xi$  is the moisture capacity ( $\text{kg}/\text{m}^3 \cdot \% \text{RH}$ ); and,  $\tau = 24 \text{ hr}$  is the load cycle period (s).

EMPD thus has an inverse relation to the square root of the product of vapor resistance factor and moisture capacity. Therefore, the settling time is inverse related to the penetration depth, as presented in Figure 5.10.

EMPD has its own physical meaning, which is to illustrate the volume of materials taking part in moisture transportation. The estimated penetration depth (Eq. 5.3) of these 10 materials under daily moisture load cycles is presented in Figure 5.11. It can be observed that materials in group B have a larger penetration depth (59-149 mm), due to their low vapor resistance factor and low moisture capacity. The small resistance and the small

capacity to hold moisture enable moisture to be transferred more easily into deeper material layers. Materials in group A, by contrast, have a smaller penetration depth (5-7mm). Penetration depth of materials in group C is between 10-82 mm, depending on their vapor resistance factors and moisture capacities.



**Figure 5.11. Penetration depths of the ten hygroscopic materials under daily moisture cycles.**

In the second stage WUFI simulations, the amount of moisture absorbed under different moisture load are compared. As shown in Figure 5.12 and Table 5.4, the moisture absorption under 10 hours moisture load is in the range of 32-54 g/m<sup>2</sup> for materials in group A and group B. Group C materials obtain much higher moisture absorption (over 70g/m<sup>2</sup>) under long term moisture load regime (10/14 hours).

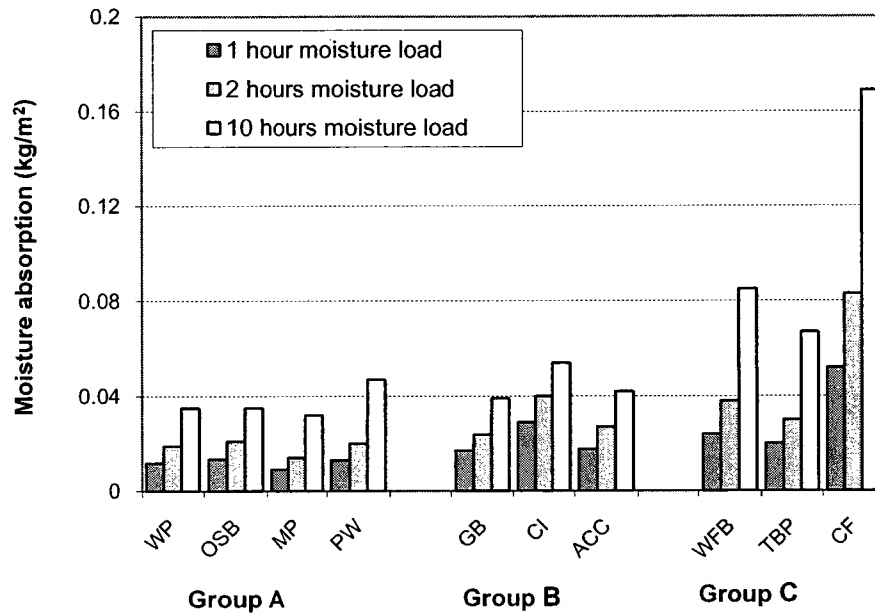


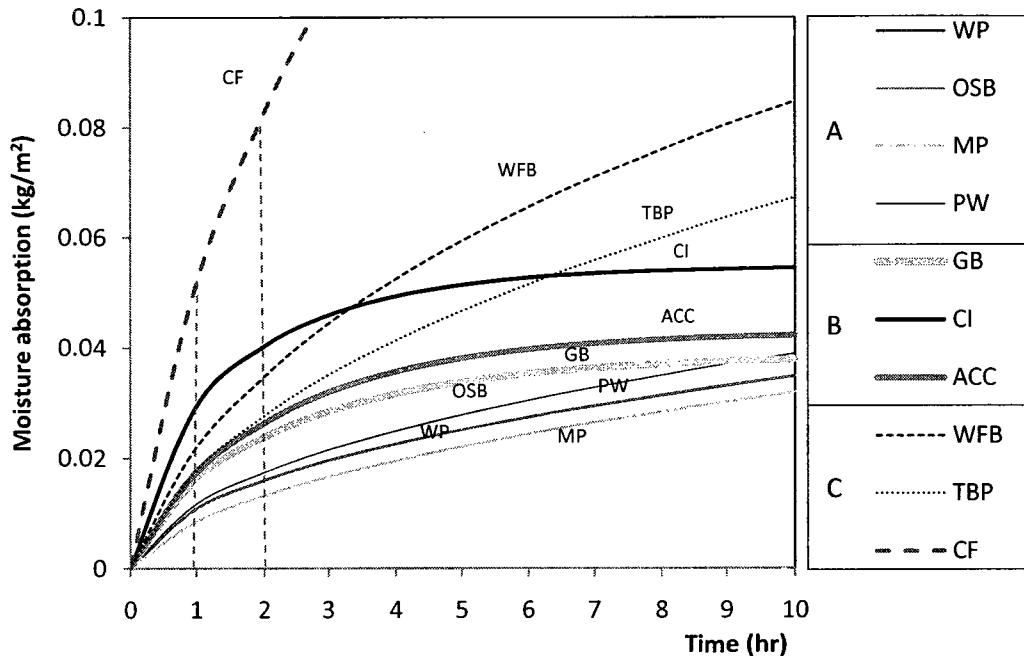
Figure 5.12. Moisture absorption under 10/14 hours and 2/22 hours moisture load schemes (obtained from the 40<sup>th</sup> moisture load cycle).

Table 5.4. Moisture absorption and reduction rate of moisture absorption under three different moisture load regime.

Materials	Moisture absorption (kg/m <sup>2</sup> )			Reduction (%)		
	1 hour	2 hours	10 hours	1 hour	2 hours	
Group A	WP	0.013	0.019	0.035	37.1	54.3
	OSB	0.014	0.020	0.035	40.0	57.1
	MP	0.009	0.014	0.032	28.1	43.8
	PW	0.013	0.020	0.039	33.3	51.3
Group B	GB	0.017	0.024	0.038	44.7	63.2
	CI	0.029	0.040	0.054	53.7	74.1
	ACC	0.018	0.027	0.042	42.9	64.3
Group C	WFB	0.024	0.038	0.085	28.2	44.7
	TBP	0.020	0.030	0.067	29.9	44.8
	CF	0.052	0.083	0.169	30.8	49.1

It is also noticed that the moisture absorption capacity is reduced for all materials under shorter term loads (1 hour or 2 hours load), as compared to absorptions under long term moisture load regime (10/14 hours). However, the reduction rates of group B materials are smaller than those of group A materials, as presented in Figure 5.12 and Table 5.4. Reduction rate is defined as the moisture absorption under shorter moisture load regime divided by the moisture absorption under long, i.e. 10 hours, moisture load. Moisture absorption of materials in group A is reduced to around 28-40 % for 1/23 hour load and 43-57% for 2 hours load compared to those under the 10/14 hour load regime. The moisture absorption for the materials in group B under 1/23 hour and 2/22 hours load schemes, in contrast, is reduced to around 42-53% and 63-74% of those under 10/14 hours load regime. Therefore, materials in group B have higher moisture absorption capacity under short term moisture load compared to those materials in group A. Group C materials show better moisture absorption than group A materials under short term moisture load but do not have any advantage in moisture absorption compared to the materials in group B materials, (except CF).

The close range of moisture buffering of group A materials and group B materials under 10/14 hours moisture load can be explained by Figure 5.13, which presents a stable moisture buffering cycle in the first 10 hours of daily moisture load cycle. Moisture absorption curves of these two group materials cross each other at point of 8-10 hour period. The moisture absorption under this long moisture load regime is determined by the combined effect of moisture capacity and vapor permeability.

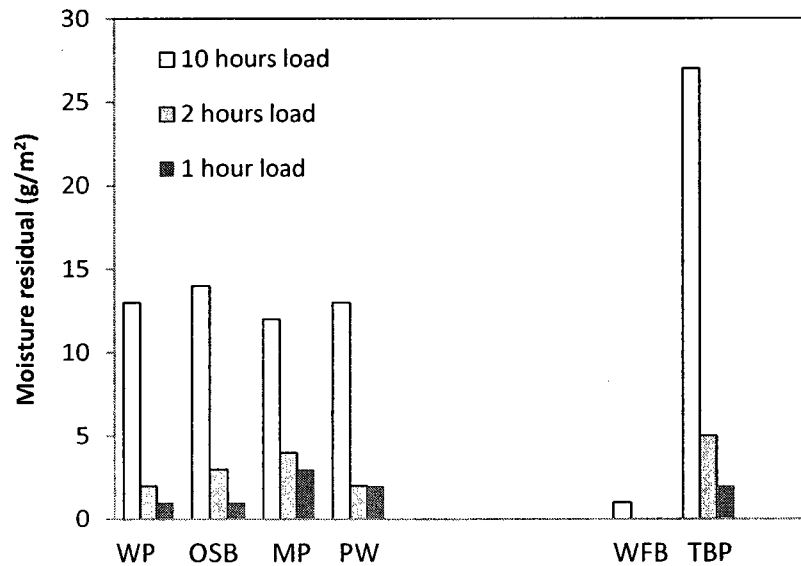


**Figure 5.13. Stable moisture buffering profile of different materials in the first 10 hours of daily moisture load.**

Under shorter moisture load regime (1/23 or 2/22 hours), high moisture permeability of group B materials determines their faster moisture reaction. For that reason, group B materials obtain high moisture absorption under short term moisture load.

Another phenomenon observed from simulation results is the daily moisture history effect on moisture absorption of materials in group A. There is up to 13 g/m<sup>2</sup> (approximately 30% of moisture absorbed) remained in materials in group A in the first 10 hours moisture load cycle, as shown in Figure 5.14. It takes over 30 days for materials in group A to achieve a stable moisture buffering cycle under 10 hours moisture load, as presented in Table 5.5. Smaller amounts of moisture residuals also occur in the first several short term moisture load (1 hour or 2 hours load) cycles for group A materials, as presented in Figure 5.14. Also less days were required to reach stable moisture buffering

cycle under short term moisture load, compared to those under 10 hours moisture load, as presented in Table 5.5.



**Figure 5.14. Moisture residual in the first moisture load cycle under three different moisture load schemes.**

**Table 5.5. Days to reach quasi-steady moisture response under three different moisture load schemes.**

Materials	EMPD (mm)	Days to reach quasi-steady moisture buffering			
		Moisture generation regime			
		10/14	2/22	1/23	
Group A	WP	4.5	40	15	4
	OSB	4.5	40	14	4
	MP	5.5	30	12	3
	PW	4.5	40	15	4
Group B	GB	103	1	1	1
	CI	149	1	1	1
	ACC	59	1	1	1
Group C	WFB	29	4	1	1
	TBP	10	13	12	8
	CF	82	1	1	1

The daily moisture history has no effect on materials in group B and influences selectively on some materials in group C. TBP, for example, has a low penetration depth and it takes a longer time for TBP to a stable moisture buffering cycle, therefore there is moisture residual in the first several each daily cycles. But for cotton fiber, which reacts fast to moisture load, has no moisture remained at the end of daily moisture cycle.

It is observed that the number of days required to reach stable moisture buffering cycles for materials under daily moisture load is inversely proportional to the penetration depths of the materials. Group A materials and materials in group C which have small penetration depth, need longer period to reach stable moisture buffering cycles

The impact of initial moisture condition on moisture buffering of all materials is investigated in the third stage simulation.

It is shown that for materials in group A, the moisture residuals under higher initial moisture (50% RH, which is almost the average ambient RH between two RH levels applied for the simulations) are much smaller than those obtained under 33% RH initial conditions, as shown in Table 5.6. The days required to reach stable moisture buffering cycles for group A materials are also shortened. Changing of initial moisture conditions has an impact on materials in group B only in the first moisture load cycle. Group C materials are influenced by the change of initial conditions selectively. For example, TBP which has small penetration depth shows the same pattern as materials in group A. But CF, which has a larger moisture penetration depth, is not influenced by the initial moisture conditions.



**Table 5.6. Moisture residual and days to reach stable moisture buffering cycle under two different initial conditions.**

Materials	Moisture residual in the first moisture load cycle (kg/m <sup>2</sup> )		Days to reach stable moisture buffering cycle(days)		
	33% RH initial	50% RH initial	33% RH initial	50% RH initial	
Group A	WP	0.013	0.007	40	15
	OSB	0.014	0.012	40	5
	MP	0.012	0.01	30	13
	PW	0.013	0.007	40	15
Group B	GB	0	0	1	1
	CI	0	0	1	1
	ACC	0	0	1	1
Group C	WFB	0.008	0.004	4	3
	TBP	0.027	0.023	13	10
	CF	0	0	1	1

### 5.3.3 Summary

The investigation in a large-scale experiment of the effect of the moisture buffering on the indoor environment has inspired two major investigations in this chapter. One is the impact of the moisture load on the moisture buffering capacity of different materials, and the other is the impact of the moisture history on moisture buffering capacities.

The relative weight of these impacts is highly related to material properties. Hence, 10 hygroscopic materials studied are categorized into three groups. Group A materials have high moisture capacities ( $\xi$  is over 20kg/m<sup>3</sup> per %RH) but low vapor permeability (vapor transfer resistance factor  $\mu > 100$ ). Wood paneling (WP), oriented strand board (OSB), magazine paper (MP) and plywood (PW) are examples of group A materials. Group B materials have high vapor permeability ( $\mu \approx 10$ ) and low moisture capacity ( $\xi < 10$  kg/m<sup>3</sup>·%RH). Group B materials include uncoated gypsum board (GB), cellulose

insulation (CI), and aerated cellular concrete (ACC). Materials in group C have both high moisture capacity and high water vapor permeability. Wood fiber board (WFB), telephone book paper (TBP), and cotton fiber (CF) belong to this group.

Under a step-change load, the moisture absorption at the new equilibrium state is determined by the isotherm curves of materials. That is the reason why groups A and C materials show much higher final moisture absorption. But higher moisture absorption does not necessarily guarantee a high moisture buffering capacity of these materials.

Under daily moisture load cycles, group A and group B materials show the same range of moisture buffering capacity under long term moisture load regime (8-10 hours moisture absorption period). This similarity arises from the fact that the moisture absorption curves of these two material groups A and B cross each other at the 8-10 hour period. However, under short daily moisture loads (1-2 hours moisture absorption period), the moisture buffering capacity of group A materials is smaller than those of group B materials. This smaller moisture buffering capacity is determined mainly by their high vapor resistance factor. Group C materials show high moisture buffering capacity under long moisture load but do not have higher moisture buffering capacity under short moisture loads, as compared to group B materials.

Penetration depths of materials can be considered as a material property that combines vapor resistance factor  $\mu$  and moisture capacity  $\xi$ . It has an inverse relationship with the time required to reach a new equilibrium state under a step-change moisture load and with the days required to reach a stable moisture buffering cycle. So the materials in groups A and materials in group C, which have small penetration depths (less than 7mm),

require much longer time to reach new equilibrium conditions or stable moisture buffering cycles, as compared to materials in group B. In addition, moisture residuals are observed in first several moisture load cycles for materials in group B and those materials in group C that have small penetration depths.

By increasing the initial humidity in the ambient air to the average RH of ambient air could shorten the time required to reach stable moisture buffering cycle for the materials in group A and the materials with low penetration depth in group C. Changing of initial humidity conditions in the ambient air does not influence the moisture buffering of group B materials and the materials in group C that have higher penetration depths.

It is concluded that under long term daily moisture load schemes (8-10 hours), group C materials are the best choice for moisture buffering application followed by materials in group B or group A. However, under short term daily moisture load schemes (less than 2 hours), materials in group B and group C with high penetration depths are better choices for moisture buffering application.

Simulation results show that the test period for group A materials and those materials in group C with low penetration depths could be longer than one month before the stable moisture buffering cycle can be reached. This longer test period required is more important in designing the large-scale experiment tests where moisture responses (for example the weight change or moisture content of materials) are difficult to be measured or analyzed to identify whether the stable moisture buffering cycle has been reached. It is also shown that test period on the moisture buffering effect for group A materials and

other materials in group C with high penetration depths can be limited to 3 days based on the fact that no significant moisture history effect is noticed.

The analyses on initial humidity conditions of ambient air indicate that increasing the initial humidity of ambient air to the average indoor RH daily variation can dramatically reduce the time required to reach stable moisture buffering cycles for materials in group A and materials in group C with low-penetration-depth. Preconditioning of these materials to reach equilibrium conditions to the average indoor RH daily variation is recommended for large-scale experimental study. With the pre-conditioning, the time required to reach the stable moisture buffering cycle can be reduced to about 15 days.

## 5.4 Using effective capacitance method (EC) to predict indoor RH and MAMBV

### 5.4.1 Methodology of effective capacitance (EC) model

- *MBV<sub>h</sub> Definition*

The Moisture Buffering Value (MBV) is the moisture accumulation under a daily moisture load, which has been investigated in Nordtest moisture buffering value protocol (Rode et al., 2007), Japanese Industrial Standard A 1470-1(JIS A 1470-1, 2002), and draft international standard 24353(ISO/DIS 24353, 2008), as reviewed in Chapter 2.

The approach to use MBV to predict indoor RH was recommended by Rode et al., 2007 and Jassen and Roels, 2008. A correction MBV\* is defined depending on the length of moisture load as,

$$MBV^* = \alpha MBV_{8h} + (1 - \alpha) MBV_{1h} \quad (5.5)$$

in which,  $MBV_{8h}$  and  $MBV_{1h}$  are derived from moisture absorption under 8 hours high RH/16 hours low RH and 1 hour high RH/23 hours low RH moisture load, respectively, based on Eq. 2.3.  $\alpha$  is weight factor, which is proposed as

0 hour < production interval  $\leq$  2 hours,  $\alpha = 0$ ;

2 hours < production interval  $\leq$  6 hours,  $\alpha = 0.5$ ;

6 hours < production interval  $\leq$  10 hours,  $\alpha = 1.0$ .

- *Moisture buffer potential in a room-enclosure*

Moisture buffer potential of a room-enclosure is characterised based on MBV\* as,

$$HIR^* = \frac{(\sum A_k \cdot MBV_k^* + \sum MBV_l^*)}{V} \quad (5.6)$$

where,  $HIR$  ( $\text{kg/m}^3 \cdot \%RH$ ) is the hygric inertia per cubic meter of room,  $MBV_k$  ( $\text{kg/m}^2 / \%RH$ ) and  $A_k$  ( $\text{m}^2$ ) are the moisture buffering value and area of finish  $k$ ,  $MBV_l$  is the equivalent moisture buffer value of object  $l$ , and  $V$  ( $\text{m}^3$ ) is the volume of the room.

- *Effective capacitance model*

The most simplified physical model to include  $HIR^*$  or  $MBV$  into room-enclosure moisture balance is the effective capacitance model, which is based on assumption that the humidity in the active part of the room enclosure is at all times in equilibrium with the room air humidity. The moisture balance of the room is described as (Jassen and Roels, 2008)

$$\underbrace{\frac{V}{R_v T_i} \cdot \frac{\partial p_{vi}}{\partial t}}_{\text{indoor humidity}} = \underbrace{(p_{ve} - p_{vi}) \frac{nV}{3600 R_v T_i}}_{\text{ventilation}} + \underbrace{G}_{\text{moisture generation}} - \underbrace{M_b}_{\text{moisture buffer}} - \underbrace{M_d}_{\text{vapor diffusion}} - \underbrace{M_l}_{\text{leakage}} \quad (5.7)$$

in which,  $T_i$  is indoor temperature;  $p_{ve}$  and  $p_{vi}$ , are the vapor pressure of ventilation supply air, interior air;  $R_v$  (462 J/kg·K) is the gas constant of water vapour;  $G$ ,  $M_b$ ,  $M_d$ ,  $M_l$  are the moisture generation, moisture buffered by the surface materials, vapour diffusion and vapour carried by air leakage. Moisture buffered by the surface materials can be computed by  $HIR^*$  as,

$$M_b = \frac{\partial RH_i}{\partial t} HIR^* \cdot V = \frac{100 \cdot HIR^* \cdot V}{\rho_{v,sat}(T_i)} \frac{\partial p_{vi}}{\partial t} \quad (5.8)$$

where,  $p_{v,sat}$  is the saturation vapor pressure at  $T_i$ . So the Eq. 5.7 can be expressed as,

$$\left( \frac{V}{R_v T_i} + \frac{100 \cdot HIR^* \cdot V}{\rho_{v,sat}(T_i)} \right) \frac{\partial p_{vi}}{\partial t} = (p_{ve} - p_{vi}) \frac{nV}{3600 R_v T_i} + G - M_d - M_l \quad (5.9)$$

Then Equation 5.9 can be rearranged as,

$$M \cdot \frac{V}{R_v T_i} \cdot \frac{\partial p_{vi}}{\partial t} = (p_{ve} - p_{vi}) \frac{nV}{3600 R_v T_i} + G - M_d - M_l \quad (5.10)$$

where,

$$M = \left( 1 + \frac{100 \cdot HIR^*}{\rho_{v,sat}(T_i)} \right) \quad (5.11)$$

in which,  $\rho_{v,sat}$  (kg/m<sup>3</sup>) is the density of saturated interior vapor.

$HIR^*$  is a constant value for one material, however, it is obvious that at higher level of indoor RH the moisture absorption of materials should be larger, compared to that at low indoor RH level at the same  $\Delta RH_i$ . For that reason, a non linear factor is introduced into the  $M_b$  calculation as,

$$M_b = \frac{C(t - t_{rev})}{\Delta t_m} \times \frac{100 \cdot HIR^* \cdot V}{\rho_{v,sat}(T_i)} \frac{\partial p_{vi}}{\partial t} \quad (5.12)$$

Thus  $M$  needs to be transformed to  $M'$  (Janseen and Roels, 2007),

$$M'(t) = \left( 1 + \frac{C(t - t_{rev})}{\Delta t_m} \frac{100 \cdot HIR^*}{\rho_{v,sat}(T_i)} \right) \quad (5.13)$$

where  $t_{rev}$  is the time point at which the most recent moisture generation starts;  $\Delta t_m$  is the period of current (at time  $t$ ) moisture load.  $C$  is estimated based on experience as 2.2 in moisture generation period and 2.8 in non-moisture generation period (Janseen and Roels, 2007).

#### 5.4.2 Application in the cases studied in this thesis research

Since MBV heavily relies on the moisture load regime, instead of using  $MBV_{1h}$  and  $MBV_{8h}$  to calculate  $HIR^*_{2h/10h}$ ,  $MBV_{2h}$  and  $MBV_{10h}$ , obtained from WUFI simulation are used.  $MBV_{2h}$  and  $MBV_{10h}$  are calculated from the maximum moisture absorption when a stable moisture buffering cycle is reached from WUFI simulations in pervious chapter as,



$$MBV_{2h/10h} = \frac{\text{Max moisture absorption}_{2h/10h}}{(RH_{high} - RH_{low})} \quad (5.14)$$

**Table 5.7.  $MBV_{1h}$  and  $MBV_{8h}$  of materials used in the effective capacitance method.**

Materials	WUFI simulation ( $\text{g/m}^2 \cdot \%RH$ )		$MBV_{8h}$ Janssen and Roels (2006 & 2007)
	$MBV_{2h}$	$MBV_{10h}$	
WP	0.48	0.88	N/A
OSB	0.50	0.98	N/A
MP	0.35	0.80	N/A
PW	0.45	0.88	0.69
GB	0.60	0.95	0.94
CI	1.00	1.35	2.01
ACC	0.68	1.05	0.81
WFB	0.95	2.13	1.92
TBP	0.75	1.68	N/A
CF	2.08	4.23	N/A

**Table 5.8 HIR\* in different materials under different moisture load schemes.**

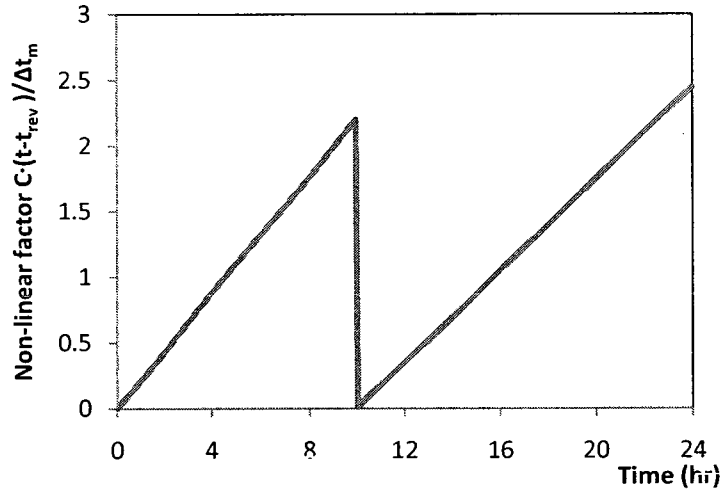
Materials	Case No.	Moisture generation in 24 hours	$HIR^*_{2h}$ ( $\text{g/m}^3 \cdot \%RH$ )	Case No.	Moisture generation in 24 hours	$HIR^*_{10h}$ ( $\text{g/m}^3 \cdot \%RH$ )
WP	13	97 g/hr 10h	0.72	19	192 g/hr 2h	0.39
OSB	B43	100 g/hr 10h	0.80	B46	200g/hr 2h	0.41
MP	N/A		0.66	N/A		0.29
PW	N/A		0.72	N/A		0.37
GB	1	103g/hr 10h	0.78	9	200 g/hr 2h	0.49
CI	N/A	100g/hr 10h	1.11	N/A		0.82
ACC	B44		0.86	B47		0.56
WFB	N/A		1.75	N/A		0.78
TBP	B45		1.38	B48		0.62
CF	N/A		3.48	N/A		1.71

The  $MBV_{2h}$  and  $MBV_{10h}$  of materials are compared with values from references as listed in Table 5.7. It is reasonable to see that the values of  $MBV_{10h}$  are a little bit larger than  $MBV_{8h}$  from Nordtest (Janssen and Roels, 2006 & 2007) due to the longer period of

moisture load regime. The only exception is MBV of CI, which is caused by the different material properties adopted in these two researches.

$HIR^*_{2h/10h}$  are calculated based on  $MBV_{2h}$  and  $MBV_{10h}$  for cases under 10 hours moisture generation and 2 hours moisture generation for different materials and listed in Table 5.8.

A non-linear factor is introduced (Figure 5.15), where  $C$  is given a value of 2.2 during the moisture generation period and 2.8 during the no moisture generation period.



**Figure 5.15. Non-linear factor introduced in the effective capacitance method.**

Using time step  $\Delta t$  and implicit differential method, Equation 5.11 can be converted to

$$M'(t^{m-1}) \cdot \frac{V}{R_v T_i} \cdot (p_{vi}^m - p_{vi}^{m-1}) = (p_{ve} - p_{vi}^{m-1}) \frac{nV}{3600 R_v T_i} \Delta t + G \Delta t - M_d \Delta t - M_l \Delta t \quad (5.15)$$

Thus the  $p_{vi}$  can be predicted from,

$$p_{vi}^m = p_{vi}^{m-1} + \left[ (p_{ve} - p_{vi}^{m-1}) \frac{nV}{3600R_v T_i} \Delta t + G\Delta t - M_d\Delta t - M_l\Delta t \right] \times \frac{R_v T_i}{M'(t^{m-1}) \cdot V} \quad (5.16)$$

and also MAMBV can be obtained from  $M_b^m$ ,

$$M_b^m = \frac{C(t-t)}{\Delta t_m} \times \frac{100 \cdot HIR^* \cdot V (p_{vi}^m - p_{vi}^{m-1})}{p_{v,sat}(T_i) \Delta t} \quad (5.17)$$

$$MAMBV = \sum_{m=0}^{\Delta t_m/\Delta t} M_b^m \cdot \Delta t \quad (5.18)$$

where m is the time step of calculation.

### 5.4.3 Calculation and discussion

The daily profile of the accumulated moisture buffering value calculated from the effective capacitance model is compared with those calculated using experimental measurements and BSim results, as shown in Figure 5.16 and 5.17. The calculated MAMBV in all cases is presented in Table 5.9, as compared to the values obtained from experimental study and BSim simulations. All the calculations are conducted with 5 min time step.

It is found that MAMBV under 2 hours moisture load regime is mostly over-estimated up to 10-25% by using effective capacitance method. MAMBV under 10 hours moisture load regime is within 10% difference compared to the values calculated either in experimental investigation or in BSim simulations.

The accumulated moisture buffering value profiles agree better with the profiles calculated based on either experimental data or BSim simulations in the moisture generation period for cases using GB, PW and WFB. Relatively larger difference in no moisture generation period can be observed in the cases using WP or WFB. It is due to the fact that HIR\*s used in the calculation are obtained from stable moisture buffering cycles and the moisture residuals as a result of the moisture load history effect is not considered in the EC model.

**Table 5.9. MAMBV obtained from the effective capacitance model vs. MAMBV calculated based on experiments and BSim simulations.**

Materials	MAMBV (10 hours moisture load)			MAMBV (2 hours moisture load)		
	EC model	experiment	BSim	EC model	experiment	BSim
WP	221	236	235	138	110	120
OSB	277	/	313	191	/	153
MP	268	/	266	163	/	155
PW	236	/	254	190	/	157
GB	244	226	236	205	186	191
CI	360	/	333	246	/	199
ACC	306	/	279	216	/	179
WFB	433	/	417	243	/	177
TBP	385	/	402	225	/	200
CF	550	/	465	295	/	261

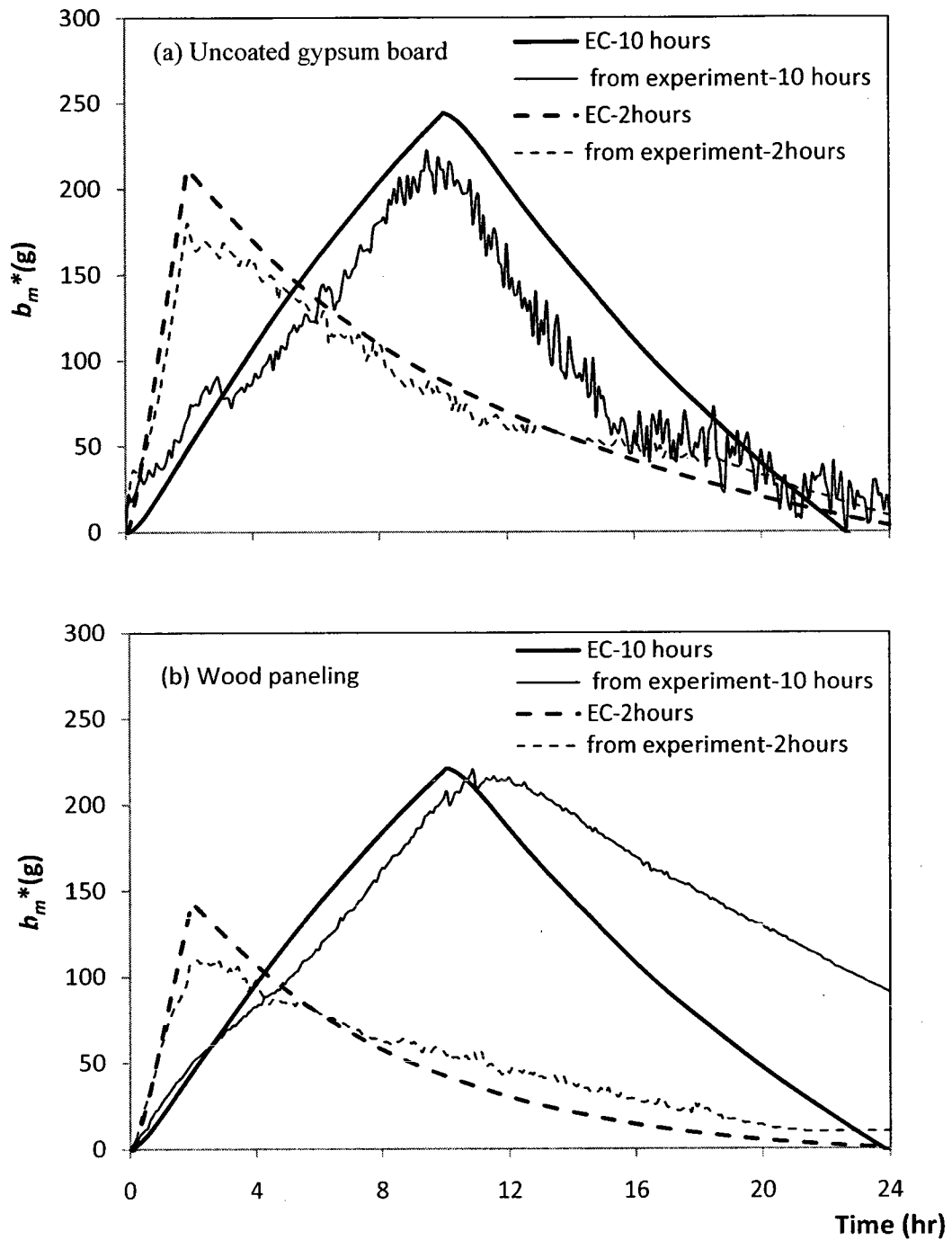
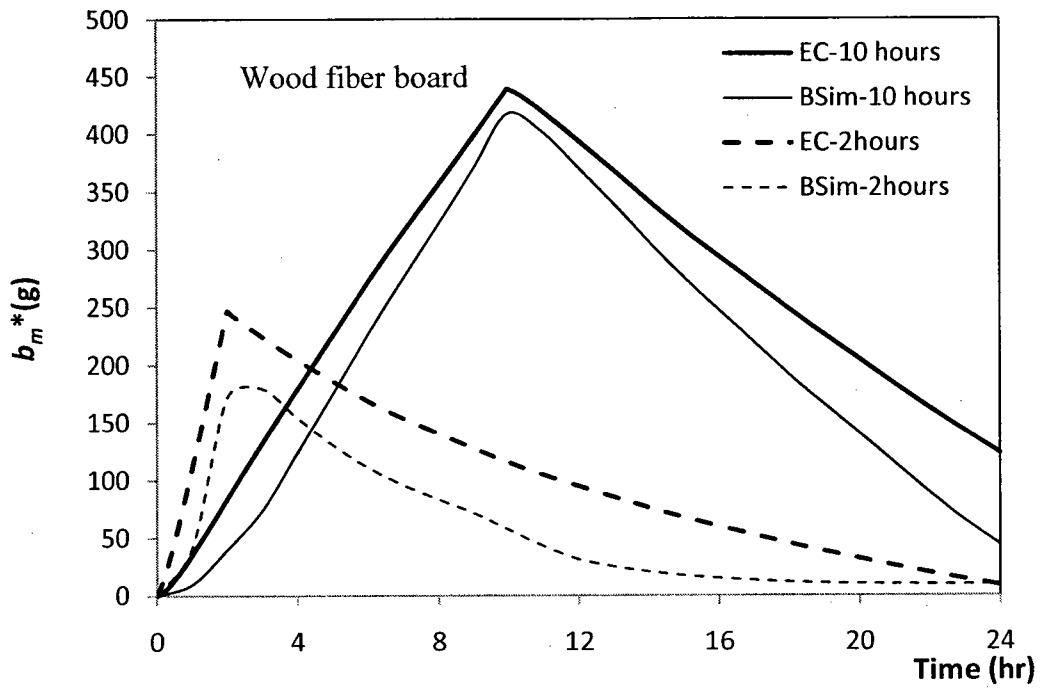
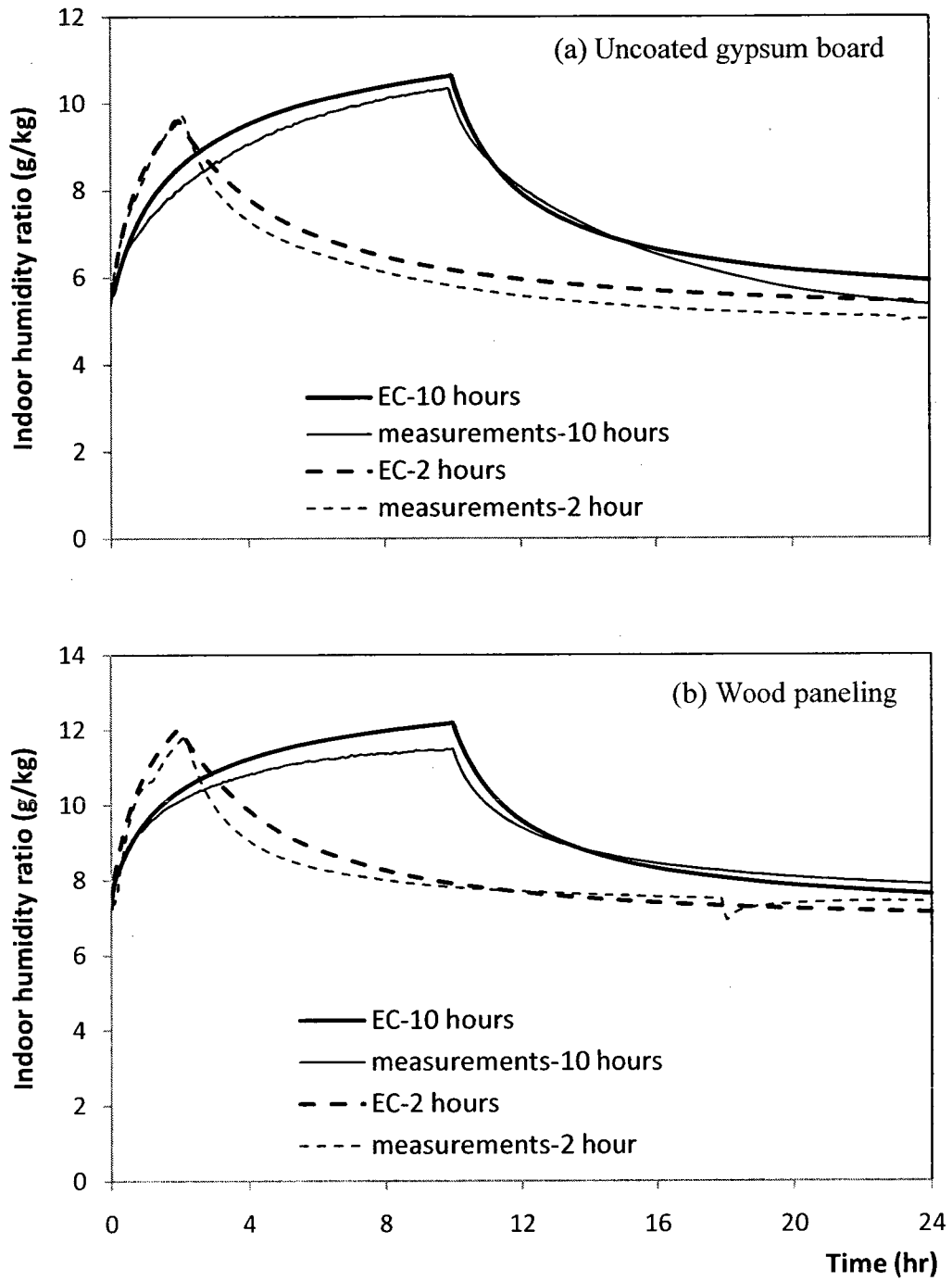


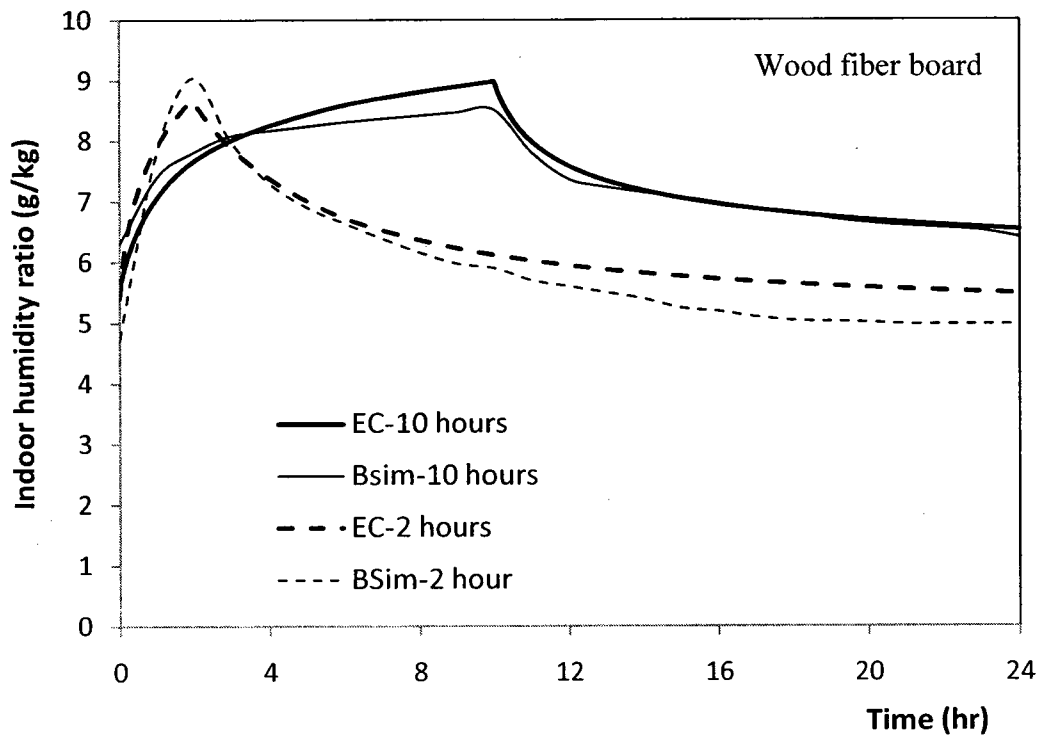
Figure 5.16. Predicted accumulated moisture buffering value ( $b_m^*$ ) using effective capacitance (EC) method compared to those calculated from experimental investigation, (a) gypsum board, (b) wood paneling.



**Figure 5.17. Predicted accumulated moisture buffering value ( $b_m^*$ ) using the effective capacitance (EC) method compared to those calculated from BSim simulations.**



**Figure 5.18. Predicted indoor HR using the effective capacitance (EC) method compared to the average indoor HR measured in experiments: (a) uncoated gypsum board (b) wood paneling.**



**Figure 5.19. Predicted indoor HR using the effective capacitance (EC) method vs. BSim simulations for wood fiberboard.**

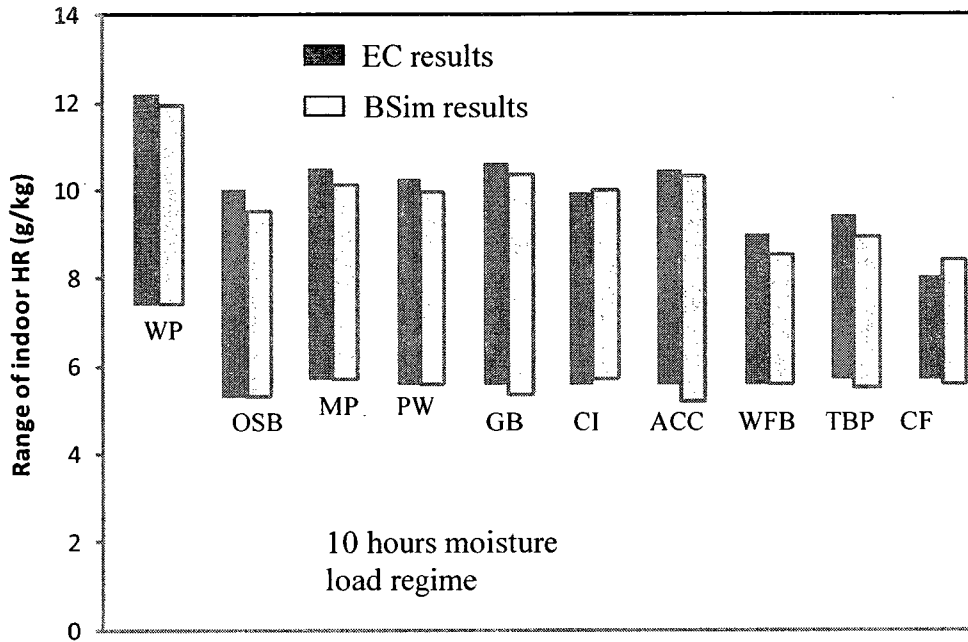
Indoor humidity ratio profile calculated by the effective capacitance model in the cases using wood paneling, gypsum board and wood fiberboard are presented in Figure 5.18 and Figure 5.19. It is observed that the indoor humidity ratio profiles calculated by effective method in cases using wood paneling and gypsum board show a good agreement to the average indoor humidity ratio profile measured in the experimental tests under both 10 hours and 2 hours moisture generation in 24 hours. The maximum differences between these two sets of profiles are 0.35 g/kg (3%) and 0.34 g/kg (3%) in the cases using wood paneling and uncoated gypsum board, respectively. The average difference is less than 0.2 g/kg (around 2%) humidity ratio for cases using either wood paneling or uncoated gypsum board. The good agreement also can be observed in the



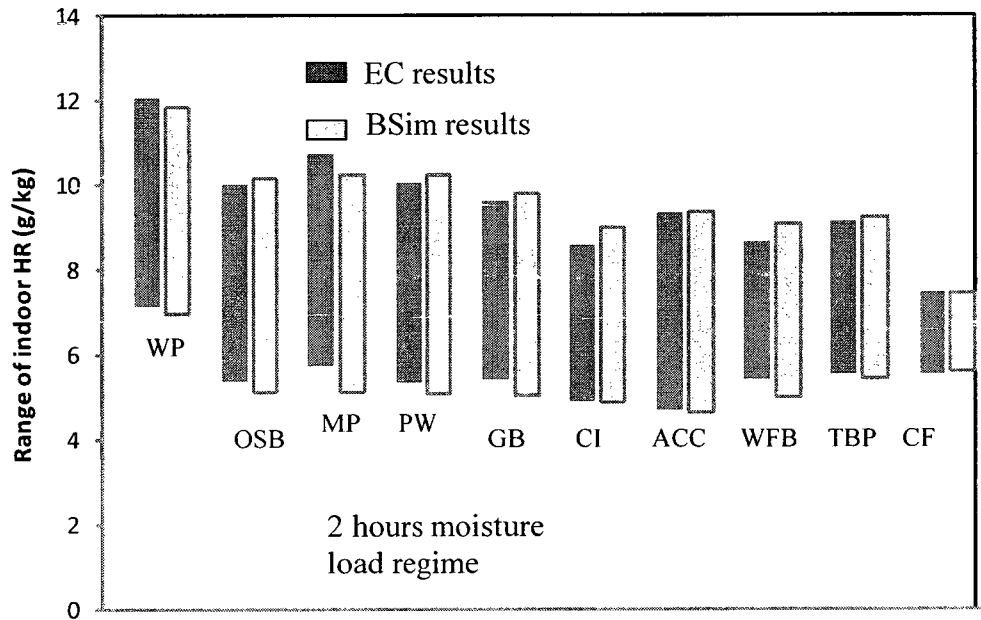
cases using wood fiberboard between effective capacitance results and BSim simulation results, with an average difference of 0.2 g/kg (2%) humidity ratio.

The variation of indoor humidity ratio calculated by the effective capacitance model and BSim simulations are compared in Figure 5.20 and Figure 5.21 for all cases under 10 hours and 2 hours moisture load schemes. It is found that the difference of indoor humidity ratio variations calculated by the effective capacitance model and BSim simulations are within 0.4g/kg humidity ratio.

In summary, it is proven that even though the difference occurs between EC calculation results and experimental calculation or BSim simulations, the effective capacitance method can estimate the indoor humidity ratio and the MAMBV with reasonable accuracy. The simplicity presented by the EC method is useful for design.



**Figure 5.20. Range of indoor HR, by effective capacitance (EC) method and BSim simulation, under 10 hours moisture generation regime.**



**Figure 5.21. Range of indoor HR, by effective capacitance (EC) method and BSim simulation, under 2 hours moisture generation regime.**

## CHAPTER 6

# LOCAL MOISTURE BUFFERING OF INTERIOR SURFACE MATERIALS

Local moisture buffering of surface materials, as results of non-uniform indoor environment, is studied based on moisture contents of surface materials obtained from experiment and from WUFI simulations applied at three locations of vertical test wall sections. The impact of furniture on the local moisture buffering of surface materials is also analyzed.

### **6.1 Local moisture content of surface materials measured from experiment**

It is observed that non-uniform indoor conditions dominate the test room environment, as presented in Appendix C. Local moisture buffering of surface materials are influenced by the local non-uniform indoor conditions. The hygrothermal performance of building envelope components behind the vapour barrier is not affected by the moisture buffering of surface materials, as shown in Appendix D.

#### **6.1.1 Temperature and RH along the test walls**

The indoor air temperature and RH close to the test walls measured in case 1 at 0.5 ACH, are presented in Figure 6.1. The temperature difference between the top and the bottom of

the test wall can be as high as 2.5 °C on the left side (close to the inlet), which is much higher than the differences in the middle and on the right side (close to outlet) of the test wall. The higher temperature on the left top corner of the test wall is attributed mainly to the baseboard heater installed at the bottom of the entry door.

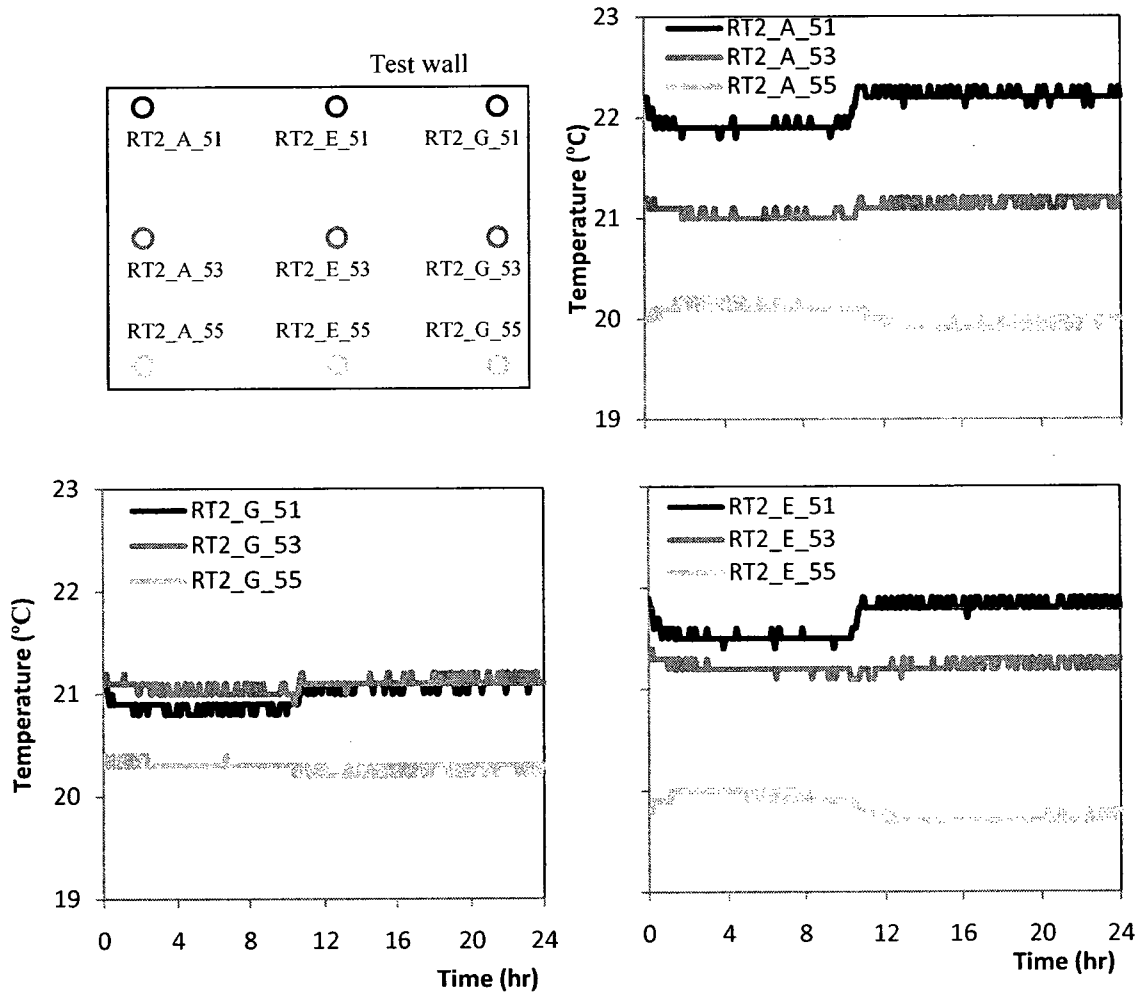
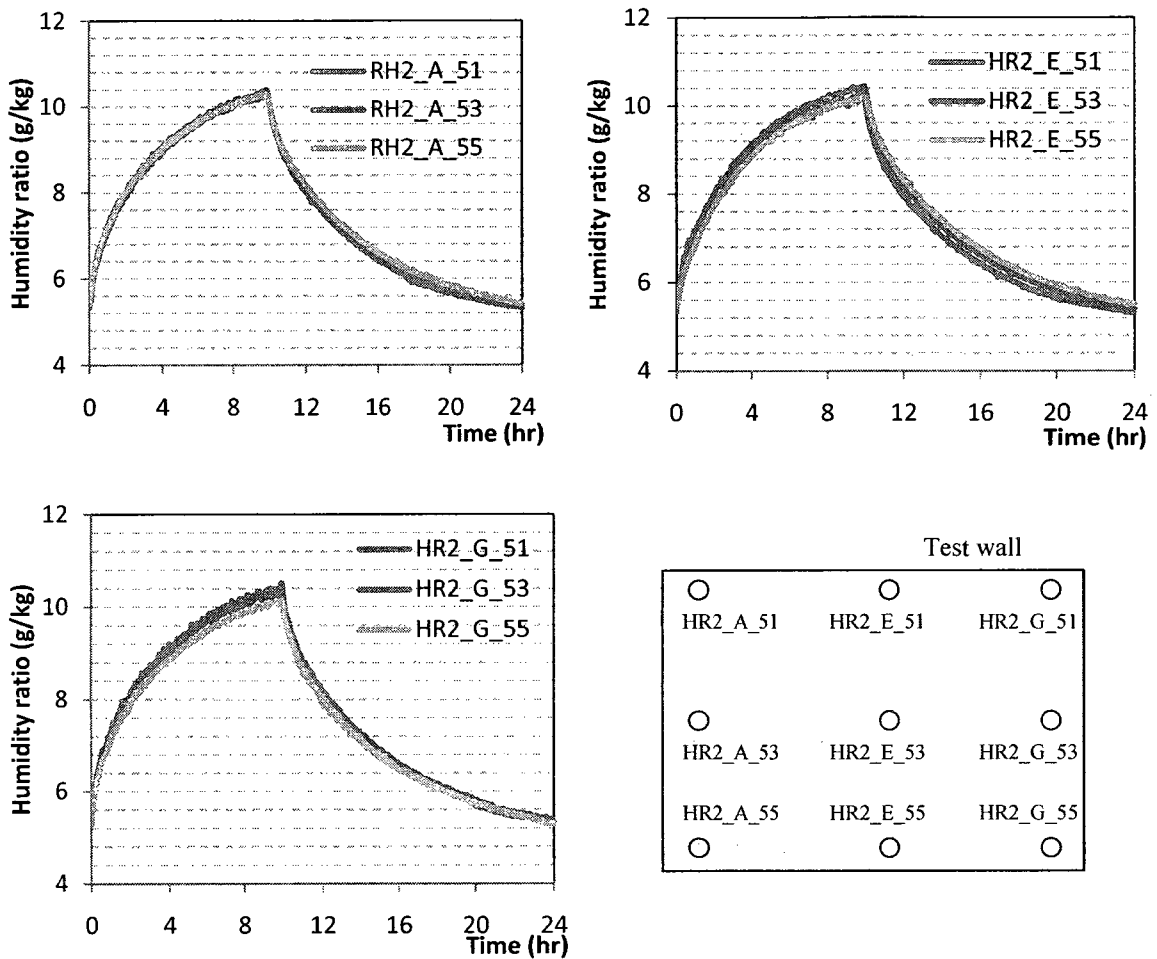


Figure 6.1. Temperatures measured by RH&T sensors close to the test wall in case

1.



**Figure 6.2. Humidity ratio close to the test wall measured in case 1.**

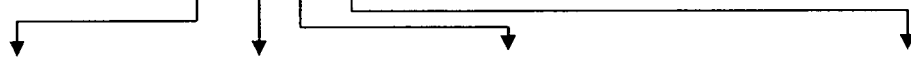
No obvious difference in air humidity at different locations close to the test walls are noticed, as shown in Figure 6.2. This lack of difference indicates that the vapour transport within the test room driven by vapour pressure differential and air movement results in a more uniform distribution of humidity than temperature.

The distribution of indoor air temperature and humidity ratio close to the test wall at other ventilation rates show the same pattern of distribution along the test walls based on the data collected from the tests.

### 6.1.2 Moisture content and temperature distribution of surface materials

Temperature of interior surface was measured by thermocouples and the moisture content was measured by the surface moisture content sensors, made of stainless screws or moisture pins, as introduced in Chapter 3. The locations of all the moisture sensors are presented in Figure 6.3.

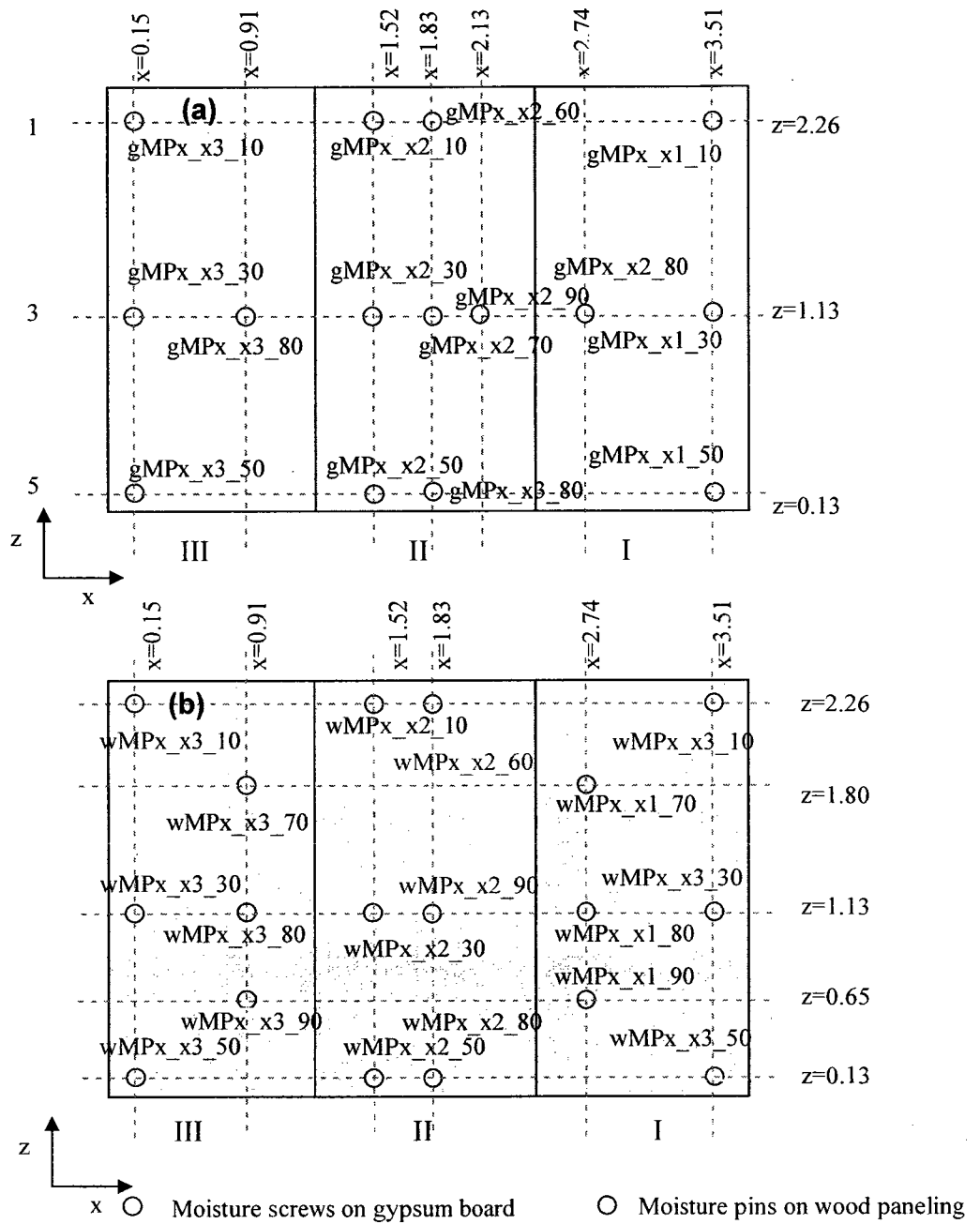
MC sensors are named as xMPx\_xx\_xx



g (GB)/w(WP); test room number; wall number: E(east)/W(west), I, II, III; location of sensors.

Thermocouples are named the same way as MC sensors: xTCx\_xx\_xx, which are accompanied with MC sensors.

The calibration of MC sensors for gypsum board is reported in Fazio et al. (2008) and the calibration of MC sensors for wood paneling is based on the experiment done by the author of this thesis, which is presented in Appendix B.



**Figure 6.3. Location of moisture content sensors on interior surface materials, (a) gypsum board, (b) wood paneling.**

Interior surface temperature is normally 1 -2 °C lower than the local indoor air temperature. For example, at edge of test wall (close to the outlets), gTC2\_E1\_10, gTC2\_E1\_30 and gTC2\_E1\_10 were 1.2-1.5 °C lower than RT2\_G\_51, RT2\_G\_53, and RT2\_G\_55, as shown in Figure 6.4.

The distribution of temperature along the interior surface materials in the periods of moisture generation and no moisture generation in case 1 (0.5 ACH) are presented in Figure 6.5. It is found that the temperature of interior surface materials during moisture generation period is influenced by the hot stream generated by the hot pot at the centre of the test room (0.45 m high), and the baseboard heater installed at the bottom of the entrance at the left corner. The left top corner (above the baseboard heater) and the center of test walls (close to the hot pot) have the highest temperatures, as shown in Figure 6.5 (a). Right bottom corner (besides outlets) is the coldest point. During the period without moisture generation, the surface temperature is mainly influence by the baseboard heater. The surface temperature shows a general trend of decreasing from the left top corner (above baseboard heater) to the right bottom corner (besides outlets), as shown in Figure 6.5 (b). In both periods, the temperature at the bottom of test walls was always lower than those at upper level. The average temperature of surface materials during the moisture generation period is higher than that in no moisture generation period.



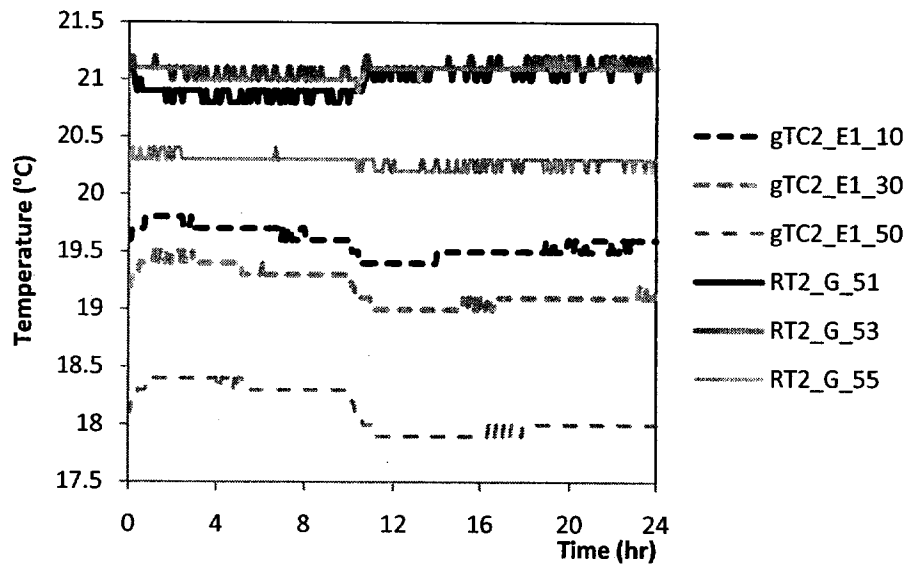


Figure 6.4. Example of interior surface temperature vs. local indoor air temperature.

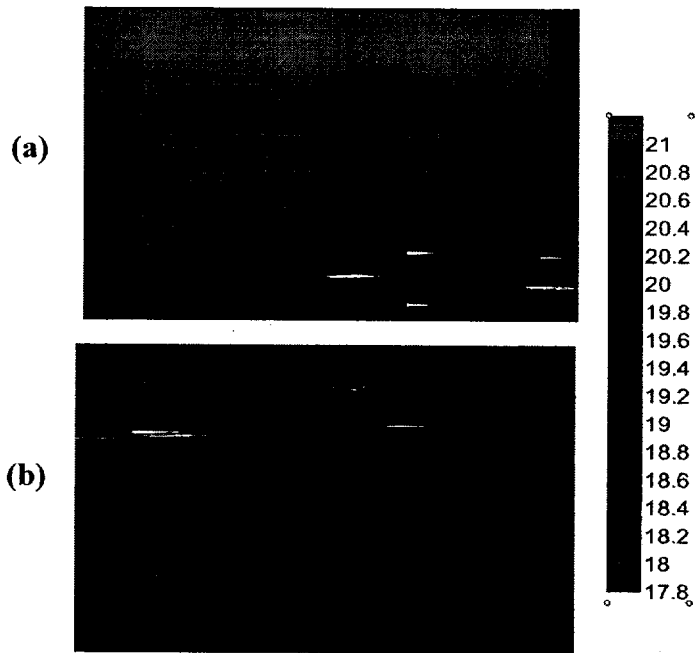


Figure 6.5. Interior surface temperature distribution on gypsum board in case 1, (a) moisture generation period, (b) no-moisture generation period.

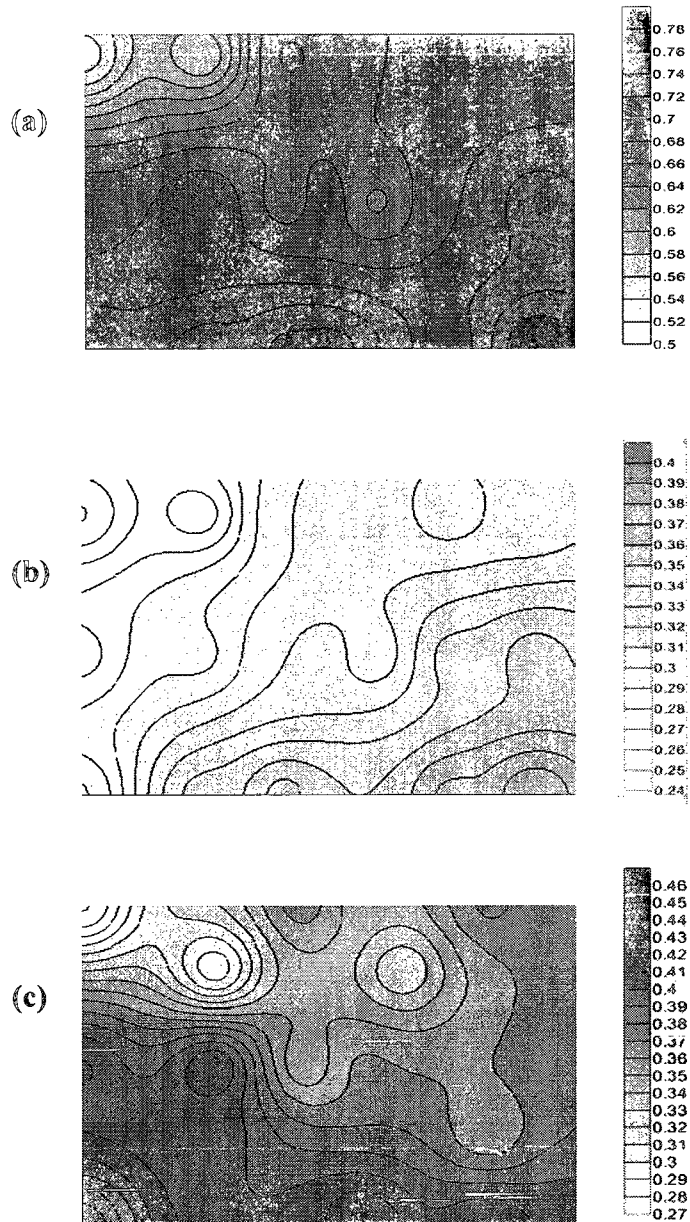


Figure 6.6. The moisture content (%) distribution on gypsum board in case 1: (a) at the end of the moisture generation period, (b) at the end of no moisture generation period, (c) maximum moisture variation in one daily moisture cycle.

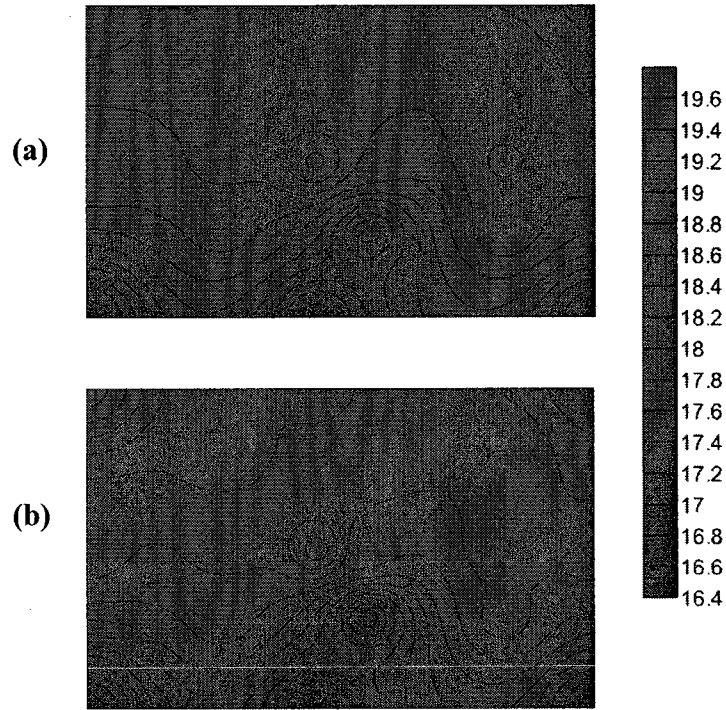
The moisture content distributions on the uncoated gypsum board in case 1 (0.5ACH) at the end of the moisture generation period and at the end of the no-moisture generation period are plotted in Figure 6.6 (a) and (b). The figures indicate that the higher moisture content is observed at areas where low surface temperature occurs. For example, at the left bottom corner of the test wall where the lowest temperature was measured, the moisture content of this area was higher than the rest of the wall. By contrast, the top left corner is the area with the highest temperature where the moisture content was lower than other areas. In summary the bottom area provides a higher moisture buffering and the top left corner shows a relatively low moisture buffering.

Similar temperature and moisture content distributions are observed in cases using wood paneling, as presented in Figure 6.7 and Figure 6.8. The difference is that the average indoor room temperature (19.5- 20.5 °C) in cases using wood paneling was lower than the indoor temperature (20 -21.5 °C) in cases using uncoated gypsum board. As a result, the surface temperatures in cases using wood paneling were around 1 °C lower than those in cases using uncoated gypsum board.

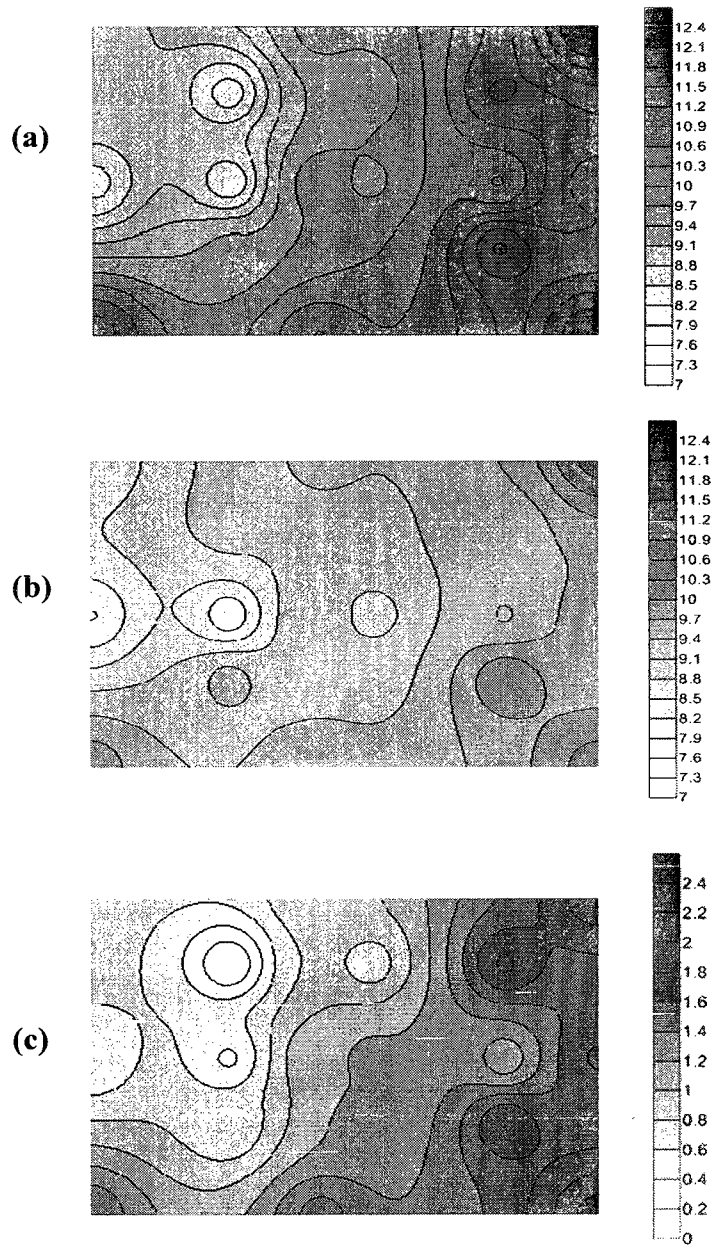
Areas at the bottom and right corner of wood paneling (interior surface of test walls) absorb more moisture during daily moisture cycle compared to other places of test walls as presented in Figure 6.8 (c).

It is necessary to mention that the distribution of surface temperature and moisture content are generated based on measurements taken at locations shown in Figure 6.2. The distribution contour was generated automatically under a gridding power of 2 and gridding smoothing factor of 0.2. The temperature and moisture content at other

locations, beyond the points where measured data are available, could be different from the real temperature and moisture content. However the figures provide the general pattern of the distribution of temperature and moisture content on the interior surface.



**Figure 6.7. Temperature distribution on wood paneling in case 13: (a) moisture generation period, (b) no moisture generation period.**

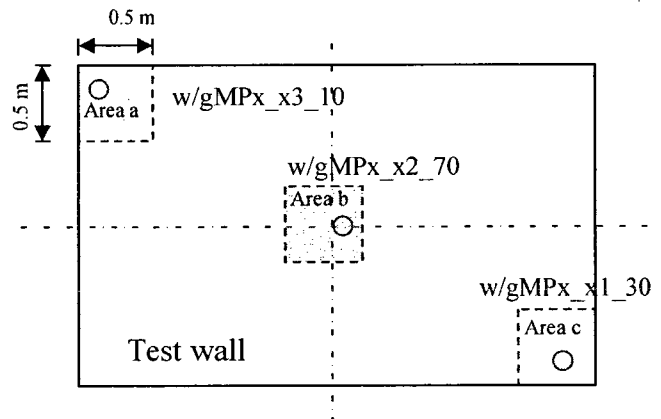


**Figure 6.8. Moisture content distribution on wood paneling in case 13: (a) at the end of moisture generation period, (b) at the end of no-moisture generation period, (c) maximum moisture content variation in one daily moisture cycle.**

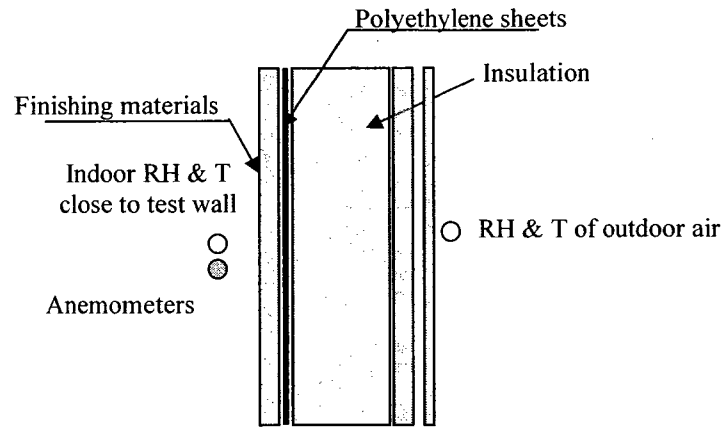
## 6.2 Local moisture buffering of surface materials and impact of ventilation rates

### 6.2.1 WUFI simulation set up and test scenarios

As seen from the previous section, the bottom section of test walls absorbs much more moisture during moisture generation period. By contrast, the left top corner and the centre of test walls are the places where less moisture is absorbed. Local moisture buffering of surface materials at these locations is analyzed by applying WUFI pro4 simulations on three areas, as shown in Figure 6.9.



**Figure 6.9. The locations of the areas on test wall (vertical section) analyzed in WUFI simulations.**



**Figure 6.10. The model of WUFI simulations on local area of interior surface materials.**

The local indoor T and RH measured by RH & T sensors are used to define air conditions that the surface area was exposed to, as shown in Figure 6.10. The measured RH & T in the outdoor air is used as ambient air conditions at the back of the vertical wall section. The local indoor air velocity measured by anemometers is used to determinate the surface mass transfer coefficient based on Re number:

$$Re = \frac{\rho V_{\infty} L}{\mu_f} \quad (6.1)$$

where,  $V_{\infty}$  is the external air velocity out of the boundary layer (m/s);  $L$  is a characteristic length, under the circumstance of interior surface; and  $\mu_f$  is viscosity at surface temperature  $T_f$ , and can be calculated based on Sutherland law as,(White, 1999)

$$\mu_f = \mu_o \left( \frac{T_f}{T_o} \right)^{3/2} \left( \frac{T_o + S}{T_f + S} \right) \quad (6.2)$$

in which,  $T_o$  is 273 K,  $\mu_o$  is viscosity of dry air at  $T_o$ , which is equal to 1.71E-5 kg/(m·s),  $S$  is 110.4 K, and  $T_f$  is the film temperature and defined as,

$$T_f = \frac{T_s + T_{in}}{2} \quad (6.3)$$

$T_s$  is the average temperature on the surface of uncoated gypsum board or wood paneling,  $T_{in}$  is the indoor air temperature close to the test walls.

Air velocities close to the test wall were measured at a time interval of 0.2 second. The local average air velocity during the moisture generation period is used as  $V_\infty$  to calculate Re number. The difference of air velocity between moisture generation period and no-moisture generation period is neglected.

The air velocities at different planes (east west) close to the test wall and at different ventilation rates are presented in Figure 6.11. Air velocity of area a and b is taken at height of 2.26 m and 1.13 m at plane B and plane E, respectively. Air velocity of area c is taken as half of air velocity at height 0.65 m at plane G. The definition of the plane can be found in Figure 3.11 and 3.12.



Thus using air velocity, Re can be calculated by Eq. 6.1.  $h_m$ , the mass transfer coefficient can then be estimated from the correlation between mass transfer coefficient and Re number obtained in the experiments by Iskra et al. (Fazio et al. 2008, Appendix A2). Mass transfer coefficient for wood paneling is set as 0.0001m/s, since there is no significant different on mass transfer coefficient in the range of 600-2200 Re number. The local air velocities and interior moisture transfer coefficients at different surface areas under different ventilation rates are presented in Table 6.1.

In WUFI simulation, surface heat transfer resistance was calculated by (Kunzel, 1995)

$$R_i = 7 \cdot 10^{-9} / h_m \quad (6.4)$$

where  $R_i$  is the surface heat resistance ( $m^2K/W$ );  $h_m$  is the water vapour transfer coefficient ( $kg/m^2 \cdot s \cdot Pa$ ), can be obtained from the relation

$$h_m = \frac{0.622 \cdot \rho \cdot \beta_p}{P_a} \quad (6.5)$$

$P_a$  is the ambient air pressure (Pa).

The exterior surface heat transfer resistance is adopted from default setting of WUFI model, which is 0.0588  $m^2K/W$ .

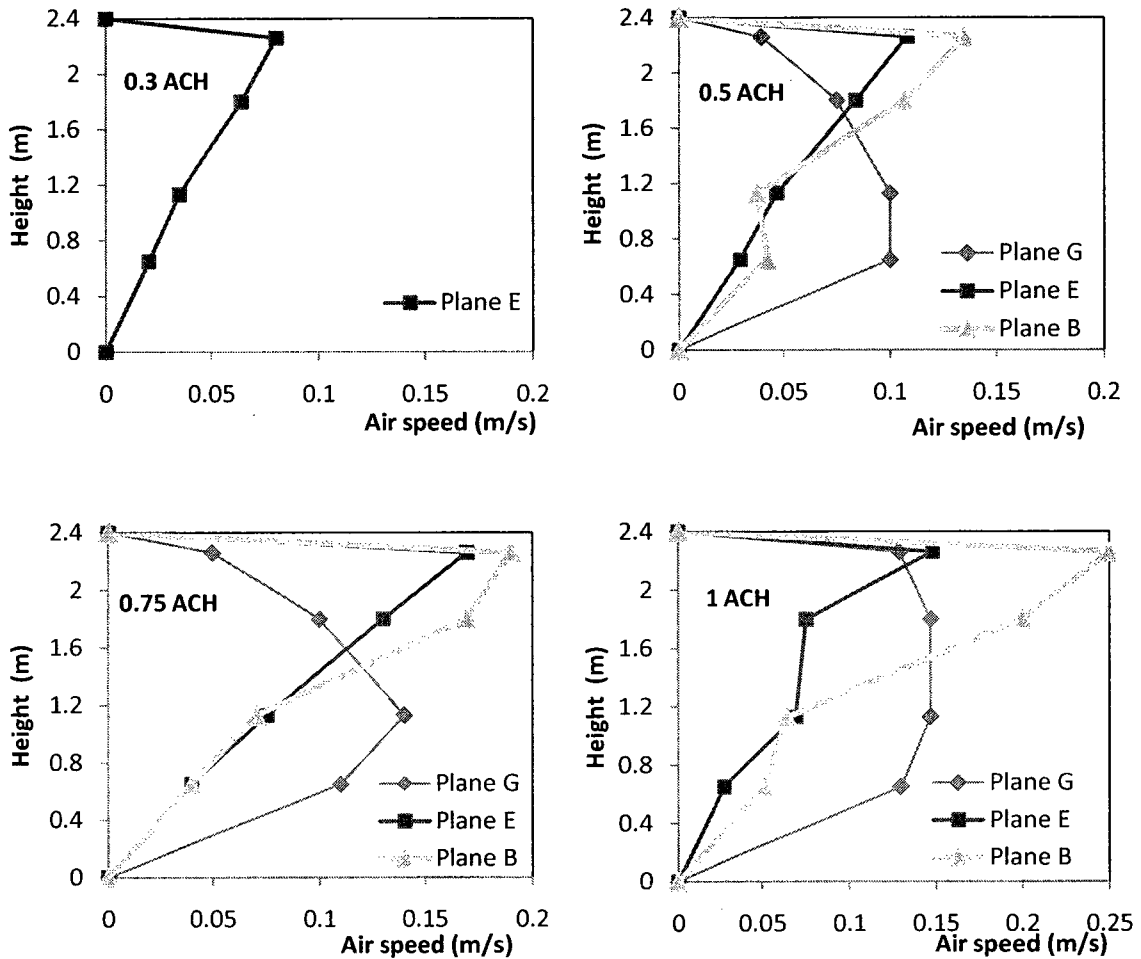


Figure 6.11. Air velocity profile close to test walls at different planes (east and west).

Table 6.1 Mass transfer coefficients and air velocity at different locations at different ventilation rates (gypsum board).

Area	0.3 ACH		0.5 ACH		0.75 ACH		1 ACH	
	Velocity (m/s)	$\beta_p$ (m/s)	Velocity (m/s)	$\beta_p$ (m/s)	Velocity (m/s)	$\beta_p$ (m/s)	Velocity (m/s)	$\beta_p$ (m/s)
Area a	x	x	0.135	0.0036	0.191	0.0025	0.250	0.0027
Area b	0.035	0.0028	0.047	0.0030	0.075	0.0033	0.051	0.0030
Area c	x	x	0.028	0.0026	0.030	0.0028	0.049	0.0029

Notes: “x” in the table resembles no data available.

### 6.2.2 WUFI simulation validation

WUFI Pro 4 was validated by comparing the predicted hygrothermal responses in the walls to those measured during the experiments. The simulations are applied to the centre cross section (Area b) of test walls as shown in Figure 6.9 and 6.10. The measured local indoor RH and T close to the section and RH and T measured at outdoor environment were used as the indoor and outdoor conditions of the wall section in WUFI simulations.

Moisture contents measured by electronic resistive probes (maximum moisture content at inner layer of surface materials) on the center area of test walls from the large-scale experiment were compared to the moisture contents at different depths calculated from WUFI simulations, as shown in Figure 6.12 (a) and (b).

It shows that the surface moisture content obtained from WUFI simulations agree well with the measurements in the moisture generation period with an average difference in moisture content (MC) of 0.02% and 0.08% for cases using uncoated gypsum board and wood paneling, respectively. It also indicates that the maximum moisture content occurs on the surface of interior surface materials during the moisture generation period.

It is noticed that there are bigger differences between the MC measured in the experiment and the surface MC obtained from simulation at the beginning segments of the no moisture generation period. This big difference is due to the fact that maximum MC does not occur on the surface any more during no-moisture generation period. The grey lines under the surface MC in Figure 6.12 (a) and (b) are the MCs at different depth of surface materials obtained from WUFI simulations under 10/14 moisture load. The maximum MC profile obtained from WUFI simulations are compared to those from measurements.

It is found that two profiles agree with each other very well during no-moisture generation period. The MC profiles within the first 8mm depth of uncoated gypsum board at different times are presented in Figure 6.13 as an additional example of moisture content distribution.

It is also noticed that the moisture content of uncoated gypsum board returns back to the level at the beginning of the moisture load cycle; however, higher moisture content (0.4 % MC) levels are observed at the end of the moisture load period in wood paneling as compared to that at the beginning of the daily cycle under 10/14 moisture load. This higher moisture content in wood paneling at the end of the moisture load cycle? represents a moisture residual in the material and corresponds to the moisture residual analyses made by MAMBV in the previous section.

Under the short moisture load regime (2/22 hours), the higher moisture content at the end of the cycle in cases using wood paneling is not observed because the longer duration of the no moisture generation period allows wood paneling to release almost all moisture absorbed back into the indoor environment.

The total moisture buffering by materials under different moisture load schemes is hard to be analyzed by only comparing the moisture content of materials, so these analyses are not discussed in this section.

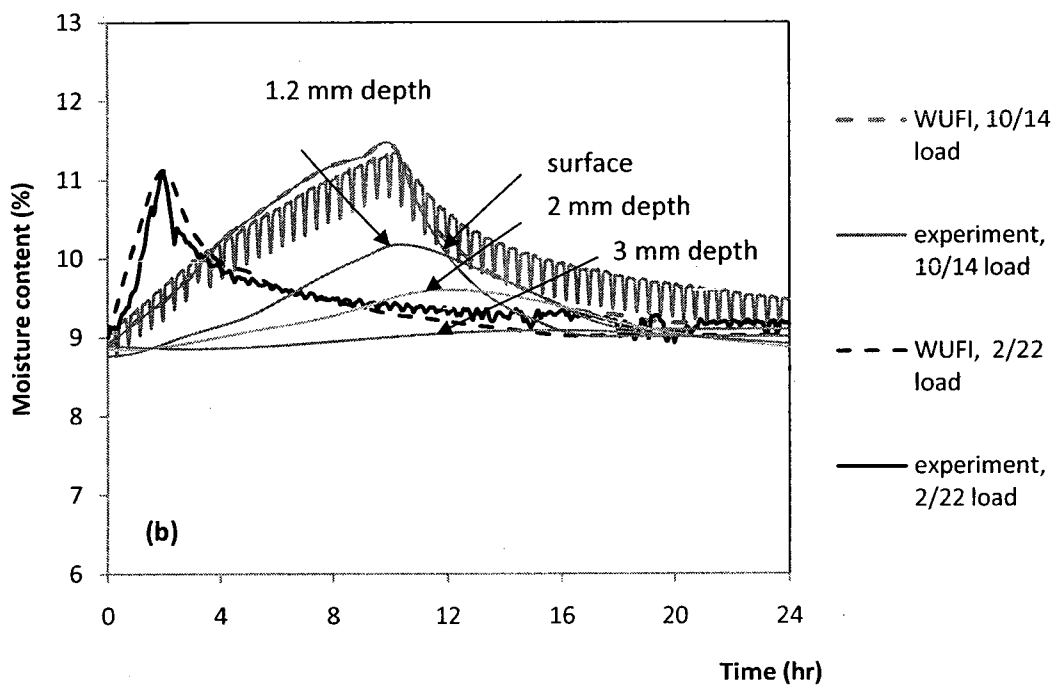
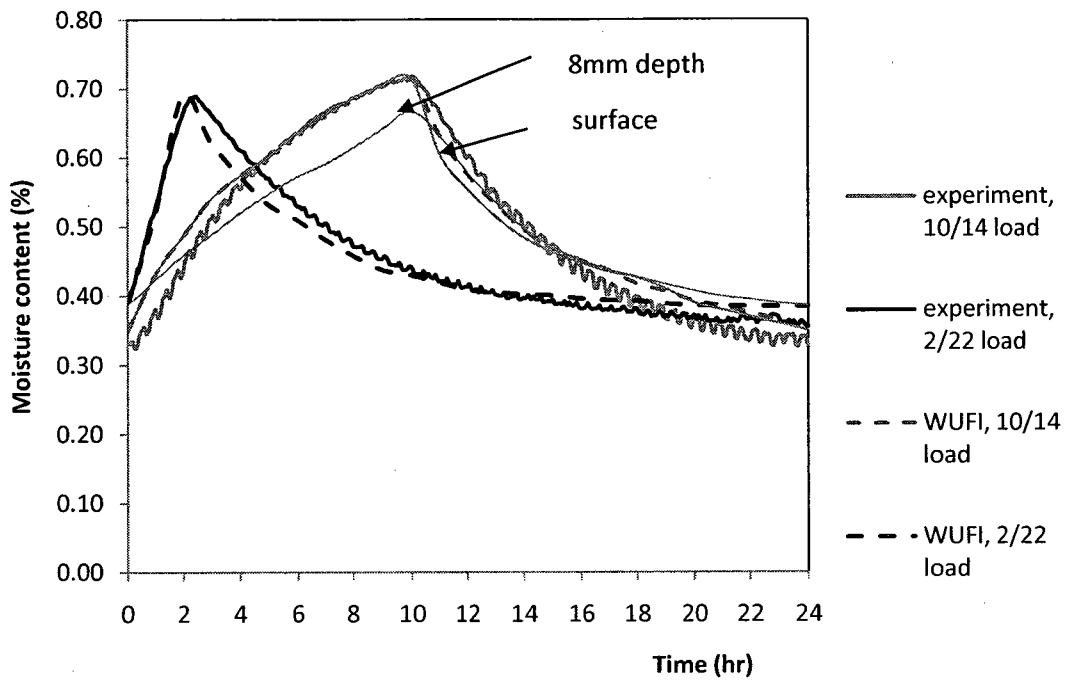
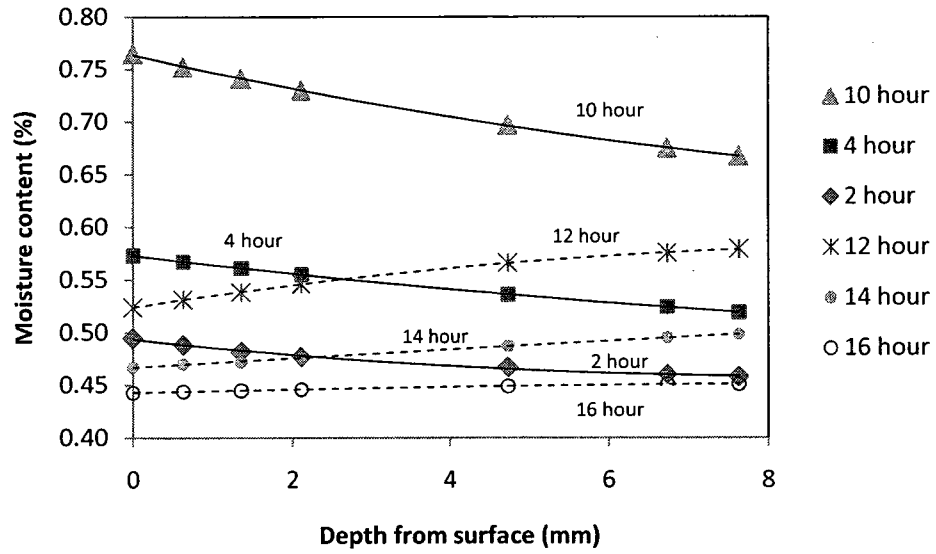
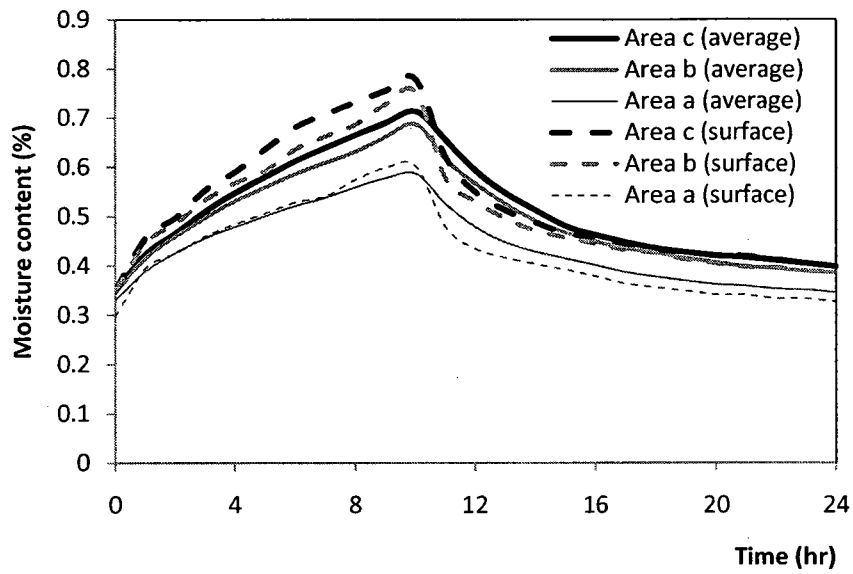


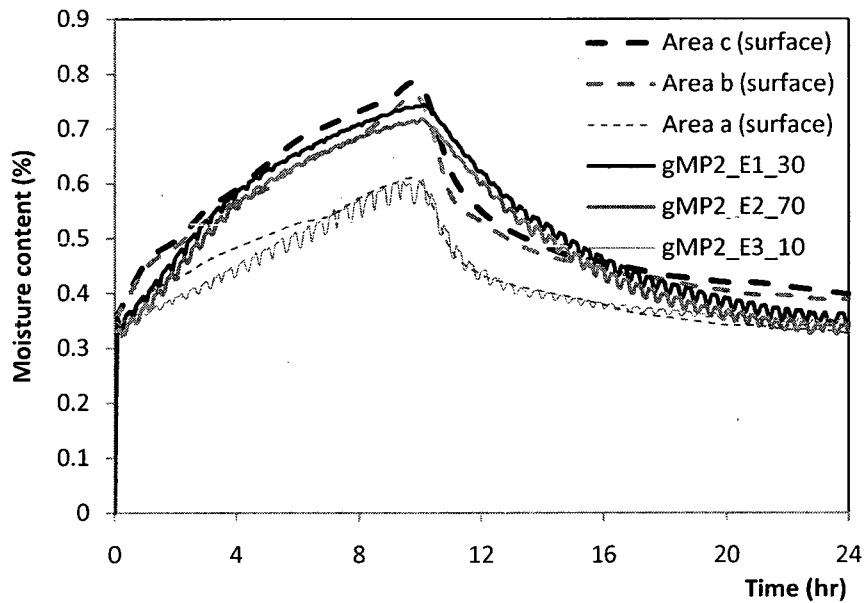
Figure 6.12. Moisture content comparison between WUFI simulations and experimental measurements, (a) uncoated gypsum board, (b) wood paneling.



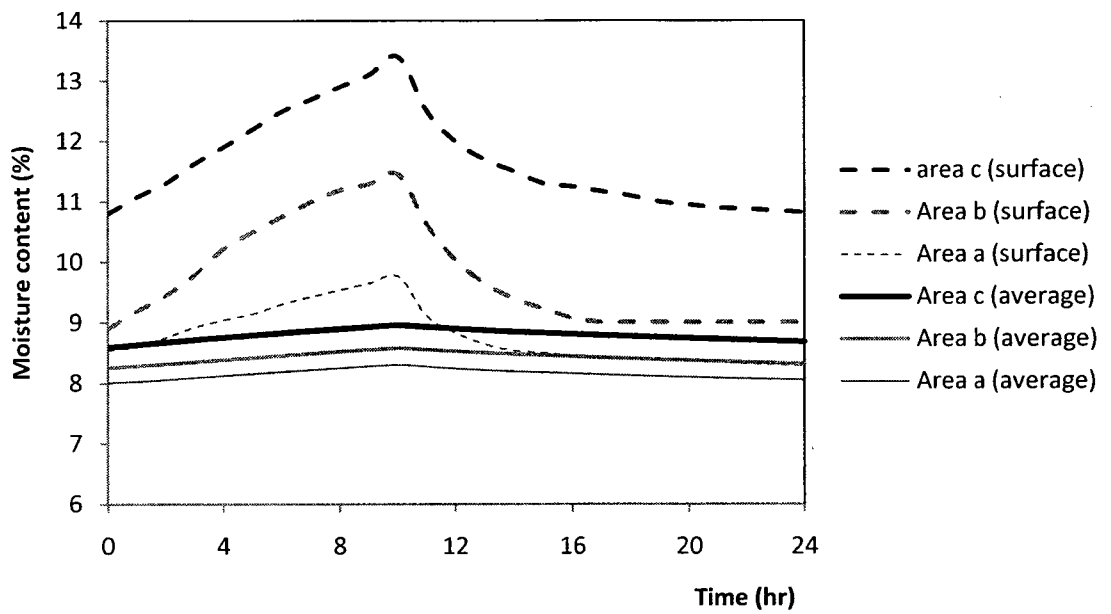
**Figure 6.13. Moisture content distribution in case 1(10/14 hours load) at different times in one day period.**



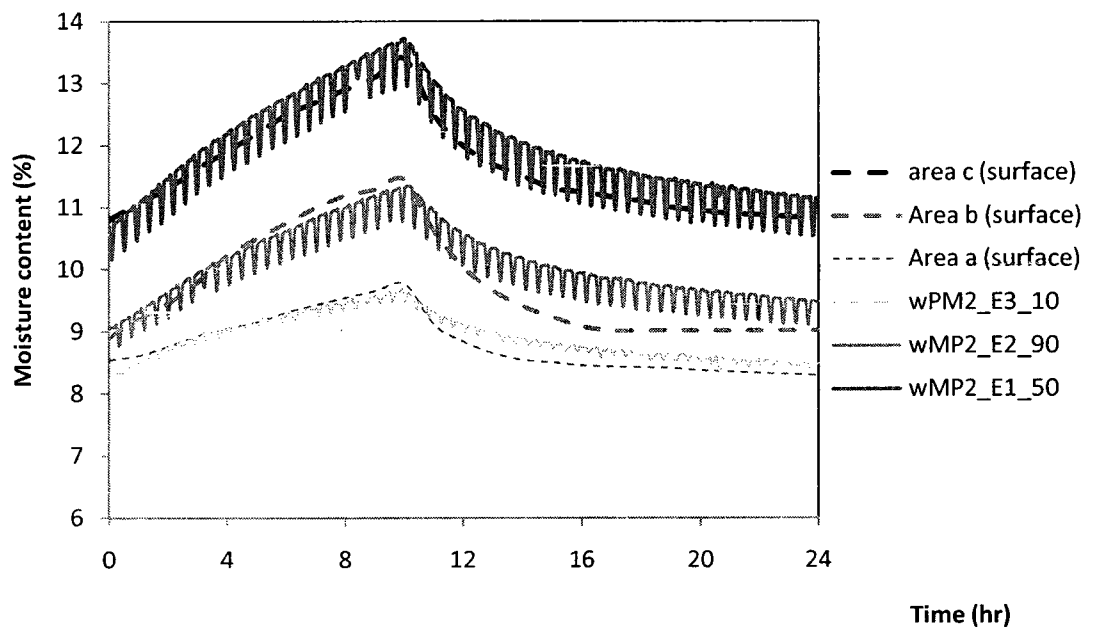
**Figure 6.14. Average moisture content in uncoated gypsum board in areas a, b, c at 0.5 ACH, from WUFI simulations.**



**Figure 6.15. Surface moisture content (at 0.5 mm) on uncoated gypsum board simulated (WUFI simulation) vs. moisture content measured at 0.5 ACH. (locations of sensors and the corresponding area are shown in Figure 6.2.)**



**Figure 6.16. Average moisture content in wood paneling in areas a, b, c at 0.5 ACH, from WUFI simulations.**



**Figure 6.17. Surface moisture content on wood paneling measured from WUFI simulation, compared to moisture content measured at areas a, b, c at 0.5 ACH.**



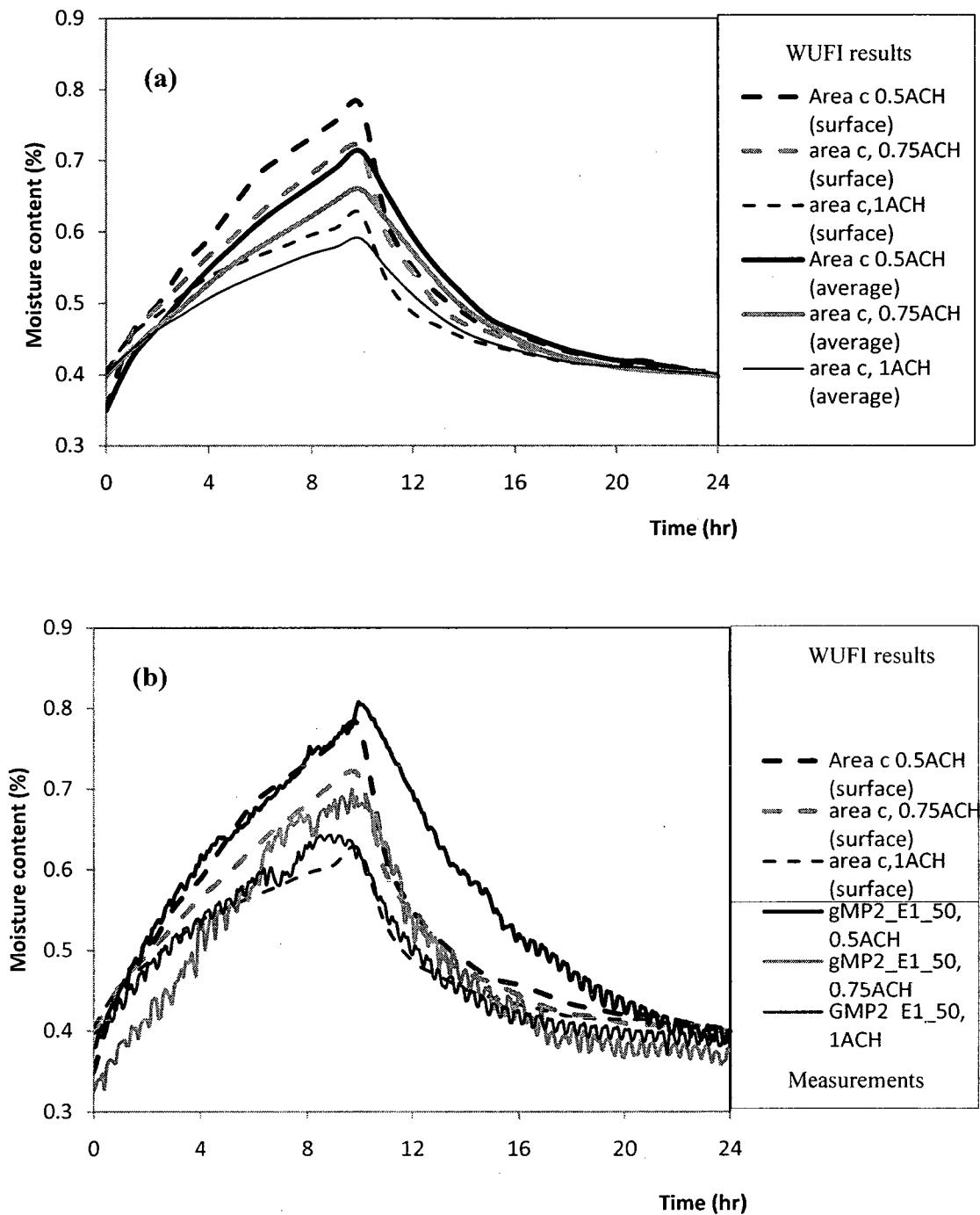
### **6.2.2 Simulation results analyses and discussion**

It is observed from Figure 6.14-17 that both average moisture content and the surface moisture content on area c are higher than those on area a and b (obtained from WUFI simulations). Area a shows the smallest amount of moisture absorption. These results provide the same moisture content distribution as shown in Figure 6.6 and Figure 6.8. Area c shows a wet and cold condition, which is susceptible to moisture damage. Surface moisture content of materials is obtained from the moisture content at 0.5 mm depth of materials in WUFI simulations.

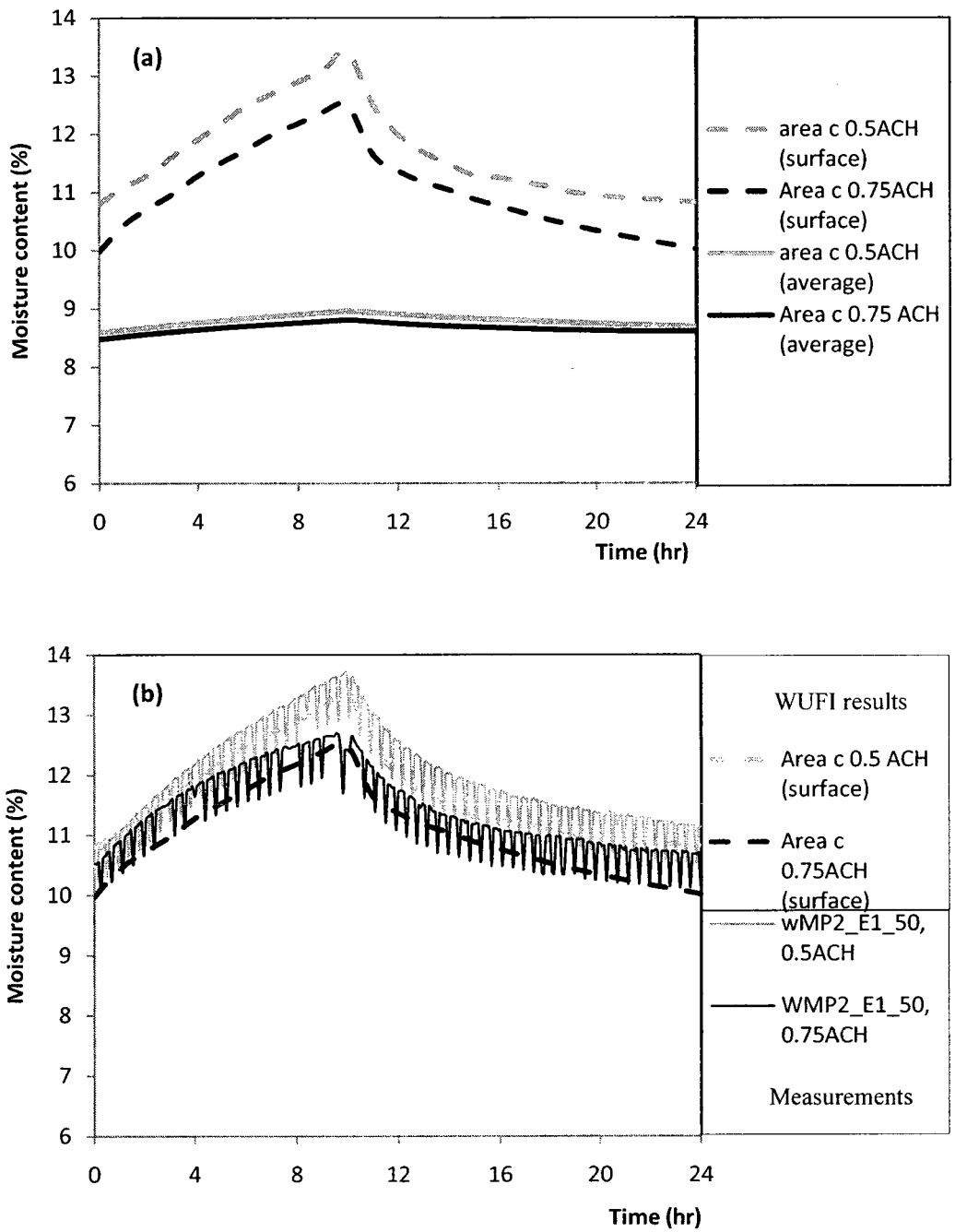
The surface moisture content profiles (at depth of 0.5 mm) calculated by WUFI simulations agree well with those obtained from experiments in the moisture generation period. However, in no-moisture generation period, surface moisture content profiles are lower than the maximum moisture content profiles measured from experiments. Under such a circumstance, the maximum moisture content may occur in the deeper layer of materials instead of at the surface of materials.

It is also shown in Figure 6.14 and 16 that the surface moisture content is higher than the average moisture content for both cases using uncoated gypsum board and wood paneling. The surface moisture content in case 13 using wood paneling is much higher than the average moisture content (up to 2-5 % MC, about 50% of MC variation). This difference may be explained by the fact that the penetration depth of wood paneling is around 5 mm, which is smaller than the thickness of wood paneling. Moisture content of the part beyond the depth of 5 mm is not influenced by indoor humidity variations. By contrast, the penetration depth of gypsum board is over 60 mm, which is much larger

than the thickness of the gypsum board itself. The whole depth of the gypsum board participates in the moisture buffering. Therefore, the difference between the surface moisture content profiles and the average moisture content profiles in uncoated gypsum board is much smaller (0.1-0.15% MC, around 20% of the MC variation).



**Figure 6.18. Moisture content in gypsum board at area c at different ventilation rates, 0.5, 0.75 and 1 ACH: (a) average vs. surface moisture content, (b) simulation results vs. measurement data.**



**Figure 6.19. Moisture content in wood paneling at area c at different ventilation rates, 0.5 and 0.75 ACH: (a) average vs. surface moisture content, (b) simulation results vs. measurement data.**

The impact of ventilation rate on local moisture content is shown in Figures 6.18 and 19. It is obvious that with the increase of ventilation rates, less moisture is absorbed in area c. In addition, higher surface temperature can be observed from both simulation results and measurements. The moisture condition of area c is improved with the increase of ventilation rate.

Hence, there should be a balance between getting maximum moisture buffering of surface materials and improving the moisture condition of surface materials at the cold corner of external walls. The solution of this problem is to increase the air velocity close to the cold corner or cold bottom surface by selecting different ventilation system (eg. changing the location of diffuser).

The impact of ventilation layout on the moisture buffering is not studied in this section. The ventilation layout and system influences the distribution of indoor conditions, which consequently influences the moisture buffering potential of surface materials. With the help of CFD simulations, further research should include more types of ventilation systems and their effect on moisture buffering effect.

### **6.3 Impact of furniture blocking on local moisture buffering of surface materials**

The moisture buffering potential of furniture cases are analyzed in Section 4.2.5. With the addition of furniture, the combined moisture buffering potential by furniture and surface materials is increased, however, the contribution of surface materials is decreased. This decrease is observed in moisture content measurements. The variation of moisture content in surface materials is smaller compared to the variation in cases with no furniture involved. However, the variation of moisture contents of surface materials blocked by furniture does not always follow the same trend.

As shown in Figure 6.20, moisture content of sensors behind curtains (wMP2\_W2\_10 and wMP2\_W2\_60) reached a higher level of moisture content in case 25 compared to those in case 23 (no curtain was installed). But other sensors, which were not blocked by curtains, showed a lower or the same moisture content as those in case 23, as shown in Figure 6.21. Colder surface temperature was also observed on the surface blocked by curtains in case 25, as shown in Figure 6.22. The surfaces blocked by furniture present colder and more humid conditions. These surfaces are easier to get moisture damage compared to other open surfaces.

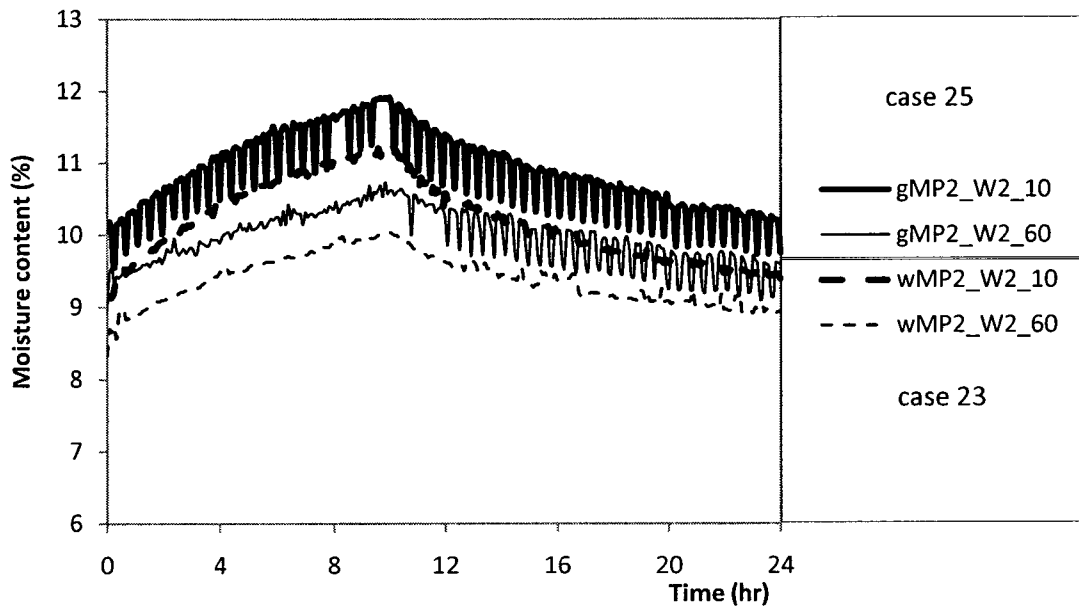


Figure 6.20. Examples of moisture content behind the curtains in case 25 vs. those in case 23.

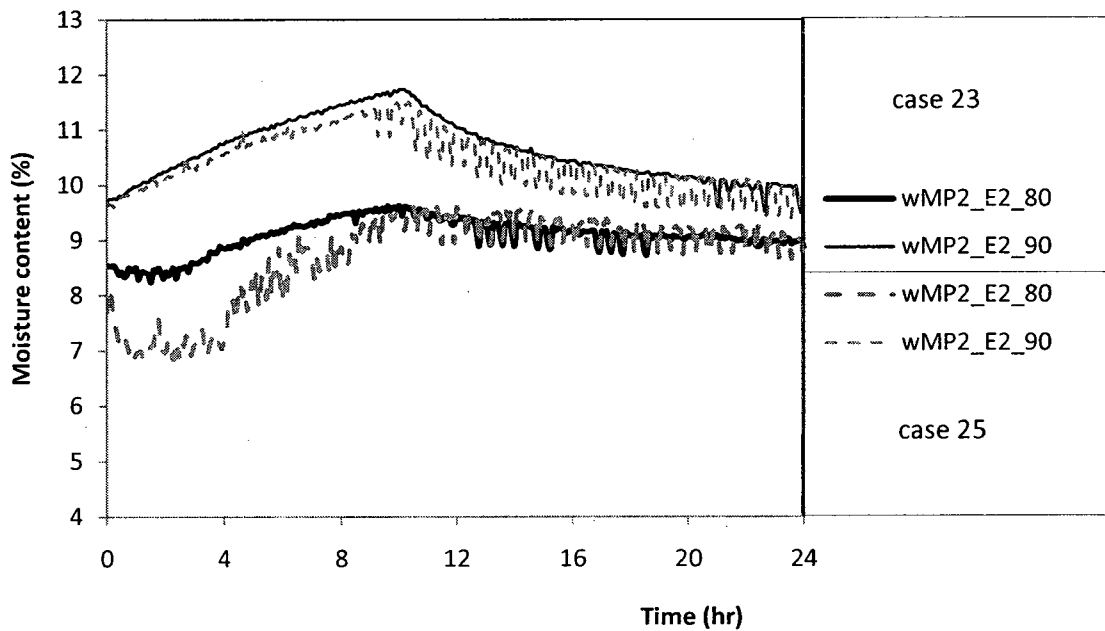
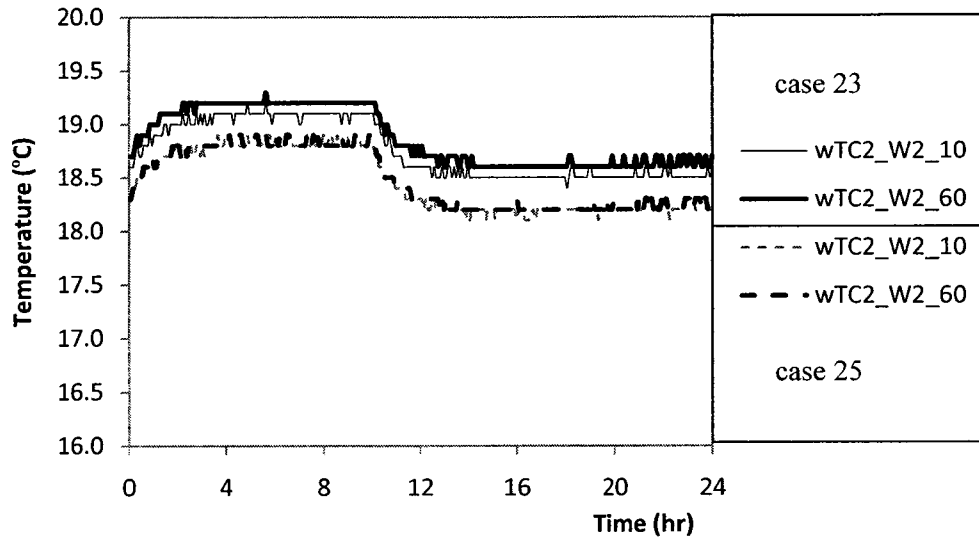


Figure 6.21. Examples of other moisture content measured in case 23 and case 25.



**Figure 6.22. Examples of temperate on the surface blocked by curtain in case 25 compared to those in case 23.**



## **CHAPTER 7**

### **CONCLUSIONS AND CONTRIBUTIONS**

The thesis research investigates the moisture buffering potential and local moisture buffering of interior surface materials in 28 cases carried out in a full-scale experimental investigation and 54 cases conducted in BSim simulations. The moisture buffering behaviour of hygroscopic materials under different moisture load schemes and the impact of moisture history on moisture buffering of materials are analyzed in three-stage WUFI simulations. Based on these analyses hygroscopic materials are categorized for practical application and recommendations are made on conducting large-scale experimental investigation in terms of experiment design and test procedure. The experimental data has contributed to the recently completed Annex 41 on the WBHAM (whole building heat, air and moisture) responses. The research findings also identify areas for future research.

#### **7.1 Summary of findings**

Results obtained from the large-scale experimental investigation and HAM simulations are summarized below. Based on these findings, recommendations are made on the test procedure of carrying out large-scale laboratory experiments or field tests and on the selection of material for moisture buffering application.

The moisture buffering effect has been investigated through the analysis of moisture balance in a full-scale experiment and in WBHAM simulations using BSim in this thesis research. A new index, MAMBV, has been developed and calculated to evaluate the moisture buffering potential of materials applied in indoor environment in different test scenarios. It is found that

- 1) The MAMBV can be used to quantify the amount of the moisture absorbed by the materials, which allows the direct comparison of moisture buffering potential of different materials under different test conditions.
- 2) Specially designed AHU (Air handling unit) provides an accurate method (condensed water method) to calculate the amount of the moisture carried in and out of test room by ventilation air, which is an essential component of moisture balance established in test rooms.
- 3) Under the same supply air conditions, with the increase of ventilation rates, the moisture buffering potential of materials decreases. No significant moisture buffering effect can be found when the ventilation rate exceeds 3 ACH. The reduction of moisture buffering potential is much more significant with the increase of ventilation rate when the ventilation rate is lower than 1 ACH.
- 4) The moisture generation protocol, including moisture generation rate and moisture generation schemes, influences the moisture buffering potential of surface materials. The higher moisture generation rate, the more moisture source is available for moisture buffering, and thus more significant moisture buffering

potential appears. The moisture buffering potential under different daily moisture load regime is determined by materials' moisture capacity and vapor permeability.

- 5) Supply air conditions partly determine the level of indoor humidity. Higher humidity level of supply air increases indoor humidity level and, as a result, enhances the moisture buffering effect. It is observed that the impact of changing the humidity level of supply air is more significant at low ventilation rates.
- 6) The larger areas of hygroscopic materials used in the indoor environment, the more moisture is buffered. However, the increase of moisture buffering is not proportional to the increase of hygroscopic materials. This impact is more significant when the volume rate is under the optimum value.

The experimental results and numerical simulations indicate that moisture buffering capacity of materials under different moisture load schemes is influenced by the material properties including moisture capacity and vapour permeability. Impact of moisture load schemes and the effect of initial conditions on moisture buffering capacity have been analyzed using HAM simulation (WUFI Pro 4) at materials level. The findings include:

- 1) Moisture capacity and vapor permeability of materials determine the moisture buffering capacity of materials under different moisture load schemes. For this reason, materials can be categorized into three groups. Group A materials have high moisture capacities ( $\xi$  is over  $\sim 20 \text{ kg/m}^3\%RH$ ), however low vapor permeability ( $\mu$  is higher than 100). Group B materials have high permeability ( $\mu$  is almost around 10), but low moisture capacity ( $\xi$  is less than  $10 \text{ kg/m}^3\%RH$ ). Group C materials have both high moisture capacity and water vapor permeability.

- 2) Materials in Group A and B have the same range of moisture buffering capacities under long term daily moisture load regime (8-10 hours), which is determined by their high moisture capacity and low vapor transfer resistance factor. Materials in group C have much higher moisture buffering capacity under long daily moisture regime. However, under short daily moisture regime (less than 2 hours), the moisture buffering capacity of group A materials decreases significantly compared to that of group B materials. This sharp reduction is due mainly to their low vapor permeability. Materials in group C that have high EMPDs (Effective Moisture Penetration Depth) have relatively high moisture buffering capacity under short term daily moisture regime loads.
- 3) Moisture residuals occur in the first several moisture load cycles for materials that have low EMPDs and the time required to reach a stable moisture buffering cycle is inversely proportional to their EMPDs. So moisture residuals appear in the first several moisture load cycles of materials in group A and group C with low EMPDs.
- 4) Initial moisture conditions of the materials with low EMPDs influence their moisture buffering and the moisture residuals. Setting the initial moisture content of materials close to the equilibrium moisture content of average ambient air humidity can significantly shorten the period required to reach a stable moisture buffering cycle.

- 5) The effective capacitance (EC) method can provide a reasonably accurate prediction of the indoor humidity and MAMBV. This method can be easily used in practice application.

The local moisture buffering of interior surface materials is analyzed based on the moisture content of surface materials obtained from measurements and WUFI simulations for three locations of the test wall. It is found that the bottom, especially bottom corner of interior surface areas show relatively low temperature and high moisture buffering potential. This is influenced by the non-uniform distribution of indoor conditions. In addition, the interior surface areas blocked by furniture show relatively low surface temperature, high moisture buffering potential, and high risk of surface moisture damage.

### **Recommendations for conducting large-scale experimental or field tests**

#### 1) Design of test conditions

It is necessary to precondition materials in group A (with high moisture capacity) and materials in group C with low-penetration-depth to an equilibrium condition under an average indoor RH. This preconditioning can significantly reduce the time required to reach the stable moisture buffering cycles. In contrast, materials in group B (with low vapour transfer resistances) and materials with high penetration depth in group C do not need to be preconditioned before the test.

#### 2) Test procedure

Tests on group A materials and group C materials with low penetration depth should last for at least one month to reach the stable moisture buffering cycles. Tests on group B materials and materials in group C with high penetration depths can be limited to 3 days since no significant moisture history effect is noticed for these materials.

A stable moisture buffering cycle can be identified by verifying the repeatability of moisture content measured within the surfacing materials in each daily moisture load cycle. Indoor humidity ratio (or RH) is not accurate enough to define the stable moisture buffering cycle due to the measurements errors or errors accumulated from calculations.

Moisture balance is an important concept in moisture buffering test design. Therefore, moisture carried in and out by ventilation and air leakage and the amount of moisture input (source) need to be carefully controlled. Additional efforts are required to determine the amount of moisture carried by ventilation air since the typical way of calculating it based on measurements of air flow rate and conditions of supply and return air is not accurate enough.

### **Recommendations for material selection for moisture buffering application**

Group C materials are the best choice for moisture buffering application in spaces with long term daily moisture load (over 8 hours) such as bedrooms and offices. Group B materials are preferred to group A materials in such applications. In contrast, materials from group B and materials in group C with high penetration depths are favourable under short term daily moisture load schemes (less than 2 hours), for example in bathrooms and kitchens. Materials in group A normally do not have good moisture buffering performance in these applications.

There is a balance to apply moisture buffering and to avoid damage due to the high surface moisture. Carefully designed ventilation operation strategy and implementation to avoid cold interior surface is the key point to avoid this damage.

## **7.2 Contributions**

The main contributions of the present research are summarized as follows:

- 1) A new experimental method, condensed water method, is developed and used to accurately determine the amount of moisture removed by ventilation, which is an essential component in establishing the moisture balance in the full-scale experiment study. A custom designed AHU is used to achieve the level of accuracy required.
- 2) A new index, MAMBV, is developed and used to quantitatively evaluate moisture potential of surface materials and furniture involved in the indoor environment, and to evaluate the impacts of different parameters on moisture buffering potential.
- 3) A unique set of experimental data is collected and included in the recently completed IEA Annex 41. The data can be used to validate current and future whole building HAM simulation tools.
- 4) A practical classification of hygroscopic materials used for moisture buffering effect is provided based on the range of the materials' moisture capacity and vapor permeability. Different groups of materials show diverse moisture buffering capacities under a variety of moisture load schemes.

- 5) Recommendations for the selections of different groups of materials used for moisture buffering under different moisture load schemes are suggested.
- 6) Moisture residuals under daily moisture load cycles, i.e. the effect of moisture history on moisture buffering of materials, are investigated for the first time. The relationship between EMPD and the time to reach a stable moisture buffering cycle is identified.
- 7) Influence of initial moisture conditions of materials on their moisture buffering and moisture residuals is investigated.
- 8) Recommendations in terms of test procedure and consideration of initial conditions are made for large-scale experimental investigation of moisture buffering effect.
- 9) Impact of non-uniform indoor conditions on local moisture buffering was investigated for the first time in large-scale experimental study. Data collected are valuable for the validation of CFD simulations.

### **7.3 Recommendations for future research**

Moisture buffering capacity of materials is evaluated at both room and materials levels by a full-scale experiment and HAM simulations in this thesis research. The impact of different parameters on moisture buffering capacity is analyzed. A number of potential research areas have been identified:

- The impact of additional parameters and scenarios can be investigated, including transient outdoor environment, various room configurations, and ventilation layout and operation strategies through either experimental testing or WBHAM simulations.



- Further investigation is required to evaluate the effect of moisture buffering for different types of room usage, for example, office, museums, library, and factory. A larger range of materials can be tested through both experimental investigation and HAM simulations.
- It is always a challenge to integrate both indoor conditions and moisture transfer of surface materials within one model. The data collected from experimental investigation, including detail information of indoor conditions and surface conditions, provide opportunity for further study and validating.
- The non-uniform moisture distribution in multi-zone rooms or buildings is a more complicated phenomenon. This would require computing and solving the HAM transportation among zones and within each zone at the same time.

## 7.4 Related publications

### *Journal publications*

1. **Yang, X.**, Fazio, P., Ge, H. and Rao, J., 2010. Investigation of influence of moisture load schemes and the effect of moisture history on moisture buffering capacities of three groups of hygroscopic materials, under preparation.
2. **Yang, X.**, Fazio, P., Ge, H and. Rao, J., 2010. Evaluation of moisture capacity of hygroscopic materials: a full-scale experimental investigation and BSim simulations. under preparation. Submitted.

### *Conference papers*

3. **Yang, X.**, Fazio, P., Ge, H., and Rao, J, 2010. Impact of moisture history and initial conditions on moisture buffering effect, preliminary accepted by 1st Central European Symposium on Building Physics (CESBP), Cracow, September 13-15.
4. **Yang, X.**, Fazio, P., Rao, J., Vera, S., and Ge, H., 2009. Experimental evaluation of transient moisture buffering of interior surface materials in a full-scale one-room test setup, Proceedings of the fourth international building physics conference, CD-rom, Istanbul, Turkey, June 15-18.
5. **Yang, X.**, Vera, S., Rao, J., Ge, H., and Fazio, P., 2007. Full-scale experimental investigation of moisture buffering effect and indoor moisture distribution, Proceedings of performance of exterior envelopes of whole buildings X (CD-rom), Clearwater beach, Florida, USA, December 2-7.

6. Vera, S., **Yang, X.**, Rao, J., Ge, H., and Fazio, P., 2007. Moisture interaction between the building envelope and indoor environment: experimental setup and preliminary results. 12th Symposium for Building Physics, Dresden, Germany, March 29-31

*Annex 41 paper and technical report*

7. Fazio, P., Vera, S., Rao, J., **Yang, X.**, and Ge, H., 2008. Datasets of whole-building HAM indoor conditions for one-room and vertical two-room experimental setups. Technical report for Annex 41.
8. Vera, S., **Yang, X.**, Rao, J., Ge, H., and Fazio, P., 2006. Test protocol of two-room setup to investigate the interaction between the building envelopes, exterior and interior environments. Paper to IEA ECBCS Annex 41 Working Meeting, Kyoto, Japan.
9. Contribution to annex 41 ST1 report.

## REFERENCES

- Aoki-Kramer, M. and Karagiozis, A.N., 2004. A new look at residential interior environmental loads. Proceeding of Performance of Exterior Envelope of Whole Buildings IX, CD-ROM, Clearwater, Florida, December 5-10.
- ANSI/ASHRAE Standard 62.1-2007, 2007. Ventilation for acceptable indoor air quality. American Society of Heating Refrigeration and Air-conditioning Engineers, Atlanta GA.
- ASHRAE, 2004. ASHRAE Handbook 2004. HVAC Systems and Equipment. American Society of Heating, Refrigerating and Air-conditioning Engineers, Atlanta GA.
- ASHRAE, 2005. ASHRAE Handbook 2005. Fundamentals. American Society of Heating, Refrigerating and Air Conditioning Engineers, Atlanta GA.
- ASHRAE Standard 119, 1988. Air leakage performance for detached single-family residential buildings. American society of heating, refrigerating and air conditioning engineers, Atlanta GA.
- ASHRAE Standard 55-04, 2004. Thermal environmental conditions for human occupancy. American Society of Heating Refrigeration and Air-conditioning Engineers, Atlanta GA.
- ASTM C1498, 2001. Standard test method for hygroscopic sorption isotherms of building materials. Annual book of ASTM Standard, 04. 06, American Society for Testing and Materials, West Conshohocken, PA.
- Aoki-Kramer, M. and Karagiozis, A.N., 2004. A new look at residential interior environmental loads, Proceedings of Performance of Exterior Envelopes of Whole Buildings X, CD-Rom, Clearwater, Florida, December 2-7.
- Barrett D., 1998. The renewal of trust in residential construction. Commission of inquiry into the quality of condominium construction in British Columbia. Submitted to the Lieutenant-Governor in Council, Government of British Columbia. <http://www.qp.gov.bc.ca/condo/>.
- Barringer, D.G. and Mcgugan, C.A., 1989. Development of a dynamic model for simulation indoor air temperature and humidity. ASHRAE Transactions, 95, 449-460.
- Berglund, L.G., 1998. Comfort and humidity. ASHRAE Journal, 40, 35-41.
- Bornehag, C.G., Blomquist, G., Gyntelberg, F., Jarvholm, B., Malmberg, P., Nordvall, L., Nielsen, A., Pershagen, G. and Sundell, J., 2001. Dampness in buildings and health. Indoor Air, 11, 72-86.

Bornehag, C.G., Sundell, J. and Sigsgaard, T., 2004 (a). Dampness in buildings and health (DBH): report from an ongoing epidemiological investigation on the association between indoor environmental factors and health effects among children in Sweden. *Indoor Air*, 14, 59-66.

Bornehag, C.G., Sundell, J., Bonini, S., Custovic, A., Malmberg, P., Skerfving, S., Sigsgaard, T., and Verhoeff, A., 2004 (b). Dampness in buildings as a risk factor for health effects, EUROEXPO: a multidisciplinary review of the literature (1998-2000) on dampness and mite exposure in buildings and health effects. *Indoor Air*, 14, 243-257.

Bornehag, C.G., Sundell, J., Hagerhed-Engman, L., Sigsgaard, T., Janson, S., Aberg, N. and the DBH study group, 2005. Dampness at home and its association with airway, nose, and skin symptoms among 10851 preschool children in Sweden: a cross-sectional study. *Indoor Air*, 15, 48-55.

Carmeliet, J., Gaublomme, J. and Janssen, H., 2004. Influence of hysteresis on the moisture buffering of wood. Paper to International Energy Agency (IEA), Energy Conservation in Buildings and Community Systems (ECBCS) Annex 41 working meeting (KUL Oct 2004 Paper A41-T1-B-04-8), Glasgow, Oct. 27-29.

CAN/CSA-F326-M91, 1991. Residential mechanical ventilation systems. Canadian Standard Association.

Christian, J.E., 1994. Moisture control in buildings, chapter 8. Book published by American Society for Testing and Materials (ASTM), Trechsel, H.R. editing.

Crawley, D. B., Linda, Lawrie, L.K., Winkelmann, F.C., Pedersen, C.O., Strand, R.K., Liesen, R.J., Fisher, D.E, Witte, M.J., Henninger, R.H., Glazer, J. and Shirey, D., 2002. EnergyPlus: New, Capable, and Linked. Proceedings of the eSim 2002 conference, IBPSA-Canada, Montreal, Quebec, Canada, September 11-13.

Cunningham, M.J., 1992. Effective penetration depth and effective resistance in moisture transfer. *Building and Environment* 27(2), 379-386.

Cunningham, M.J., 2003. The building volume with hygroscopic materials-an analytic study of a classical building physics problem, *Building and Environment*, 38, 329-337.

Delgado, J. M.P.Q., Ramos, N. M. M. and De Freitas, V.P., 2006. Can moisture buffer performance be estimated from sorption kinetics? *Journal of Building Physics*, 29, 281-298.

Downing, C.C. and Bayer, C.W., 1993. Classroom indoor air quality vs. ventilation rate. *ASHRAE Transactions*, 99, 1099-1103.

El Diasty, R., Fazio, P. and Budaiwi, I., 1993. Dynamic modeling of moisture absorption and desorption in buildings. *Building and Environment*, 28 (1), 21-32.

Fazio, P., Athienitis, A., Marsh C. and Rao J., 1997. Environmental chamber for investigation of building envelope performance. *Journal of Architectural Engineering*, 3(2): 97-103.

Fazio, P., Vera, S., Rao, J., Yang, X. and Ge, H., 2007. Datasets of whole-building HAM indoor conditions for one-room and vertical two-room experimental setups. Submitted to International Energy Agency (IEA), Energy Conservation in Buildings and Community Systems (ECBCS), for Annex 41 report.

Hagentoft, C., 2001. Introduction to building physics. Studentlitteratur, Sweden.

Hagentoft, C., Kalagasidis A., Adl-Zarrabi B., Roels S., Carmeliet J., Hens H., Grunewald J., Funk M., Becker R., Shamir, D., Adan, O., Brocken, H., Kumaran, K. and Djebbar, R., 2004. Assessment method of numerical prediction models for combined heat, air and moisture transfer in buildings components: benchmark for one-dimensional cases. *Journal of Thermal Envelope and Building Science*, 27(4), 327-352.

Hamlin, T.L., 1991. Ventilation and airtightness in new detached Canadian housing. *ASHRAE Transactions*, 97(2), 904-910.

Harriman, L., Brundrett, G. and Kittler, R., 2001. Humidity control design guide. Book published by American Society of Heating, Refrigerating and Air-conditioning Engineers.

Hedeegard, L., Rode, C. and Peuhkuri, R., 2005 (a). Full scale test of moisture buffer capacity of wall materials, 7<sup>th</sup> Nordic Building Physics Symposium, (2), 662-669. Reykjavik, Iceland, June 13-15.

Hedeegard, L., Rode C. and Peuhkuri R., 2005 (b). Effect of airflow velocity on moisture exchange at surfaces. Paper to International Energy Agency (IEA), Energy Conservation in Buildings and Community Systems (ECBCS) Annex 41 working meeting (DTU Oct 2005 Paper A41-T3-Dk-05-4), Trondheim, October 26-28.

Hens, H., 1996. Heat, air and moisture transfer through new and retrofitted insulated envelope parts: final report. International Energy Agency Energy Conservation in Buildings and Community Systems Program (IEA-ECBCS), Laboratorium Bouwfysica, Dept. Burgerlijke Bouwkunde.

Hens, H., 2005. Impact of hygric inertia on indoor climate: simple models. Paper to International Energy Agency (IEA), Energy Conservation in Buildings and Community Systems (ECBCS) Annex 41 working meeting (KUL Oct 2005 Paper A41-T1-B-05-6), Trondheim, October 26-28.

Holm, A. and Lengsfeld, K., 2007. Moisture-buffering effect- experimental investigations and validation. Conference Proceedings Performance of Exterior Envelope of Whole Buildings. X, CD-ROM, Clearwater, Florida, December 2-7.

Iskara, C., James, C. and Simonson, C.J., 2007. Experimental determination of convective mass transfer coefficients for gypsum board and pine paneling. Datasets of whole building HAM and indoor conditions for one-room and vertical two-room experimental setups, submitted to annex 41, International Energy Agency (IEA), Energy Conservation in Buildings and Community Systems (ECBCS).

ISO/DIS 24353, 2008. Hygrothermal performance of building materials and products-determination of moisture adsorption/ desorption properties in response to humidity variation. International Standards for Business, Government and Society.

Janssen, H. and Roels, S., 2006. A comparison of Nordtest and Japanese test methods for the moisture buffering performance of building materials, *Journal of Building Physics*, 30(2), 137-161.

Janssen, H. and Roels, S., 2007. The hygric inertia of building zones: characterization and application. Available at <http://www.kuleuven.be/bwf/projects/annex41/protected/data/DTU%20Apr%202007%20Paper%20A41-T4-Dk-07-1.pdf>

Janssen, H. And Roels, S, 2009. Qualitative and quantitative assessment of interior moisture buffering by enclosures, *Energy and Buildings*, 41 (4), 382-394.

JIS A 1470-1, 2002. Japanese industrial standard. Japanese Standard Association.

Kariagozis, A.N., 2001 (a). Advanced hygrothermal models for hygrothermal research, Chapter 6 moisture analysis and condensation in building envelopes. Manual 40. American Society for Testing and Materials (ASTM), West Conshohocken, PA.

Karagiozis, A.N., Kuenzel, H. and Holm, A., 2001 (b). WUFI-ORNL/IBP hygrothermal model, Solutions to moisture problems in building enclosures. Ontario Building Envelope Council, Toronto, Canada.

Karagiozis, A.N., 2004. Importance of moisture control in building performance. available in <http://www.esim.ca/2002/English/proceedings.htm>, revised in October 2004.

Kerestecioglu, A. and Gu, L., 1990. Theoretical and computational investigation of simultaneous heat and moisture transfer in buildings: “evaporation and condensation” theory. *ASHRAE Transactions*, 96 (2), 455-464.

Kerestecioglu, A., Swami, M. and Kamel, A., 1990. Theoretical and computational investigation of simultaneous heat and moisture transfer in buildings: “effective penetration depth” theory. *ASHRAE Transactions*, 96 (2), 447-454.

Koronyhalyova, O., Mihalka, P. and Matiasovsky, P., 2004. Model for whole HAM-transfer simulation in room. Paper to International Energy Agency (IEA), Energy Conservation in Buildings and Community Systems (ECBCS) Annex 41 working meeting (SAS May 2004 Paper A41-T2-SI-04-2), Zurich, May 12-14.

- Künzel, H. M., 1995. Simultaneous heat and moisture transport in building components, one- and two-dimensional calculation using simple parameters, (ISBN 3-8167-4103-7), Fraunhofer IRB Verlag Stuttgart.
- Künzel, H. and Kiessl. K., 1997. Calculation of heat and moisture transfer in exposed building components. *Heat and Mass Transfer*, 40 (1), 159-167.
- Künzel, H. and Holm, A., 2003. The hygrothermal behaviour of rooms: combining thermal building simulation and hygrothermal envelope calculation. Eighth International IBPSA Conference Proceeding, 491-499, Eindhoven, Netherlands, August 11-14.
- Künzel, H., Holm, A. and Sedlbauer, K., 2004. Experimental investigation of the hygric buffering capacity of wood based interior paneling. Paper to International Energy Agency (IEA), Energy Conservation in Buildings and Community Systems (ECBCS) Annex 41 working meeting (FhG May 2004 Paper A41-T2-D-04-1), Zurich, May 12-14.
- Kurnitski, J., Kalamees, T., Palonen, J., Eskola, L. and Seppanen, O., 2007. Potential effects of permeable and hygroscopic lightweight structures on thermal comfort and perceived IAS in a cold climate. *Indoor Air*, 17, 37-49.
- Kwiatkowski, J., Feret, K. and Woloszyn, M., 2007. Predicting indoor relative humidity using building energy simulation tools. Proceeding of Indoor Air Quality, Ventilation & Energy Conservation in Buildings (IAQVEC) conference, Sendai, Japan, October 28-31.
- Lucas, F., Adeland, L., Garde, F. and Boyer, H., 2002. Study of moisture in buildings for hot humid climates. *Energy and Buildings*, 34, 345-355.
- Malonvaara, M., Ojanen, T., Holm, A., Kunzel, H.A. and Karagiozis, A.N., 2004. Moisture buffering effects on indoor air quality-experimental and simulation results. Conference Proceedings Performance of Exterior Envelope of Whole Buildings IX, CD-ROM, Clearwater, Florida, December 5-10.
- Mitamura, T., Hasegawa, K., Yoshino H., Mastumoto S. and Takshashi N., 2004. Experiment for moisture buffering and effects of ventilation rate, volume rate of the hygrothermal materials, Paper to International Energy Agency (IEA), Energy Conservation in Buildings and Community Systems (ECBCS) Annex 41 working meeting (THU Oct 2004 Paper A41-T2-J-04-3), Glasgow, Oct. 27-29.
- NRCC, 2005, National Building Code of Canada 2005, published by National Research Council of Canada.
- Ojanen, T., Salonvaara, M., Kohonen, R. and Nieminen, J., 1989. Moisture transfer in building structures: numerical methods. Technical Research Center of Finland, Report No. 595, 113.
- Ojanen, T. and Kumaran, K., 1996. Effect of exfiltration on the hygrothermal behavior of a residential wall assembly. *Journal of Thermal Insulation and Building Envelopes*, 19, 215-227.



Ojanen, T. and Salonvaara, M., 2004. Comparison of measured and simulated moisture buffering results. Paper to International Energy Agency (IEA), Energy Conservation in Buildings and Community Systems (ECBCS) Annex 41 working meeting (GCU Oct 2004 Paper A41-T3-UK-04-2), Glasgow, Oct. 27-29.

Osanyintola, O.F. and Simonson, C.J., 2005 (a). Transient moisture buffering capacity of plywood. Paper to International Energy Agency (IEA), Energy Conservation in Buildings and Community Systems (ECBCS) Annex 41 working meeting (UofS May 2005 Paper A41-T2-C-05-2), Montreal, May 16-18.

Osanyintola, O.F. and Simonson, C.J., 2005 (b). Experimental and numerical studies of transient heat and moisture transfer within spruce plywood. Paper to IEA ECBCS Annex 41 Working Meeting. Paper to International Energy Agency (IEA), Energy Conservation in Buildings and Community Systems (ECBCS) Annex 41 working meeting (UofS Oct 2005 Paper A41-T2-C-05-4), Trondheim, Oct. 26-28.

Osanyintola, O. F., 2005. Transient moisture characteristic of spruce plywood. Master Thesis, Department of Mechanical Engineering, University of Saskatchewan, Canada.

Osanyintola, O.F. and Simonson, C.J., 2006. Moisture buffering capacity of hygroscopic building materials: experimental facilities and energy impact. *Energy and Buildings*, 38, 1270-1282.

Padfield, T., 1998. The role of absorbent building materials in moderating changes of relative humidity. Ph.D. Thesis, Department of Structural Engineering and Materials, The Technical University of Denmark, Denmark.

Peuhkuri, R., 2003. Moisture dynamics in building envelopes. PhD Thesis, Technical University of Denmark, Copenhagen, Denmark.

Peuhkuri, R. and Rode, C., 2005. Using the dynamic moisture loading tests for determination of moisture buffer value. Paper to International Energy Agency (IEA), Energy Conservation in Buildings and Community Systems (ECBCS) Annex 41 working meeting (DTU May 2005 Paper A41-T2-Dk-05-1), Montreal, May 16-18.

Ramos, N.M.M. and de Freitas, V.P., 2004. Hygroscopic inertia as a function of transient behavior of veering materials. Conference Proceedings Performance of Exterior Envelope of Whole Buildings IX, CD-ROM, Clearwater, Florida, December 5-10.

Roles, S. and Janssen, H., 2005. Is the moisture buffering value a reliable material property to characterize the hygric buffering capacities of building materials? Paper to International Energy Agency (IEA), Energy Conservation in Buildings and Community Systems (ECBCS) Annex 41 working meeting (KUL Oct 2005 Paper A41-T2-B-05-7), Trondheim, Oct. 26-28.

Roles, S. and Janssen, H., 2006. A comparison of the Nordtest and Japanese test methods for the moisture buffering performance of building materials. *Journal of Building Physics*, 30 (2), 137-161.

Roels, S., 2008. Subtask 2- Experimental analysis of moisture buffering. Annex 41 Final Report, International Energy Agency (IEA), Energy Conservation in Buildings and Community System Program (ECBCS).

Rode, C. and Grau, K., 2001. Synchronous calculation of transient hygrothermal conditions of indoor spaces and building envelopes. Building Simulation 2001 (ISBN), 491-498, International Building Performance Simulation Association.

Rode, C., Grau K. and Mitamura T., 2001. Model and experiments for hygrothermal conditions of the envelope and indoor air of buildings. Conference Proceeding of Performance of Exterior Envelope of Whole Buildings, VIII, CD-ROM, Clearwater, Florida, December 2-7.

Rode, C., Mendes M. and Grau, K., 2004 (a). Evaluation of moisture buffer effects by performing whole building simulations. Conference Proceedings Performance of Exterior Envelope of Whole Buildings IX, CD-ROM, Clearwater, Florida, December 5-10.

Rode, C., Holm, A. and Padfield, T., 2004 (b). A review of humidity buffering in the interior spaces, Journal of Thermal Environment and Building Science, 27, 221-226.

Rode, C., Peuhkuri, R., Hansen, K., Time, B., Svennberg, K., Arfvidsson, J. and Ojanen, T., 2005. BYG DTU R-126, Nordtest project on moisture buffering of building materials. Department of Civil Engineering, Technical University of Denmark.

Rode, C., Peuhkuri, R., Time, B., Svennberg, K. and Ojanen, T., 2007. Moisture buffer value of building materials, Journal of ASTM International 4(5), 22-34.

Rode, C. and Grau, K., 2008. Moisture buffering and its consequence in whole building hygrothermal modeling. Journal of Building Physics, 31 (4), 333-360.

Salonvaara M. and Ojanen, T. and Karagiozis, A., 2003. Indoor air humidity variations and its effects on the moisture performance of building envelope. Eighth International Building Performance Simulation Association (IBPSA) Conference, Eindhoven, August 11-14.

Salonvaara, M., Holm A., Kunzel H. and Karagiozis. A., 2004. Moisture buffering effects on Indoor Air Quality – experimental and simulation results. Conference Proceedings Performance of Exterior Envelope of Whole Buildings IX, CD-ROM, Clearwater, Florida, December 5-10.

Satio, H., 2005 (a). Simple parameters for moisture buffering effect to predict indoor humidity variation. Paper to International Energy Agency (IEA), Energy Conservation in Buildings and Community Systems (ECBCS) Annex 41 working meeting (BRI May 2005 Paper A41-T2-J-05-7), Montreal, May 16-18.

Satio, H., 2005 (b). Review of researches regarding moisture sources in Japan. Paper to International Energy Agency (IEA), Energy Conservation in Buildings and Community

Systems (ECBCS) Annex 41 working meeting (BRI May 2005 Paper A41-T3-J-05-5), Montreal, May 16-18.

Sherman, M. and Matson, N., 1997. Residential ventilation and energy characteristics. ASHRAE Transactions, 103 (1), 717-730.

Simonson, C.J. and Solonvaara, M., 2000 (a). Mass transfer between indoor air and a porous building envelope: Part I-field measurements. Proceeding of Healthy Buildings, 3, 117-122, Espoo, Finland, August 6-10.

Simonson, C.J. and Solonvaara, M., 2000 (b). Mass transfer between indoor air and a porous building envelope: Part II- validation and numerical studies. Proceeding of Healthy Buildings, 3, 123-128, Espoo, Finland, August 6-10.

Simonson, C.J., Solonvaara, M. and Ojanen, T., 2002. The effect of structures on indoor humidity- possibility to improve comfort and perceived air quality. Indoor Air, 12, 243-251.

Simonson, C.J., Solonvaara, M. and Ojanen, T., 2004. Heat and mass transfer between indoor air and a permeable and hygroscopic building envelope: Part I- field measurements. Journal of Thermal Envelope and Building Science, 28, 63-101.

Straube, J.F., 2002. Moisture in building. ASHRAE Journal, January, 1-5.

Straube, J.F. and Burnett, E.F.P., 2005, Building Science for Building Enclosures. Building Science Press.

Svennberg, K., Hedegaard, L. and Rode, C., 2004. Moisture buffer performance of a fully furnished room. Proceedings of Performance of Exterior Envelopes of Whole Buildings IX, CD-ROM, Clearwater, Florida, December 5-10.

Talukar, P. Olutmayin, S.O., Osanyintola, O.F. and Simonson, C.J., 2007 (a). An experimental data set for benchmarking 1-D, transient heat and moisture transfer models of hygroscopic building material. Part I: experimental facility and material property data. Heat and Mass Transfer, 50, 4527-4539.

Talukar, P. Olutmayin, S.O., Osanyintola, O.F. and Simonson, C.J., 2007 (b). An experimental data set for benchmarking 1-D, transient heat and moisture transfer models of hygroscopic building material. Part II: experimental, numerical and analytical data. Heat and Mass Transfer, 50, 4519-4526.

Tariku, F., 2008. Whole building heat and moisture analysis, Ph. D. Thesis. The Department of Building Civil and Environmental Engineering, Concordia University, Canada.

Tenwolde, A. and Walker, L.S., 2001. Interior moisture design loads for residences. Conference Proceeding of Performance of Exterior Envelope of Whole Buildings, VIII, CD-ROM, Clearwater, Florida, December 2-7.

- Teodosiu, C., Hohota, R., Rusaouen, G. and Woloszyn, M., 2003. Numerical prediction of indoor humidity and its effect on indoor environment. *Building and Environment*, 38, 655-664.
- Toftum, J., Jorgensen, A.S. and Fanger, P.O., 1998 (a). Upper limits for indoor air humidity to avoid uncomfortably humid skin. *Energy and Buildings*, 28, 1-13.
- Toftum, J., Jorgensen, A.S. and Fanger, P.O., 1998 (b). Upper limits for preventing warm respiratory discomfort. *Energy and Buildings*, 28, 15-23.
- Toftum, J. and Fanger, P.O., 1999. Air humidity requirements for human comfort. *ASHRAE Transactions* 105(2), 641-647.
- Thomas, W. C. and Burch, D. M., 1990. Experimental validation of a mathematical model for predicting water vapor sorption at interior building surfaces. *ASHRAE Transactions*, 96 (1), 487-496.
- Vera, S., Yang, X., Rao, J., Ge, H. and Fazio, P., 2006. Test protocol of two-room setup to investigate the interaction between the building envelope, exterior and interior environments. Paper to International Energy Agency (IEA), Energy Conservation in Buildings and Community Systems (ECBCS) Annex 41 working meeting, (CON Apr 2006 Paper A41-T2-C-06-2), Kyoto, Japan, April 3-5.
- Vera, S., Yang, X., Rao, J., Ge, H. and Fazio, P., 2007. Moisture interaction between the building envelope and indoor environment: experimental setup and preliminary results. 12<sup>th</sup> Symposium for Building Physics, Dresden, Germany, March 29-31.
- Woloszyn, M. and Rode, C., 2008 (a). Subtask 1- Modeling principles and common exercises. Annex 41 Final Report, International Energy Agency (IEA), Energy Conservation in Buildings and Community System Program (ECBCS).
- Woloszyn, M and Rode, C., 2008 (b). Tools for performance simulation of heat, air and moisture conditions of whole buildings. *Building Simulation*, 1, 5-24.
- White F.M., 1999. *Fluid Mechanics*, fourth ed., McGraw-Hill, Boston.
- Wu, Y., Fazio, P. and Kumaran, K., 2008. Moisture buffering capacities of five north American building materials. *Journal of Testing and Evaluation*, 36, (1), 1-7.
- Wu, Y., 2007. Experimental study of hygrothermal properties of building materials, Master Thesis. The Department of Building Civil and Environmental Engineering, Concordia University, Canada.
- Zhao, H., 2004. An integrated zonal model to predict transient indoor humidity distribution. Master Thesis, The Department of Building Civil and Environmental Engineering, Concordia University, Canada.

Yang, X., Vera, S., Rao, J., Ge, H. and Fazio, P., 2007. Full-scale experimental investigation of moisture buffering effect and indoor moisture distribution, Proceedings of Performance of Exterior Envelopes of Whole Buildings X, CD-Rom, Clearwater, Florida, December 2-7.

Yang, X., Fazio, P., Rao, J., Vera, S. and Ge, H., 2009. Experimental evaluation of transient moisture buffering of interior surface materials in a full-scale one-room test setup. Proceeding of 4th International Building Physics Conference, Istanbul, Turkey, June, 15-18.

## APPENDIX A: MATERIAL PROPERTIES

Moisture sorption isotherm and vapor transfer resistance factor can be expressed as (Janssen and Roels, 2009)

$$w = w_{sat} \times [1 + m \cdot \ln(RH)^n]^{\frac{1-n}{n}}$$

$$\mu = \frac{1}{a + b \cdot e^{c \cdot RH}}$$

where  $w_{sat}$  is the saturation moisture content of materials ( $\text{kg}/\text{m}^3$ ); a, b, c, m, n are constants calculated from fitting. The values of these constants for different materials are listed in the Table A-1. The other properties are listed in Table A-2.

Material properties of the uncoated gypsum board, oriented strand board plywood, and wood fiber board are obtained from the database created by Wu (2007). The material property of wood paneling was measured by one of the authors of this paper. Material properties of the magazine paper, Tel. book paper, and cotton fiber are drawn from Roels (2008). Material properties of aerated cellular concrete and cellulose insulation are taken from Peuhkuri (2003).

Table A-1. Constants used for sorption isotherm curve vapour transfer resistance factor.

Materials	$w_{sat}$	m	n	a	b	c
Wood paneling (PW)	588	-625.404	1.4639	1.98e-5	2.72e-4	5.930
Oriented strand board (OSB)	903	-1057.568	1.449	3.90e-5	1.06e-3	3.241
Magazine paper (MP)	151	-14.262	1.626	0.002	1.67e-6	9.925
Plywood (PW)	271	-127.901	1.454	1.98e-5	2.72e-4	5.931
Uncoated gypsum board (GB)	805	-8416.602	1.652	0.650	-0.512	-0.224
Cellulose insulation (CI)	448	-8437.193	1.523	0.558	-1.45e-8	3.893
Aerated cellular concrete (ACC)	498	-8414.644	1.515	0.101	6.59e-6	8.930
Wood fiber board (WFB)	1003	-1784.981	1.597	0.095	8.04e-7	7.671
TEL. book paper (TBP)	165	-14.172	1.594	0.009	2.57e-4	5.656
Cotton fiber (CF)	64	-8.263	1.737	0.469	1.25e-3	5.869

Table A-2. Other material properties.

Materials	Thickness (m)	Density (kg/m <sup>3</sup> )	heat capacity (J/kg·K)	Thermal conductance (w/m·K)
Wood paneling (PW)	0.018	520	1880	0.120
Oriented strand board (OSB)	0.012	664	1880	0.090
Magazine paper (MP)	0.010	840	1300	0.130
Plywood (PW)	0.013	456	1880	0.085
Uncoated gypsum board (GB)	0.013	592	870	0.150
Cellulose insulation (CI)	0.010	65	1382	0.040
Aerated cellular concrete (ACC)	0.010	450	900	0.110
Wood fiber board (WFB)	0.010	840	1300	0.130
TEL. book paper (TBP)	0.010	690	1300	0.130
Cotton fiber (CF)	0.010	478	1340	0.042

## APPENDIX B: MOISTURE CONTENT SENSOR CALIBRATION

The accurate measurement of moisture content of the surface material is important for analyzing the moisture buffering potentials in this large-scale experiment. To ensure accuracy, moisture content sensors (screws and pins) used on two surface materials are calibrated.

### 1. Test set up and procedure

There are six gravimetric samples for both uncoated gypsum board and wood paneling. Three of them are gravimetric samples without moisture content sensors while the other three samples are installed with screws or pins, as shown in Figure B-1.

Uncoated gypsum board samples have a dimension of 16.51 cm x 16.51 mm (6.5 in. x 6.5 in.). Dimension for wood paneling samples is 13.34 cm x 11.74 cm (5.25 in. x 4.625 in.). The edge, side surface and back surface are all sealed by aluminum tape to avoid any moisture absorptions on these surfaces. The open surfaces thus have dimensions of 15.86 cm x 15.86 cm for uncoated gypsum board and 12.7 cm x 11.11 cm for wood paneling.

The readings of moisture content sensors are calibrated at different RH levels by the true moisture content calculated by

$$MC = \frac{Weight_{RH} - dry\ weight}{dryweight}$$

where  $weight_{RH}$  is weight of samples when they are exposed to a certain RH level at their equilibrium conditions in a small environmental chamber. Dry weight is obtained by oven drying samples.

Samples are placed in a small environmental chamber. The temperature of chamber is set at 20.5 °C while the RH of environment chamber is maintained at 5% RH step each in the range of 30-80% RH for uncoated gypsum board and 50-80% for wood paneling based on indoor RH variation recorded in the full-scale experiment. The weight of samples is measured by a scale with an accuracy of 0.001g. The measurement of moisture content is taken by the same transmitter (MTC-60) used in the full-scale experiment and data are recorded by a small DAS (Data Acquisition System) manually, as shown in Figure B-2. The weight of all samples and the moisture content readings are recorded every week in the first three weeks. After the fourth week, the measurement is taken every 24 hours until the weight change of the samples is less than 0.1% of the sample weight.

Then the samples are put in the oven with a set temperature at 58 °C to get their dry weight. Weight of the samples is taken every day until the weight change is less than 0.1% of the sample weight.



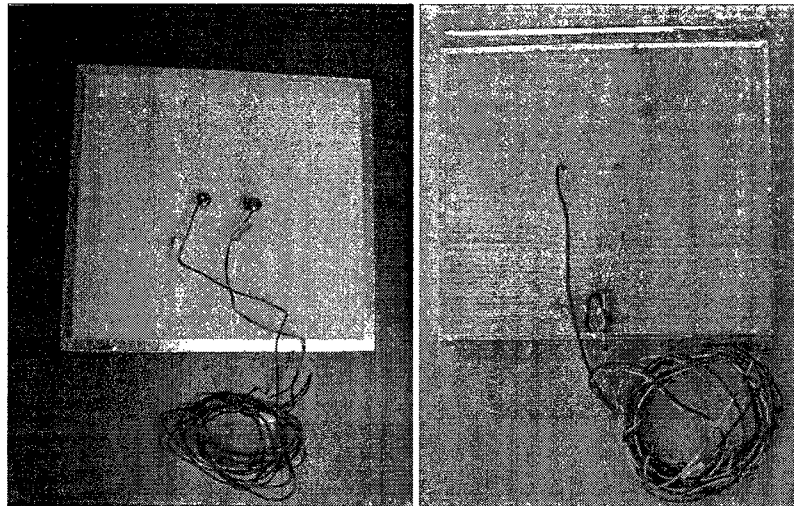


Figure B-1. Samples of wood paneling and gypsum board.

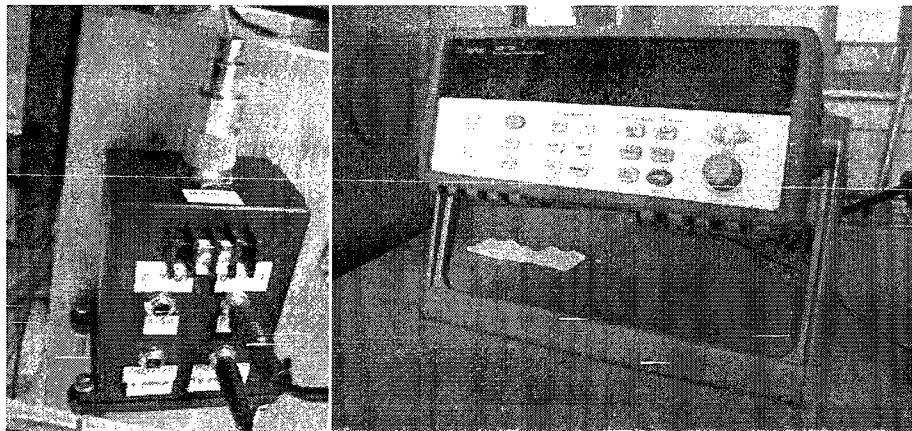


Figure B-2. MTC-60 transmitter and small DAS station

## 2. Data collected

Since the moisture content reading is taken under equilibrium condition, the sorption curve is obtained at the same time, as shown in Figure B-3 and B-4. Comparing to the data from Wu (2007), the difference for gypsum board is very small. But for wood paneling, the data obtained from this experiment is always below the curve from Wu's. That is because Wu's data is carried out for plywood instead of wood paneling. There is no sorption curve data in literature for wood paneling so far.

The voltage reading compared to the moisture content reading from gravimetric method is listed in Table B-1. Based on this data and the calibration data provided by the manufacturer, the calibration curve is created, as shown in Figure B-5 and B-6.

Table B-1. Moisture content voltage reading vs. moisture content

RH (%)	MC (%), gypsum board	MC reading. (v) Gypsum board	MC (%), Wood paneling	MC reading, (v) wood paneling
50	0.58	1.53	5.83	1.97
55	0.65	1.49	6.82	1.89
60	0.70	1.46	7.02	1.88
65	0.78	1.47	7.47	1.85
70	0.85	1.43	9.03	1.73
75	0.89	1.40	9.96	1.70
80	1.10	1.37	10.99	1.67

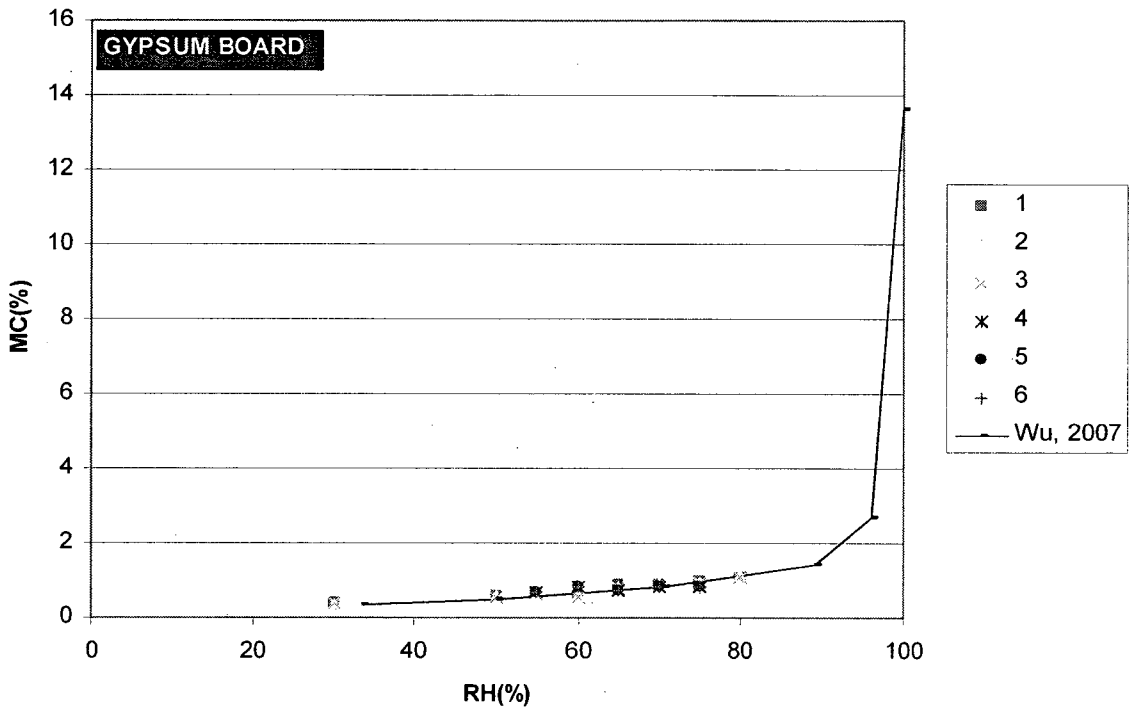


Figure B-3. Sorption curve for gypsum board

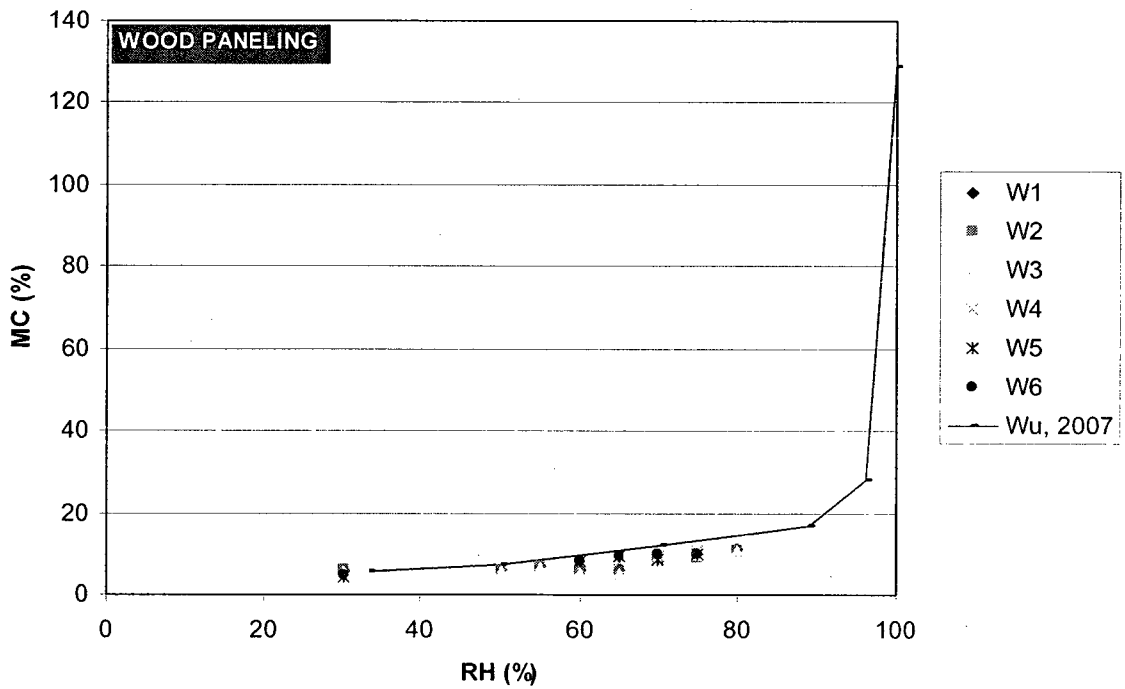


Figure B-4. Sorption curve for wood paneling.

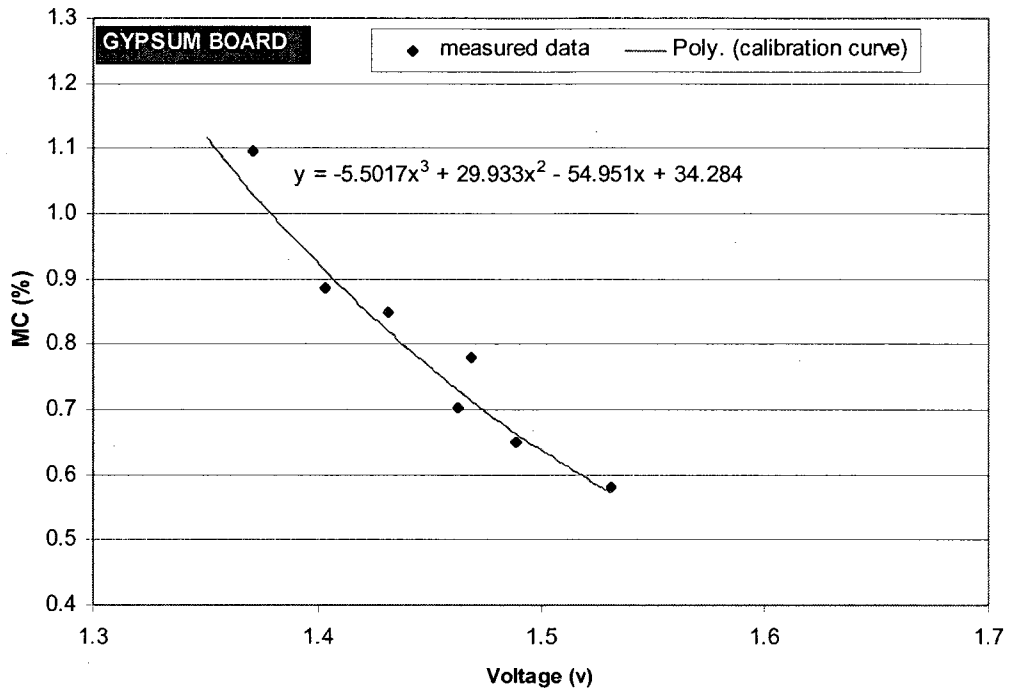


Figure B-5. Calibration curve for gypsum board.

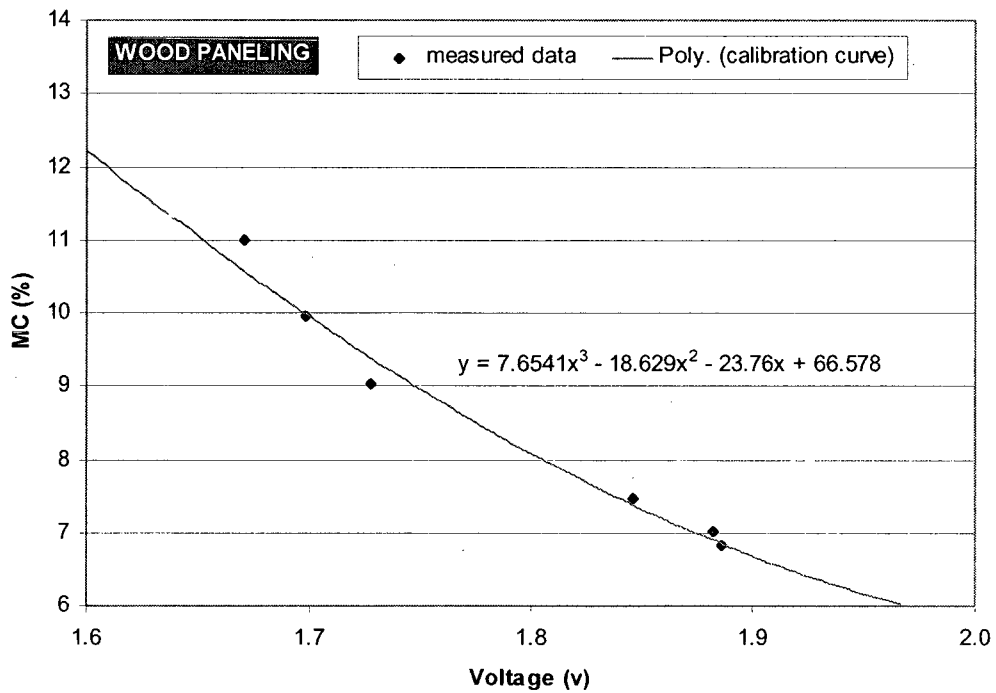


Figure B-6. Calibration curve for wood paneling.

The moisture content measurement on wood paneling and sheathing board (plywood) are also calibrated by handheld meter in the full-scale experiment.

The MC recorded by handheld meter is used to calibrate the voltage reading taken by DAS system used in the experiment. It is proved that the calibration curve obtained from the small chamber calibration test for wood paneling is very close to the data collected by handheld meter, as shown in Figure B-7. The calibration curve for sheathing board is fitted according to the handheld meter measurement and is presented in Figure B-8. Reference data from manufacturer of transmitter (Delmhorst) are also presented in the chart.

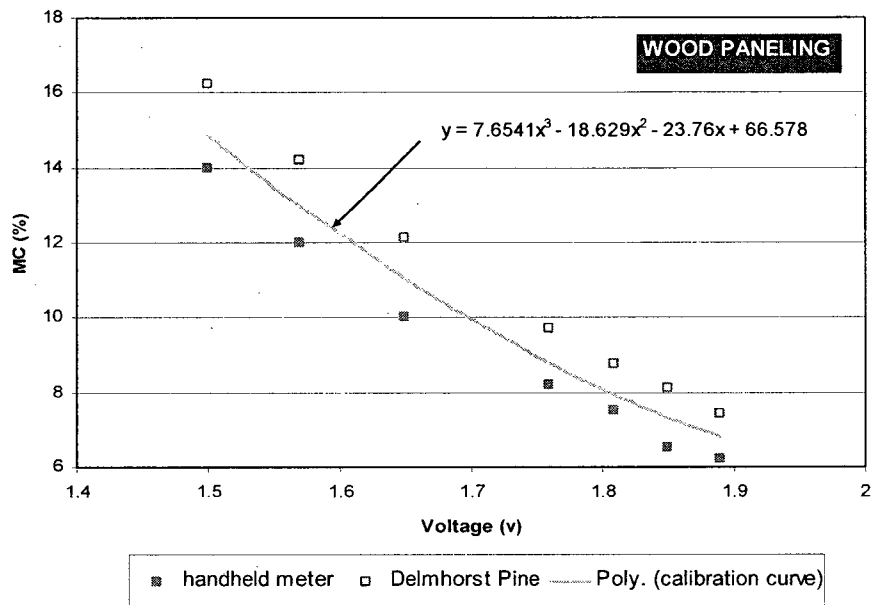


Figure B-7. Calibration of MC on wood paneling by handheld meter.

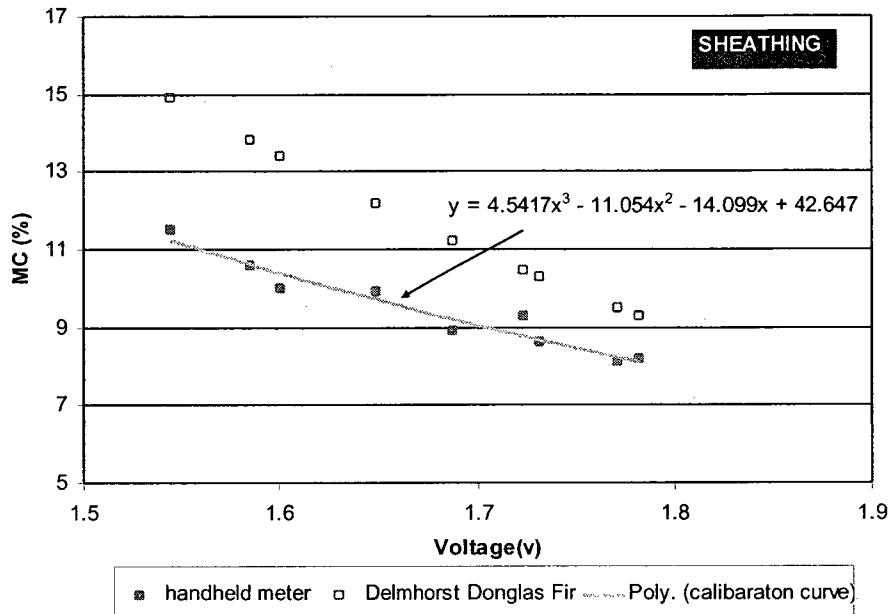


Figure B-8. Calibration of MC on sheathing board by handheld meter.

## **APPENDIX C: NON-UNIFORM INDOOR ENVIRONMENT**

Non-uniform indoor environment are the prevalent conditions within rooms in reality, which has an impact on the local moisture buffering of the surface materials. However, most of large-scale experiments investigate moisture buffering effect in a uniform indoor environment by fully circulating indoor air using one or several fans inside of test rooms.

### **1 Distribution of indoor RH and T in test rooms**

In this study, non-uniform indoor environment was studied by measuring indoor temperature and relative humidity using totally 32 sets of RH and T sensors (HMP 50, Vaisala Inc.) installed across the test rooms. The name and location of these sensors are provided in Figure 3.11 and section 3.5.2.

Indoor temperature and RH are strongly influenced by ventilation air and the hot pot installed in the centre of test rooms. It is observed that the temperature difference at different height of test room could be over 2 °C, as shown in Figure C-1. Air temperature close to and above the hot pot (RT2\_C\_32) is strongly influenced by the heat generation of hot pot, which is 0.5 °C higher in the moisture generation period (hot pot operating period). The air temperature close to the up right corner of the test room (RT2\_E\_32 and RT2\_E\_31) is influenced by the re-circulation of air and hot stream made by hot pot, so it is 0.3 °C lower than those at no-moisture generation period. The same pattern can be observed at locations, RT2\_F\_21, RT2\_F\_22, RT2\_F41 and RT2\_F42, as shown in Figure C-2.

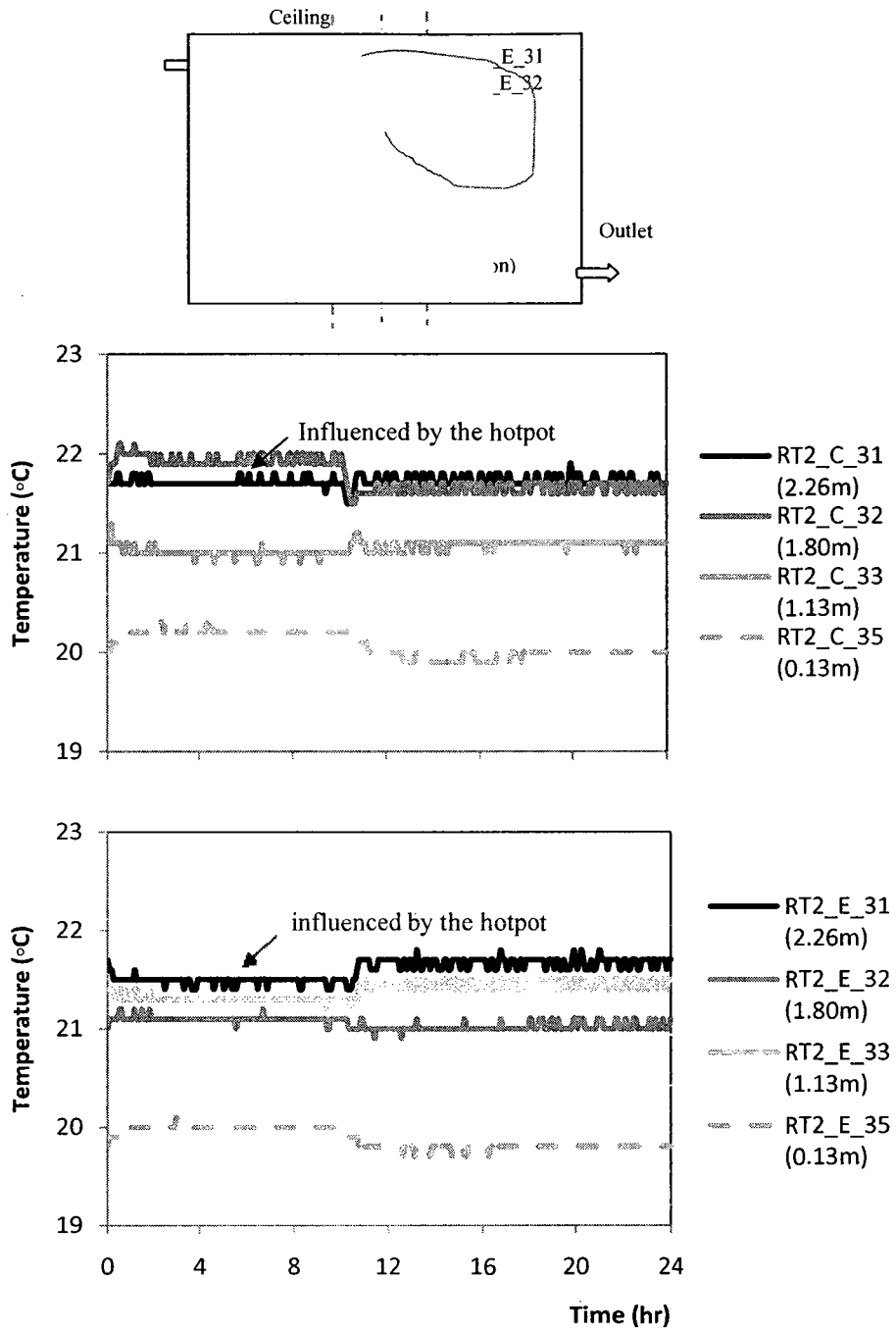


Figure C-1. Temperature at different heights around the centre of test rooms in case 1 at 0.5ACH.



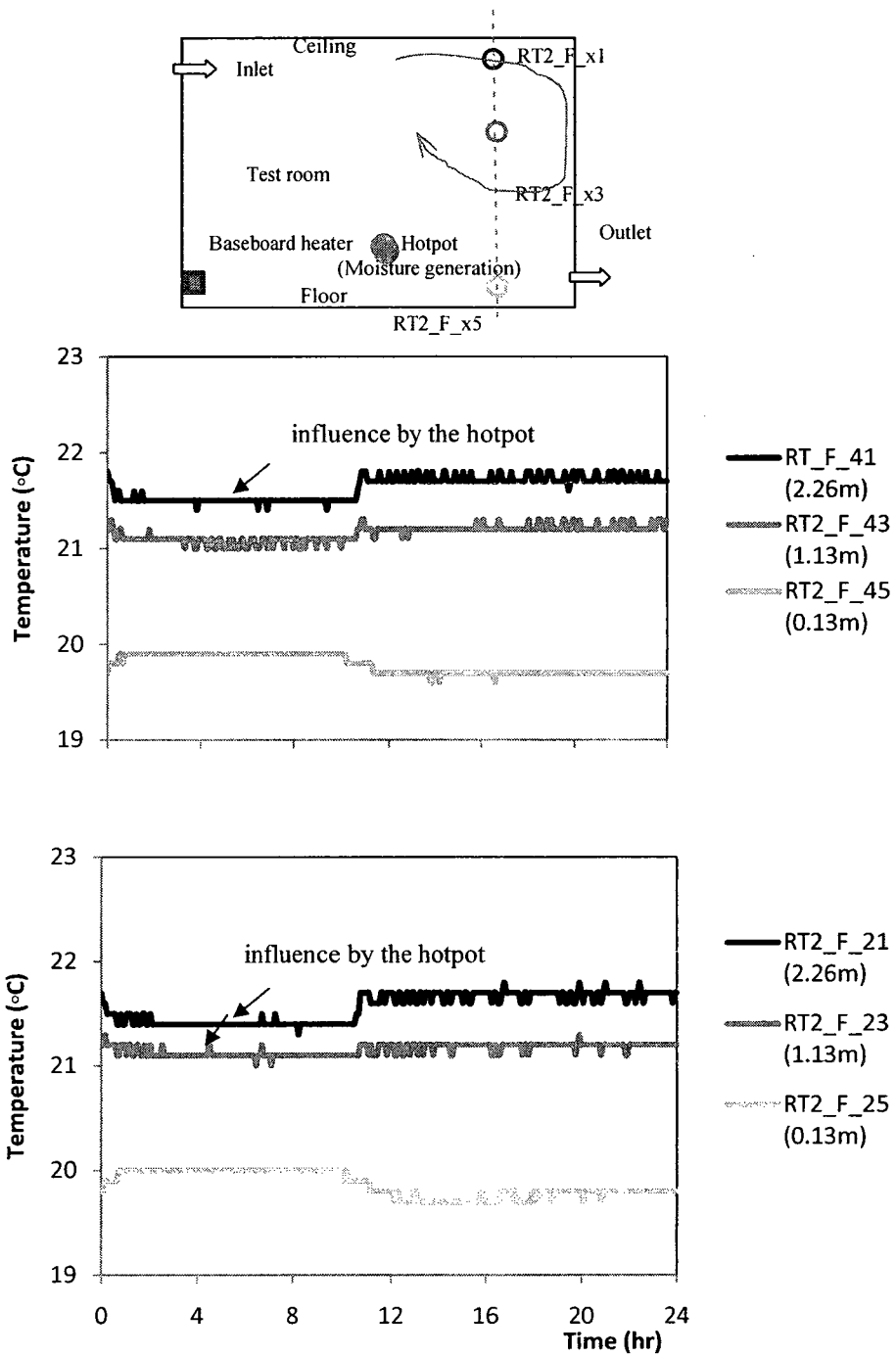


Figure C-2. Temperatures at top right corner of test rooms in case 1 at 0.5ACH.

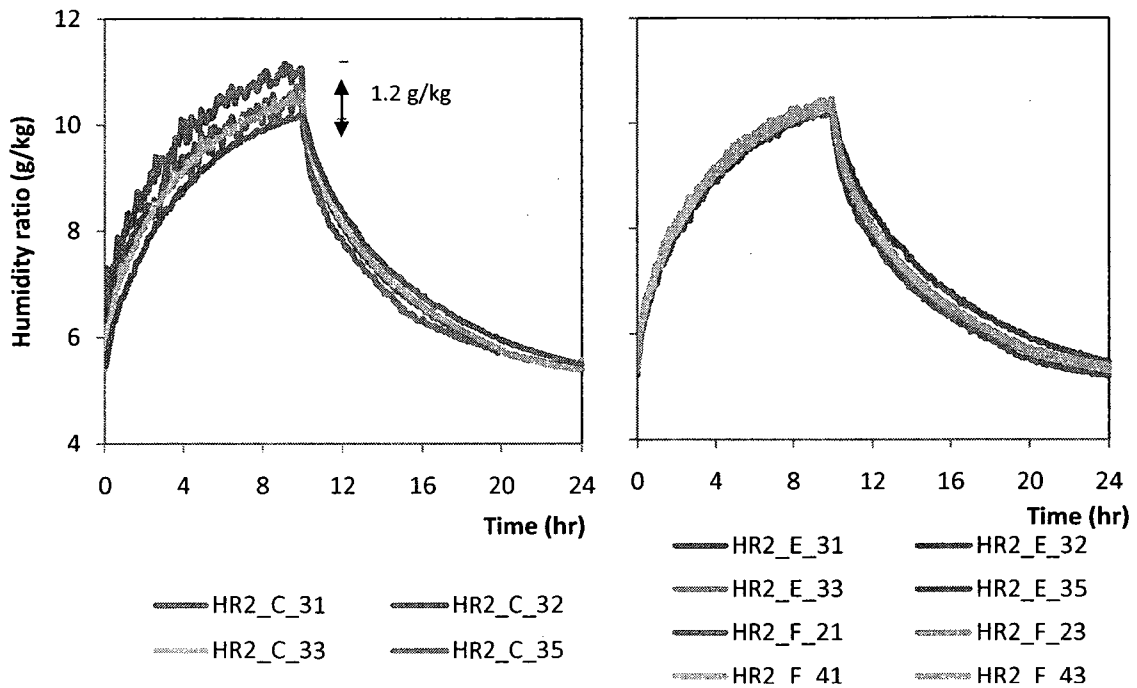


Figure C-3. Indoor humidity at locations close to the centre of test rooms in case 1 at 0.5 ACH.

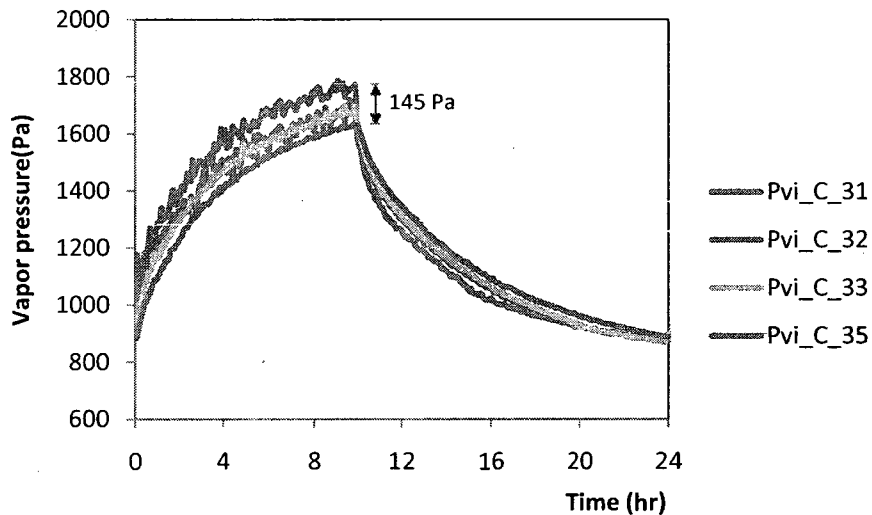


Figure C-4. Indoor vapor pressure difference close to the centre of test rooms in case 1 at 0.5 ACH.

The indoor humidity ratio is influenced by the ventilation and hot pot as well. HR2\_C\_32 is close to and above the hot pot. It is impacted by the hot stream generated by the hot pot and has 1.2 g/kg higher humidity ratio than HR2\_C\_35, which is close to the floor, as presented in Figure C-3. The higher moisture content in the air can be also observed from indoor vapor pressure, as shown in Figure C-4. There is up to 145 Pa higher vapor pressure at C\_32 compared to C\_35. However, the air is better mixed by the air

circulating at top right area of test rooms (HR2\_E\_32, HR\_F\_21, HR\_F\_23, HR\_F\_41 HR\_F\_43), so the humidity ratio of air in this area is close to each other, as shown in Figure C-3.

The same pattern of air flow and distribution of indoor temperature and humidity ratio can be observed in cases at 0.3, 0.75, 1 ACH. A validated CFD simulation on indoor environment can better illustrate the non-uniform distribution of indoor conditions, which is beyond this research due to the limit of time.

# APPENDIX D: BUILDING ENVELOPE PERFORMANCE IN MOISTURE BUFFERING EXPERIMENTAL INVESTIGATION

## 1. Temperature distribution across test walls

Since indoor temperature and outdoor temperature (chamber) were kept constant during tests, except for the impact of moisture generation, the temperature profile through the test wall were constant. Temperature across the centre of test wall (east) in case 1 is presented as an example of temperature distribution, as shown in Figure D-1. Indoor temperature and interior surface temperature in the period of moisture generation is slightly higher than those in no-moisture generation period. But this difference of indoor temperature does not have any influence on the temperatures of insulation cavity and sheathing board.

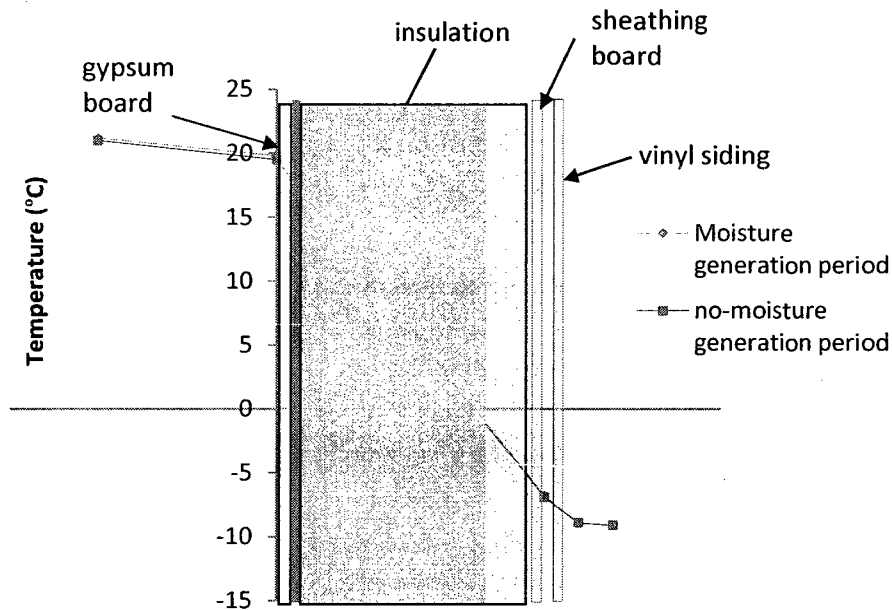


Figure D-1. Temperature distribution across test walls.

Interior surface temperature in case 2 (non-hygroscopic case) was 0.7 °C lower than that in case 1 (hygroscopic case). In addition, increasing ventilation rates enhance the heat transfer on interior surface, but the impact is too small to detect (the difference of interior surface temperature is within 0.1 °C).

## 2. Moisture conditions of insulation cavity and sheathing board

The moisture content of interior surface materials has been discussed in the section 6.1.2. Moisture content measured on sheathing board and RH measured in insulation cavity in case 1 (hygroscopic) and case 2 (non-hygroscopic) are presented as an example of the humidity conditions of building envelope components, as shown in Figure D-2 and D-3. It is proved that, moisture buffering only has its effect on interior surface materials. No

influence of moisture buffering can be found in other building envelope components behind vapor barrier. Also the daily variation of indoor humidity does not have any impact on the moisture condition of insulation cavity and sheathing board.

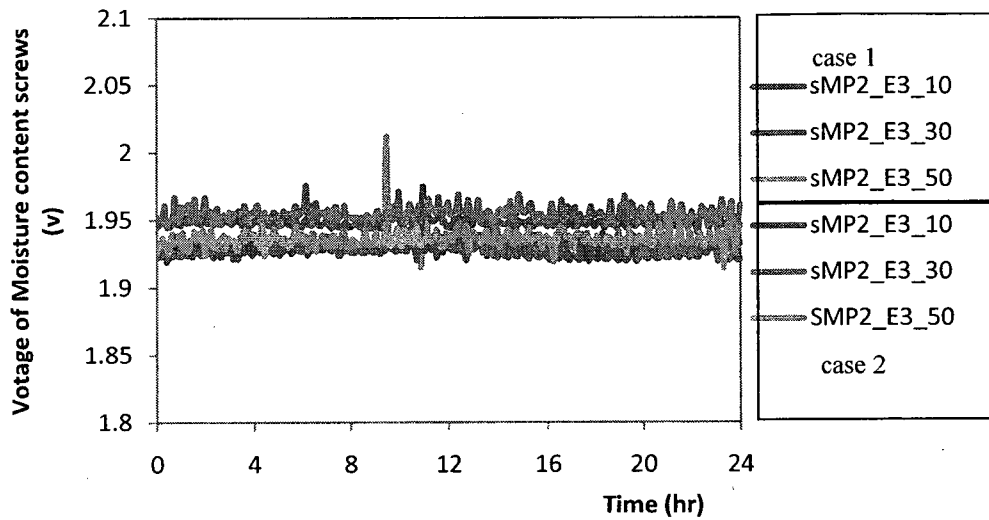


Figure D-2. Comparison of moisture content measured on sheathing board in case 1 and case 2.

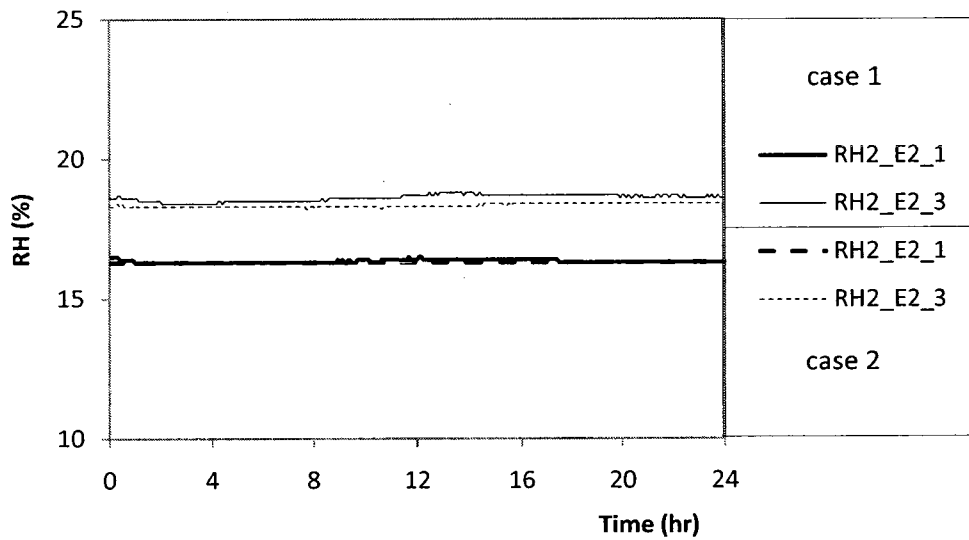


Figure D-3. Comparison of RH measured in insulation cavity in case 1 and case 2.